7. SITE 674[1]

Shipboard Scientific Party[2]

HOLE 674A

Date occupied: 1315, 28 July 1986

Date departed: 0830, 3 August 1986

Time on hole: 5.8 days

Position: 15°32.29′N, 58°51.09′W

Water depth (sea level, corrected m; echo-sounding): 4549.8

Water depth (rig floor, corrected m; echo-sounding): 4560.3

Bottom felt (rig floor, m; drill pipe measurement): 4560.7

Distance between rig floor and sea level (m): 10.5

Total depth (rig floor; m): 5013.3

Penetration (m): 452.6

Number of cores (including cores with no recovery): 48

Total length of cored section (m): 452.6

Total core recovered (m): 354.58

Core recovery (%): 78.3

Deepest sediment cored:
Depth sub-bottom (m): 452.6
Nature: claystone and mudstone
Age: early Oligocene
Measured velocity (km/s): 1.9

Principal results: Site 674 is located 17 km arcward of the Barbados Ridge deformation front. The main objectives at this site were to study the continuing structural and hydrologic evolution of accreted deposits well arcward of the deformation front.

The site drilling penetrated three main tectonic units composed of sediments ranging in age from early Pleistocene to middle Eocene. Tectonic unit A (0–101 mbsf) includes 10 m of sheared Oligocene and lower Miocene claystone and mudstone with an undeformed cover of upper Miocene to Pleistocene noncalcareous to calcareous clay(stone). This slope cover contains Miocene (?) material reworked from upslope and is locally deformed by thrust faults propagating from the underlying complex. Unit B (101–253 mbsf) encompasses Miocene and Pliocene claystone and mudstone with steep bedding dips and conspicuous scaly fabric. Unit C (253–452 mbsf) comprises lower Miocene to upper Eocene claystone and mudstone, plus alternating sequences of middle Eocene limestone, marl, claystone, and sandstone. This unit shows intense deformation, with overturned beds, thrust faults, and prominent development of scaly fabric, calcite veins, and stratal disruption. These three tectonic units are separated by low-angle thrust faults that postdate the internal deformation of each unit.

The presence of Eocene and Oligocene rocks in the accretionary wedge demonstrates that the décollement has been at a deeper stratigraphic depth than it is now at Site 671. The water content of these offscraped sediments is still 20%–40% of their total weight, and their porosity about 40%–50%. The chloride content shows a slight progressive decrease with depth, with negative anomalies close to the surface (30 mbsf) and in tectonic unit C. These anomalies apparently result from water circulation along fault zones. The absence of methane in these waters suggests that they have originated from a depth shallower than 2000 m, above the zone where thermogenic methane could have formed. Eight downhole temperatures measurements were made and they indicate a superficial gradient of 143°C/km (down to 48 mbsf), and a deeper gradient of 28°C/km. Warm waters are either being laterally supplied at a depth of about 30 m and there create the superficial gradient or, alternatively, elevated temperatures below 48 m result from heat input along numerous paths, with the upper gradient resulting from the presence of the 2.2°C isotherm at the water/sediment interface.

Site 674 provides unique insight into the development of intensively deformed rocks at a low degree of consolidation. These sedimentary rocks were accreted only a few million years ago but have continued to deform substantially during uplift. This site links present accretionary processes at the deformation front to rocks of emergent accretionary complexes, such as those exposed on Barbados Island.

BACKGROUND AND OBJECTIVES

The lower slope of the Barbados accretionary complex is characterized by a rough seafloor morphology as depicted on Seabeam maps (Valery et al., 1985), and by the absence of slope basins or pelagic draping of significant thickness (Speed, Westbrook et al., 1984; Mascle et al., 1986). The lower slope, inclined about 2° seaward, is 40 km wide at the latitude of the ODP Leg 110 site transect. This slope corresponds to the zone of initial accretion as defined by Westbrook et al. (1984), where sediments initially deposited in the oceanic plain are tectonically transported to the accretionary complex. The lower slope marks the eastern limit of a 100-km-wide plateau (water depth about 4000 m) where former accreted series are blanketed by a gently deformed hemipelagic cover several hundred meters thick.

Although accretion of oceanic sediments or underplating is probably occurring at the base of the prism and thickening the

---

[1] Mascle, A., Moore, J. C., et al., 1988. *Proc., Init. Repts. (Pt. A), ODP,* 110: College Station, TX (Ocean Drilling Program).

[2] Alain Mascle (Co-Chief Scientist), Institut Français du Pétrole, 1-4 Ave Bois-Preau, B.P. 311, 92506 Rueil Malmaison Cedex, France; J. Casey Moore (Co-Chief Scientist), Dept. of Earth Sciences, University of California at Santa Cruz, Santa Cruz, CA 95064; Elliott Taylor (Staff Scientist), Ocean Drilling Program, Texas A&M University, College Station, TX 77840; Francis Alvarez, Borehole Research Group, Lamont-Doherty Geological Observatory, Columbia University, Palisades, NY 10964; Patrick Andreieff, BRGM, BP 6009, 45060 Orleans Cedex-2, France; Ross Barnes, Rosario Geoscience Associates, 104 Harbor Lane, Anacortes, WA 98221; Christian Beck, Département des Sciences de la Terre, Université de Lille, 59655 Villeneuve d'Ascq Cedex, France; Jan Behrmann. Institut für Geowissenschaften und Lithosphärenforschung, Universität Giessen, Senckenbergstr. 3, D6300 Giessen, FRG; Gerard Blanc, Laboratoire de Géochimie et Métallogénie U. A. CNRS 196 U.P.M.C., 4 Place Jussieu, 75252 Paris Cedex 05, France; Kevin Brown, Dept. of Geological Sciences, Durham University, South Road, Durham, DH1 3LE, U.K. (current address: Dept. of Earth Sciences, University of California at Santa Cruz, Santa Cruz, CA 95064); Murlene' Clark, Dept. of Geology, LSCB 341, University of South Alabama, Mobile, AL 36688; James Dolan, Earth Sciences Board, University of California at Santa Cruz, Santa Cruz, CA 95064; Andrew Fisher, Division of Marine Geology and Geophysics, University of Miami, 4600 Rickenbacker Causeway, Miami, FL 33149; Joris Gieskes, Ocean Research Division A-015, Scripps Institution of Oceanography, La Jolla, CA 92093; Mark Hounslow, Dept. of Geology, Sheffield University, Brook Hill, Sheffield, England S3 7HF; Patrick McLellan, Petro-Canada Resources, PO Box 2844, Calgary, Alberta Canada (current address: Applied Geotechnology Associates, 1-817 3rd Ave. NW, Calgary, Alberta T2N OJ5 Canada); Kate Moran, Atlantic Geoscience Centre, Bedford Institute of Oceanography, Box 1006, Dartmouth, Nova Scotia B2Y 4A2 Canada; Yujiro Ogawa, Dept. of Geology, Faculty of Science, Kyushu University 33, Hakozaki, Fukuoka 812, Japan; Toyosaburo Sakai, Dept. of Geology, Faculty of General Education, Utsunomiya University, 350 Mine-machi, Utsunomiya 321, Japan; Jane Schoonmaker, Hawaii Institute of Geophysics, 2525 Correa Road, Honolulu, HI 96822; Peter J. Vrolijk, Earth Science Board, University of California at Santa Cruz, Santa Cruz, CA 95064; Roy Wilkens, Earth Resources Laboratory, E34-404 Massachusetts Institute of Technology, Cambridge, MA 02139; Colin Williams, Borehole Research Group, Lamont-Doherty Geological Observatory, Columbia University, Palisades, NY 10964.

accreted complex, it is along the lower slope that present frontal accretionary processes or offscraping are clearly depicted on seismic records. Here, we can directly sample recently offscraped material, measure its physical properties, and analyze its pore-water content with the present capabilities of deep-sea drilling. Several holes on a single transect across this lower slope are necessary for a full understanding of tectonic processes related to the growth of accretionary complexes. Site 674 is located 17 km west of the deformation front (Fig. 1) and is the shallowest (water-depth: 4560 m) and the farthest arcward (17 km from the front) of a series of penetrations that already include ODP Sites 673-671 and DSDP Sites 541-542 downslope (Fig. 2).

The main objectives of Site 674 are quite similar to those of Site 673, located only 5 km downslope. They are as follows:

1. To define the age, facies, and structural fabric of the accreted series and the age and facies of the hemipelagic slope sediments that, according to seismic data, should not be thicker than a few tens of meters. We also hope to compare the depositional paleoenvironment and deformation history of sediments at Site 674 with those of same age drilled downslope.
2. To determine the physical properties of the accreted series and to compare their state of consolidation with presently accreting sediments at the toe of the prism and with the sedimentary cover of the adjacent Atlantic plain. Also to attempt correlations with the few discontinuous and arcward-dipping reflectors observed on seismic records.
3. To measure *in-situ* temperature and calculate a heat-flow gradient to determine if the anomalously high values obtained at Sites 671, 672, and 673 are representative of the entire slope.
4. To determine the pore-water chemical content of sediments and to determine if fluids are still advecting along thrust faults.
5. To constrain various models of prism thickening (see Background and Objectives section, Site 673 chapter, this volume) as the accreted series at this site is five times thicker than at the initial offscraping zone at the deformation front.

OPERATIONS

Site 674 was approached by dynamic positioning offset from Site 673. A beacon was dropped at 1315 on 28 July 1986 for a site location 2.5 nmi west of Hole 673B at 15°32.29′N, 58° 51.09′W. This location is the westernmost drill site on the Lesser Antilles forearc. The coring objectives here were similar to those at Site 673; to investigate the continuing deformation of the accretionary sequence and the thickening of offscraped sediments. Hole 674A was drilled with a six-drill-collar BHA and an 11-7/16″ APC deep throat core bit spudded into a sediment pond to provide lateral support for the BHA. The hole was continuously cored from mudline, at 4560.7 m drill pipe, to 452.6 mbsf.

Cores 110-674A-1H through -4H were taken with the APC. Recovery was 97.3% but high pull-out forces required a switch to the XCB system below 34.6 mbsf. An APC shoe with the Von Herzen temperature recorder was deployed on Core 110-674A-3H.

The XCB system was used on Cores 110-674A-5X through -48X. Recovery in this mode was 76.7%. Hole problems were encountered twice, but mud sweeps and short trips reduced the fill between cores. The bulk of the coring was accomplished with 65 pump strokes and 75 RPM on the bit. Recovery was

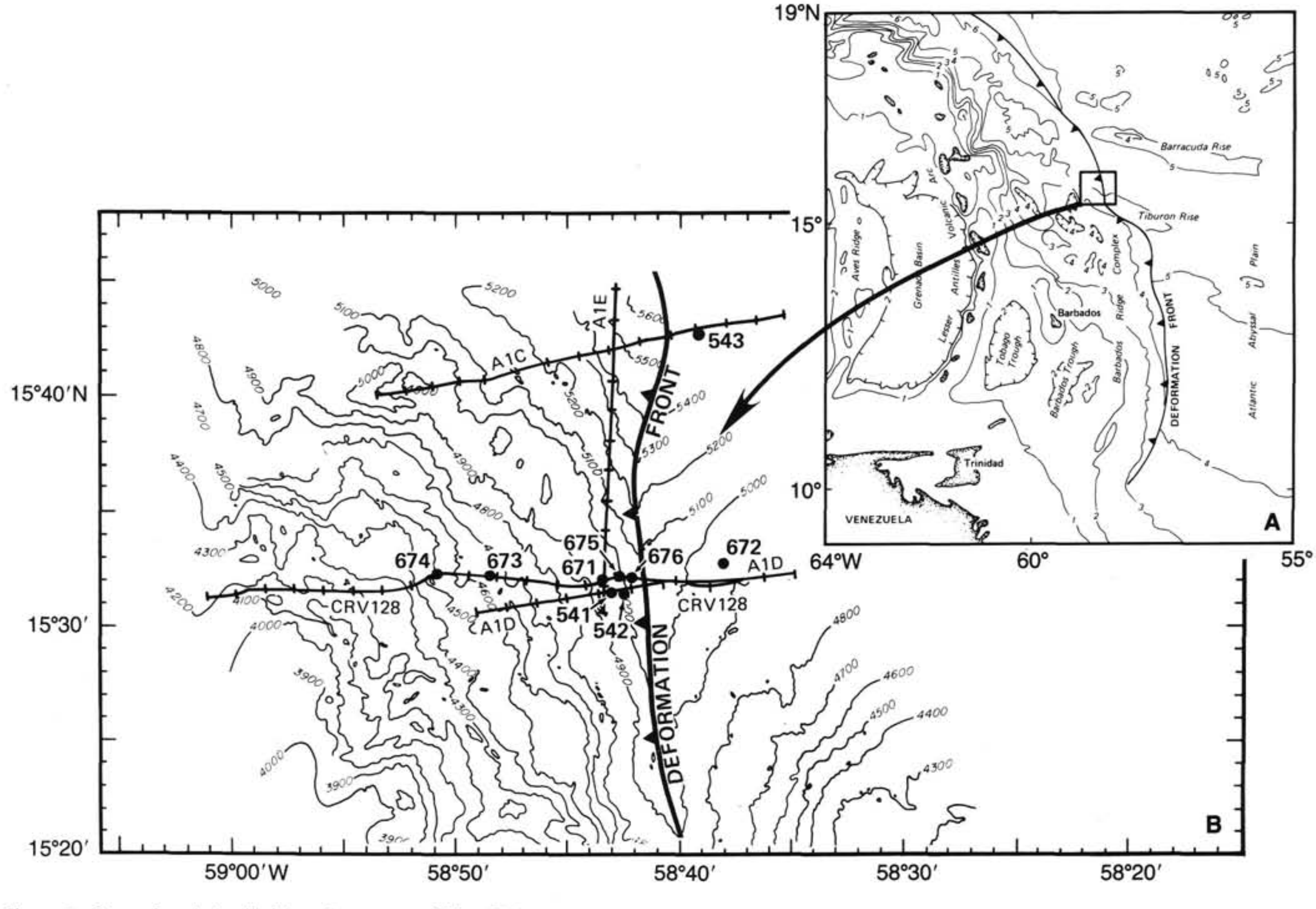

Figure 1. General and detailed location maps of Site 674.

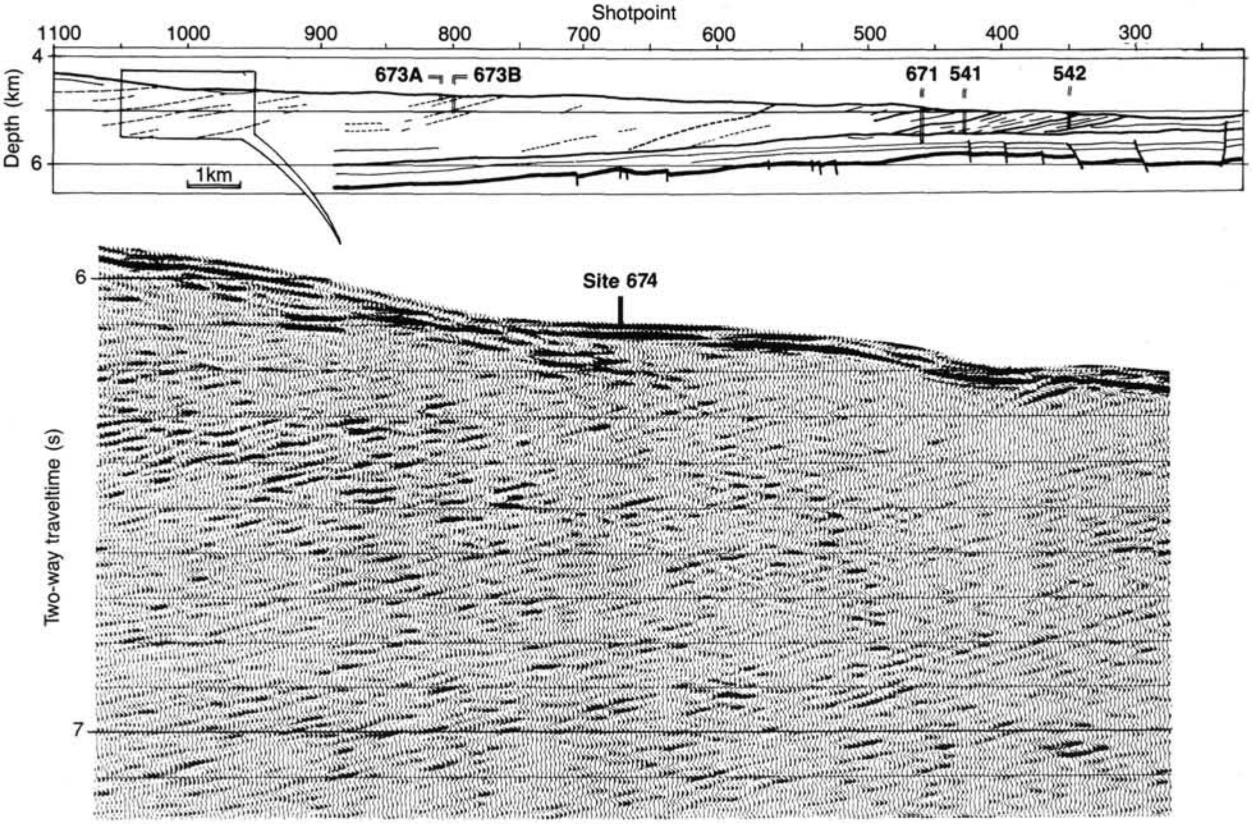

Figure 2. Top: Depth section (no vertical exaggeration) of line CRV 128. Bottom: Seismic line CRV 128 and location of Site 674.

good in the sediments, which varied from chalky green clay to waxy clay. The recovered cores were characterized by repeating-age stratigraphy, steep (locally overturned) bedding dips. The new Venturi XCB sub was used on Cores 110-674A-46X to -48X. Results are given in the special tools section of the ODP Operations Report. Coring was suspended at the request of the Co-chief Scientists for scheduling purposes of other Leg 110 drilling objectives. The coring summary for Site 674 operations is listed in Table 1. The hole was plugged with heavy mud and the ship departed for Site 675 at 0830 on 3 August 1986 after 5.8 operational days.

STRUCTURAL GEOLOGY

Site 674 is located 17 km arcward of the accretionary front, in the oldest portion of the Barbados Ridge complex cored during DSDP Leg 78A and ODP Leg 110. Good core recovery and quality at Site 674 revealed a number of large-scale structures and intense fabrics which have previously only been observed in sub-aerially exposed ancient accretionary complexes. This site therefore provides crucial links between ancient and modern accretionary processes. The sequence recovered at Site 674 is made up of two main structural units; an upper slope cover sequence and a lower unit of accreted sediments.

Slope Sediments

The slope sediments at Site 674 are at least 63 m thick (Cores 110-674A-1H to -7X) and may be as much as 90 m thick (i.e., down to Core 110-674A-10X; see Lithostratigraphy section). The top 10–15 m of the cored section (Cores 110-674A-1H to -2H) consists of approximately horizontally bedded, lower Pleistocene marl (Fig. 3). This marl overlies matrix-supported, polymictic breccias which extend from 15–34 mbsf (Cores 110-674A-2H to -4H). The breccia clasts include both Miocene mudstones and sediments of indeterminate age (see Lithostratigraphy, this chapter). Within the breccias, bedding dips range between 0 and 40°. The majority of the dips are thought to record random orientation of blocks. The breccias overlie a bedded sequence of lower Pleistocene and upper Pliocene mud and marl that extends from 40 to 63 mbsf (Cores 110-674A-5X to -7X). Variations in bedding dip decrease downsection, from 0 to 40° at around 50 mbsf to horizontal at 60 mbsf (Fig. 3).

A small but well-documented geochemical anomaly, corresponding to a chloride minimum, is centered around 25 to 35 mbsf (Core 110-674A-4H) and suggests that fluids from deeper within the complex are migrating along fractures or faults through this zone (see Geochemistry, this chapter). The nearest identified faults (which are not thought to be in eroded blocks in the breccias) are two zones of scaly clay that occur near 20 mbsf (Core 110-674A-3H, Fig. 3). The scaly clay fabrics in these fault zones dip between 15° and 50°. In the fault zone at 21 mbsf (Core 110-674A-3H), folding of a disrupted calcite vein suggests a reverse sense of shear (Fig. 4). In addition, two low-angle fault contacts occur at 42 and 53 mbsf (Core 110-674A-5X and -6X). Any, or all of the fault zones may be the product of either slumping or tectonic activity. However, the association of the fault at 21 mbsf with the calcite vein suggests that it is tectonic. No fault zones were observed closer to the immediate vicinity of the chloride minimum, suggesting that this geochemical anomaly may be associated with only a small structural feature.

It is not clear whether the lower Pleistocene to upper Pliocene slope sediments unconformably overlie the accretionary complex at 65 mbsf or whether they extend down through the section of indeterminate age to 90 mbsf. The basal portion of this sequence (65–90 mbsf) appears to be relatively undeformed and has a high porosity, suggesting that it has not been deeply buried (see Physical Properties section). However, lithologic correlations with the biostratigraphically dated sequences at Site

Table 1. Coring summary for Site 674.

Core no. 110-674A-	Date July/August 1986	Time	Sub-bottom top (m)	Sub-bottom bottom (m)	Meters cored (m)	Meters recovered (m)	Percent recovery
1H	29	0020	0	6.1	6.1	6.08	99.7
2H	29	0138	6.1	15.6	9.5	9.30	97.9
3H	29	0310	15.6	25.1	9.5	9.54	100.0
4H	29	0430	25.1	34.6	9.5	8.84	93.0
5X	29	0730	34.6	44.1	9.5	6.50	68.4
6X	29	0915	44.1	53.6	9.5	4.78	50.3
7X	29	1100	53.6	63.1	9.5	5.71	60.1
8X	29	1250	63.1	72.6	9.5	5.86	61.7
9X	29	1430	72.6	82.1	9.5	9.58	101.0
10X	29	1620	82.1	91.6	9.5	7.97	83.9
11X	29	1957	91.6	101.1	9.5	4.44	46.7
12X	29	2310	101.1	110.6	9.5	6.19	65.1
13X	30	0302	110.6	120.1	9.5	6.73	70.8
14X	30	0450	120.1	129.6	9.5	6.86	72.2
15X	30	0650	129.6	139.1	9.5	4.02	42.3
16X	30	0910	139.1	148.6	9.5	4.98	52.4
17X	30	1105	148.6	158.1	9.5	2.93	30.8
18X	30	1300	158.1	167.6	9.5	9.65	101.0
19X	30	1900	167.6	177.1	9.5	4.68	49.2
20X	30	2100	177.1	186.6	9.5	8.71	91.7
21X	30	2255	186.6	196.1	9.5	5.55	58.4
22X	31	0043	196.1	205.6	9.5	8.14	85.7
23X	31	0425	205.6	215.1	9.5	5.45	57.3
24X	31	0640	215.1	224.6	9.5	8.56	90.1
25X	31	0840	224.6	234.1	9.5	9.32	98.1
26X	31	1030	234.1	243.6	9.5	6.45	67.9
27X	31	1520	243.6	253.1	9.5	8.21	86.4
28X	31	1800	253.1	262.6	9.5	4.69	49.3
29X	31	1950	262.6	272.1	9.5	4.55	47.9
30X	31	2150	272.1	281.6	9.5	6.36	66.9
31X	01	0020	281.6	291.1	9.5	3.07	32.3
32X	01	0217	291.1	300.6	9.5	8.64	90.9
33X	01	0635	300.6	310.1	9.5	9.29	97.8
34X	01	0830	310.1	319.6	9.5	5.50	57.9
35X	01	1030	319.6	329.1	9.5	7.37	77.6
36X	01	1240	329.1	338.6	9.5	9.60	101.0
37X	01	1515	338.6	348.1	9.5	9.73	102.0
38X	01	1720	348.1	357.6	9.5	9.73	102.0
39X	01	1920	357.6	367.1	9.5	9.49	99.9
40X	01	2132	367.1	376.6	9.5	9.00	94.7
41X	02	0155	376.6	386.1	9.5	8.34	87.8
42X	02	0400	386.1	395.6	9.5	7.02	73.9
43X	02	0640	395.6	405.1	9.5	9.62	101.0
44X	02	1200	405.1	414.6	9.5	9.00	94.7
45X	02	1348	414.6	424.1	9.5	9.68	102.0
46X	02	1543	424.1	433.6	9.5	9.59	101.0
47X	02	1933	433.6	443.1	9.5	9.56	100.0
48X	02	2130	443.1	452.6	9.5	9.72	102.0
					452.6	354.58	

671 and the reference site (Site 672), suggest that it could be of Miocene age (see Lithostratigraphy section). In either case, an angular unconformity representing a period of moderate erosion may be present at either 60 or 90 mbsf. An unconformity at this level would account for the presence of lower Oligocene sediments in the fault zone at 100 mbsf (correlation with sediment thicknesses at Site 672 would indicate that on the order of 100 to 150 m or more of section may have been removed).

Accreted Sequence

The accreted sequence at Site 674 is divided into seven packets separated by biostratigraphic and structural discontinuities. These discontinuities correspond to zones of scaly clay fabrics that are developed along thrust zones. Evidence that these packets may form subdivisions of three major tectonic units will be discussed later (Fig. 3).

Packet 1

Packet 1 is bounded above by an erosional unconformity and below by thrust 1. Lithologically, the packet is largely composed of a 20-m-thick section (Core 110-674A-8X to -9X) of indeterminant age (Miocene?) mud with local ash beds. If the indeterminate aged sediments are part of the slope cover sequence then most of Packet 1 has been completely eroded away, leaving only its basal thrust zone (thrust 1, see below). The section is upright and bedding dips are horizontal. Thrust 1 corresponds to a complex zone of deformation that lies between 91.6 and 105 mbsf (base of Core 110-674A-10X to top of -12X). The upper margin of the fault zone is a sharp, subhorizontal contact between the nonscaly green gray mudstone of Packet 1, and an underlying fault zone sequence dominated by orange brown scaly mudstone. Radiolarians extracted from the scaly clay along this contact give both early and late Oligocene ages. The distinctive orange brown mud, stained by a black amorphous (manganese) phase, is not biostratigraphically dated. The brown mud is, however, identical in character to the horizon along which the décollement was localized at Site 671 and a horizon at the same stratigraphic level in the reference hole (Site 672), both of which have an early Miocene biostratigraphic age. Internally, the muds of this unit have a well-developed scaly fabric. The basal contact

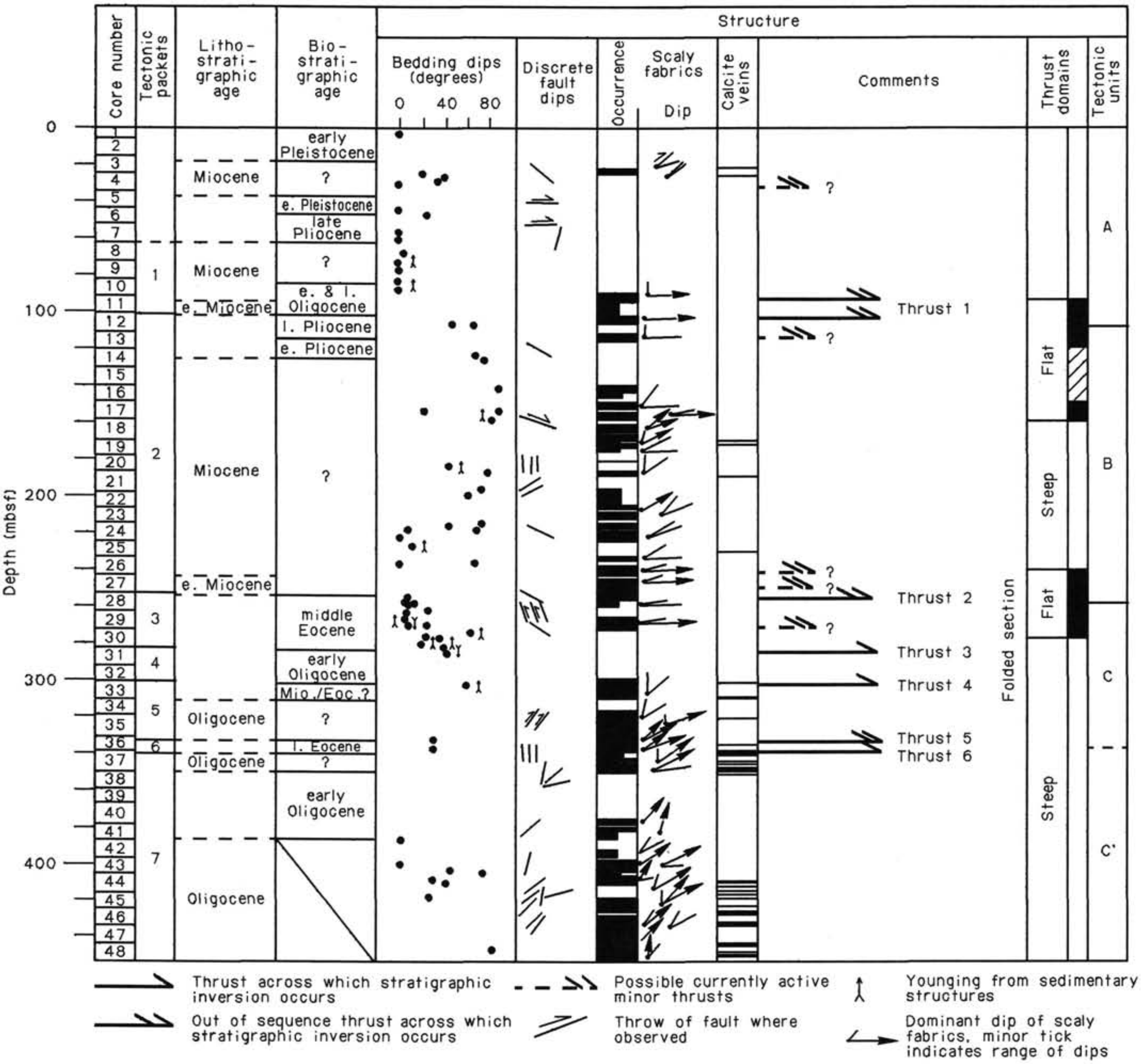

Figure 3. Structural log of Hole 674A. Range and dominant dip of scaly fabrics is denoted by angle between two bars and arrowhead, respectively. See text for discussion.

of the fault zone is marked by a zone of intense scaly clay 20–30 cm wide with horizontal fabrics in which blue gray staining occurs. The deformation dies away downward through approximately 4 m of sheared muds with an almost planar horizontal fabric (Fig. 5). The apparent range in ages of the fault zone material suggests that a series of tectonized slivers of a number of lithological units from the accretionary complex have been incorporated into this fault zone.

Packet 2

Packet 2 is bounded by thrust 1 above and thrust 2 below and extends from 100 to 250 mbsf (Cores 110-674A-12X to -27X, Fig. 3). The packet is composed of an upper section of upper and lower Pliocene sediments with a downhole thickness of 30 m and a lower section of sediments with an indeterminate age and a downhole thickness of 110 m. Lithological correlation with the reference hole (Site 672) indicates that the indeterminate age section is very probably of Miocene age (see Lithostratigraphy section). Both sections dip at between 60° and 80° from 180 to 220 mbsf (Cores 110-674A-12X to -23X), with dips then decreasing to 0–10° at the base of the packet at 240 mbsf (Core 110-674A-26X). Local sedimentary structures indicate that the section is upright. After correcting for dip, the Pliocene section has a true thickness between 5 and 15 m and the indeterminate section has a true thickness between 35 and 65 m.

Zones of scaly clays are common in Packet 2 and make up over 50% of the section. No biostratigraphically defined offsets occur across these scaly fault zones and they appear to be the product of intrapacket thickening. Near thrust 1, between 100 and 150 mbsf, the scaly fabrics generally have low to horizontal

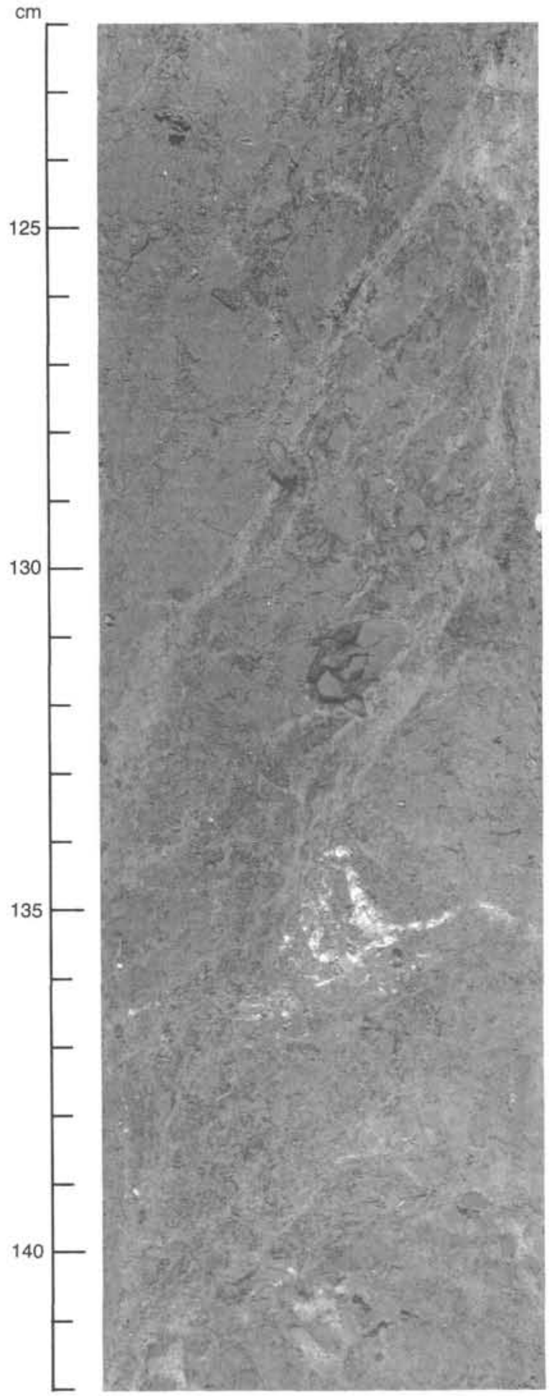

Figure 4. Folded and disrupted calcite indicates a reverse sense of shear across a fault zone in which scaly fabrics are well developed. Basal contact of fault zone dips at 35°, upper contact dips at 60°. (Core 110-674A-3H.)

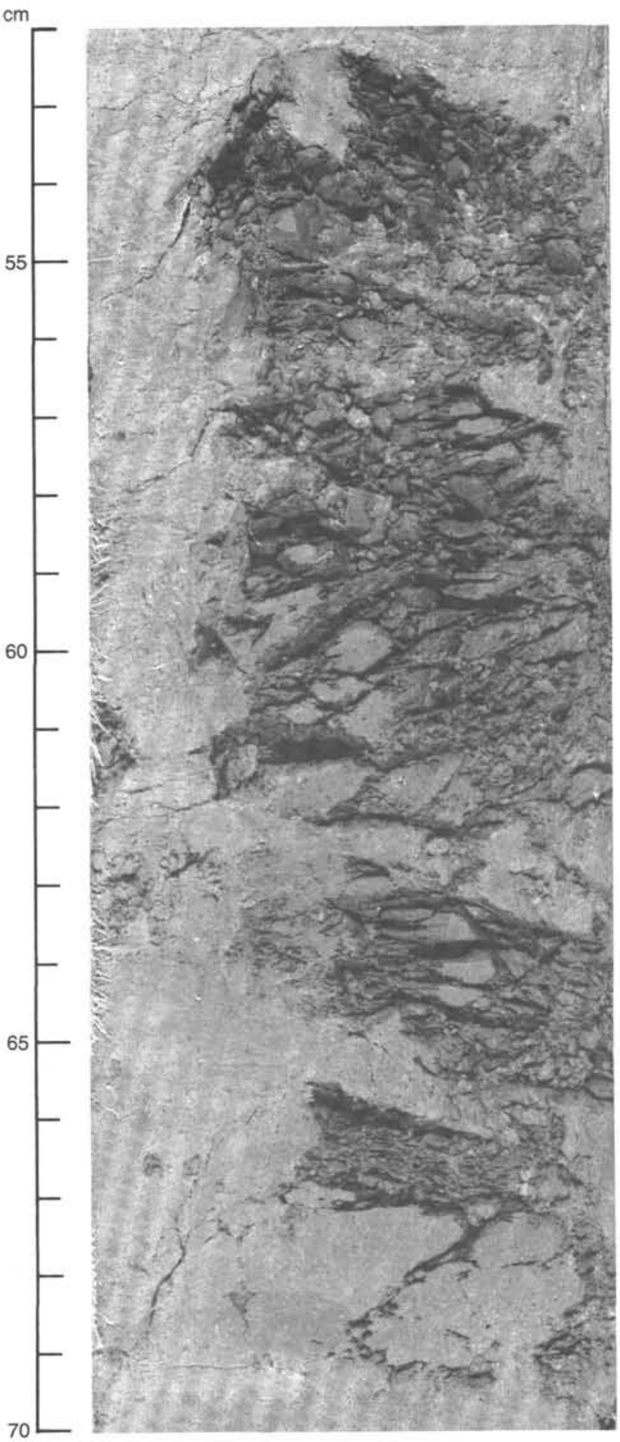

Figure 5. Subhorizontal, subplanar fabrics developed in mudstones just beneath thrust 1, Core 110-674A-12X.

dips (Cores 110-674A-12X to -17X). Locally, these scaly fabrics are associated with relatively intense stratal disruption (see Fig. 6 for an example of stratal disruption). The low-angle fault zones cut across the steeply dipping beds in this upper part of the packet. Below 150 mbsf and down to about 230 mbsf (Cores 110-674A-18X to -24X), the scaly fabrics generally dip between 30° and 65°. Calcite veins oriented subparallel to the scaly fabrics occur locally within this interval. Syncline and postdisruption relationships between veins and fault zone fabrics are particularly well developed around 165 mbsf (Core 110-674A-18X), in a zone of stratal disruption (Fig. 6). The scaly fabrics dip at low angles near thrust 2, between 230 and 250 mbsf (Cores 110-674A-25X to -27X). In the middle and basal portions of Packet 2, the scaly fault zones are subparallel to the dominant bed dip. Thrust 2 lies at approximately 250 mbsf (Cores 110-674A-26X to -28X). It is characterized by intense subhorizontal scaly clay fabrics (Fig. 7), and well-developed zones of stratal disruption, boudinage, and brecciation (Figs. 8 and 9). A distinctive orange

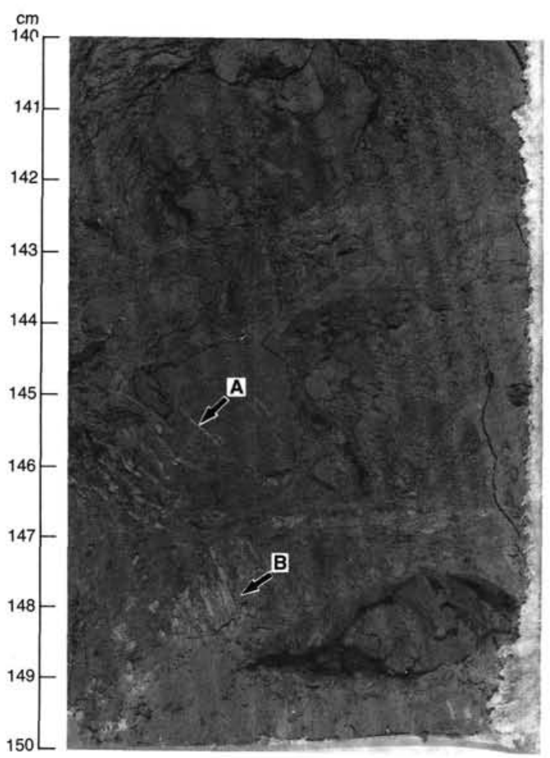

Figure 6. A zone of stratal disruption in which syntectonic calcite veining is developed in Core 110-674A-18X. Note the subrounded-to-partially dismembered mudstone fragments in the matrix of scaly clays. Slightly sigmoidal calcite vein arrays cut across matrix and fragment alike (Arrow A), indicating a postdisruptive episode of calcite veining. Predisruptive calcite veining is indicated by the dense network of veins contained within fragment at base of plate (Arrow B).

brown mudstone, stained with an amorphous black (manganese) phase previously mentioned in connection with thrust 1, is also present in the thrust 2 fault zone (Core 110-674A-27X). If these lithologically similar horizons have the same age, early Miocene material is present in the fault zone.

Packet 3

Packet 3 is bounded by thrust 2 above and thrust 3 below and extends from 250 to 280 mbsf (Cores 110-674A-28X to -30X, Fig. 3). The packet is composed of a middle Eocene sequence (see Lithostratigraphy section) that dips approximately 10–40°. Well-developed networks of shear fractures (web structure), occur in sandstone sequences in this packet just below thrust 2 (Fig. 10). Sedimentary structures in this packet indicate that the section is locally overturned and that the sequence is folded (fold half wavelengths are approximately 10 m). Assuming that the axial planes of the folds bisect their limbs, they have a dip of approximately 10° at the top of the packet, steepening to around 40° near the bottom. Fold hinges tend to be faulted out along thin scaly clay zones. Thrust 3 is not directly seen and has been inferred from biostratigraphic evidence. This evidence indicates that the middle Eocene sequence of Packet 3 directly overlies the lower Oligocene strata of Packet 4 (see below). The contact between packets is not thought to be conformable, but instead represents an overturned age boundary, as the upper Eocene sediments are missing. The missing lithologies correspond to about 40 m of section when compared to the reference section Site 672. As Packet 4 is similarly folded, it is possible that thrust 3 predates the episode of folding and is itself folded. On the other hand, folding episodes in both packets may be unrelated.

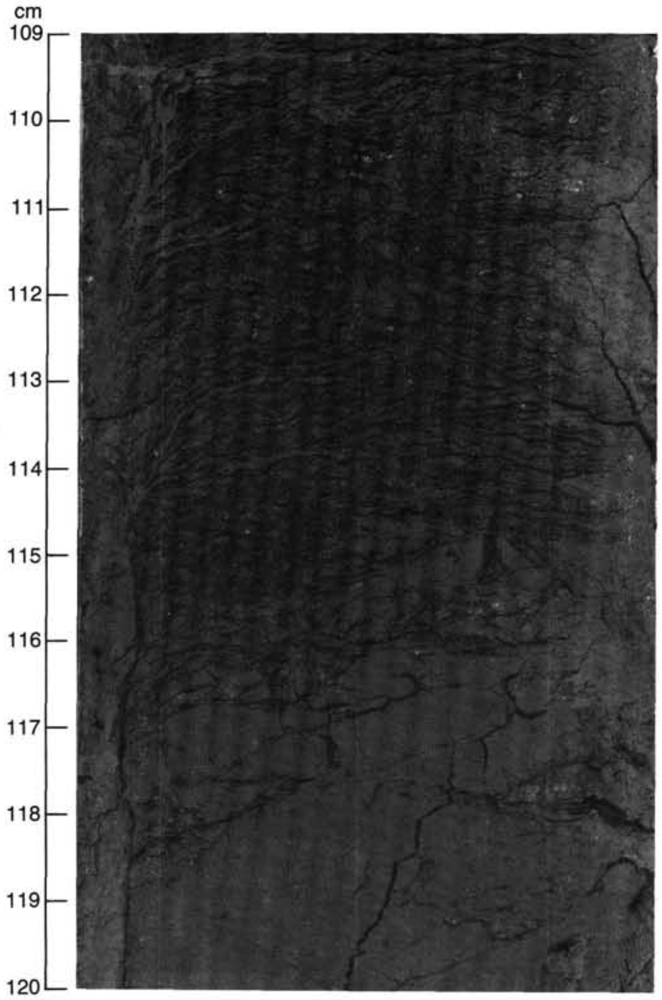

Figure 7. Intense subhorizontal scaly fabrics in minor splay fault just above thrust 2 in Core 110-674A-26X.

Packet 4

Packet 4 is bounded by thrust 3 above and thrust 4 below and extends from 280 to 300 mbsf (Cores 110-674A-31X to -32X). This packet consists of biostratigraphically delineated lower Oligocene sediments, with bedding dips between 40 and 60° (Fig. 3). The packet contains a synclinal fold with an axial plane dipping at around 50°. Thrust 4 separates the lower Oligocene of Packet 4 from the lower Miocene sequence of Packet 5 below. The scaly fabrics in this fault zone dip between 60° and 90° and occur over an interval a little more than 10 m wide (Core 110-674A-33X and top of -34X). There is abundant calcite veining within this fault zone. The veins have generally developed subparallel to the scaly clay fabric.

Packet 5

Packet 5 is bounded by thrust 4 above and thrust 5 below and extends from 300 to 330 mbsf (Cores 110-674A-33X to -35X). The top of the packet is early Miocene in age; however, the basal portions of this sequence are indeterminate in age. Lithological correlation suggests that the lower section of Packet 5 is of Oligocene age (see Lithostratigraphy section). No bedding dips were recorded within this packet but scaly fabrics, which dip between 35° and 90° and are well developed throughout much of the sequence (Cores 110-674A-34X to -35X). These scaly clays

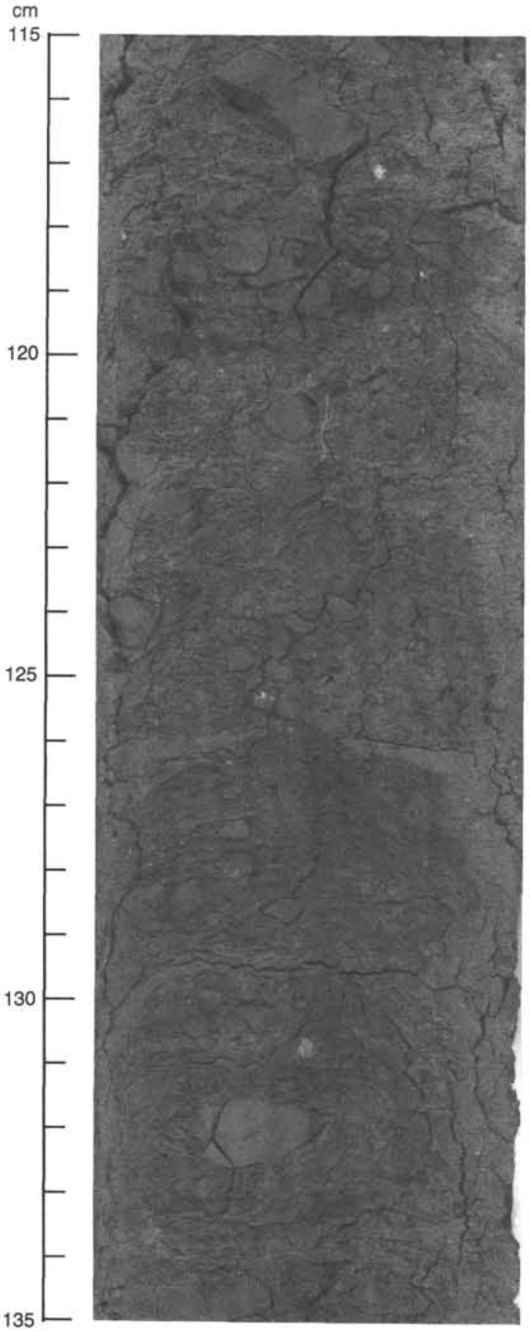

Figure 8. Well-developed zone of stratal disruption in the fault zone of thrust 2, Core 110-674A-27X. Note variation in the shapes (rounded, angular to phacodial) of the mudstone fragments in the scaly clays.

correspond to thrust 5, which may be interpreted as an out-of-sequence structure that places a structurally thinned Oligocene section (by about 100 m) onto the upper Eocene section below.

Packet 6

Packet 6 is bounded by thrust 5 above and thrust 6 below and extends from 330 to 340 mbsf (Core 110-674A-36X). The sediments in this packet comprise an upper Eocene, laminated fine sandstone or siltstone unit in which weblike structures are well developed in places. The sequence has typical bedding dips of 30°. Scaly clay fabrics are well developed throughout the packet and commonly have dips of 30° to 90°. The packet appears to be part of a large-scale thrust zone that stretches between 310 and 350 mbsf (Cores 110-674A-34X to -37X).

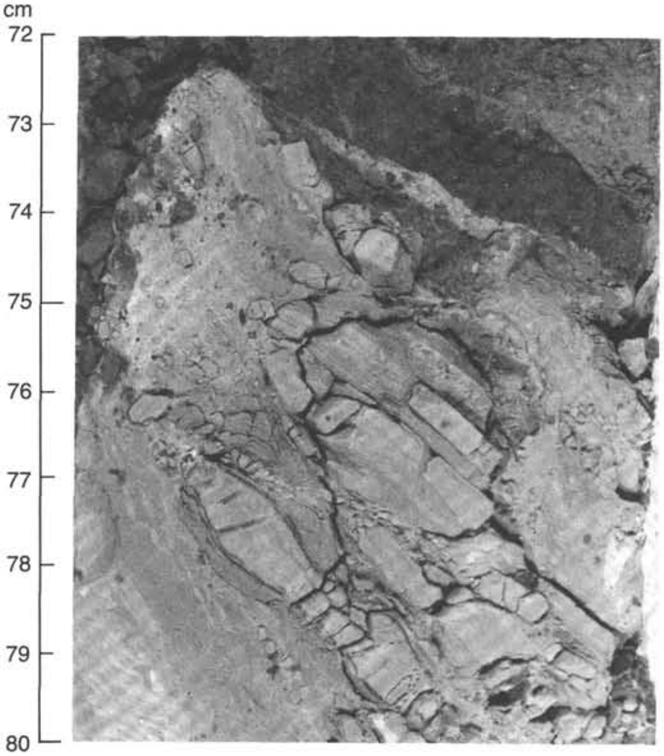

Figure 9. Boudinaged, laminated siltstone beds in the middle Eocene section of Packet 3, immediately below thrust 2, Core 110-674A-28X.

Packet 7

Packet 7 is bounded by thrust 6 above and extends to the base of the hole at 452 mbsf (Cores 110-674A-37X to -49X). It is composed of lower Oligocene strata at the top, for which no bedding dips were recorded. The lower sediments have a mixed fauna of late Oligocene to middle Eocene age. Bed dips are variable, ranging between 0° and 75°, with the dips generally steepening toward the base of the packet. Intensely developed scaly clays and zones of strata disruption occur throughout most of the packet, which may be part of a major thrust zone. The mixing of the fauna may be a result of tectonic processes. The scaly fabrics dip between 40° and 90°. Calcite veining is common throughout the scaly zones and is folded and disrupted in Cores 110-674A-37X, -45X, and -47X (Figs. 11 and 12). In general, the intensity of the fabrics increases downward through the packet. Almost 100% of the sequence is composed of scaly and stratally disrupted zones (Fig. 13) below 420 msbf (Core 110-674A-45X).

Discussion

Despite the apparent structural complexity of the thrusted sequence cored at Site 674, an overall structural pattern can be extracted. The packets of accreted material are divided into three major "tectonic units" (termed A, B, and C, see Figs. 3 and 14), thought to relate to currently active deformation within the accretionary complex. The delineation of these units is based on four criteria:

1. Division of the accreted sequence into thrust domains, with distinctions being made between regions in which high-an-

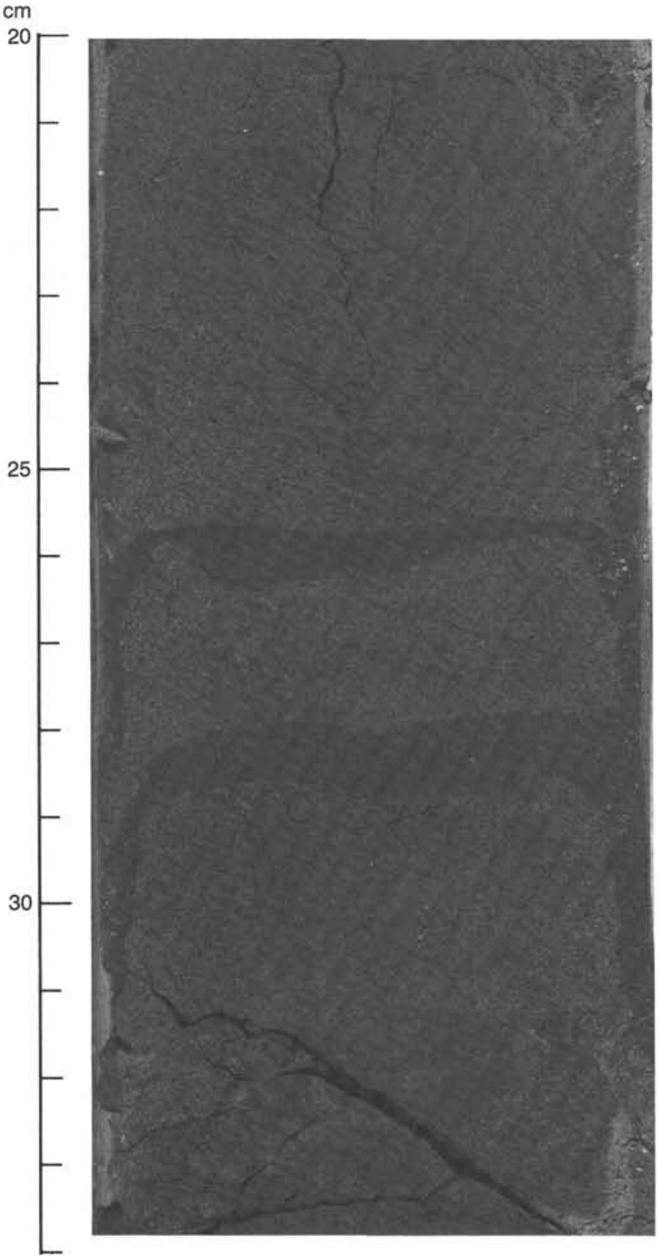

Figure 10. Anastomosing networks of crosscutting shear fractures that form a 'web structure', Core 110-674A-28X.

gled and low-angled thrust zones are dominant (see Figs. 3 and 14). The tectonic unit boundaries correspond to low-angle faults.

2. Separation by major out-of-sequence thrusts (see Boyer and Elliott, 1982) across which either stratigraphic section is missing or in which a wide variety of disparate formations are present as tectonic slivers.

3. Large changes in physical properties such as porosity and bulk density (see Figs. 3 and 14).

4. Division of the accreted sequence into regions in which bedding dips are dominantly steep or shallow. The division boundaries correspond to the tectonic unit boundaries (Fig. 3).

Tectonic unit A corresponds to the upper 100 m of the accretionary complex at this site (Packet 1 + slope sediments). It consists of predominantly shallow-dipping strata except for the slumped slope sequence. The lower boundary to this tectonic unit is thrust 1. The low-angle faults just below thrust 1 may be splays off the main thrust zone. An abrupt downhole decrease in porosity occurs across the shallow-dipping thrust 1 (Fig. 14). The fault zone is very complex and contains thrust slivers of lower and upper Oligocene sediments as well as a possible lower Miocene unit. These are emplaced over upper Pliocene strata,

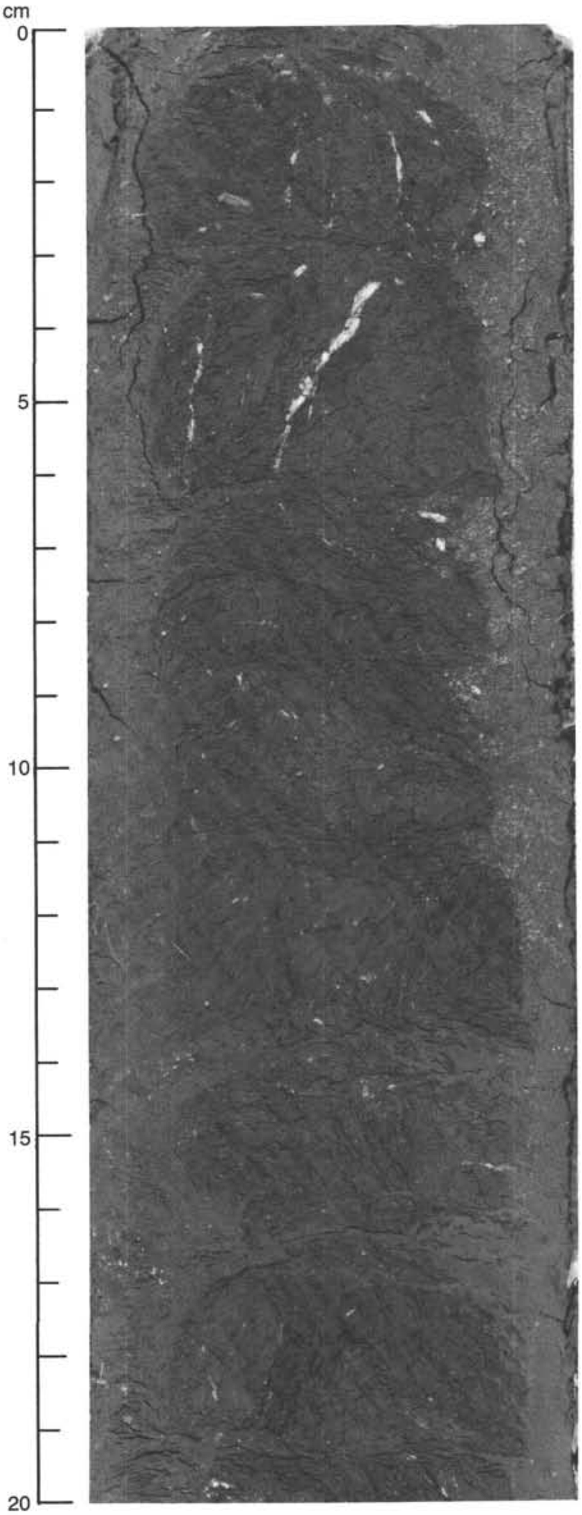

Figure 11. Disrupted calcite veins in scaly clays just below thrust 6, Core 110-674A-37X.

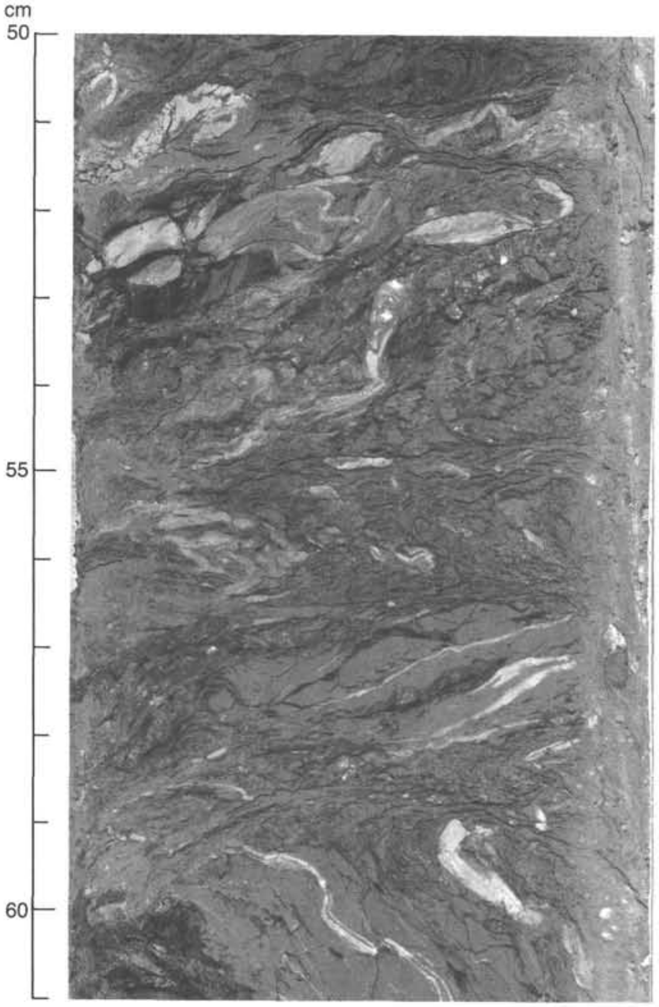

Figure 12. Folded and disrupted calcite veins in the scaly clays toward the base of Packet 7, Core 110-674A-45X.

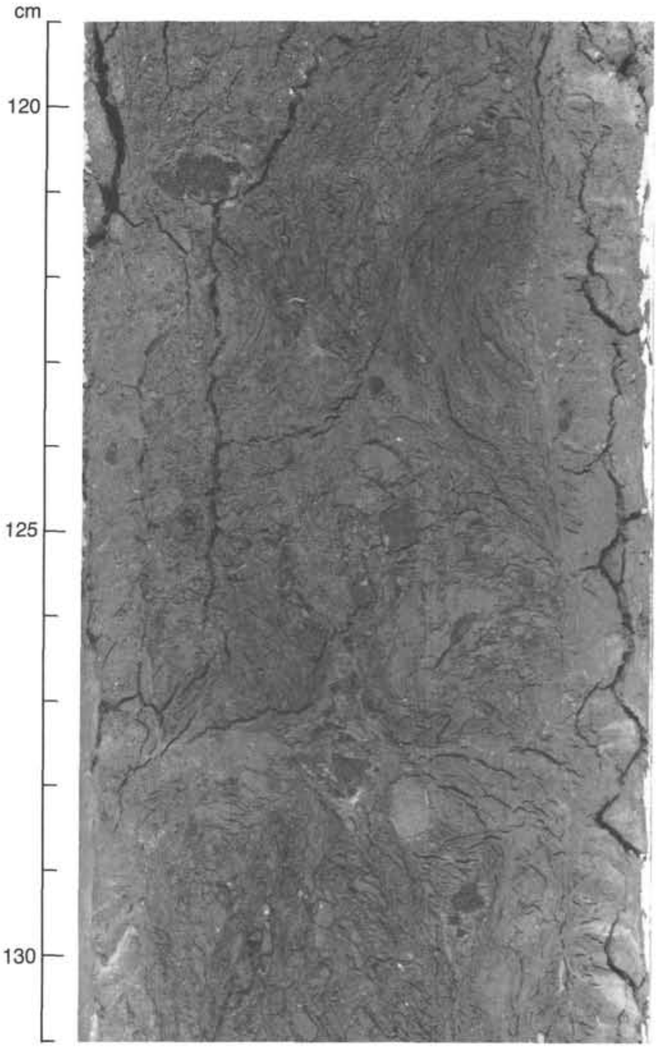

Figure 13. Well-developed zone of stratal disruption. Note phacoidal and subrounded shapes of mudstone fragments in scaly clays. The scaly fabric is dominantly steeply dipping, but is deflected along subhorizontal drilling laminations in Core 110-674A-48X.

resulting in the largest stratigraphic jump across a fault zone so far identified in either ODP Leg 110 and DSDP Leg 78A. The fault places generally older strata over younger.

The complexity of thrust 1 suggests that it is an out-of-sequence structure that has cut through, and incorporated, slices of an accretionary wedge that was already structurally complex. The low-angle splays below thrust 1 that cut through the steeply dipping sequence at the top of Packet 2 may be examples of how these thrust slices formed.

Tectonic Unit B extends from 100 mbsf to approximately 255 mbsf and is made up of Packet 2. Structures and strata in this unit are generally steeply dipping (greater than 60°). The steeply-dipping faults and beds appear to abruptly terminate at a high angle against thrust 1 at the top of this tectonic unit. Thrust 1 is, therefore, thought to postdate these now inactive steeply-dipping thrust faults. The latter were presumably active before back rotation of the strata in this tectonic unit occured. The scaly zones generally dip at angles similar to the bedding, and may represent bedding-parallel thrusts. If the indeterminate age section in this unit is of Miocene age, tectonic unit B represents a disrupted and structurally thickened stratigraphic sequence. The downhole porosity decrease across thrust 1 (Fig. 14) probably results from the greater tectonism of the sequence in tectonic unit B. The basal thrust of tectonic unit B corresponds to the low-angle thrust 2 and surrounding low-angle splays. A large stratigraphic section is missing across thrust 2, with probable lower Miocene strata emplaced directly on much older middle Eocene material. This fault could be interpreted as having a normal displacement across it on purely stratigraphic grounds; however, no normal offsets were seen in any part of the section at Site 674. Furthermore, the intensity and form of the fabrics in the fault zone were identical to these associated with thrust faults. This interpretation requires thrust 2 to have cut through an already structurally complex sequence so that it most probably represents an out-of-sequence structure. There is a sharp decrease in porosity downhole across the thrust as a result of emplacing a younger (and originally shallower) section onto a much older and more consolidated section.

Tectonic units C and C′ extend from 255–454 mbsf. Internally, they are the structurally most complex of the tectonic units, being made up of at least five packets (Packets 3–7). Bedding dips are variable in these units, but are predominantly below 40° to 50°. The thrust faults that separate the packets dip between 40° to 70°. As with the steeply-dipping thrusts in tectonic unit B, they are probably not active at the present time. The thrust faults may have been originally lower angle, flat and ramp structures that have been rotated to steep orientations during imbrication or by folding. The basal thrust to tectonic unit C

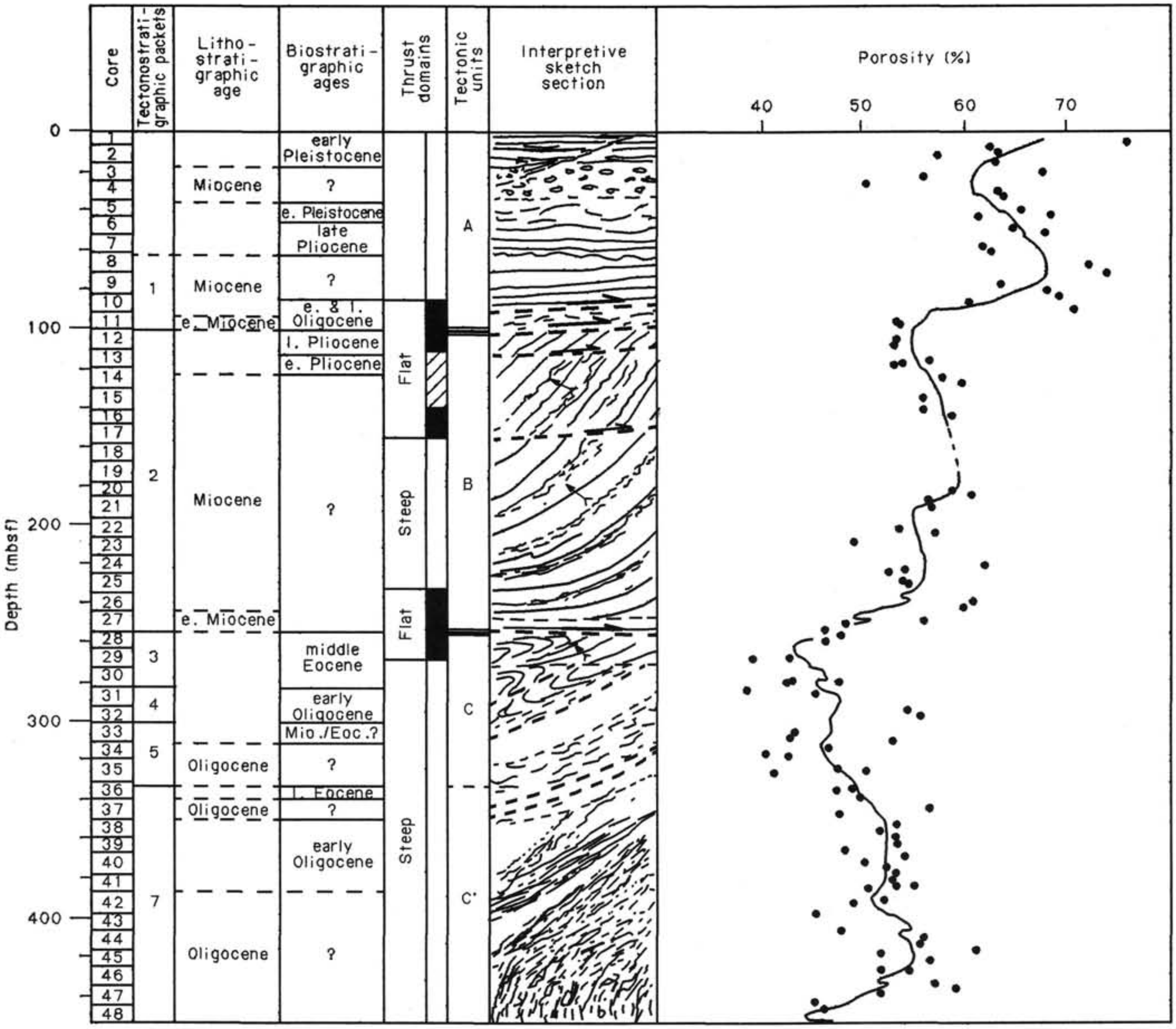

Figure 14. Sketch section and downhole porosity profile illustrating general relationships of the tectonic Units A, B, and C to the main features of the complex seen in cores from Site 674.

is not seen. An individual out-of-sequence thrust, across which some lithologic section is missing (thrust 5), occurs at 330 mbsf and dips between 30° and 50°. This thrust has not been made a major tectonic unit boundary because it is steeply dipping and is probably not currently active; however, it has been used to separate this tectonic unit into the C and C′ subunits as it may have been a former tectonic unit boundary.

The thrust faults (thrusts 1 and 2) that form the boundaries to tectonic units A, B, and C, show large changes in acoustic impedance across them (see Seismic Stratigraphy and Physical Properties sections). The faults also occur at depths in the accretionary complex at which low-angle reflectors in the seismic sections are interpreted to intersect Hole 674A. It is therefore possible that such reflectors correspond to out-of-sequence low-angle thrusts that are currently redeforming and thickening this region of the accretionary complex.

Summary

In summary, the following are the most important features of Site 674:

1. Out-of-sequence thrusts subdivide the accretionary complex into three large tectonic units (tectonic units A, B, and C) that are thought to have developed during the continued thickening of the accretionary complex after the initial period of frontal accretion.
2. The tectonic units are relatively internally homogeneous regarding stratal and structural dips, but these dips are strongly discordant with respect to adjacent units.
3. Physical properties change rapidly across the tectonic unit boundaries.
4. The tectonic unit-bounding thrust faults appear to correspond to low-angle landward-dipping reflectors in the seismic reflection profiles.
5. A series of small overturned-to-recumbent folds have been identified within the complex.
6. Intense scaly fabrics and zones of stratal disruption occur within thrust zones. The overall proportion of the complex that is composed of scaly mudstones increases downhole until it is well above 50%. The intensity of the fabric development also increases downhole.

7. The calcite veining shows a close spatial relationship to the scaly fabrics. Veins have been folded and disrupted in places. The presence of veins indicates that fluids are using the scaly clay zones as migration pathways. The veining appears to be more commonly associated with the steeply-dipping scaly zones than with the low-angle out-of-sequence thrusts.

LITHOSTRATIGRAPHY

Introduction

The lithostratigraphy at Site 674 is complicated by intense tectonic deformation, including initial offscraping at the leading edge of the accretionary complex and continued deformation and shortening throughout the complex (see Structural Geology section). We have divided the cored section at Site 674 into thirteen units based on lithology and sediment age (Table 2, Fig. 15); many boundaries coincide with tectonic contacts.

Sediment Lithology: Description

Unit 1 (0–8.7 mbsf)

The unit consists of interbedded brown to gray calcareous mud and marl, thin ash beds, and thick carbonate-free claystone breccia (Fig. 16). Both carbonate-free and slightly calcareous breccia matrices occur. The foraminifera and nannofossils in the calcareous muds and marls are of early Pleistocene age. The age of the breccia clasts is unknown.

Unit 2 (8.7–40.1 mbsf)

This unit contains carbonate-free, matrix-supported claystone breccias with olive claystone clasts and clay matrix, but here

Table 2. Site 674 lithologic units.

Unit	Lithology	Core range (core-section cm level) 110-674A-	Depth (mbsf)	Age
1	Brown to gray calcareous mud and marl, ash layers and thick carbonate-free clay breccia; $CaCO_3$ up to 45%	1H-1 to 2H-2, 110	0–8.7	early Pleistocene
2	Green to olive carbonate-free breccia with clay matrix and claystone pebbles; interbedded clay with a few ash layers;	2H-2, 110 to 5X-4, 93	8.7–40.1	indeterminate
3	Brown to gray calcareous mud, marl, with ash layers; $CaCO_3$: 20 to 45%	5X-4, 93 to 7X-CC	40.1–63.1	early Pleistocene to late Pliocene
4	Green to olive carbonate-free claystone and mud-stone, with a few ash layers	8X-1 to 10X-CC, 40	63.1–91.5	indeterminate
5	Brownish green to reddish, radiolarian-bearing, siliceous to slightly siliceous, mudstone and claystones	10X-CC, 40 to 11X-CC	91.5–101.1	early Oligocene to late Oligocene
6	Gray, calcareous to slightly calcareous mudstones and claystones, with a few ash layers; $CaCO_3$ decreases from 25% to 1%	12X-1 to 13X-CC	101.1–120.1	late Pliocene to early Pliocene
7	Olive to yellowish brown carbonate-free claystone with dispersed ashy fraction; thin breccia layers in Cores 17 and 24	13X-CC to 28X-2, 70	120.1–255.3	indeterminate
8	White to green chalk, limestone, calcareous mudstone (often silky), and carbonate-free claystone; interbedded glauconite quartz sandstone; $CaCO_3$ from 0 to 70%	28X-2, 70 to 31X-CC	255.3–291.1	middle Eocene
9	Yellowish brown, radiolarian-, spicule-, diatom-bearing siliceous claystone and mudstone	32X-1 to 32X-CC	291.1–300.6	early Oligocene
10	Dark olive claystone, with laminated, slightly calcareous mudstone, one recrystallyzed limestone layer; $CaCO_3$ up to 1%	33X-1 to 34X-CC	300.6–319.6	early Miocene? and indeterminate
11	Varicolored (olive, brown, reddish), locally ashy, mudstone and claystone, with a few radiolarian-, spicule-, diatom-bearing siliceous intervals and one silt layer	35X-1 to 36X-CC	319.6–338.6	late Eocene
12	Green to brown, radiolarian-bearing, siliceous claystone and mudstone, with local ashy fraction and one silt layer	37X-1 to 43X-CC	338.6–405.1	early Oligocene
13	Varicolored (olive, reddish, brown) claystone and mudstone with ashy fraction and a few ash layers; one recrystallized limestone layer in Core 48	44X-1 to 48X-CC	405.1–452.6	indeterminate

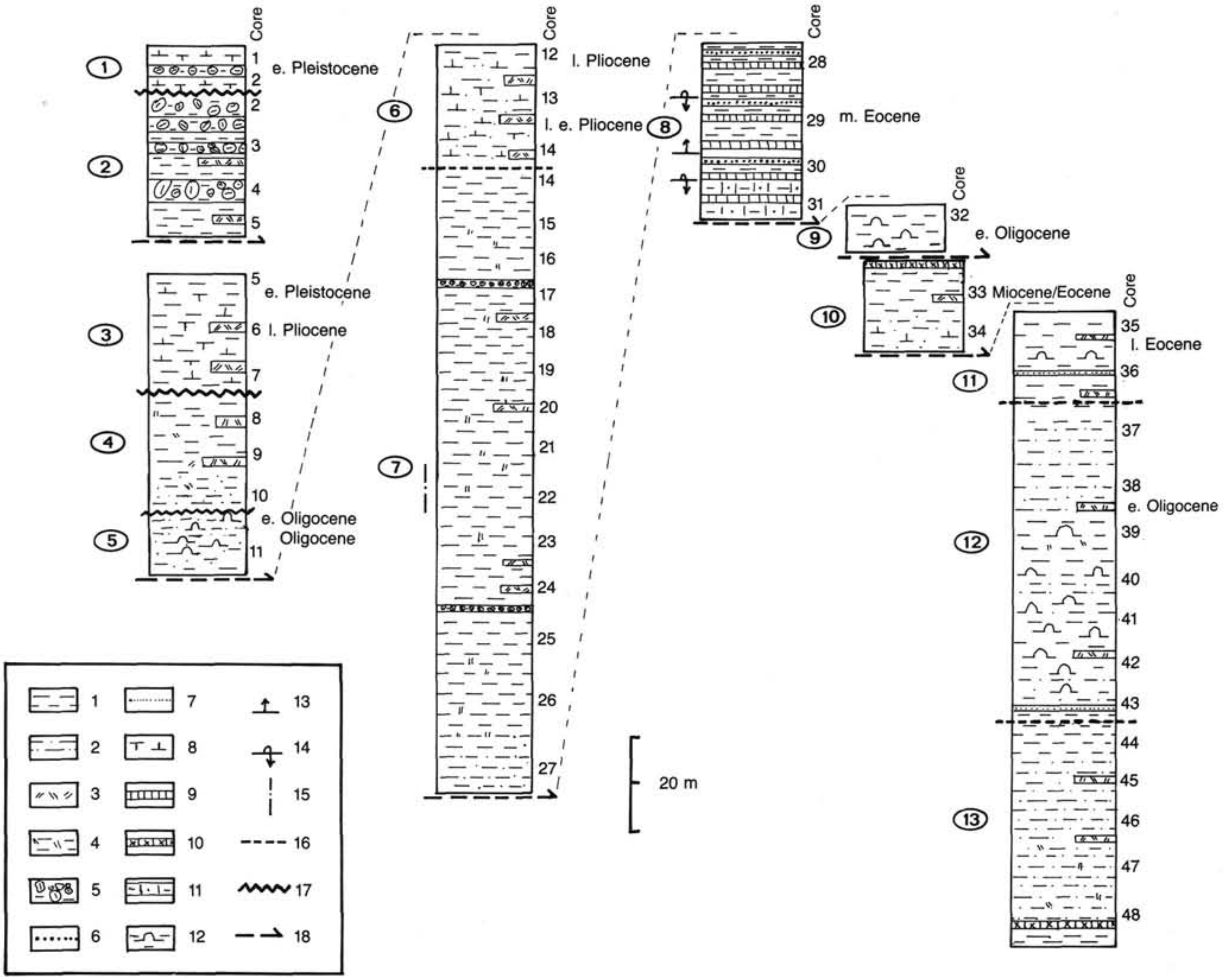

Figure 15. Lithologic units and inferred relationships. Explanation: 1. clay(-stone); 2. mud(-stone); 3. volcanic ash; 4. ash-rich mud(-stone); 5. claystone breccia; 6. sand(-stone); 7. silt(-stone); 8. calcareous mud(-stone); 9. chalk, limestone; 10. recrystallized limestone; 11. silty chalk, silty marl; 12. siliceous clay(-stone) or mud(-stone); 13. upright bedding; 14. overturned bedding; 15. subvertical bedding; 16. stratigraphic gradational contact; 17. unconformity, nonconformity, or hiatus; 18. thrust fault. (Numbers in ovals correspond to lithologic units of Table 2).

they are interbedded with green to olive claystone of indeterminate age. Clasts contain deformation-related features such as vein structures (Fig. 17). Ash occurs interbedded with breccia and claystone intervals.

Unit 3 (40.1–63.1 mbsf)

Brown to gray foraminifera/nannofossil calcareous claystone and mudstone plus marl make up the unit. Ash beds also occur. Although lithologically similar to Unit 1, Unit 3 ranges in age from early Pleistocene to late Pliocene.

Unit 4 (63.1–91.5 mbsf)

The unit consists of homogeneous, carbonate-free olive to greenish gray claystone and mudstone with ash-rich intervals. This unit is barren of microfossils. Because the main distinction between Units 3 and 4 is the absence of carbonate in Unit 4, and because carbonate may disappear gradually down-section, Unit 4 may rest conformably below Unit 3.

Unit 5 (91.5–101.1 mbsf, including the bottom 1 cm of Core 110-674A-10X)

Although no strong lithologic distinction exists between Units 4 and 5, this unit has a distinctly scaly, highly deformed fault zone (see Structural Geology section). In contrast, Unit 4 is only very mildly deformed. Unit 5 is made up of reddish brown and orange brown, slightly siliceous mudstone that is age-dated as early and late Oligocene. Biostratigraphy reveals that these ages appear in reverse stratigraphic sequence, either as a result of overturned folding or of thrust repetition.

Unit 6 (101.1–120.1 mbsf)

The unit includes gray and brownish gray calcareous to slightly calcareous claystone and mudstone with interbedded ash layers. Nannofossils were used to age-date this unit as early to late Pliocene.

Unit 7 (120.1–255.3 mbsf)

The absence of carbonate distinguishes Unit 7 from the overlying unit. Unit 7 consists of olive to yellowish brown mudstone and claystone with minor disseminated ash and stratally disrupted ash beds (Fig. 18). Thin pebble conglomerate beds occur in Cores 110-674A-17X and -24X (Fig. 19). In one interval (Sample 110-674A-17X-2, 8–28 cm), possible small syn-sedimentary dikes and sills are preserved in laminated mudstone (Fig. 20). Bedding dips of laminated mudstone locally approach vertical (Fig. 21). One Oligocene radiolarian age date occurs at the base

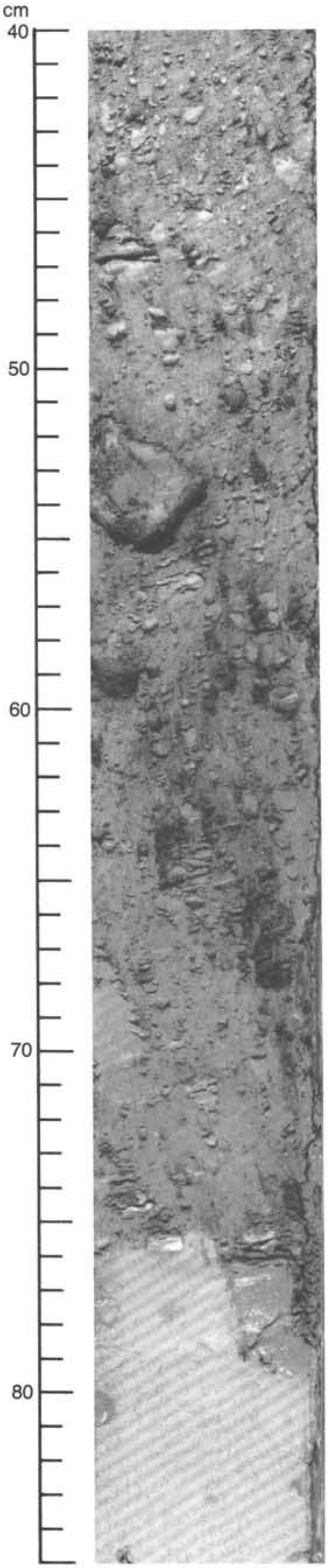

Figure 16. Matrix-supported claystone breccia overlying marl in Unit 1. These beds are interpreted as slope deposits (debris flows?).

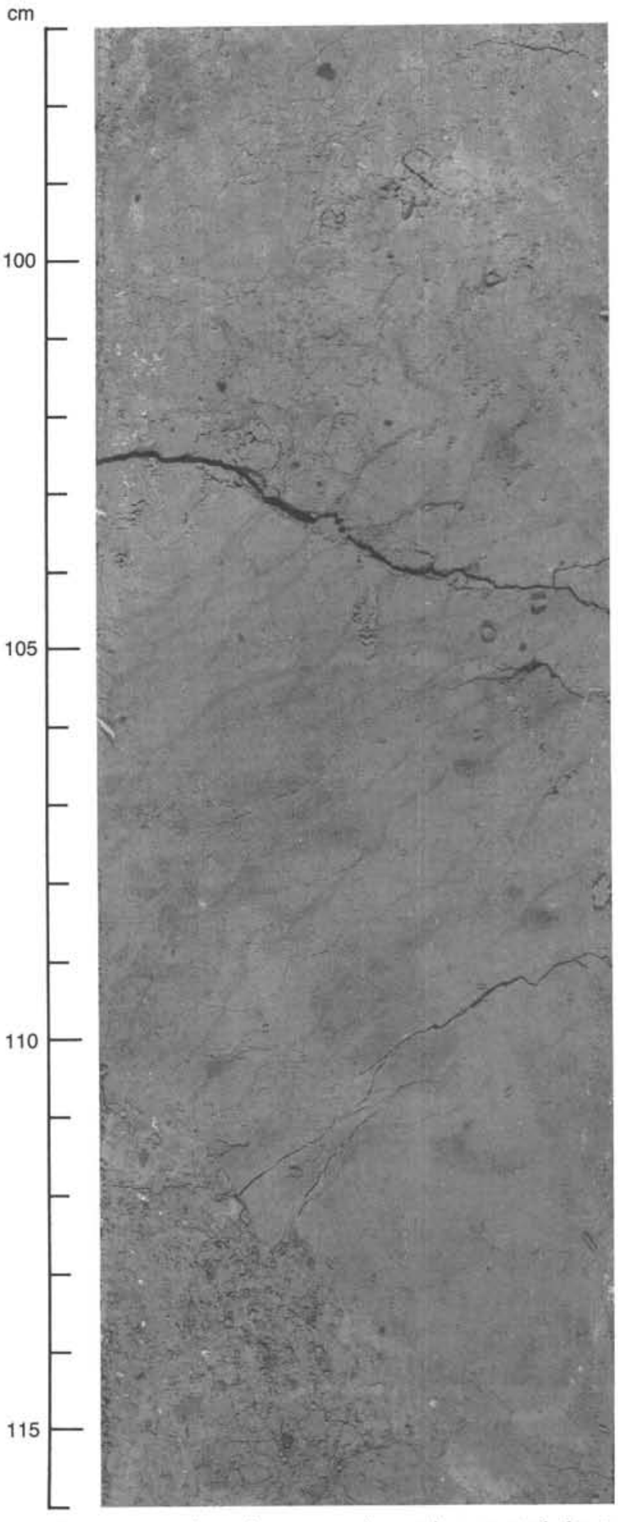

Figure 17. Anastomosing vein structure in matrix-supported claystone breccia. Age of deformation is uncertain.

of this unit (see Biostratigraphy section), but the sample comes from a fault zone. Therefore Unit 7 remains largely undated.

Unit 8 (255.3–291.1 mbsf)

This unit consists of distinctive middle Eocene lithologies equivalent to those described at Site 672 (see Site 672 chapter). At Site 674 this interval is composed of interbedded white to

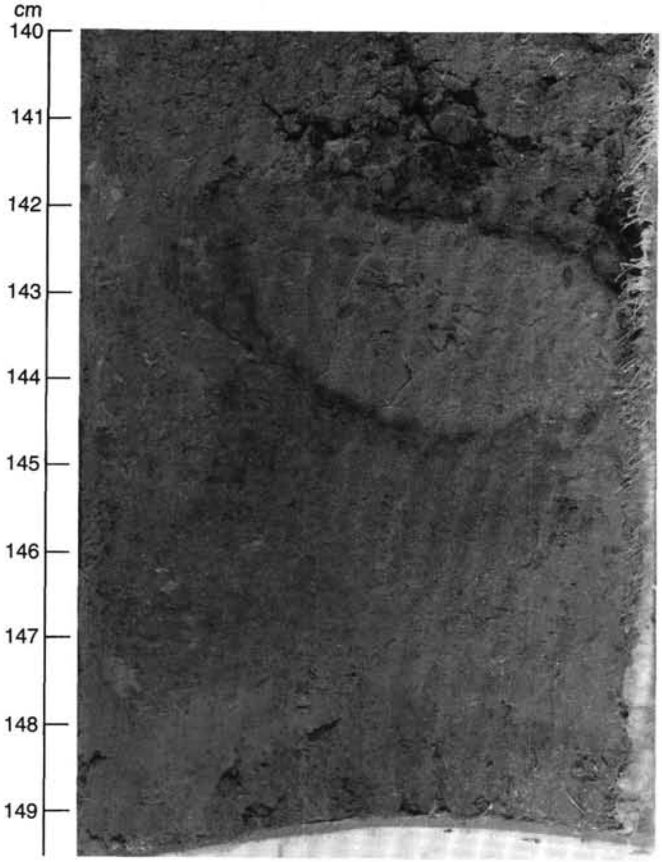

Figure 18. Stratally disrupted ash strata rimmed by alteration halo. This relationship clearly demonstrates that stratal disruption in this example precedes drilling.

green chalk, limestone (often silty with rounded quartz grains), calcareous mudstone, claystone, and glauconitic quartz sandstone. Preserved bedding-top indicators demonstrate local overturned bedding (Fig. 22). The middle Eocene age is based on nannofossil, foraminifera, and radiolarian age determinations.

Unit 9 (291.1–300.6 mbsf)

The unit consists of yellowish brown siliceous claystone and siliceous mudstone. Radiolaria indicate that this sequence is early Oligocene in age.

Unit 10 (300.6–319.6 mbsf).

Dark-olive claystone of indeterminate age makes up most of the unit. However, rare, laminated, slightly calcareous mudstone beds in the upper part of the unit provide a possible middle Miocene age. The top of the unit contains a thin bed of fine-grained, recrystallized chalk.

Unit 11 (319.6–338.6 mbsf)

This unit includes multicolored olive, brown, and dark brown mudstone and claystone with local disseminated ash. Minor siliceous intervals containing radiolaria, diatoms, and sponge spicules indicate that this sequence is late Eocene in age. A single 3 cm-thick silty mudstone layer also occurs at Section 110-674A-36X-4, 31 cm.

Unit 12 (338.6–405.1 mbsf)

Green to brown siliceous (radiolaria, diatoms, and sponge spicules) to slightly siliceous claystone and mudstone make up the unit. Minor ash-rich(?) beds are important features of this early Oligocene unit because ash was absent from the reference Oligocene section (Site 672), but present in Leg 78A's reference site (Site 543). Ash intervals found further downsection are interbedded with undated mudstone. Radiolaria in siliceous intervals in the upper part (338.6–386.1 mbsf) age-date Unit 12 as early Oligocene. A single silt layer occurs at the base of the section.

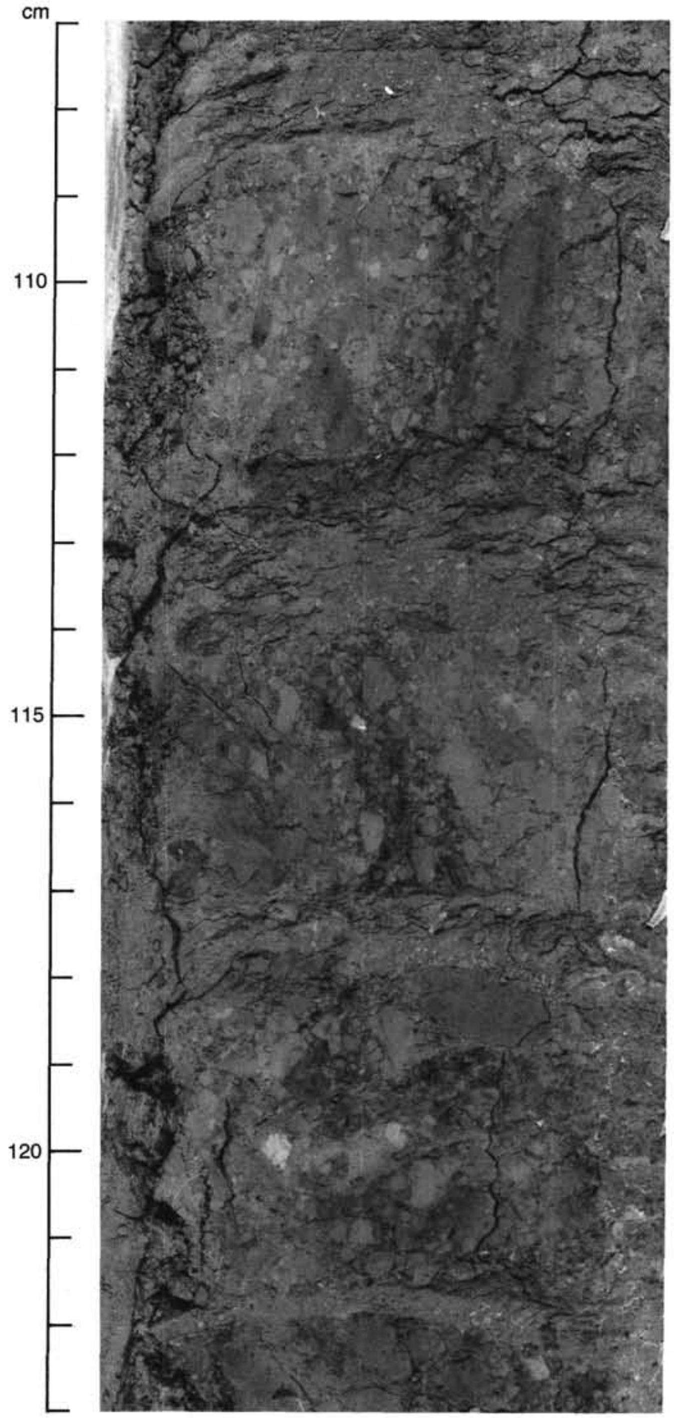

Figure 19. Clast-supported pebble conglomerate beds in undated (Miocene?) claystone of Unit 7. Beds appear crudely graded.

Unit 13 (405.1–452.6 mbsf)

This unit consists of multicolored olive, greenish gray, gray, and brown claystone and mudstone. Ash occurs in this unit both

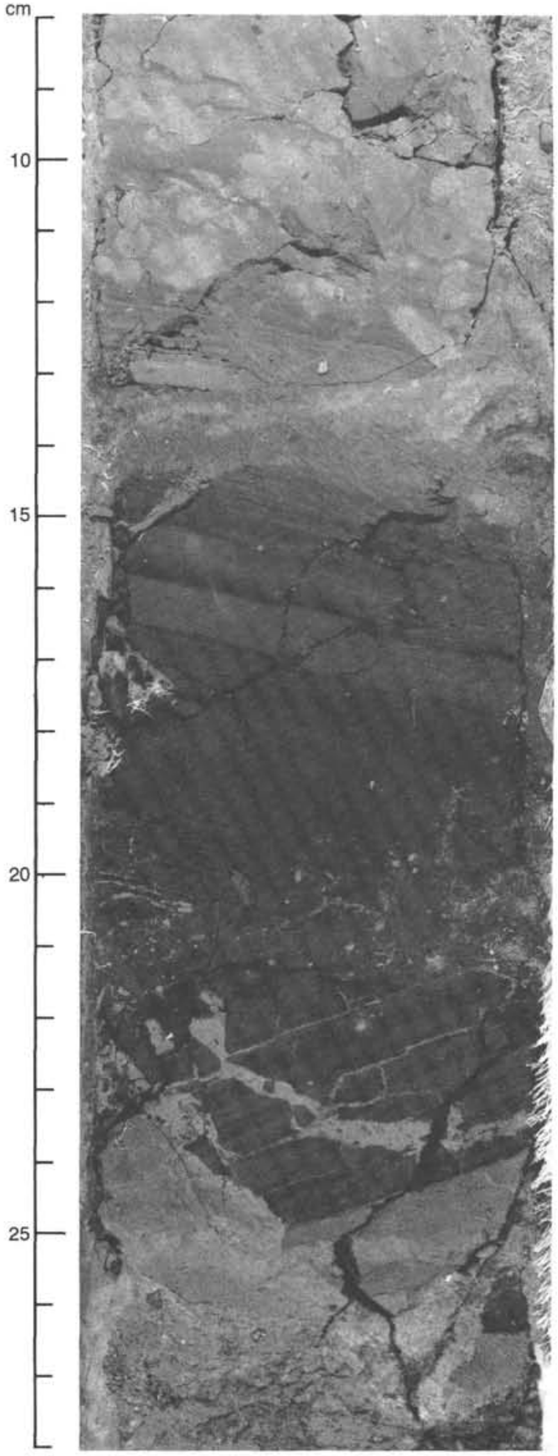

Figure 20. Clastic dikes and sills in semiconsolidated, laminated mudstone. Top of interval between 10 and 15 cm is gradational into strongly bioturbated hemipelagic mudstone. Low-angle striations in 13–15 cm interval are saw-blade marks.

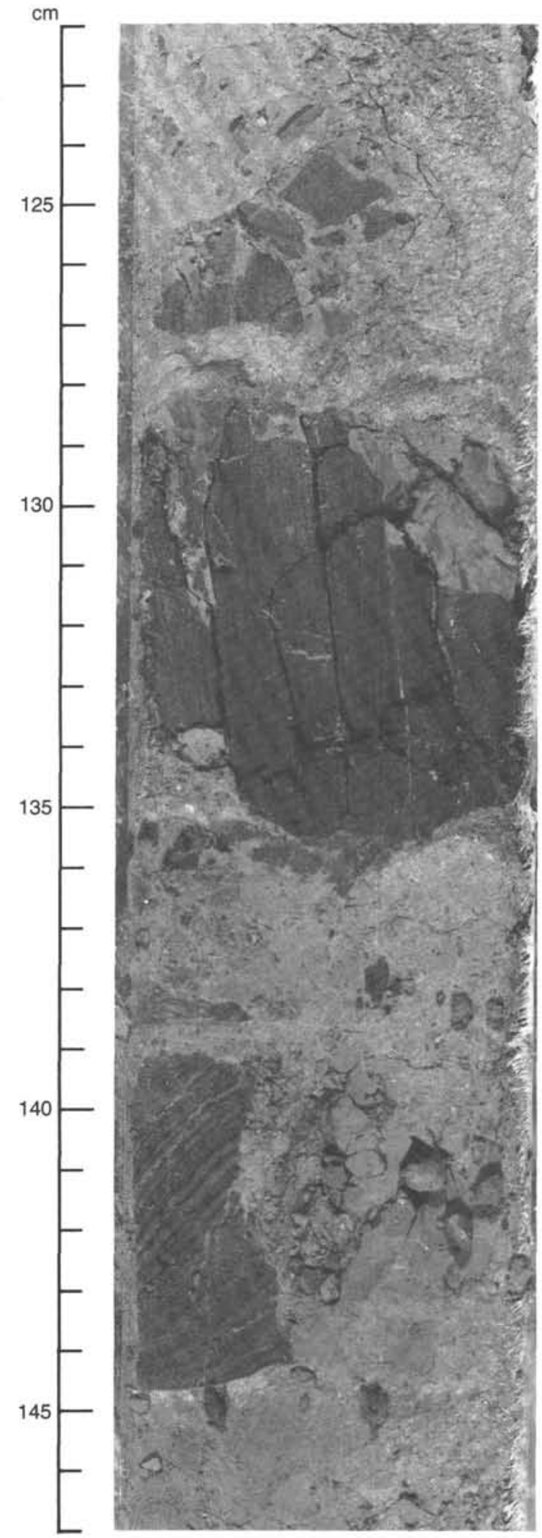

Figure 21. Steeply dipping, finely laminated mudstone in Unit 7.

as discrete beds (Figure 23) and disseminated through the sediment. A solitary thin, recrystallized limestone bed (Sample 110-674A-48X-6, 75–105 cm) yielded no biostratigraphic information.

Lithostratigraphic Age Estimates of Undated Intervals

The lack of biostratigraphic control at Site 674 has led us to attempt to correlate the barren intervals at this site with age-dated lithologies at the reference Site 672; important trends are further confirmed by comparison with Site 671. At Site 674, two main intervals are barren of microfossils, coinciding with Units 7 and 13. Additionally, four minor intervals remain undated, including parts of Units 2, 4, 10, 11, and 12.

Ash Stratigraphy

The graphic ash log (Fig. 24) results from analysis of visual core descriptions and smear-slide descriptions. Although this

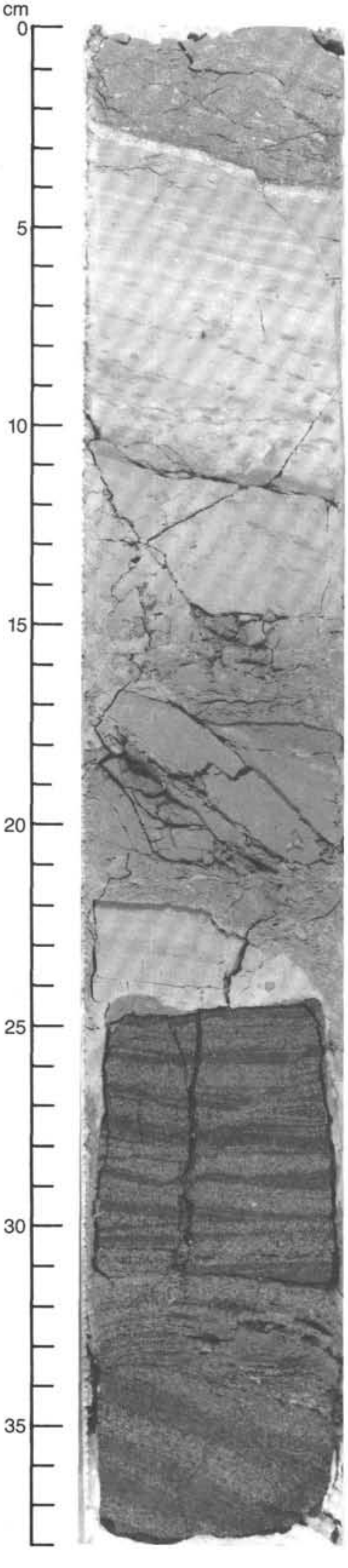

Figure 22. Overturned bedding in Unit 8. The bed located between 2 and 15 cm has a sharp base and a gradational top (11-15 cm) into claystone. Additionally, the finely laminated bed between 22 and 25 cm has a sharp base but is subsequently truncated by cross-laminated mudstone (25-38 cm).

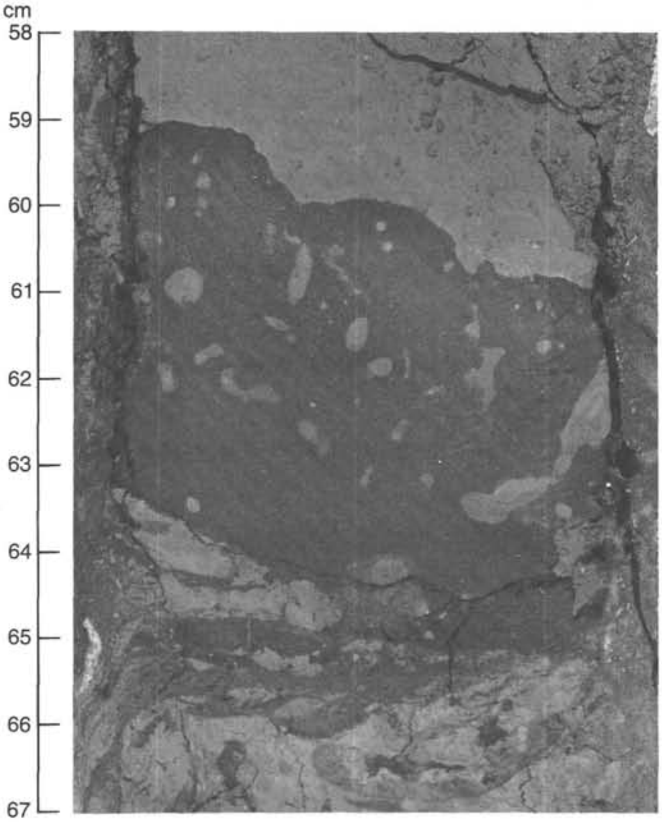

Figure 23. Bioturbated ash bed in lowermost undated (Oligocene?) sequence of Site 674 (Unit 13).

analysis strives to present the position and abundance of ash through the stratigraphic column, several uncertainties persist. Bedding dips at Site 674 were rare (see Structural Geology section), so true thicknesses of ash intervals are unknown. Furthermore, in the uppermost 40 m of section at this site, ash occurs in slump and breccia blocks as well as in the matrix of conglomerates, breccias, and hemipelagic deposits; some ash beds occur in older blocks surrounded by younger deposits.

Further complicating our estimate of ash abundance is diagenesis, which has locally strongly altered ash beds; XRD analyses may be able to confirm tentative ash occurrences. Structural disruption may also have dispersed ash, causing ash abundances to be underestimated. For example, in Fig. 18 an ash layer has been disrupted before diagenetic alteration at its margins. A further example occurs nearby where small fragments of ash were observed smeared out along scaly surfaces.

Proposed Age Criteria

Three aspects of the sediments cored at Site 672 and DSDP Leg 78A, Site 543, appear to be useful for lithologic correlation with the sediments cored at Site 674 (Fig. 24). First, essentially no volcanic ash is found below the Miocene/Oligocene boundary at the reference Site 672 but is present in the Oligocene section at Site 543. Second, the Miocene section at Sites 672 and 543 are almost completely devoid of carbonate material. Third, XRD bulk mineralogy data show a clear distinction between the plagioclase/clay ratio in the Miocene and Oligocene/Eocene sections at Site 672 (Site 674, Table 3). Volcanic ash occurrence, carbonate content, and bulk mineralogy information provide constraints on the age of undated sections.

The two main barren zones (Unit 7 and Unit 13) at Site 674 contain significant ash (Fig. 24). Furthermore, both sections are nearly devoid of carbonate. However, the bulk mineralogy of

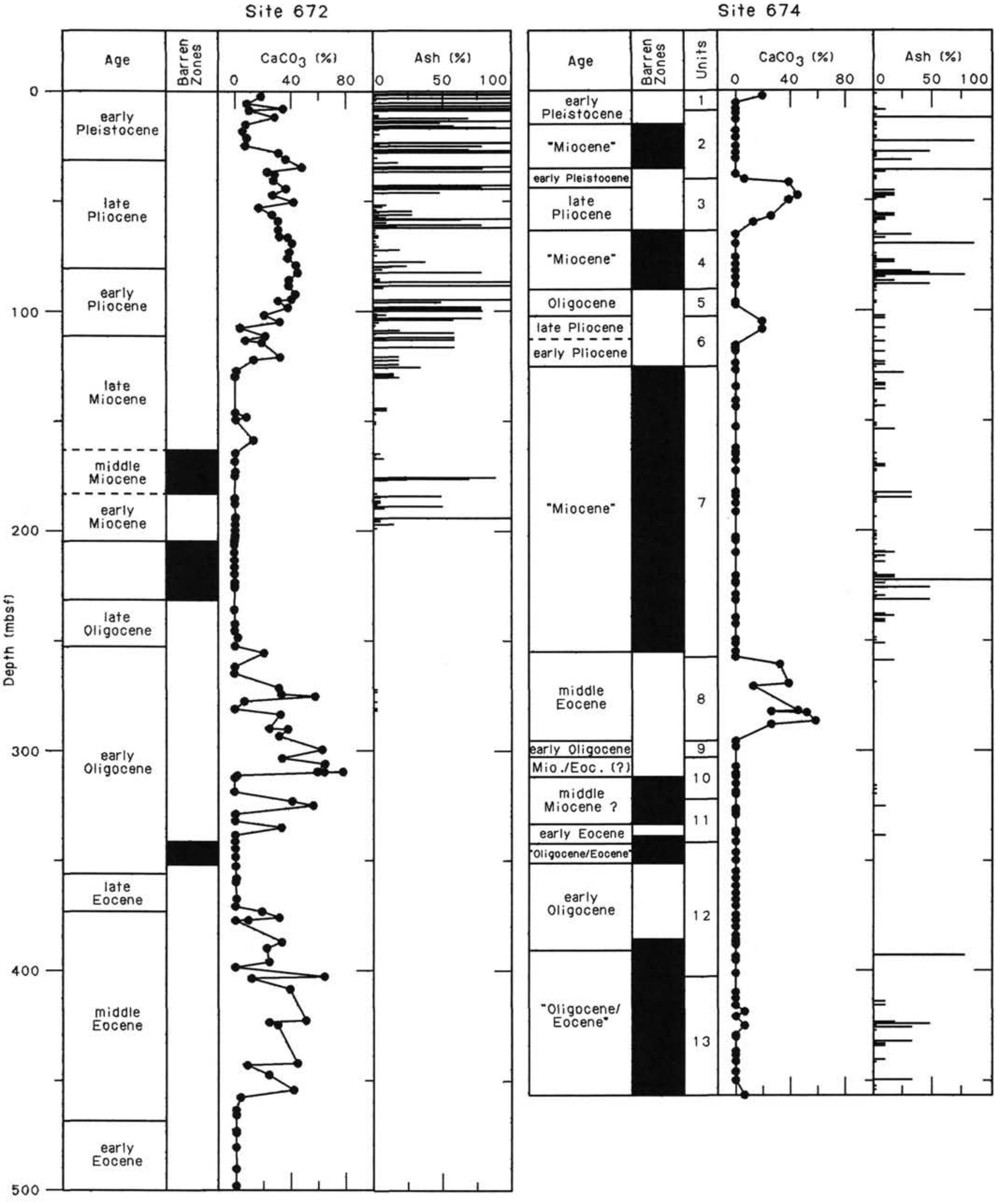

Figure 24. Comparative graphic ash log and carbonate content log for Sites 672 and 674. Note that ash is absent at Site 672 below the Miocene and that the Miocene section is essentially carbonate-free. At Site 674 undated intervals generally contain significant ash and no carbonate, suggesting a correlation with the reference site Miocene section, although bulk mineralogy data suggest that the undated sections in Unit 10 and below may be Oligocene/Eocene in age. (Additional correlation criteria are discussed in the text.)

the upper zone more closely matches the Miocene section at Site 672, whereas the mineralogy of the lower zone is closer to the Oligocene/Eocene section (Site 674, Table 3). Based on these three observations and supporting evidence, such as sediment color and composition (determined by smear-slide examination), we suggest that the upper section (Unit 7) is Miocene in age and the lower section (Unit 13) is Oligocene/Eocene in age. In addition, the absence of siliceous beds and the minor facies of Unit 13, including a limestone bed and a silty mudstone bed, further supports an Oligocene/Eocene age. Of the four minor barren zones, we suggest the barren sections in Units 2 and 4 may be Miocene in age while the barren sections in Units 10, 11, and 12 may be Oligocene/Eocene in age, based primarily on bulk mineralogy data.

The age of Unit 10 presents an interesting problem. Sparse nannofossils in the upper part of the unit indicate a Miocene age, whereas bulk mineralogy correlations suggest an Oligocene/Eocene age for the entire unit. Either the nannofossil samples in Unit 10 were derived from some higher level in the drill hole and therefore represent a contaminated sample, or the bulk mineralogy comparisons are imprecise, or both ages are correct and Unit 10 represents a tectonically interleaved sequence. Resolution of this problem depends on either further biostratigraphic age dates or rejection of our correlation criteria.

Discussion

Our lithologic age correlations are based partly on the fundamental assumption that ash occurrence and carbonate content are areally continuous and correlatable features. This assumption may be untrue. First, there is a marked difference in the Oligocene/Eocene facies at Sites 672 and 674. Because many carbonate beds deposited in the Oligocene section at Site 672 may have been derived from the nearby Tiburon Rise, carbonate content may be misleading. Secondly, essentially no ash occurs in the Oligocene and Eocene sections at Site 672. However, ash may be present in Oligocene and Eocene sections at Site 674, albeit in small quantities. Core 110-674A-11X (91.6–101.1 mbsf), dated as Oligocene, contains ash, but intense deformation of this interval may have caused interleaving of thin fault slices of exotic lithologies (see Structural Geology section). Cores 110-674A-28X and -29X (254.8–265.4 mbsf) are clearly dated as middle Eocene and contain possible ash beds. The presence of ash is based on the interpretation of low relief, low birefringence grains in smear slides as volcanic glass, but these grains may also be zeolites. Further XRD and coarse-fraction analyses may resolve this problem. Lastly, ash may be present in Core 110-674A-26X (334.0–334.1 mbsf) in Eocene rocks. If the Eocene and Oligocene sections at Site 674 contain ash because they were closer to the Antilles volcanic arc than Site 672, then lithologic correlations based on ash occurrence are weakened.

Table 3. Ratios of plagioclase to total clay content (×100) for sediments of Sites 672 and 674. The means, minima, and maxima of the ratios for each sediment unit are given. For Site 672, the sediment units are based on biostratigraphically determined ages, with the exception of the barren unit between the late and early Miocene age units, which is assumed to be the middle Miocene. For Site 674, the units are all barren and are identified by depth.

Site 672				
	Plagioclase/Clay ratio × 100			
Age	Mean	Minimum	Maximum	No. of Samples
l. Miocene	10.74	2.59	51.45	17
m. Miocene (barren)	37.37	4.56	96.58	6
e. Miocene	9.20	0	38.41	16
l. Oligocene	1.47	0	4.25	21
e. Oligocene	1.54	0	8.25	29
e. Oligocene/l. Eocene (barren)	3.34	0	10.72	9
l. Eocene	3.87	0	10.93	10
m. Eocene	2.01	0	26.04	31
e. Eocene	1.58	0	7.91	5
Site 674				
Depth (mbsf)				
15.6–34.6	34.89	9.23	49.86	4
63.1–82.1	23.83	20.24	28.49	4
120.1–253.1	26.57	6.33	60.54	24
310.1–329.1	4.02	3.08	5.05	3
338.6–348.1	4.80	2.66	7.70	3
376.6–452.6	4.16	0.31	10.29	21

Depositional Processes and Discussion

Because of the structural complexities at Site 674, precise facies analysis is difficult. In this discussion only deviations from the patterns observed at Sites 671 and 672 will be treated fully.

Slope Deposits

Units 1, 3, and 6 are interpreted to have been deposited on the slope of the accretionary complex. Two types of sediments make up this facies: a) Homogeneous hemipelagic calcareous muds and marls with a significant biogenic component, and b) Redeposited claystone breccias and slump and slide blocks. Depositional patterns are interpreted to have been similar to those described at the top of Hole 673B. However, at Site 674 only Unit 1 represents an unambiguous, age-dated slope deposit because it contains thick breccia deposits. Units 3 and 6 contain no breccias and may have been deposited as hemipelagic deposits on the abyssal plain. Therefore slope deposits may be as young as early Pleistocene or as old as early Pliocene.

Units 2 and 4 may also be interpreted as slope deposits. Unit 2 clearly contains slope deposits, using the criterion of breccia beds, but the age of the breccia matrix remains unknown. However, the lowest claystone interval in Unit 2 may represent abyssal deposits. Unit 4 is a carbonate-free, homogeneous, clay-rich sequence, possibly Miocene(?) in age. If this age is correct, then the contact between Units 3 and 4 may be conformable. No tectonic break is observable between these two units. The marked lack of deformation in both units argues for deposition on the slope (see Structural Geology section), as well as for the relatively high porosities measured in Unit 4 (see Physical Properties). If these two units are slope deposits, and if our tentative lithologic age correlation is correct, then slope deposits first formed in the Miocene at this site.

Abyssal Hemipelagic Deposits

All other units are interpreted as various types of hemipelagic (with the exception of Unit 8) deposits that accumulated on the Atlantic abyssal plain and were subsequently offscraped and incorporated into the Lesser Antilles accretionary complex.

Unit 5 corresponds to a more siliceous hemipelagic deposit; however, most sedimentary features have been obliterated by intense deformation. An Oligocene age for this unit indicates a significant tectonic contact between Units 4 and 5, either a large unconformity or a fault contact.

Unit 7 is a homogeneous, carbonate-free, clay-rich hemipelagic interval. There appears to be no clear break between this unit and the overlying Pliocene unit (Unit 6). The boundary between the two units was drawn on the basis of the disappearance of carbonate and on a color change from olive to green. This may be a conformable contact if Unit 7 is Miocene in age.

Unit 8 consists of a distinctive sequence of chalk, siltstone, sandstone, and claystone that correlates with the lower Oligocene/upper Eocene to middle Eocene section of Site 672. The quartz-rich detrital component of this unit probably represents an influx of sediment from South America (quartz, glauconite, other heavy minerals; see Site 672 chapter). This unit contains a far greater component of coarse-grained detritus than the other units. A tectonic break, probably a thrust fault, separates Units 7 and 8.

Units 9, 10, 11, 12, and 13 are all homogeneous, clay-rich hemipelagic deposits. The Oligocene and Eocene units contain a greater siliceous component whereas the undated sequence (Unit 13) contains more ash. Diagenesis affects these deposits with common alterations of ash and claystone; claystone is altered mostly along fractures. Contacts between all of these units are interpreted as faults.

Relationships between age and depth (Fig.25) are completely obscured by intense tectonic deformation and by the lack of biostratigraphic resolution. Continuous age-depth gradients appear only in Units 3 and 6.

Bulk Mineralogy

Ninety-six samples from Site 674 were analyzed for bulk mineralogy by the X-ray diffraction methods outlined in Chapter 1. The results are given in Figure 26. The mineralogical trends with depth at Site 674 reflect the tectonic interleaving of lithologic units similar in mineralogy to those described at Site 672 (and other sites of Leg 110).

The upper 120.1 m of section at Site 674 (lithologic Units 1-6) are characterized by clay mineral contents that vary widely between 30% and 90%. From 120.1 to 255.3 mbsf (Unit 7) the percentage of total clay minerals varies from about 60% to 90%. The middle Eocene sediments of Unit 8 (255.3-291.1 mbsf) have variable, but generally lower, clay contents compared to other sediments sampled at Site 674. Units 9 to 13 (291.1-452.6 mbsf) all have relatively high percentages of total clay minerals ranging from 60% to 90%.

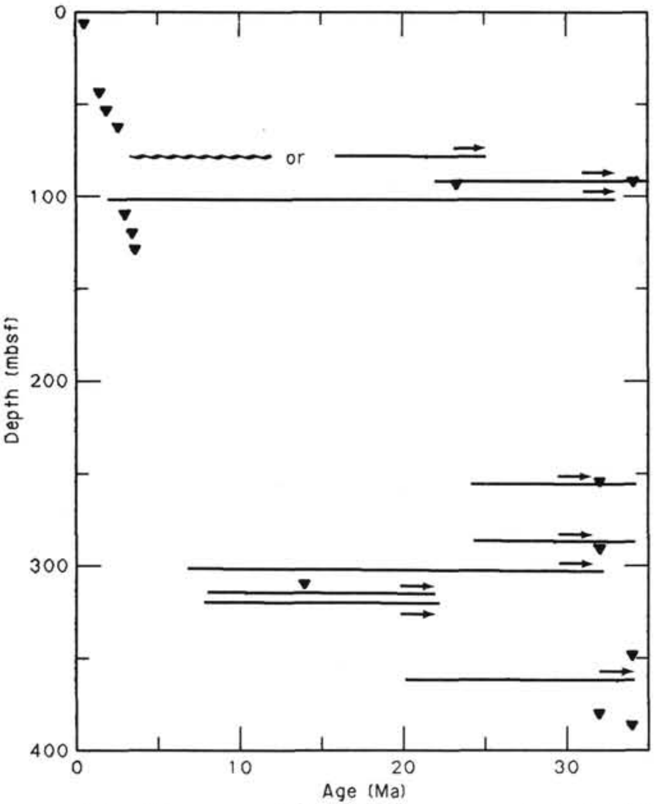

Figure 25. Plot of age vs. depth for Site 674. Lack of trends clearly reflects the structural complexities at this site.

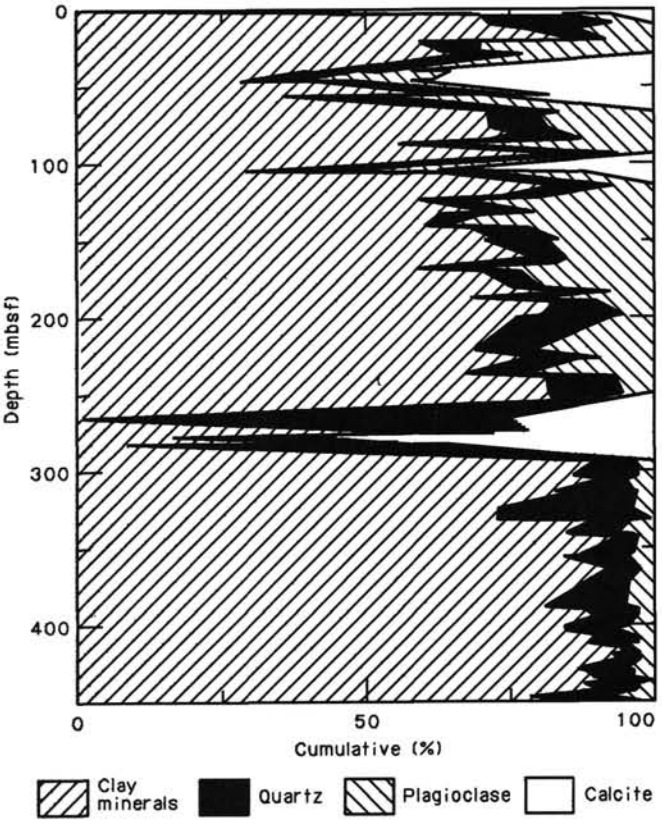

Figure 26. Bulk mineralogy of Site 674. Samples expressed as cumulative percentages of total clay minerals, quartz, plagioclase, and calcite.

Calcareous sediments, mostly marls containing 10% to 45% calcite, are present in Units 1, 3, 6, and 8. The remainder of the sequence at Site 674 is calcite-free. Coulometric analyses of calcium carbonate content are similar to XRD results, and are listed in Table 4 for Hole 674A sediments.

The quartz content of Site 674 sediments generally varies between 0% and 20% and shows no trend with depth. The only exceptions are the Eocene silt and sand-rich sediments of Units 8 and 11 that show high and variable quartz contents (4%-75%).

The sediments between 0 and 255.3 mbsf (Units 1-7) have highly variable plagioclase contents (5%-39%). From 255.3 mbsf to the base of the hole, the fluctuations of percent plagioclase are of much smaller amplitude, and plagioclase contents vary between 0%-8%. As was the case at other sites, the percent of plagioclase reflects the ash content. This bulk analytical technique therefore is useful for age correlations based on lithology (see above). Table 3 shows the plagioclase-to-clay ratios characteristic of various ages of sediments from Site 672 and of the barren intervals from Site 674. As was discussed above, these ratios are useful in determining probable ages of barren sequences.

BIOSTRATIGRAPHY

Biostratigraphic Summary

Figure 27 summarizes Site 674 biostratigraphy. Sediments recovered range in age from early Pleistocene to middle Eocene. Downhole occurrence of dissolution is observed stratigraphically higher at this site than at Sites 671 through 673. This is particularly obvious in foraminifers, which are severely dissolved in sediments as young as late Pliocene.

Table 4. Calcium carbonate, Hole 674A.

Core 110-674A-	Sec.	Int. (cm)	Depth (mbsf)	Carbonate (% dry wt.)
1	2	75	2.25	20.3
1	4	78	5.28	0.7
2	2	63	8.23	0.3
2	4	55	10.05	0.5
2	6	29	12.79	0.3
3	2	81	17.91	1.5
3	5	37	20.78	2.1
3	8	128	24.58	0.3
4	2	123	27.83	0.3
4	4	67	30.27	0.4
5	2	110	37.20	0.9
5	4	32	39.42	9.8
5	5	12	40.72	40.7
6	2	70	46.30	47.2
6	4	31	48.41	43.2
7	2	91	56.01	30.4
7	4	62	58.72	16.3
8	2	15	64.75	0.1
8	4	95	68.55	0.5
9	2	64	74.74	0.5
9	4	76	77.86	0.4
9	6	63	80.73	1.0
10	2	33	83.93	0.3
10	4	60	87.20	0.4
11	3	0	94.60	0.4
11	10	20	95.86	0.3
12	2	92	103.52	24.4
12	4	118	106.78	19.2
13	3	77	114.37	2.75
13	4	73	115.83	1.08
13	5	11	116.71	4.17
14	2	69	122.29	0.50
14	4	65	125.25	0.25
15	3	58	133.18	0.25
16	1	4	139.14	0.42
16	2	131	141.91	0.33
17	2	66	150.76	0.33
18	2	71	160.31	0.58
18	3	107	162.17	0.42
18	4	69	163.29	0.42
18	6	34	165.94	0.33
19	2	111	170.21	0.50
19	3	4	170.64	0.42
20	2	118	179.78	0.25
20	4	54	182.14	0.08
20	6	27	184.87	0.33
21	2	57	188.67	1.00
22	3	73	199.83	0.92
22	4	102	201.62	0.33
23	1	145	207.05	0.42
24	2	67	217.27	0.42
24	4	75	220.35	0.33
24	4	79	220.39	0.50
25	1	119	225.79	0.83
25	3	40	228.00	0.50
26	2	32	235.92	0.42
26	4	36	238.96	0.42
27	2	82	245.92	0.75
27	3	94	247.54	1.83
27	6	39	251.49	0.25
28	1	55	253.65	1.25
28	3	76	256.86	32.53
29	2	128	265.38	38.36
29	3	100	266.60	13.51
30	4	79	277.39	47.37
30	4	130	277.90	25.10
30	10	15	278.23	52.54
31	1	59	282.19	56.30
31	2	85	283.95	25.02
32	1	35	291.45	0.50
32	3	19	294.29	0.25
33	2	104	303.14	0.67
33	4	110	306.20	0.50
33	5	75	307.35	0.33
34	1	76	310.86	0.50
34	3	127	314.37	0.58
34	4	88	315.48	0.42
35	2	57	321.67	0.50
35	3	48	323.08	0.42
35	4	16	324.26	0.83
36	2	109	331.69	0.25
36	3	74	332.84	0.25
36	5	114	336.24	1.08
37	3	12	341.72	1.42
37	5	56	345.16	0.67
38	2	44	350.04	0.25
38	4	74	353.34	0.17
38	6	96	356.56	0.25
39	2	76	359.86	0.33
39	4	74	362.84	0.25
39	6	61	365.71	0.17
40	2	110	369.70	0.17
40	4	49	372.09	0.25
40	6	63	375.23	0.17
41	2	63	378.73	0.17
41	4	4	381.14	0.25
41	4	84	381.94	0.25
41	5	41	383.01	0.33
42	2	70	388.30	0.42
42	3	87	389.97	0.33
43	1	5	395.65	0.17
43	6	127	404.37	0.33
44	2	49	407.09	0.25
44	4	57	410.17	1.50
44	6	47	413.07	8.59
45	1	53	415.13	3.75
45	4	29	419.39	8.34
45	7	15	423.75	0.58
46	1	12	424.22	0.08
46	5	92	431.02	0.42
46	6	93	432.53	0.25
47	2	71	435.81	0.17
47	5	72	440.32	0.33
48	1	68	443.78	0.25
48	6	58	451.18	8.34

Miocene microfossils are extremely rare at this site. A few lower Miocene nannofossils are noted in Core 110-674A-33X, as well as within the first recovered Eocene interval (Cores 110-674A-28X through -30X) where their occurrence remains anomalous.

Oligocene sediments are mostly barren of calcareous microfossils but provide generally good radiolarian assemblages.

A middle Eocene sequence is identified by the three fossil groups between Cores 110-674A-28X and -32X. Within this interval, a lower middle Eocene foraminiferal assemblage has been recognized from a level underlain by younger middle Eocene (nannofossil Zone CP14) sediments. As long as these microfossils are autochthonous, the data are consistent with overturning of the sequence.

The biostratigraphic succession at Site 674 is frequently interrupted by intervals barren of microfossils; the longest interval is approximately 130 m thick (Cores 110-674A-14X through -27X) and is probably equivalent to the usual nonfossiliferous upper-middle Miocene sequence.

Calcareous Nannofossils

Nannofossil biostratigraphy at Hole 674A is punctuated by a series of rather extensive barren intervals which may result from a combination of reverse thrust faulting and dissolution. Nannofossiliferous sediments range from lower Pleistocene to middle Eocene.

Samples 110-674A-1H-1, 68–70 cm through -2H-2, 86–88 cm are restricted to the early Pleistocene *Pseudoemiliania lacunosa/* small Gephyrocapsa Zone of Gartner (1977) based on the presence of *Pseudoemiliania lacunosa* without *Helicosphaera sellii.* Samples 110-674A-5X-4, 99–101 cm through -6X-2, 80–82 cm

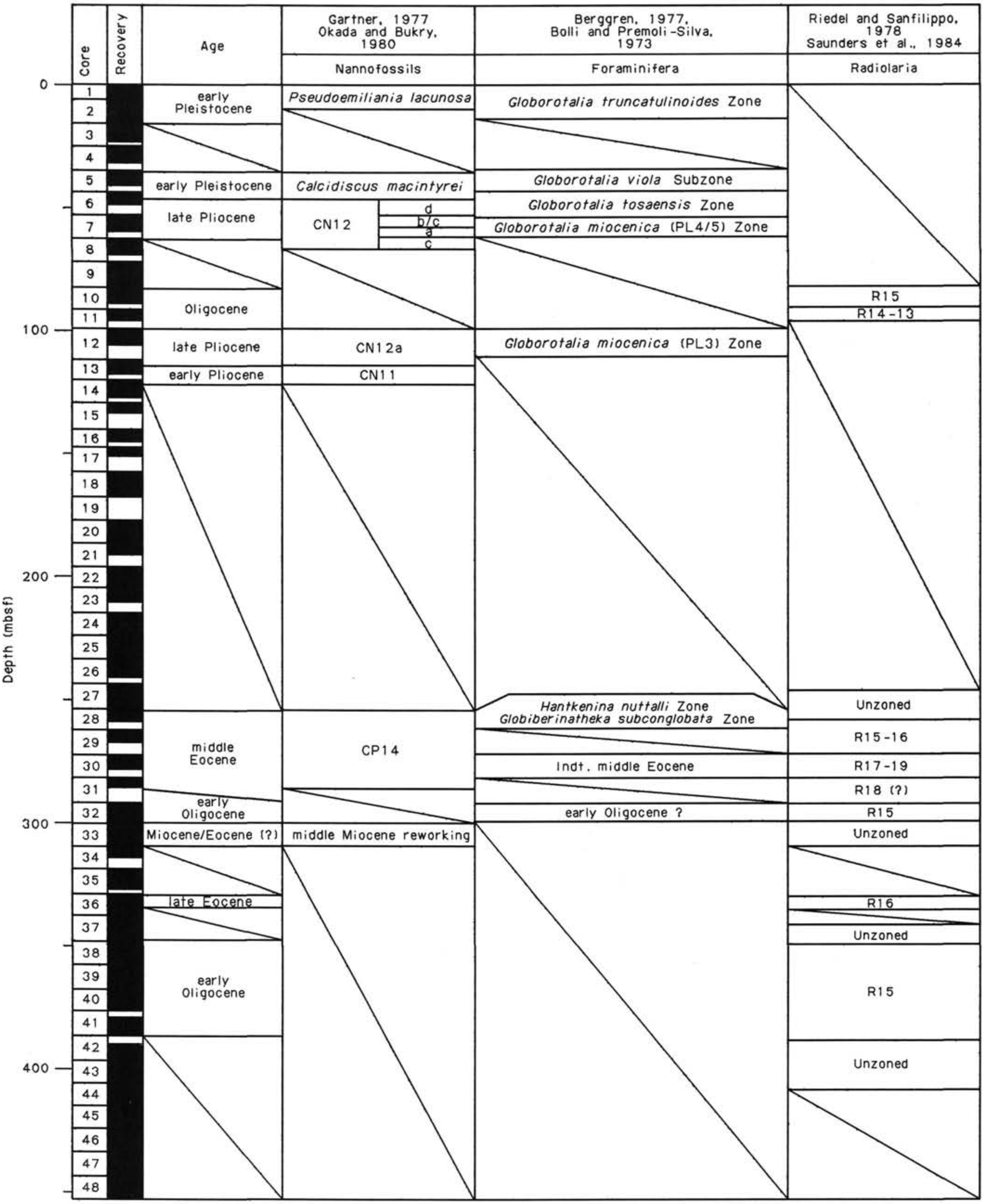

Figure 27. Site 674 biostratigraphic summary. R14: *Dorcadospyris ateuchus* Zone, R15: *Theocyrtis tuberosa* Zone (-1: upper part, -2: lower part), R16: *Theocyrtis bromia* Zone (a: *Cryptopora ommata* Subzone, b: *Calocyclas bandyca* Subzone, c: *Carpocanistrum azyx* Subzone), R17: *Podocyrtis goetheana* Zone, R18: *Podocyrtis chalara* Zone, R19: *Podocyrtis mitra* Zone, R20: *Podocyrtis ampla* Zone, R21: *Thyrsocyrtis triacantha* Zone, R22: *Dictyoprora mongolfieri* Zone.

are also early Pleistocene in age and occur below a barren interval between Samples 110-674A-2H-4, 86–88 cm and -5X-3, 99–101 cm. Samples 110-674A-5X-4, 99–101 cm through -6X-2, 80–82 cm are placed within the *Calcidiscus macintyrei* Zone of Gartner (1977) owing to the presence of *C. macintyrei* without *Discoaster brouweri*. The *Helicopontosphaera sellii* Zone of Gartner (1977) was not noted in the section.

The last occurrence datum of *D. brouweri* marks the top of the Pliocene in Sample 110-674A-6X-3, 80–82 cm. The Pliocene/Pleistocene boundary appears to be biostratigraphically continuous at Site 674. The interval between Sample 110-674A-6X-3, 80–82 cm and -6X, CC contains *D. brouweri* without *D. pentaradiatus* and is, therefore, assigned to the late Pliocene Subzone CN12d of Okada and Bukry (1980). Sample 110-674A-7X-1, 78–80 cm contains *D. pentaradiatus* without *D. brouweri*, whereas Sample 110-674A-7X-2, 78–80 cm contains *D. surculus* without *D. tamalis*. These intervals are placed within the CN12c and CN12b Zones, respectively, of Okada and Bukry (1980). Samples 110-674A-7X-3, 78–80 cm through 7X, CC and 110-674A-12X-1, 70–72 cm through -13X-4, 80–82 cm contain *D. tamalis* without *Reticulofenestra pseudoumbilica* and are placed within subzone CN12a. This subzone is interrupted by a recurrence of the *D. surculus* subzone in Sample 110-674A-8X-1, 85–87 cm and by a barren interval between Samples 110-674A-9X-1, 86–88 cm and 110-674A-11X, CC.

An extensive barren interval is present in Samples 110-674A-13X, CC through -27X, CC. This interval is correlated with the nonfossiliferous upper-middle Miocene section at other ODP and DSDP sites in the Barbados accretionary wedge. Sample 110-674A-14-1, 13–15 cm, at the top of the dissolved interval, contains an assemblage assigned to the early Miocene CN11 Zone of Okada and Bukry (1980).

Well-indurated middle Eocene sediments occur in Samples 110-674A-28X-3, 4–6 cm through -31X-2, 107–109 cm. This interval contains a somewhat recrystallized nannofossil assemblage of poor-to-moderate preservation. *Chiasmolithus grandis* and *Reticulofenestra umbilica* occur in all of the above samples and are indicative of Zone CP14 of Okada and Bukry (1980). A rare component of early Miocene species is also found in Sample 110-674A-28X, CC.

Samples 110-674A-31X, CC through -48X, CC are barren of nannofossils except for Sample 110-674A-33X-2, 50–52 cm, which contains a sparse nannofossil assemblage that includes *Sphenolithus heteromorphus* of early to middle Miocene age. *Discoaster variabilis, D. pentaradiatus, D. brouweri*, and *D. quinqueramus* are also observed in this interval and collectively range in age from middle Miocene to Pliocene. The combined ranges of these species suggests a Miocene age for the sample.

Planktonic Foraminifers

Planktonic foraminifer-bearing sediments are very rare at Site 674; in fact, they are restricted to the Pleistocene and upper Pliocene (i.e., the first 63 m of the section and the upper part of the short repeated Pliocene sequence recovered between 110.60 and 129.60 mbsf) and to some Paleogene levels. Preservation is good in Pleistocene and uppermost Pliocene assemblages but deteriorates rapidly in the late Pliocene *Globorotalia miocenica* Zone. Sediments assigned to the lower Pliocene on the basis of nannofossil data yield strongly dissolved microfaunas, composed of a few small benthic forms and rare fragments of indeterminate planktonic foraminifers. Paleogene assemblages are poor and moderately preserved.

Thus, dissolution starts in younger sediments at Site 674 than in the previous sites, where well-dissolved assemblages have not been observed above the lowermost Pliocene-upper Miocene section.

Sections 110-674A-1H, CC and -2H, CC belong to the Pleistocene *Globorotalia truncatulinoides* Zone. No subzonal assignment was attempted because of the absence of the usual key species.

Cores 110-674A-3H and -4H are barren of foraminifers; they could correspond to an older (late/middle Miocene?) package.

Section 110-674A-5X, CC, which yielded *Globorotalia tenuitheka* and the last observed specimens of *G. truncatulinoides*, is dated from the earliest Pleistocene *Globorotalia viola* subzone of the *G. truncatulinoides* Zone.

Sections 110-674A-6X, CC and -7X, CC are late Pliocene in age. Section 110-674A-6X, CC contains a rich and well-preserved assemblage, assigned to the *Globorotalia tosaensis* Zone on the basis of the absence of either *G. truncatulinoides* or *G. miocenica*. Sparse and badly preserved planktonic foraminifers identified in Section 110-674A-7X, CC include *Sphaeroidinella dehiscens, Pulleniatina obliqueloculata, Neogloboquadrina dutertrei* and *Globorotalia crassaformis*. Accurate zonal assignment is not possible from this poor assemblage; nevertheless, the presence of *S. dehiscens s.s.* indicates a biostratigraphic level younger than the lower part of the *Globorotalia miocenica* Zone (PL 3).

Cores 110-674A-8X through -11X are barren of foraminifers.

Section 110-674A-12X, CC is assigned to the lowest part of the *G. miocenica* Zone (PL 3), based on the occurrence of *G. multicamerata, G. praehirsuta, G. pseudopima* and *Globigerinoides extremus*, without *Sphaeroidinella dehiscens* or *Globorotalia margaritae*.

Very rare fragments of indeterminate planktonic foraminifers are noted in Section 110-674A-13X, CC. Below this level, sediments recovered down to Section 110-674A-27X, CC are barren of foraminifers.

Some Paleogene assemblages have been recognized between Cores 110-674A-28X and -32X. Section 110-674A-28X, CC contains sparse and recrystallized foraminifers including *Morozovella aragonensis, Globigerinatheka* sp., *Acarinina broedermanni* and *Globorotalia* gr. *boweri-possagnoensis*. Co-occurrence of the first two taxa marks the lower part of the middle Eocene, *Hantkenina nuttalli* Zone or *Globigerinatheka subconglobata* Zone. On the other hand, this same sample is dated by nannofossils from the *upper* part of the middle Eocene (CP14). This disagreement may be attributed to one or two causes: a) reworking of foraminifers, or b) mixing of sediments in the core catcher.

Finally, sparse microfaunas have been identified in Sections 110-674A-30X, CC and -32X, CC. The former belongs to the middle Eocene, owing to the presence of sparse *Globigerinatheka* gr. *mexicana* and *Truncorotaloides rohri*. The latter is assigned to a doubtful early Oligocene age on the basis of occurrence of very rare *Globigerina* cf. *officinalis, Pseudohastigerina micra* and small *Globorotalia* sp.

Cores 110-674A-33X through -48X are barren of foraminifers.

Radiolaria

Cores 110-674A-1H through -10X are barren of radiolarians, except Sample 110-674A-10X, CC, 46–47 cm taken from the extreme bottom of Core 110-674A-10X. The sample contains abundant and well-preserved radiolarians assigned to the lower part of *Theocyrtis tuberosa* Zone of Riedel and Sanfilippo (1978).

Theocyrtis tuberosa is common, *Lithocyclia crux, Lithocyclia angusta*, and *Tristylospyris triceros* are present, and *Lithocyclia aristotelis* group, *Dorcadospyris ateuchus*, and *Theocyrtis annosa* are absent from this sample. The upper part of the next core, Sample 110-674A-11X-1, 96–98 cm, also contains abundant but remarkably dissolved radiolarians. The sample is assigned to the *Dorcadospyris ateuchus* Zone or *Lychnocanoma elongata* Zone of Riedel and Sanfilippo (1978) because of the presence of *Liriospyris longicornuta*, ranging from the middle part of the *D. ateuchus* Zone to the middle part of the *L. elongata* Zone (Goll, 1972, as upper *Theocyrtis annosa* Zone to middle *Lychnocanium bipes* Zone). In Samples 110-674A-11X-2, 95-97 cm through -11X, CC, rare to common radiolarians occur but are badly dissolved. No speciation is available.

Samples 110-674A-12X-2, 58-60 cm through -27X-3, 54-56 cm are entirely barren of radiolarians.

In Samples 110-674A-27X-4, 59-61 cm, through -27X, CC, radiolarians are few to common, but the state of their preservation is very poor (badly dissolved).

Sample 110-674A-28X-1, 104-106 cm contains abundant well-preserved radiolarians and is assigned to the upper part of *T. tuberosa* Zone based on the following: *L. crux* is present, *T. triceros* and *Artophormis gracialis* are common, *T. tuberosa* and *D. ateuchus* are very rare, and *L. aristotelis* group and *T. annosa* are absent.

Samples 110-674A-28X-2, 18-20 cm through -28X, CC contain *T. triceros* and lack *Dictyoprora mongolfieri* and *Lithocyclia occerus* group.

Sample 110-674A-29X-1, 96-98 cm contains common but poorly preserved radiolarians and is assigned to the middle or lower part of the *Thyrsocyrtis bromia* Zone of Riedel and Sanfilippo (1978) (= *Calocyclas bandyca* Zone or *Carpocanistrum azyx* Zone of Saunders et al., 1984), owing to the presence of *T. bromia* and *D. mongalfieri*.

In Samples 110-647A-29-2, 132-134 cm through -31-2, 20-22 cm, the state of preservation is also very poor but *Dictyoprora mongolfieri* and *Eusyringium fistuligerum* could be identified.

Samples 110-674A-30X-1, 140-142 cm through 31X-2, 20-22 cm contain rather abundant radiolarians, although the preservation state is still poor. *Podocyrtis chalara* is found as well as *Sethochytris triconiscus, Lithochytris vespertilio, D. mongolfieri*, and *E. fistuligerum*. These samples are assigned to the interval between the upper part of the *Podocyrtis mitra* Zone and the lower part of the *Podocyrtis goetheana* Zone (possibly to the *Podocyrtis chalara* Zone).

Sections 110-674A-31X, CC through -32X, CC are assigned to the early Oligocene *Theocyrtis tuberosa* Zone because of the presence of *T. tuberosa, T. triceros, L. angusta*, and *L. crux*, and the absence of *L. aristotelis* group and *T. annosa*. Samples 110-674A-33X-1, 29-31 cm through -35X, CC are barren of radiolarians with the exception of Section 110-674A-53X, CC.

In Section 110-674A-33X, CC, rare and moderately preserved early Oligocene radiolarians occur together with several badly dissolved ones. This may be attributed to redeposition of the latter or the downhole mixing of the former. In this sample, the downhole mixing explanation is probable because middle Miocene nannofossils are obtained in the same core (samples from Sections 110-674A-33X-2 and -3).

Samples 110-674A-36X-1, 75-77 cm and -36X-2, 74-76 cm contain poorly preserved but abundant radiolarians, and are assigned to the late Eocene *Thyrsocyrtis bromia* Zone (*Calocyclas bandyca* Zone of Saunders, et al. (1984). *Calocyclas bandyca* occurs in these samples, as well as *Thyrsocyrtis tetracantha, T. bromia, Calocyclas turris, D. mongolfieri*, and *T. triceros*.

In samples 110-674A-36X-3, 60-62 cm and -36X-4, 59-61 cm, partly dissolved radiolarians commonly occur.

In Sample 110-674A-36X-5, 59-61 cm through -37X-5, 76-78 cm, no radiolarians occur.

In Samples 110-674A-37X-6, 76-78 cm through -37X, CC, partly dissolved radiolarians commonly occur.

Samples 110-674A-38X-1, 66-68 cm through -42X-2, 78-80 cm are assigned to the *Theocyrtis tuberosa* Zone (early Oligocene) owing to the presence of *L. angusta*, the absence of *L. aristotelis* group, and the predominant occurrence of *T. triceros*. Within the interval, Samples 110-674A-41X-3, 57-59 cm through -41X, CC contain few *T. tuberosa*. Thus the age of these latter samples is judged younger than that of upper and lower samples.

Samples 110-674A-3, 78-80 cm through -42X, CC contain a few radiolarians in two different preservational states. One group is badly dissolved, and does not yield a specific age. The other group is rather well preserved and is of the overlying *T. tuberosa* Zone. No definite age assignment is suggested.

Samples 110-674A-43X-1, 48-50 cm through -43X, CC contain abundant, middle to late Eocene radiolarians, but precise age assignment is impossible because of their partly dissolved state.

Cores 110-674A-44X through -48X are barren of radiolarians.

PALEOMAGNETICS

Paleomagnetics samples were collected from Site 674, both from visibly deformed and undeformed areas. The samples from areas of scaly fabric development are specifically for examination of the magnetic fabrics, although the remanent magnetization of these samples has been subjected to the normal demagnetization techniques (see Chapter 1). Whole-core susceptibility was also initially measured on some of the first APC cores although this was discontinued when the structural complexity of the sequence became apparent (Fig. 28).

Remanence Measurements

Samples from Cores 110-674A-1H to -14X were demagnetized onboard the *Resolution*, whereas samples from Cores 110-674A-15X to -48X were measured and demagnetized at Sheffield. The NRM intensity and inclination are shown in Figure 29. The NRM is again dominated by the drilling-induced remanence at least to approximately 280 mbsf. The demagnetization behavior of samples show a similar range of response to those

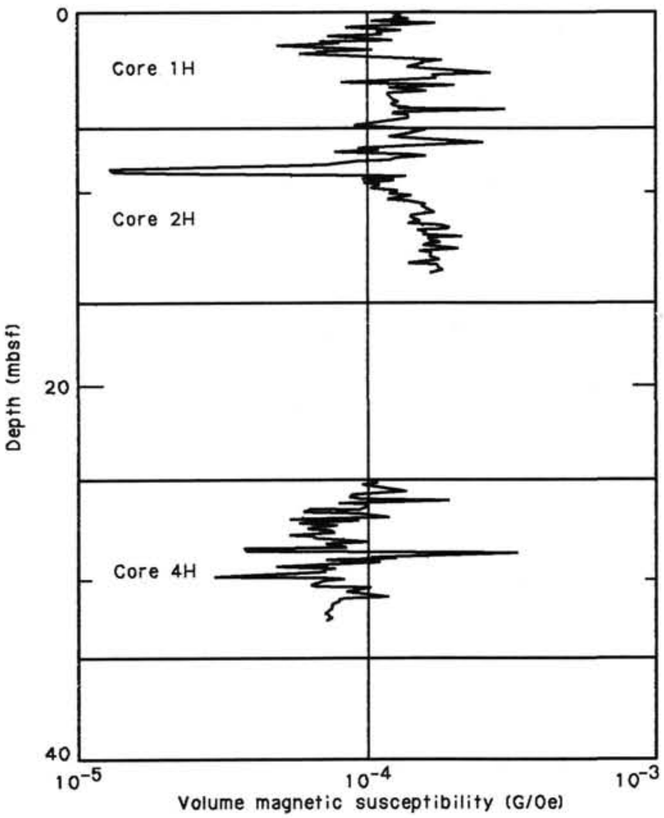

Figure 28. Whole-core susceptibility data for Hole 674A.

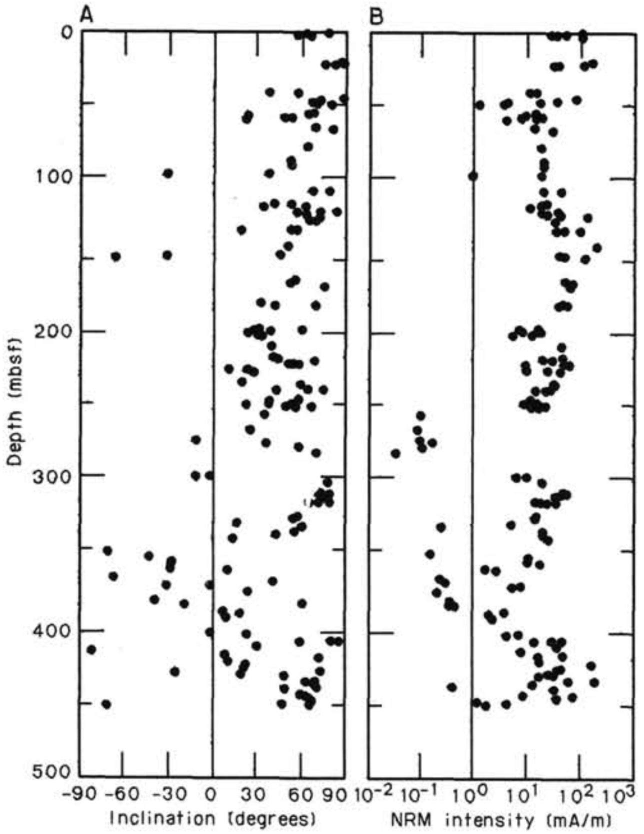

Figure 29. A. NRM inclination and B. NRM intensity for Hole 674A.

outlined in the report for Site 671 (Paleomagnetics section), examples of which are shown on Figures 30 through 33.

The steep positive vertical component is generally removed by demagnetization (Fig. 34), giving shallower or negative inclinations. The group of samples between 350 and 400 mbsf have consistently negative stable endpoints, in most cases little different from the NRM directions. This group of samples also corresponds to the top of tectonic package 7, of early Oligocene age, which is relatively undeformed. The samples from Hole 674A cannot be interpreted in terms of a polarity sequence until the inclinations are corrected for tectonic tilt.

GEOCHEMISTRY

Introduction

Site 674 was drilled 5 km to the west of Site 673. In this report we present a brief summary of the geochemical data obtained in Hole 674A.

Inorganic Geochemistry

The data are presented in Tables 5 and 6, and in Figure 35.

Discussion

Chloride

The chloride profile in the upper 30 mbsf (Fig. 35) shows a clearly established minimum that appears to be related to the advection of lower chlorosity waters from greater depths. The data for Ca and Mg (Fig. 35) appear little affected by advection in this zone, with Ca concentrations being lower but Mg concentrations being higher than expected. The major part of this section is undatable (barren) and has relatively little volcanic material. We postulate that the low chlorosity observed in Core 110-674A-4H is associated with a potential fault in this section along which advection of low-chloride waters from greater depths may have occurred. A clear-cut anomaly in heat flow appears to be associated with this same interval, strongly supporting the concept that the chloride anomaly is of a recent origin, resulting in a non-steady-state both in chloride and temperature distributions.

From 30 mbsf to 200 mbsf the chloride concentrations show a decrease along an essentially diffusive gradient, the waters gradually freshening with depth.

Below 200 mbsf concentration variations are greater, but low sulfate concentrations emphasize the essential validity of the samples, so that the observed extrema do not appear to be artifacts. We suggest that the dashed line in Figure 35 represents the baseline for the general depth trend in chloride and that the minima located at recently active faults (250 m and 310 m, and presumably at a depth just below 450 m—major reflector) are representative of inputs of low chlorosity waters from greater depths. The time of these injections was sufficiently in the past for a normal heat flow gradient to be reestablished (see Heat Flow section).

Calcium and Magnesium

The upper 30 m of Hole 674A show smooth concentration gradients of Ca and Mg (Fig. 35). The curvature of the gradients is unlike those in Sites 671 and 672, perhaps owing to the lesser amounts of volcanic matter in the Miocene block below 10 mbsf. Below 30 m to about 220 m, continued decreases in magnesium and an increase in calcium are observed. Ash occurs in the upper 250 m, but is relatively more abundant above 220 mbsf, though variable with the age of the sediments (see Lithostratigraphy section). We submit that the decrease in Mg and the increase in Ca are mainly related to the alteration of volcanic ash.

Below 250 mbsf, increased Mg concentrations occur as well as a general decrease in Ca. The increase in Mg is reminiscent of the higher Mg concentrations below the décollement of Site 671. The decrease in Ca is in part owing to removal into the ubiquitous calcite cements noticed in the lower sediment sections. In addition, the influence of the drop in chlorosity as a result of pore-water freshening is a contributing factor. Of note is the lack of an increase in Ca with depth within this lower section, as was the case in the décollement zone at Site 671. The (Na + K)/Cl ratio (Fig. 35) also changes slightly with depth (see below).

Sodium and Potassium

As usual, the sum (Na + K) follows to a large extent the dissolved chloride profile (Fig. 35). However, the ratio (Na + K)/Cl (Fig. 35) is lower at Site 674 than at Site 673, showing perhaps a small influence of the lower (Na + K)/Cl ratio which should occur at greater depths.

Sulfate and Ammonia

The sulfate profile (Fig. 35) indicates almost complete depletion of dissolved sulfate below 290 mbsf, mostly as a result of bacterial sulfate reduction processes. Similar observations were made at Site 673.

Ammonia concentrations (Fig. 35) also show changes similar to those in Site 673, but with slightly lower absolute values (300–400 μmol/L vs. 500 μmol/L at Site 673). In part this is owing to uptake of ammonium ions into clay minerals.

Silica

The dissolved silica data (Fig. 35) indicate relatively low concentrations, primarily because of the lack of control by biogenic silica. Notable exceptions to this are the radiolarian-rich zones where opal solubility plays a dominant role.

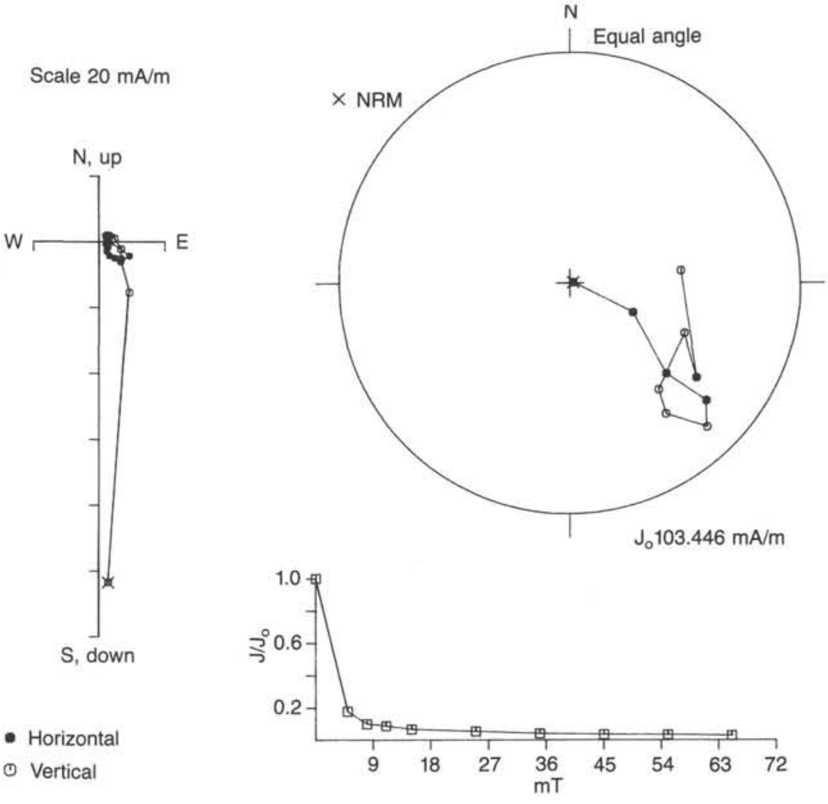

Figure 30. Demagnetization data for Section 110-674A-3H-5, 101 cm, which shows the very large, low-coercivity, drilling-induced remanence (refer to Site 671 chapter, Paleomagnetics section for an explanation of the diagrams).

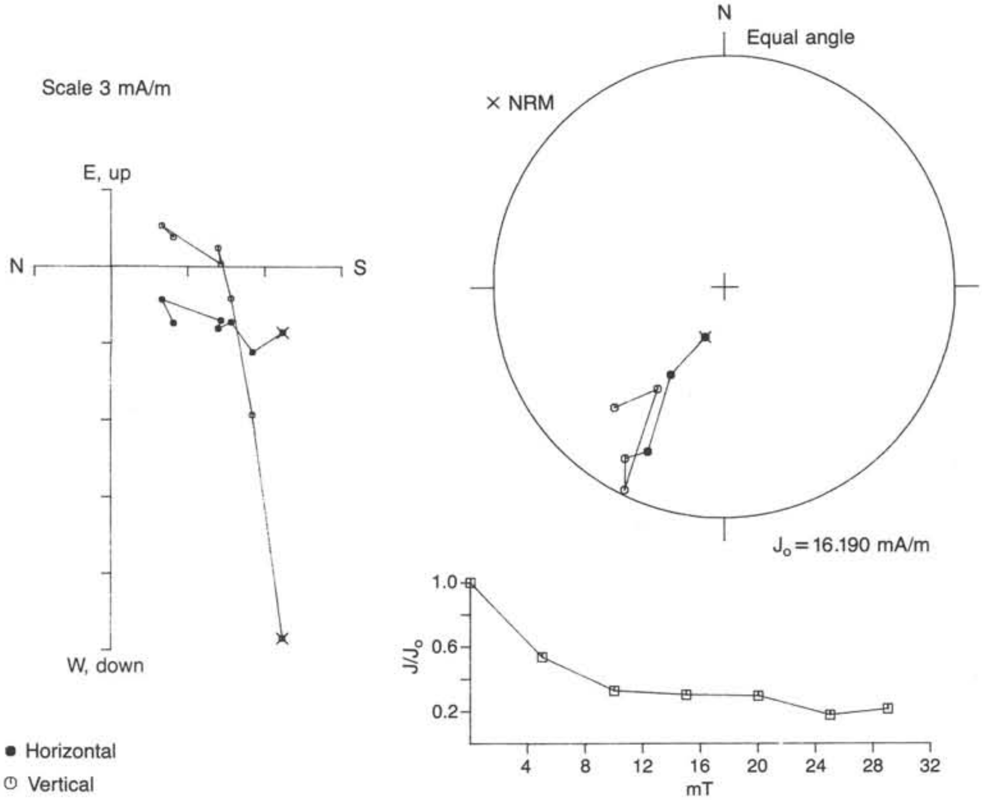

Figure 31. Demagnetization data for Section 110-674A-9X-4, 50 cm.

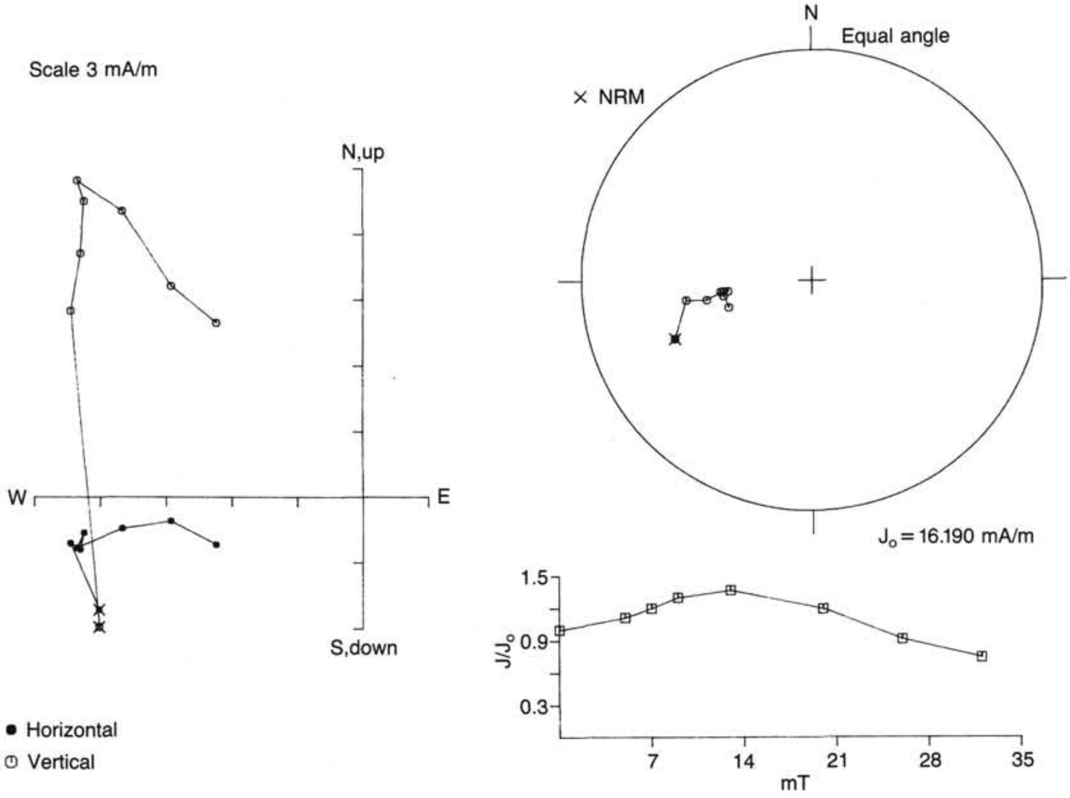

Figure 32. Demagnetization data for Section 110-674A-22X-4, 57 cm, which has the positive inclination, drilling-induced remanence superimposed upon a stable negative inclination.

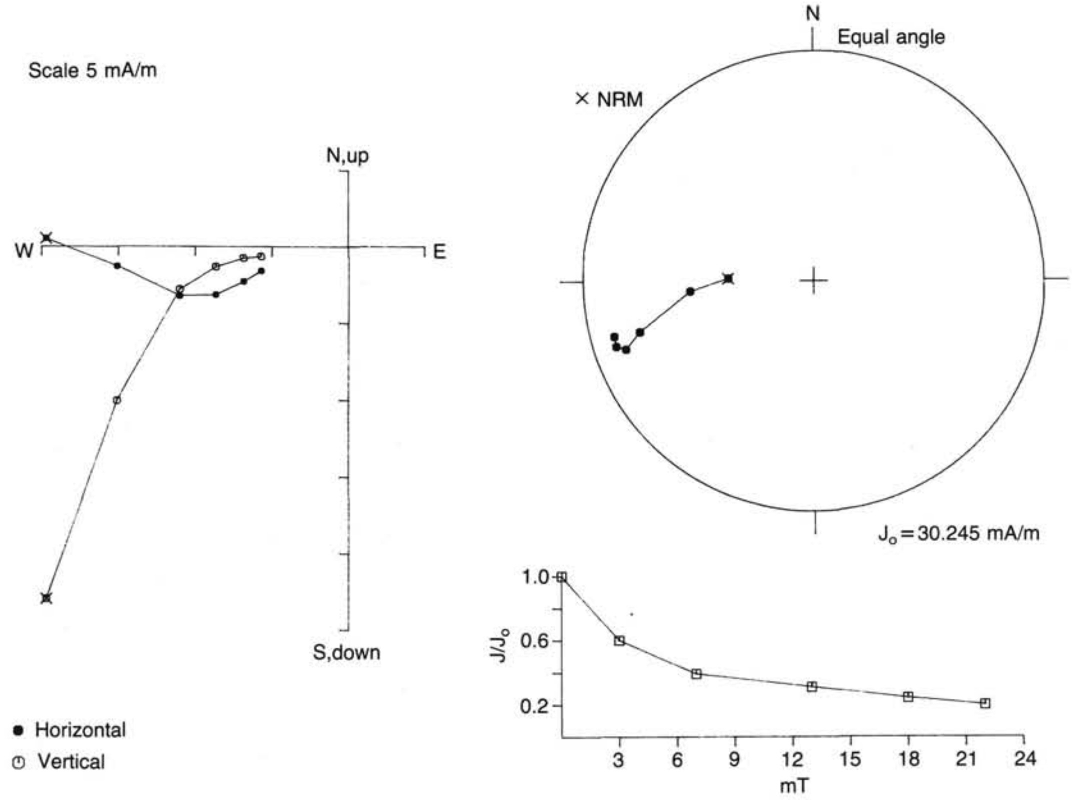

Figure 33. Demagnetization data for Section 110-674A-47X-5, 70 cm, which shows planar movement on the stereonet. At its termination the stereonet defines a stable endpoint.

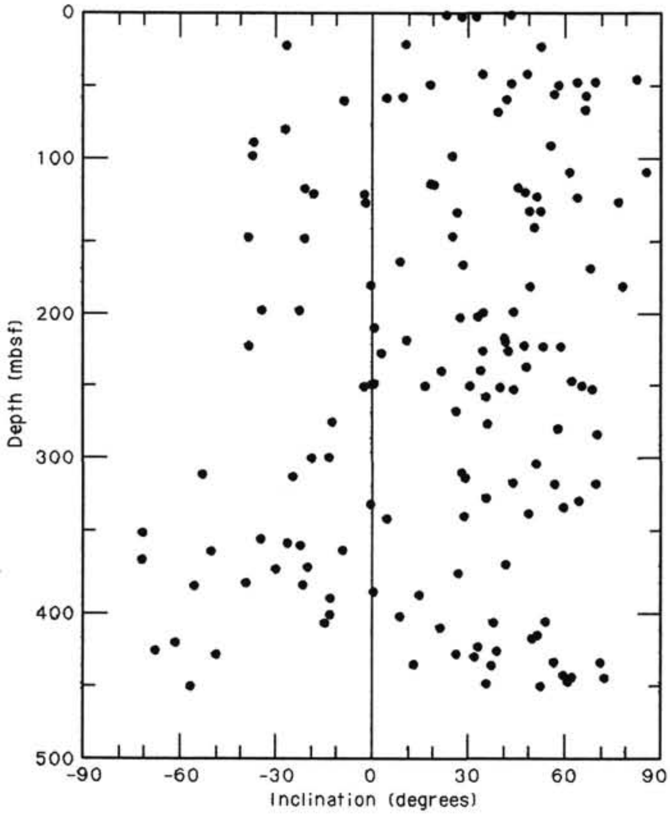

Figure 34. The inclination of high-coercivity components in Hole 674A.

Conclusions

1. Chloride decreases in the upper 30 mbsf suggest upward transport of relatively low-chlorosity waters from greater depths along a possible fault zone identified at about 30 mbsf.

2. Below 250 mbsf, extremes in chloride attest to heterogeneity, probably related to local processes of faulting, which creates varying conduits for the advection of low-chlorosity waters.

3. Small increases in magnesium and decreases in the (Na + K)/Cl ratio in the sediments below 250 mbsf suggest remnant traces of concentration profiles below the décollement as observed in Sites 671 and 672. The associated signal in dissolved calcium appears to have vanished.

Table 5. Interstitial water composition: pH, alkalinity, salinity, chlorinity, Site 674.

Core 110-674A-	Sec.	Interv. (cm)	Depth (mbsf)	pH	Alkalinity (mmol/L)	Salinity (‰)	Chlorinity (mmol/L)
1	3	145–150	4.5	7.86	3.51	34.2	546
2	6	145–150	15.5	8.15	3.34	34.0	543
3	5	145–150	23.5	n.d.	n.d.	33.5	537
4	3	145–150	30	n.d.	n.d.	32.0	518
5	4	145–150	40.5	7.73	1.32	34.3	569
7	2	145–150	57	6.87	0.67	33.7	565
9	6	145–150	82	n.d.	n.d.	n.d.	553
12	3	145–150	105	7.77	1.18	33	558
15	2	140–150	132	8.11	0.93	33	543
18	5	140–150	165	8.07	1.20	31.8	530
21	3	140–150	190	n.d.	n.d.	32.2	527
24	5	140–150	220	n.d.	n.d.	29	501
27	5	140–150	250	n.d.	n.d.	26.5	481
30	3	140–150	275	7.85	2.88	29.5	508
33	5	140–150	308	n.d.	n.d.	26.2	455
36	5	140–150	336	n.d.	n.d.	n.d.	465
39	5	140–150	365	n.d.	n.d.	n.d.	489
42	3	140–150	391	n.d.	n.d.	25.5	455
45	4	140–150	421	n.d.	n.d.	n.d.	459
48	3	140–150	448	n.d.	n.d.	23.5	394

n.d. = not determined.

Organic Geochemistry

Discussion

Methane

As at Site 673, dissolved methane was not detected in interstitial waters at Site 674. Despite zero sulfate concentrations in the deeper parts of both Sites 673 and 674, no biogenic production of methane is apparent. The lack of methane at Site 674 also yields an additional argument that no methane diffusion occurs from the décollement towards offscraped sediments, and methane is essentially advected with low chlorosity waters along the décollement.

Rock-Eval Results

Similar to Site 673, the plot of total organic carbon (TOC) vs. depth in Hole 674A (Fig. 36) shows very low and quite constant organic carbon (<0.02%) (Table 7). In this lower Pleisto-

Table 6. Interstitial water composition; Ca, Mg NH_4, Si, SO_4, Na + K, (Na + K)/Cl, Site 674.

Core 110-674A-	Depth (mbsf)	Calcium (mmol/L)	Magnesium (mmol/L)	Ammonia (μmol/L)	Silica (μmol/L)	Sulfate (mmol/L)	Na + K (mmol/L)	(Na + K)/Cl
1	4.5	11.5	50.1	8	420	24.3	475	0.87
2	15.5	15.8	46.4	82	180	24.0	470	0.86
3	23.6	21.2	40.8	145	175	20.0	456	0.85
4	30	25.2	38.4	155	455	18.0	429	0.83
5	40.5	29.8	27.5	235	400	15.5	486	0.85
7	57	33.3	22.3	295	195	13.0	480	0.85
9	82	37.5	20.0	303	335	11.1	461	0.83
12	105	38.6	13.9	306	320	7.3	468	0.84
15	132	40.6	12.5	243	210	8.5	455	0.84
18	165	46.2	4.9	287	200	4.0	437	0.82
21	190	44.5	5.1	433	225	4.8	439	0.83
24	220	42.7	5.0	313	130	2.4	412	0.82
27	250	38.8	9.5	317	930	1.6	390	0.81
30	275	40.2	11.7	493	550	0.8	408	0.80
33	308	35.7	11.6	333	130	3.6	370	0.81
36	336	35.9	8.8	421	170	1.8	381	0.82
39	365	37.8	9.9	380	935	0.0	396	0.81
42	391	34.4	9.6	414	935	0.8	371	0.815
45	421	32.0	10.3	398	120	0.4	378	0.82
48	448	25.6	10.7	322	285	1.0	325	0.825

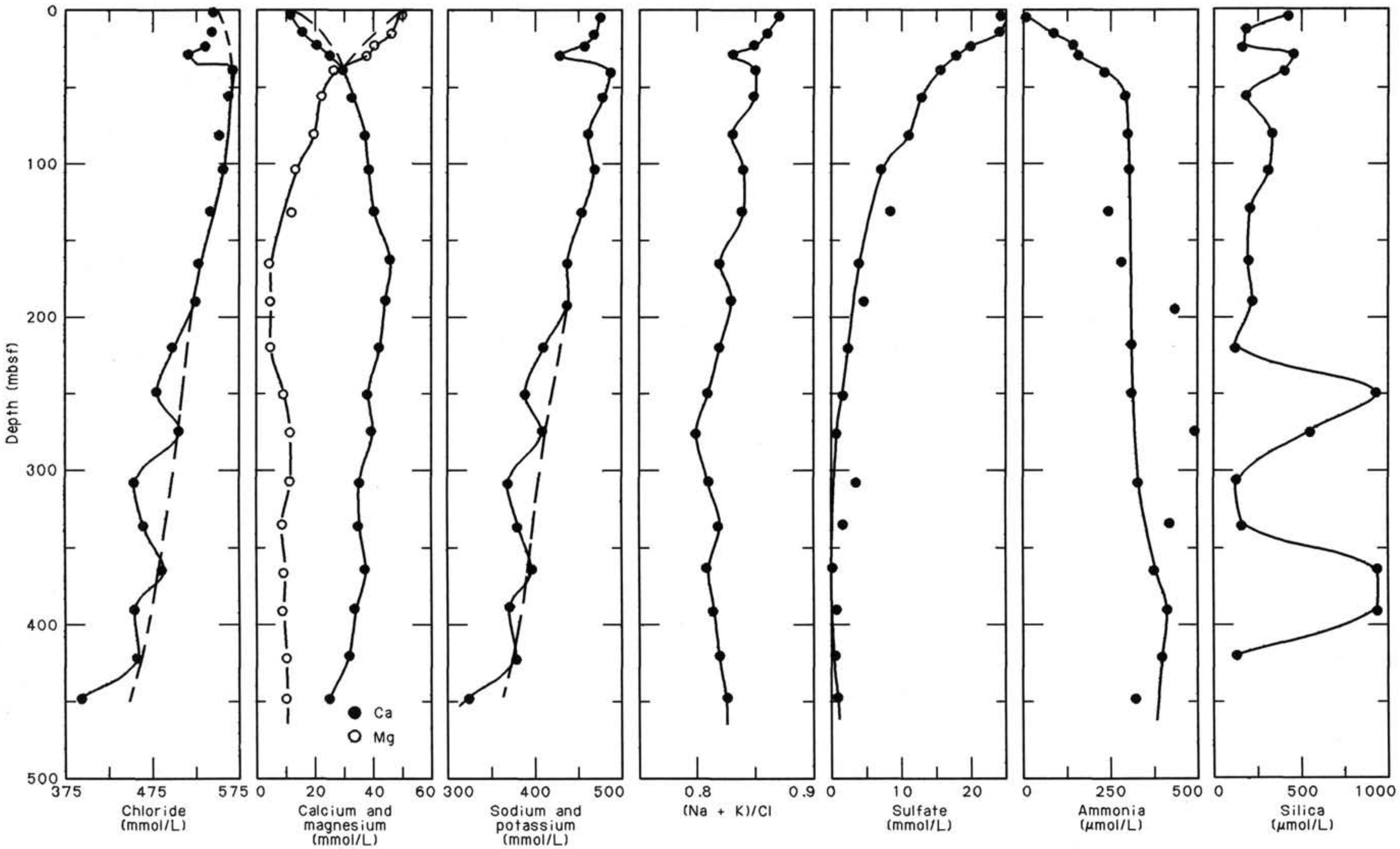

Figure 35. Chloride, calcium, magnesium, (Na + K), (Na + K)/Cl, sulfate, ammonia, and silica profiles, Site 674.

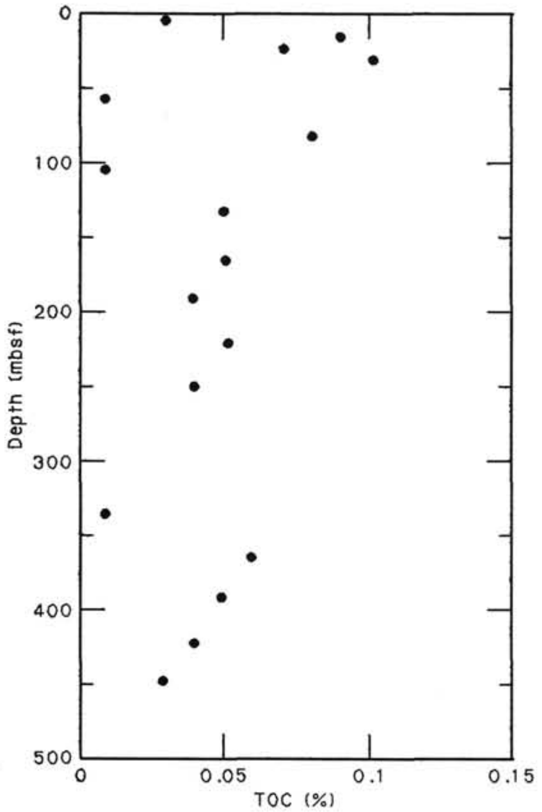

Figure 36. Plot of Total Organic Carbon (TOC) vs. depth, Site 674.

cene to middle Eocene sedimentary series, the organic matter is residual.

PHYSICAL PROPERTIES

Introduction

The objectives of the physical properties program at Site 674 were to characterize the nature of sediments that had been involved in more extensive deformation than at previous Leg 110 drilling locations and to shed some light on the obscure record of seismic reflections seen in the accretionary prism to the west of Site 671. The full suite of measurements were carried out according to the Leg 110 plan, which is described in Chapter 1.

Index Properties

Results

Values of index property determinations from Site 674 are listed in Table 8 and are plotted vs. depth in Figure 37. The plots of index properties reflect the very complicated nature of the lithostratigraphy at this site. There are three major subdivisions of the property profiles which individually contain local maxima and minima related to the finer scale breakdown of the stratigraphy. The major units coincide with the identification of three major fault-bounded tectonic units described by the shipboard stratigraphers and structural geologists, although, in detail, exact boundary levels may differ by 5 to 10 m between the physical property and tectonic units.

The boundaries of the three major physical property units are seen clearly in the plots of bulk density and porosity vs. depth below seafloor. The uppermost interval extends from the seafloor to a depth of around 90 mbsf. Throughout most of this

Table 7. Rock-eval geochemistry data, Site 674.

Core 110-674A-	Sec.	Interval (cm)	Depth (mbsf)	Temp. (°C)	S1	S2	S3	PI	S2/S3	PC	TOC (%)	HI	OI
1	3	145–150	4.5	543	0.05	0.34	1.89	0.13	0.17	0.03	0.03	1133	6300
2	6	145–150	15.5	455	0.06	1.06	0.26	0.05	4.07	0.09	0.09	1177	288
3	5	145–150	23.5	446	0.04	0.83	0.15	0.05	5.53	0.07	0.07	1185	214
4	3	145–150	30	477	0.03	1.30	0.20	0.02	6.50	0.10	0.10	1300	200
7	2	145–150	57	361	0.05	0.15	2.66	0.25	0.05	0.01	0.01	1500	26600
9	6	145–150	82	495	0.04	1.03	0.36	0.04	2.86	0.08	0.08	1287	450
12	3	145–150	105	350	0.04	0.13	2.00	0.25	0.06	0.01	0.01	1300	20000
15	2	140–150	132	479	0.04	0.58	0.22	0.06	2.63	0.05	0.05	1160	440
18	5	140–150	165	564	0.03	0.61	0.66	0.05	0.92	0.05	0.05	1220	1320
21	3	140–150	190	524	0.02	0.52	0.48	0.04	1.08	0.04	0.04	1300	1200
24	5	140–150	220	520	0.04	0.67	0.56	0.06	1.19	0.05	0.05	1340	1120
27	5	140–150	250	535	0.02	0.48	0.22	0.04	2.18	0.04	0.04	1200	550
36	5	140–150	336	472	0.04	0.17	0.41	0.20	0.41	0.01	0.01	1700	4100
39	5	140–150	365	480	0.02	0.74	0.09	0.03	8.22	0.06	0.06	1233	150
42	3	140–150	391	473	0.02	0.67	0.08	0.03	8.37	0.05	0.05	1340	160
45	4	140–150	421	526	0.00	0.60	0.25	0.00	2.40	0.04	0.04	1500	625
48	3	140–150	448	535	0.01	0.43	0.22	0.02	1.95	0.03	0.03	1433	733

S1 (mg hydrocarbon/g rock): the quantity of free hydrocarbons present in the rock and which are volatilized below 300°C.

S2 (mg hydrocarbon/g rock): the amount of hydrocarbon-type compounds produced by cracking of kerogen as the temperature increases to 550°C.

S3 (mg CO_2/g rock): quantity of CO_2 produced from pyrolysis of the organic matter in the rock.

S2/S3 : A means of determining the type of organic matter in the rock.
- — from 0.0 to 2.5: gas, type III
- — from 2.5 to 5.0: oil/gas, type III
- — from 5.0 to 10.0: oil, types I and II

Temperature (°C): maximum temperature at which maximum generation of hydrocarbon from kerogen occurs.

PI (Productivity Index): $PI = S1/(S1 + S2)$.
PI characterizes the evolution level of the organic matter.

PC "Pyrolysized carbon": $PC = k(S1 + S2)$ where $k = 0.083$ mg C/g rock. PC corresponds to the maximum quantity of hydrocarbons capable of being produced from the source rock given sufficient burial and time.

TOC: Total Organic Carbon

HI "Hydrogen index": $HI = (100 \times S2)/TOC$

OI "Oxygen index": $OI = (100 \times S3)/TOC$

Table 8. Index properties summary, Hole 674A.

Core 110-674A-	Sec.	Int. (cm)	Depth (mbsf)	% Water (total)	% Water (dry)	Porosity (%)	Bulk density	Grain density
1	2	75	2.25	54	118	76.3	1.44	2.72
1	4	78	5.28	37	60	62.8	1.72	2.73
2	2	70	8.30	39	64	63.6	1.68	2.63
2	4	56	10.06	33	49	57.7	1.80	2.69
2	6	29	12.79	37	60	63.4	1.74	2.65
3	2	80	17.90	43	76	68.0	1.61	2.69
3	5	38	20.79	31	45	56.3	1.86	2.65
3	8	128	24.58	26	35	50.8	1.99	2.83
4	2	122	27.82	39	63	63.7	1.69	2.61
4	4	68	30.28	39	64	64.3	1.70	2.68
5	2	111	37.21	40	66	66.1	1.70	2.70
5	4	33	39.43	44	79	68.9	1.60	2.68
5	5	21	40.81	37	59	61.7	1.71	2.67
6	2	70	46.30	40	66	65.2	1.67	2.76
6	4	31	48.41	45	81	68.3	1.56	2.60
7	2	91	56.01	38	61	62.2	1.68	2.70
7	4	62	58.72	38	63	63.1	1.68	2.65
8	2	15	64.75	48	94	72.8	1.54	2.65
8	4	95	68.55	51	104	74.6	1.50	2.69
9	2	64	74.74	40	66	64.2	1.65	2.70
9	4	75	77.85	44	80	68.6	1.58	2.59
9	6	62	80.72	46	84	69.9	1.57	2.68
10	2	33	83.93	36	57	61.0	1.73	2.71
10	4	60	87.20	48	92	71.4	1.53	2.66
11	3	0	94.60	29	41	53.9	1.89	2.71
11	CC	20	95.86	30	43	54.3	1.84	2.74
12	2	92	103.52	30	42	53.9	1.86	2.67
12	4	118	106.78	29	41	53.6	1.89	2.68
13	3	78	114.38	31	46	57.3	1.87	2.75
13	4	74	115.84	30	43	54.7	1.86	2.72
13	5	12	116.72	29	41	53.7	1.89	2.70
14	2	70	122.30	33	50	58.6	1.79	2.62
14	4	65	125.25	35	53	60.4	1.79	2.71
15	3	52	133.12	31	46	56.6	1.85	2.65
16	1	1	139.11	32	47	56.7	1.81	2.62
16	2	132	141.92	34	52	59.4	1.77	2.64
20	2	118	179.78	34	51	59.7	1.81	2.69
20	4	54	182.14	36	57	61.4	1.73	2.57
20	6	27	184.87	32	47	57.2	1.83	2.67
21	2	55	188.65	32	48	57.6	1.82	2.65
22	3	73	199.83	30	42	54.6	1.88	2.71
22	4	102	201.62	33	48	57.9	1.82	2.69
23	1	145	207.05	28	39	50.1	1.84	2.76
24	2	77	217.37	38	60	62.8	1.71	2.68
24	4	75	220.35	31	44	55.0	1.84	2.70
24	5	77	221.87	29	41	53.5	1.90	2.71
25	1	120	225.80	30	43	54.7	1.86	2.74
25	3	39	227.99	31	45	55.4	1.82	2.69
26	2	32	235.92	35	55	61.7	1.79	2.82
26	4	36	238.96	36	55	60.8	1.75	2.69
27	2	82	245.92	32	47	56.9	1.81	2.69
27	3	94	247.54	26	35	49.2	1.95	2.69
27	6	39	251.49	25	33	47.1	1.94	2.60
28	1	55	253.65	26	35	48.7	1.93	2.64
28	3	76	256.86	25	33	47.2	1.96	2.61
29	2	128	265.38	23	30	43.6	1.93	2.51
29	3	100	266.60	21	26	39.9	1.99	2.46
30	4	79	277.39	22	29	43.9	2.02	2.67
30	4	130	277.90	26	35	48.6	1.92	2.59
30	CC	19	278.27	23	29	43.4	1.96	2.54
31	1	59	282.19	19	24	39.5	2.09	2.65
31	2	84	283.94	25	34	46.2	1.88	2.43
32	1	34	291.44	32	47	55.4	1.77	2.53
32	3	17	294.27	33	49	56.6	1.76	2.59
33	2	105	303.15	22	28	44.3	2.05	2.69
33	4	110	306.20	22	28	43.9	2.07	2.71
33	5	75	307.35	30	42	54.0	1.87	2.67
34	1	76	310.86	24	32	47.5	2.02	2.79
34	3	126	314.36	20	25	41.4	2.11	2.73
34	4	88	315.48	22	28	43.7	2.03	2.69
35	2	57	321.67	25	34	48.7	1.98	2.68
35	3	48	323.08	27	37	51.3	1.96	2.74
35	4	16	324.26	21	26	42.3	2.08	2.73
36	2	109	331.69	28	39	50.0	1.83	2.51
36	3	74	332.84	26	36	48.5	1.89	2.56
36	5	114	336.24	26	36	50.6	1.97	2.77
37	3	13	341.73	32	47	57.7	1.86	2.79
37	5	56	345.16	25	33	48.7	1.99	2.76

Table 8 (continued).

Core 110-674A-	Sec.	Int. (cm)	Depth (mbsf)	% Water (total)	% Water (dry)	Porosity (%)	Bulk density	Grain density
38	2	44	350.04	30	43	54.3	1.85	2.64
38	4	74	353.34	29	42	52.7	1.84	2.54
38	6	96	356.56	30	43	54.2	1.83	2.59
39	2	76	359.86	31	45	54.4	1.80	2.61
39	4	74	362.84	27	36	49.3	1.90	2.60
39	6	61	365.71	31	45	55.2	1.82	2.62
40	2	110	369.70	28	39	51.3	1.86	2.60
40	4	49	372.09	30	43	53.5	1.82	2.60
40	6	63	375.23	31	45	54.2	1.79	2.65
41	2	64	378.74	31	44	54.1	1.80	2.56
41	4	4	381.14	33	48	56.1	1.76	2.59
41	4	84	381.94	31	44	54.4	1.81	2.62
41	5	41	383.01	29	40	51.7	1.86	2.54
42	2	68	388.28	30	43	53.0	1.80	2.55
42	3	87	389.97	27	38	50.4	1.89	2.56
43	1	7	395.67	24	32	46.4	1.94	2.59
43	6	126	404.36	26	35	48.9	1.93	2.65
44	2	49	407.09	32	47	57.1	1.83	2.69
44	4	57	410.17	30	42	56.7	1.95	2.98
44	6	47	413.07	37	59	62.3	1.71	2.64
45	1	53	415.13	29	41	52.9	1.88	2.70
45	4	29	419.39	32	47	57.7	1.84	2.72
45	7	15	423.75	29	40	53.0	1.89	2.91
46	1	12	424.22	30	44	55.6	1.87	2.71
46	5	92	431.02	32	48	58.1	1.83	2.72
46	6	95	432.55	35	53	60.1	1.78	2.74
47	2	71	435.81	28	39	52.8	1.92	2.74
47	5	75	440.35	24	31	46.3	2.02	2.72
48	1	70	443.80	25	33	47.3	1.95	2.73
48	6	60	451.20	24	32	47.9	2.01	2.68

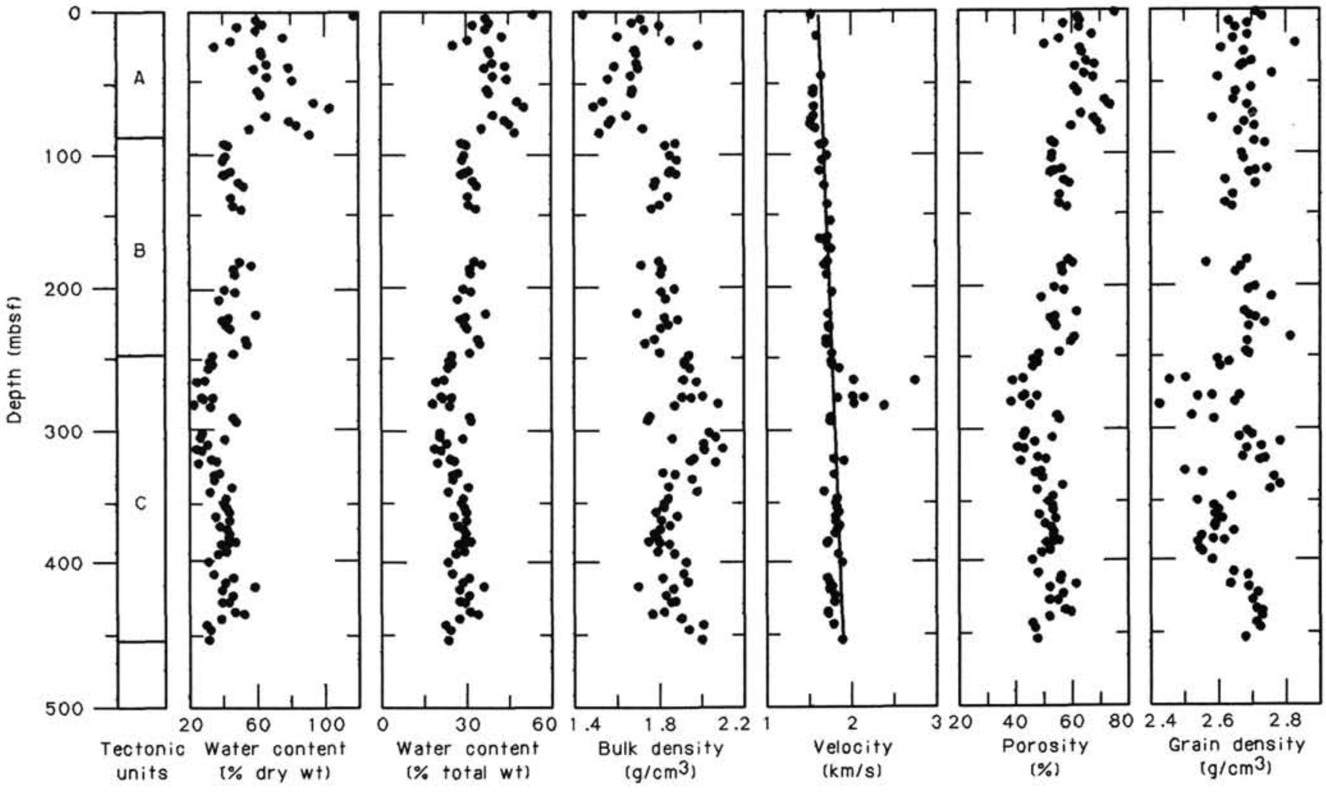

Figure 37. Index properties and compressional wave velocity vs. depth at Site 674. Lines are least-squares linear fits to data discussed in text.

unit, bulk density values range between 1.5 and 1.7 g/cm^3. Several values higher than this range were seen at very shallow depths, but they represent measurements of clasts in what appears to be a debris flow, and are not characteristic of the lithologic interval as a whole. Porosity is relatively high within this unit, with almost all of the values between 60% and 70%. Several porosity values between 60 and 90 mbsf suggest a positive gradient in porosity, but it must be kept in mind that tectonic Unit A is made up of five separate lithologic units, and assigning any overall trend to the data might be superfluous.

There is a large increase in bulk density and concomitant decrease in porosity between Samples 110-674A-10X-4, 60 cm (87.2 mbsf) and -11X-3, 0 cm (94.6 mbsf) that corresponds roughly to the boundary between tectonic Unit A and tectonic Unit B. Below this level almost all of the samples from tectonic Units B and C exhibit densities near to or greater than 1.80 g/cm^3 and porosities less than 60%. Within tectonic Unit B, bulk density values are almost exclusively limited to the range of 1.80 to 1.90 g/cm^3 while porosities range between 50% and 60%. This unit extends to a depth of between 247 and 254 mbsf. It should also be noted that grain density values within both Units A and B are relatively uniform (2.70 g/cm^3) and suggest, by their lack of excursions to densities less than 2.60 g/cm^3, that there is very little biogenic silica in the sediments of the upper two tectonic units (grain densities of clays and calcite are near 2.70 g/cm^3 and biogenic silica has a grain density of around 2.20 g/cm^3). These two tectonic units, though distinct from each other, are internally relatively uniform.

The break between the lower two units might be assigned to either 247 or 254 mbsf based on index property values. Measurements within this zone (Sections 110-674A-27X-3, 94 cm; -27X-6, 39 cm; and -28X-1, 55 cm) are from three samples of a scaly brown claystone layer that separates overlying green claystones of tectonic Unit B from rather anomalously well-cemented Eocene sandstones and marls. These three samples have bulk densities near 1.95 g/cm^3, much like the Eocene claystones below, but do not exhibit the greater velocities characteristic of the underlying sediments (see the velocity discussion below). With no rational evidence to make a clear-cut assignment one way or the other, these samples are placed into a transition zone until other information suggests to which unit, if either, these claystones belong.

The Eocene sediments below 254 mbsf exhibit a scatter of index properties that is characteristic of other Eocene sediments sampled during Leg 110. The break between tectonic Units B and C is best seen in the plot of grain densities, at the point where grain densities decrease to less than 2.50 g/cm^3. All excursions of the grain density profile to values lower than 2.65 g/cm^3 from below the Eocene sand layers to the bottom of the hole correlate with radiolarian-rich zones. Barren intervals, such as the interval from 300 to 325 mbsf, have grain densities near 2.70 g/cm^3. The increase in grain density from about 2.55 g/cm^3 at 390 mbsf to 2.70 g/cm^3 at 410 mbsf is a direct reflection of the dissolution of the radiolaria seen in paleontologic descriptions.

It is interesting to note that the presence of biogenic silica in the sediments does not seem to create local porosity maxima to the degree observed in Miocene sediments of Site 672 or in other oceanic locations. In fact, the opposite appears to be true in upper levels of tectonic Unit C, where a local minimum in porosity is coincident with low grain densities. At about 300 mbsf there is an increase in grain density that can be explained by the disappearance of radiolaria from the core.

Discussion

In general there are three main divisions seen in the index properties data. Each of the three divisions describes a stepwise reduction in porosity and increase in bulk density with depth, although there are some local minima of density in the lowermost sediments (300–390 mbsf) that are counter to this general trend. The upper two units, predominantly Neogene in age, have fairly uniform grain densities, indicating some reasonable homogeneity of composition, whereas the lowermost unit (Paleogene-Neogene) displays much more diversity. Local maxima and minima perturb the individual units and are probably reflections of less drastic differences in composition, structure, or state of compaction.

Compressional Wave Velocity

Results

The compressional wave velocity measured at Site 674 is generally consistent with the changes described in the tectonic units. Results are listed in Table 9. An increase in velocity occurs at the boundary between tectonic Units A and B; and another, sharper, increase in velocity occurs near the boundary between tectonic Units B and C. The only deviation from this conformity with the tectonic interpretation is a profile of decreasing velocity vs. increasing depth at the bottom of the hole. The results are presented in three major zones, roughly corresponding to the tectonic unit breakdown.

In the upper zone (tectonic Unit A), the velocity varies only slightly with depth in a range of 1.52 to 1.65 km/s (Fig. 37). This profile is consistent with an almost constant bulk density profile, although no velocity measurements were made in the upper portion of this zone, where there is high variability in the bulk density measurements.

Just above the tectonic Unit A/B boundary, the velocity increases sharply from 1.58 km/s at 83.9 mbsf to 1.69 km/s at 94.6 mbsf (Fig. 37). Within tectonic Unit B the velocity is consistent with increases in bulk density. The data agree well with a linear least-squares fit to the entire velocity and density profiles, having the same slope (0.6). The velocity increases from 1.63 km/s near the top of the unit to 1.78 km/s at the tectonic Unit B/C boundary.

Just below the tectonic Unit B/C boundary, the velocity increases to the maximum values measured at this site. The major change occurs between 256.9 mbsf (where the measured velocity is 1.87 km/s) and 265.38 mbsf (where the velocity increases to 2.04 km/s). Below this boundary the velocities are scattered. Measurements above 2.15 km/s are representative of fine sandstone and velocities between 2.03 and 2.05 km/s represent marl. This high-velocity zone is only apparent in the upper portion of tectonic Unit C where, as at Site 672, middle Eocene sandstone and marl produced anomalous measurements. Between 291.4 and 395.6 mbsf, the velocity decreases to values which can be represented by the slope of the linear least-square fit (Fig. 37). At the base of tectonic Unit C, between 400 and 450 mbsf, the velocity decreases to values comparable to those measured within tectonic Unit B (1.72 to 1.81 km/s). The deepest measurement (1.9 km/s at 451.2 mbsf), however, is closer to the linear approximation.

Discussion

The velocity measurements at Site 674 are linearly related to bulk density measurements (Fig. 37). The only exception to this trend is the increase in velocity within the upper section of tectonic Unit C where the high-velocity measurements can be attributed to well-cemented sandstones and marls.

At the bottom of the hole, the velocities are low, but exhibit the same trends as the density profile. This is a scaly clay zone (between 400 and 450 mbsf) and has an abundance of calcite veins. It is also of note that the deepest velocity measurement is higher than those between 400 and 450 mbsf and, although it is only one measurement, it may indicate a change in tectonic units which is coincident with reflections on the seismic record.

Table 9. Compressional wave velocity, Hole 674A.

Core 110-674A-	Sec.	Int. (cm)	Depth (m)	Vel(A)* (km/s)	Vel(B)* (km/s)
1	2	106	2.56	1.52	1.53
3	2	80	17.90		1.60
6	2	70	46.30		1.65
7	2	91	56.01	1.55	1.56
7	4	62	58.72	1.55	1.55
8	4	95	68.55		1.56
9	2	64	74.74	1.56	1.56
9	4	75	77.85	1.54	1.53
9	6	62	80.72	1.53	1.52
10	2	33	83.93	1.50	1.58
11	3	0	94.60	1.70	1.69
11	CC	20	95.86	1.64	1.64
12	2	92	103.52		1.72
12	4	118	106.78		1.66
13	3	106	114.66		1.63
14	4	65	125.25		1.69
16	1	1	139.11		1.73
17	2	66	150.76		1.77
18	3	107	162.17		1.73
18	4	69	163.29	1.61	1.63
18	6	34	165.94	1.69	1.71
19	2	111	170.21	1.73	1.73
19	3	4	170.64	1.75	1.77
20	2	118	179.78		1.72
20	4	54	182.14		1.68
21	2	55	188.65		1.71
22	4	102	201.62		1.78
24	2	77	217.37		1.73
25	1	119	225.79		1.74
25	3	39	227.99		1.74
26	2	32	235.92		1.71
26	4	36	238.96		1.71
27	2	82	245.92		1.78
27	3	94	247.54	1.76	
27	6	39	251.49	1.75	1.77
28	1	55	253.65	1.77	1.78
28	3	76	256.86	1.85	1.87
29	2	128	265.38	1.88	2.04
29	3	100	266.60	2.71	2.76
30	4	79	277.39		2.03
30	4	130	277.90		1.85
30	CC	19	278.27	2.12	2.16
31	1	59	282.19		2.05
31	1	59	282.19		2.05
31	2	84	283.94		2.40
32	1	34	291.44		1.76
32	3	17	294.27		1.76
35	2	57	321.67	1.82	1.80
35	3	48	323.08	1.90	1.92
36	2	109	331.69	1.72	
36	3	74	332.84	1.82	1.80
37	5	56	345.16	1.80	1.68
38	2	44	350.04	1.82	1.84
38	4	74	353.34	1.82	1.82
38	6	96	356.56	1.80	1.84
39	2	76	359.86	1.85	1.86
39	4	74	362.84	1.92	1.82
39	6	61	365.71	1.83	1.82
40	2	110	369.70		1.87
40	4	49	372.09	1.83	1.84
40	6	63	375.23	1.80	1.81
41	4	4	381.14		1.73
41	4	84	381.94		1.72
42	3	87	389.97		1.85
43	1	7	395.67		1.90
44	2	49	407.09		1.72
44	4	57	410.17	1.75	
44	4	57	410.17		1.75
44	6	47	413.07	1.73	1.78
45	1	53	415.13		1.75
45	4	29	419.39		1.81
46	1	12	424.22	1.81	1.81
46	5	92	431.02		1.73
46	6	93	432.53		1.73
47	5	72	440.32	1.81	1.79
48	6	58	451.18	1.80	1.90

*Vel(A): measured parallel to core axis
Vel(B): measured perpendicular to core axis

Thermal Conductivity

Results

Thermal conductivity values measured at Site 674 are listed in Table 10 and plotted vs. depth below seafloor in Figure 38. There is a general increase in thermal conductivity with depth at Site 674. Overall control of thermal conductivity values appears to be related to water content, as is illustrated in Figure 39. We have included the data from Hole 671B as a reference and to illustrate the similarity of relationships at both sites. As at Site 671, Site 674 values suggest that there is a change from a fluid to a matrix-dominated system of thermal conduction as the sediments dewater and lithify. The lack of very low conductivity values at Site 674 is probably a reflection of the rather evolved (i.e., more compacted) nature of the sediments at shallow depths (less than 40 mbsf). This compaction has been noted in both formation factor and vane shear measurements (see below) in the uppermost sections of the hole.

Formation Factor

Results

Formation factor values measured at Site 674 are listed in Table 11 and plotted vs. depth in Figure 40. This figure does not include four measurements made on Cores 110-674A-48X which were between 443 and 452 mbsf and had values between 5.2 and 6.4. The formation factor increases very rapidly with depth in the upper 25 m of sediment at Site 674, reflecting the presence of some rather anomalously low porosity sediments at very shallow levels. When plotted against porosity, all of the formation factor values measured agree well with results from previous sites (see Fig. 41, with Hole 671B as a reference) and conform to

Table 10. Thermal conductivity, Hole 674A.

Core 110-674A-	Sec.	Int. (cm)	Depth (mbsf)	Cal/cm·°C·s ($\times 10^{-3}$)	W/m°C
1	4	75	5.25	2.92	1.22
2	2	70	8.30	2.82	1.18
2	4	70	10.20	3.18	1.33
2	6	70	13.20	2.52	1.06
3	2	75	17.85	2.83	1.18
3	5	75	21.16	3.33	1.39
4	2	75	27.35	2.71	1.13
4	4	75	30.35	2.83	1.19
9	1	50	73.10	2.92	1.22
10	2	70	84.30	2.59	1.08
10	4	70	87.30	3.04	1.27
11	CC	18	95.84	3.12	1.31
12	4	75	106.35	3.28	1.38
13	4	75	115.85	3.81	1.59
17	2	60	150.70	3.10	1.30
18	6	70	166.30	2.84	1.19
22	3	70	199.80	3.32	1.39
22	4	70	201.30	3.48	1.46
24	4	80	220.40	2.88	1.21
24	6	74	223.34	2.74	1.15
26	4	70	239.30	2.97	1.24
28	1	57	253.67	3.60	1.51
30	2	90	274.50	3.21	1.34
35	2	60	321.70	3.56	1.49
36	2	58	331.18	3.32	1.39
37	5	58	345.18	3.93	1.64
40	6	115	375.75	3.15	1.32
41	2	60	378.70	3.22	1.35
42	2	70	388.30	2.92	1.22
44	4	30	409.90	2.85	1.19
46	4	110	429.70	3.10	1.30
46	6	110	432.70	3.08	1.29
47	2	75	435.85	3.48	1.46
47	5	75	440.35	3.87	1.62
48	1	68	443.78	3.17	1.33
48	6	56	451.16	4.14	1.74

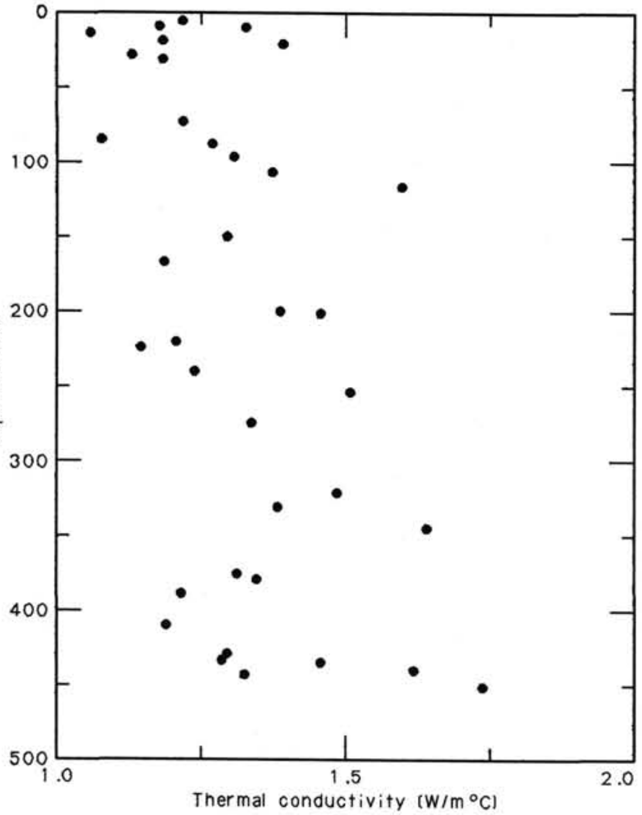

Figure 38. Thermal conductivity vs. depth at Site 674.

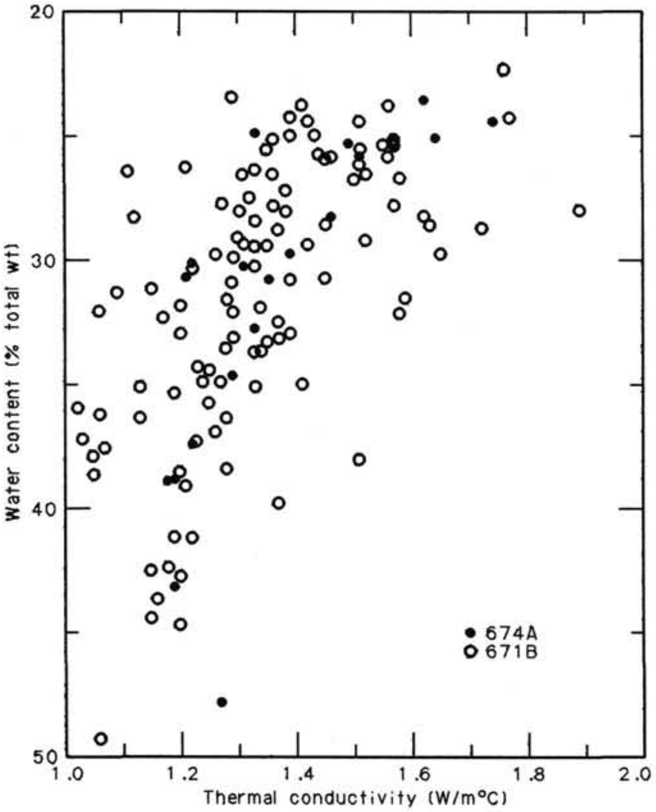

Figure 39. Thermal conductivity vs. water content (% total weight) at Sites 674 and 671.

Table 11. Sediment formation factor, Hole 674A.

Core	Sec.	Int. (cm)	Depth (mbsf)	F-Horiz.	F-Vert.
1	2	70	2.20	1.50	1.53
1	4	70	5.20	3.30	3.27
2	2	70	8.30	2.67	3.00
3	2	2	17.12	3.17	3.50
3	8	120	24.50	4.50	4.67
6	2	75	46.35	2.73	2.80
7	2	98	56.08	2.87	3.00
7	4	70	58.80	2.37	2.50
8	2	20	64.80	1.76	1.91
8	4	86	68.46	1.88	2.06
9	2	60	74.70	2.64	2.75
9	4	70	77.80	2.21	2.47
9	6	80	80.90	2.13	2.31
10	2	39	83.99	3.19	3.62
10	4	64	87.24	2.66	2.87
48	1	46	443.56		6.40
48	1	98	444.08		6.20
48	6	82	451.42		5.40
48	7	15	452.25		5.20

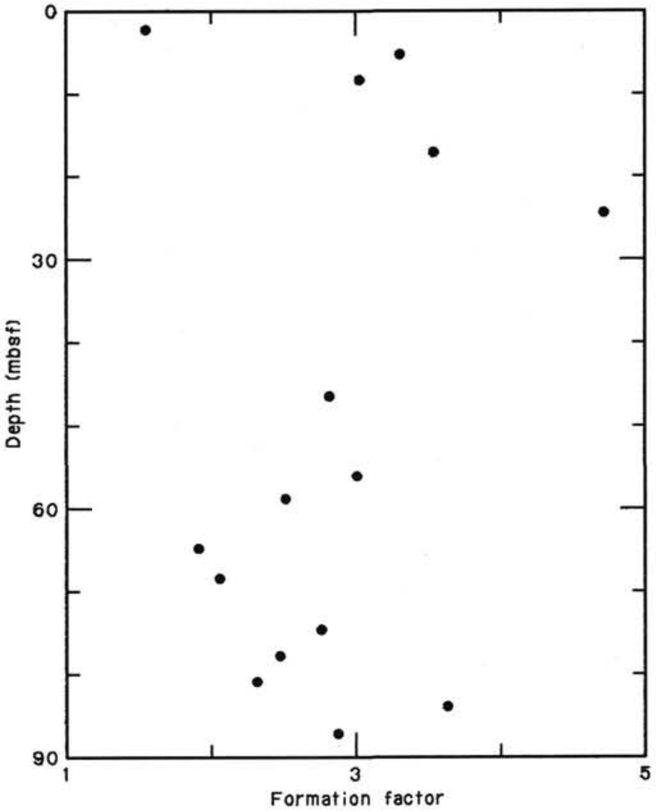

Figure 40. Formation factor vs. depth at Site 674, measurements from APC cores only.

the expected logarithmic relationship. The paucity of data from this site again reflects the overall disturbed nature of the recovered core. The good agreement between sites for the porosity/formation factor relationship suggests that a reasonable estimate of formation factor values might be obtained from index property measurements of porosity and an empirical fit to the existing data. Caution must be exercised, however, if this method is employed to estimate values for unusual lithologies, such as the well-cemented Eocene sands cored at some of the sites.

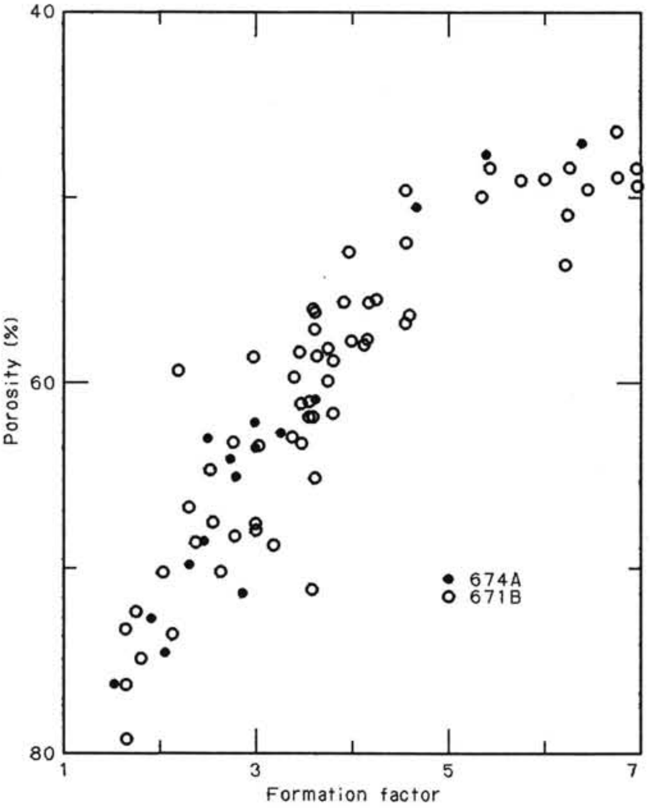

Figure 41. Formation factor vs. porosity at Sites 674 and 671. Data includes two measurements made at 445 mbsf as well as data displayed in Figure 40.

Shear Strength

Methods

The undrained shear strength at Site 674 was measured following the procedures outlined in Chapter 1. The only variation from these procedures was a change in the rate of rotation from 56°/min to 72°/min.

Results

Measurements were made in the upper 87 m of core samples where sample quality was good and a minimum (or no) drilling disturbance was observed. Results are listed in Table 12. Between 10 and 40 mbsf, the core samples were interpreted to be debris flow material. This material is inherently variable in strength and consequently, no shear strength was measured within this interval. In the upper 10 m, the peak shear strength increased from 20 kPa to 80 kPa with only one variation from the increasing trend at 8.35 mbsf (Fig. 42A and B). From 40 to 87 mbsf the peak shear strength increases monotonically with depth although there is scatter in the data. The maximum peak strength is 129 kPa, which occurs at 84 mbsf.

Table 12. Vane shear strength, Hole 674A.

Core 110-674A-	Sec.	Int. (cm)	Depth (mbsf)	Peak (kPa)	Residual (kPa)
1	2	75	2.25	19.61	4.61
1	3	0	3.00	39.89	
1	4	75	5.25	59.95	
2	2	75	8.35	25.37	
2	4	75	10.25	80.69	57.64
5	5	5	40.65	83.00	28.81
6	2	80	46.40	62.24	30.20
7	2	90	56.00	63.22	29.97
7	4	62	58.72	101.43	23.05
8	2	26	64.86	78.38	23.05
8	4	98	68.58	73.77	
9	2	70	74.80	110.67	23.06
9	4	80	77.90	85.30	11.53
9	6	70	80.80	80.69	13.84
10	2	34	83.94	129.12	16.13
10	4	57	87.17	101.44	

The residual shear strength is fairly consistent over the measured intervals (Fig. 42C), with a variation of 4 to 57 kPa and a mean of 24 kPa. The general trend is toward decreasing residual strength with increasing depth below seafloor. One measurement of remolded shear strength was made at 75 mbsf to check the variance with the residual measurement. The remolded shear strength was measured as 25 kPa and the residual as 23 kPa, a very small difference.

As at the previous sites, the residual shear strength was used to calculate the sensitivity of the sediment. The sensitivity reflects the decrease in residual strength below 40 mbsf, increasing from 3 to 8 between 41 and 84 mbsf (Fig. 42D) and possibly indicating a change in the physicochemistry of the sediment within this zone.

The total stress and hydrostatic stress conditions were calculated for Site 674 using the bulk density measurements incremented with depth. The stresses are very close to linear with depth (Fig. 43) and show only small deviations at this scale. A slight change in the slope of the total stress line occurs near 80 and 300 mbsf.

Discussion

The undrained shear-strength data can be broken into two separate regions. The upper region at the top of the core is char-

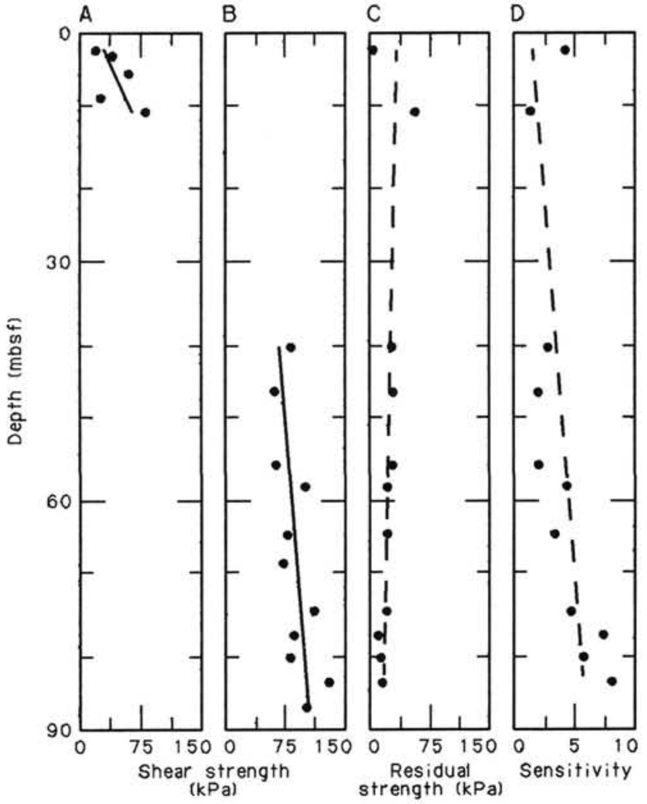

Figure 42. Shear strength (A, B), residual strength (C), and sediment sensitivity (D) at Site 674. Lines are least-squares regression fits to data discussed in text.

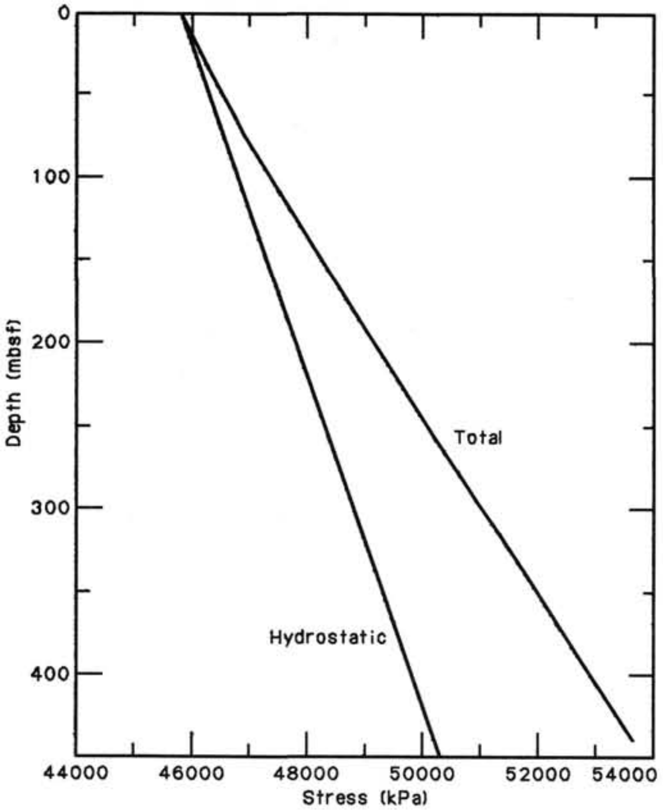

Figure 43. Total and hydrostatic stress vs. depth at Site 674. Assumed water depth is 4650 m.

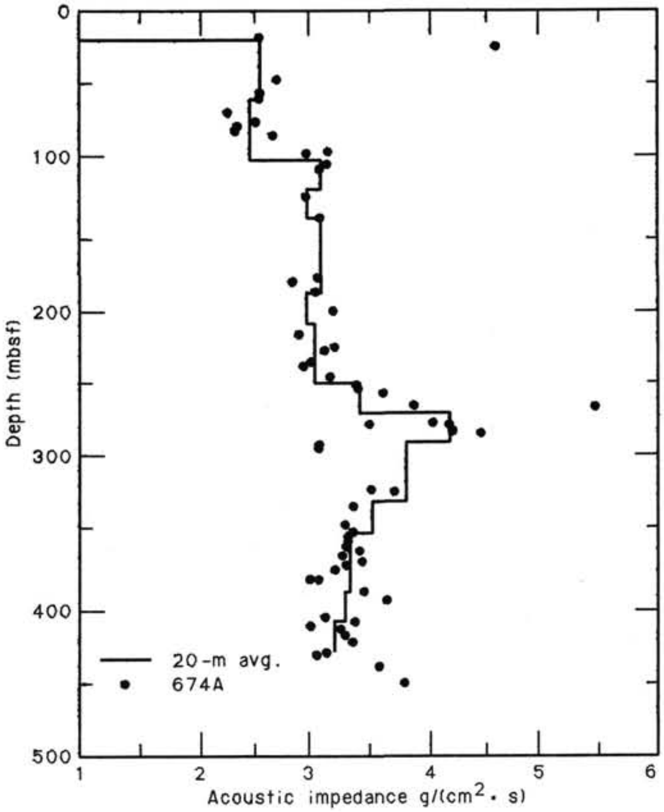

Figure 44. Acoustic impedance vs. depth at Site 674. Line represents results of running average of 20-m window calculated at 10-m intervals.

acterized by a rapid increase in strength over a very small depth interval. A linear least-square approximation to this upper sequence (Fig. 42A) results in the following correlation:

$$\text{Strength} = 20 + (4.4 * \text{Depth}),\ r = 0.59,\ N = 5$$

where depth is in meters and strength is in kilopascals, r is the correlation coefficient and N is the number of measurements.

Both the slope of the approximation and the intercept are high compared to the reference Site 672, which was characterized by a linear approximation with a slope of 0.8 and an intercept of 13. This is the highest strength increase measured in the Leg 110 study area. It suggests that the sediment could be overconsolidated in this upper sequence.

Below 40.7 mbsf, the shear strength increase with depth is much lower (Fig. 42B) and identical to that of the reference site with the following linear least-squares approximation:

$$\text{Strength} = 36 + (0.8 * \text{Depth}),\ r = 0.58,\ N = 11$$

where depth and strength units are as above. However, the intercept at the seafloor is much greater than at the reference site (36 kPa for Site 674 and 13 for Site 672). We suggest that this high intercept may be indicative of sediment erosion from the upper 40-mbsf sediment interval on the order of tens of meters, perhaps prior to the deposition of the debris flow sediments.

Summary

The index property and velocity data gathered at Site 674 serve to identify the three major tectonic units found by the paleontologic and stratigraphic observers. A profile of acoustic impedance (Fig. 44) illustrates that the boundaries between each of these units are the source of clear-cut reflections in the seismic records. The physical properties of the samples from within each of these tectonic units reflect the complexity of the stratigraphy.

A major question throughout the cruise has been to what extent the accretionary prism dewaters, at least in the realm that we are able to sample. We have plotted porosity vs. depth for Site 674 and also for the reference section, Site 672, in Figure 45. We have also plotted empirical curves for terrigenous sediment and radiolarian ooze taken from Hamilton (1976). The data from Site 672 agree well with the empirical curve, including the local maximum in porosity seen in the radiolarian-bearing Miocene sediments. These data suggest that our reference site data may represent a fairly regular sequence of sediment accumulation and dewatering. The data from Site 674, however, are not nearly as consistent. Entire intervals appear to have porosities greater than might be expected, while other segments have porosities below predicted values. It is reasonable to assume that faulting has played an important role in producing the observed profile. Each excursion from the empirical relationship may have a different explanation, and further study will be needed before they are understood. It is apparent from the plot, though, that there has not been a major amount of water lost from the sediments cored at Site 674.

A final interesting note concerns the bottom of the hole at Site 674. The index properties exhibit a reversed trend, seen most clearly in an increase in porosity (and density decrease) with depth from 300 to almost 400 mbsf. Several lines of stratigraphic evidence suggest that there is a large-scale fold, or at least reversal of section, within the zone from 300 mbsf to the bottom of the hole. The reversed trend would tend to support this sort of conclusion.

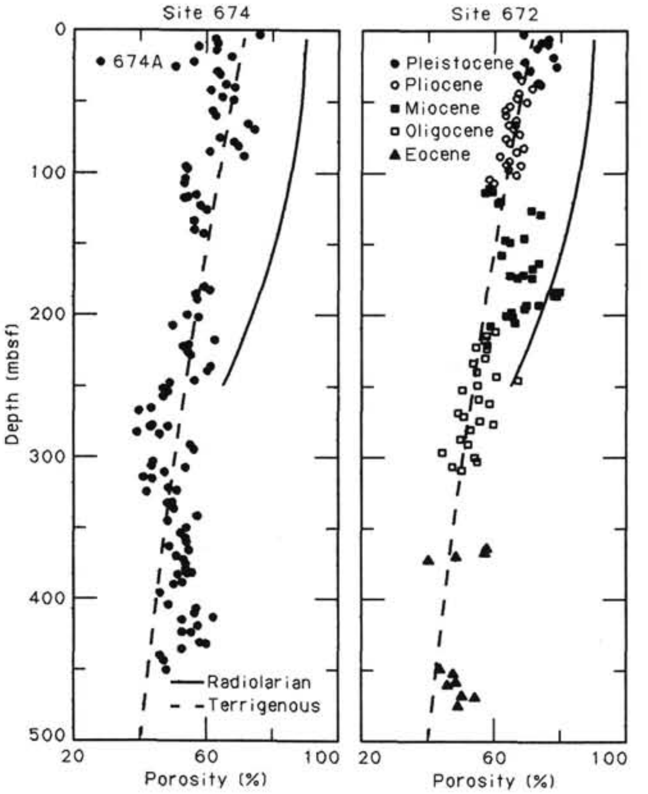

Figure 45. Porosity vs. depth at Sites 674 and 672 (reference site). Lines plotted are empirical curves for terrigenous sediments and radiolarian ooze (Hamilton, 1976).

SEISMIC STRATIGRAPHY

Site 674 is located 17 km arcward of the Barbados Ridge deformation front. Seismic reflection profiles across this location show very poor coherent reflectors. At Site 673, a few kilometers downslope, weak and discontinuous reflectors were still reasonably depicted on both seismic lines A3 and CRV 128. This is not the case at Site 674, although a cluster of small, discontinuous, weak to moderately strong reflectors can be observed. Accordingly we can only make tentative correlations between the well data and the seismic records.

Our tentative interpretation of line CRV 128 has been conducted in three stages as shown in the upper part of Figure 46. On the left is a line drawing with all observed reflectors. Assuming that large and continuous geological structures (such as thrust faults) are present in the accretionary complex, we selected the reflectors that appear to form continous and linear patterns (middle). Lastly, we only consider the reflectors that correlate with acoustic impedance contrasts as determined from the physical properties of Hole 674A sediments.

Site 674 is located at the foot of a relatively steep slope, possibly related to recent thrust faulting (see the Seabeam map, back pocket). Unfortunately, the true thickness of slope sediment, or the location of any structural features, are badly defined in the upper 50 m of Hole 674A. The first sharp increase in acoustic impedance appears at a depth of 95 mbsf. This event can be correlated with a sharp density contrast between Oligocene claystones (tectonic Unit A) and upper Pliocene calcareous mudstones (tectonic Unit B). The acoustic impedance vs. depth curve does not show any significant change from 95 mbsf down to 245 mbsf. A second increase of acoustic impedance is noted between 250 and 280 mbsf. This increase is clearly related to a sharp velocity change between lower Miocene green and brown claystones at the base of tectonic Unit B and the diversified clastic and calcareous lithologies of the middle Eocene at the top of tectonic Unit C.

If our seismic stratigraphic interpretation is correct, tectonic Units A, B, and C are bound by large eastward-verging thrust faults. The upper fault is subhorizontal while the lower fault is slightly dipping (10°) to the west. A relatively continuous reflector (R) just below hole penetration depth can be interpreted as a third and deeper thrust fault, but we do not have clear indication of it in the last cores. The interpretation of seismic line A3 is improved by projecting Site 674 onto it (Fig. 47). The seismic record shows a few westward-dipping reflectors that may be traces of the above-mentioned thrust faults. These faults are parallel to the thrust faults inferred at Site 673, most of which appear to originate at sea floor slope anomalies. The topographic expression of these thrusts implies that they are active, or have been recently reactivated.

HEAT FLOW

Introduction

Site 674 is located 17 km west of the deformation front of the Lesser Antilles accretionary complex. This site is the farthest arcward of any drilled on ODP Leg 110. A single hole was drilled to 452 mbsf and eight sediment and bottom-water temperatures were measured.

Methods and Results

See Chapter 1 for a discussion of experimental methods, intertool calibration and data reduction. Two different sampling intervals were used with the T-probe during measurements at Site 674: 5.12 s with the new electronics and 60 s with the old electronics. These different recorders used the same thermistor probes. Tool properties are summarized in Table 13 and temperature measurements are summarized in Table 14.

Hole 674A

The APC tool was deployed once in Hole 674A to a depth of 25.1 mbsf, while taking Core 110-674A-3H. A 10-min bottom-water measurement was made prior to measuring the sediment (Figs. 48A and B) resulting in a temperature of 2.20°C (±0.05°C). This value is in excellent agreement with bottom-water readings from Sites 671, 672, and 673. After pausing at mudline, the cutting shoe was thrust into the sediment, giving an extrapolated equilibrium temperature of 5.8°C (±0.2, Fig. 48B). There is a larger estimated error associated with this temperature measurement than is normal for the APC tool, because the cutting shoe was held in the sediment for 5 min before removal. With only 5 min of data available, several different cooling curves, with different final temperatures, were found to fit the data equally well. Each of these fits has an estimated error of 0.05 to 0.1°C, but the range in final values suggested an overall error of 0.2°C.

The T-probe was deployed a total of nine times before pulling out of Hole 674A. The new recorder was run first after Core 110-674A-10X, to a depth of 92.0 mbsf (Fig. 49A), with an extrapolated temperature of 10.3°C (±0.1°C). There was over 2 m of fill lining the bottom of the hole during the T-probe deployment at 110.0 mbsf. This fill prevented the probe from penetrating the formation, as is evident from the lack of a frictional heating spike in the temperature record (Fig. 49B). Other successful runs with the new electronics package were after Cores 110-674A-18X (168.0 mbsf), -22X (206.0 mbsf), and -26X (244.0 mbsf). The records from these runs (Figs. 49C through 50B) indicate equilibrium temperatures of 12.3°C (±0.1°C), 13.7°C (±0.1°C), and 14.6°C (±0.1°C), respectively. Two additional runs were made with the T-probe after Cores 110-674A-32X (301.0 m) and -40X (377.0 m). These runs produced records

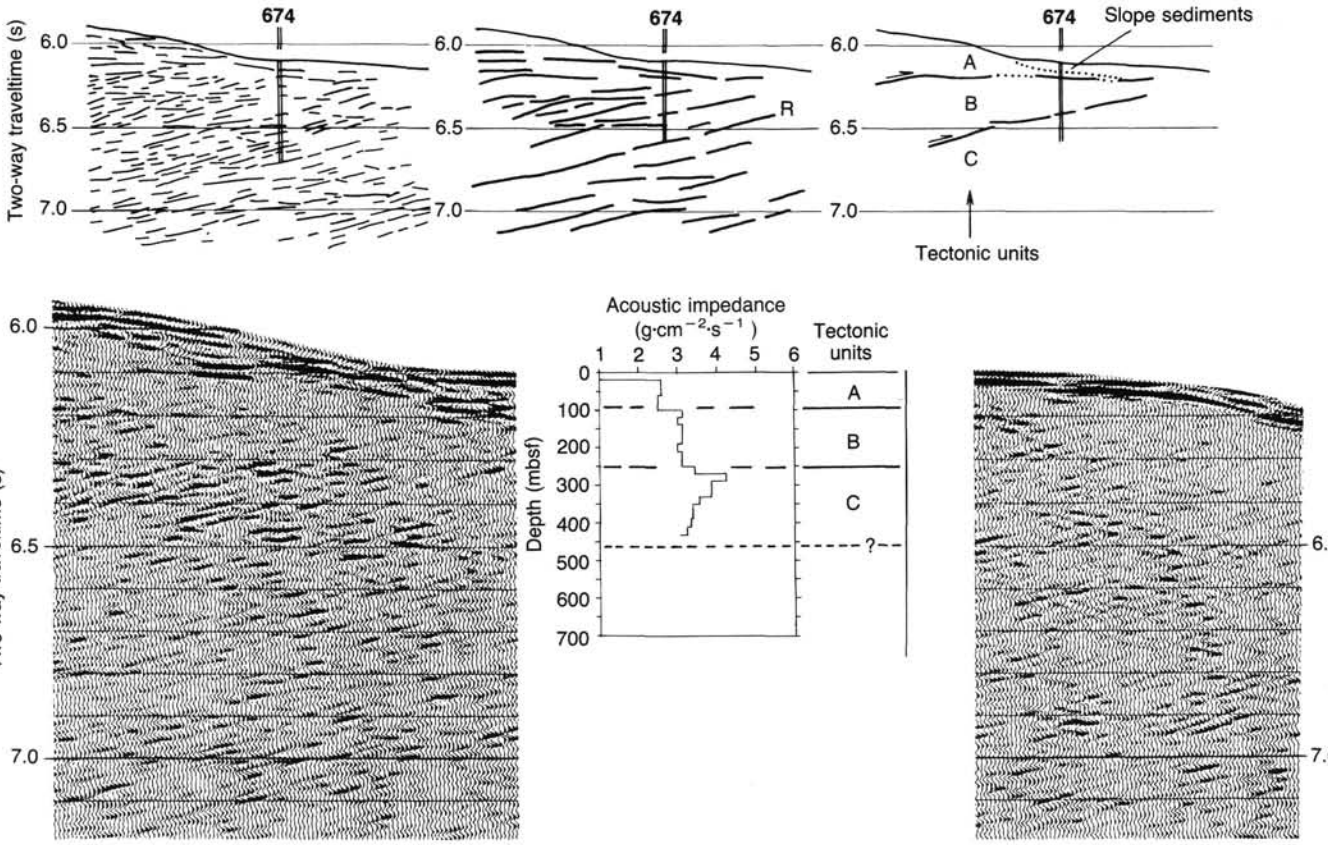

Figure 46. Location of Site 674 on line CRV 128. Bottom: Correlation of the seismic record with the acoustic impedance diagram. Top: Tentative scenario from successively interpreted line drawings.

which at first extrapolated to anomalously low temperatures. It was determined that a broken "high-calibration" resistor in the digital recording package caused the thermistor resistances to be calculated incorrectly. The recording unit was then checked with a precision decade box, and a systematic malfunction was found to have raised all resistances measured (lowered temperatures) during these runs by 25.7%. A resistance correction was applied, and the corrected, processed results are reproduced in Figures 50C and 51A with final temperatures of 16.15°C (±0.05°C) at 301.0 mbsf and 18.2°C (±0.1°C) at 377.0 mbsf.

The T-probe lance was slightly bent during penetration at 377.0 m. The old T-probe lance (Uyeda tool) and digital-recorder package was then deployed for two final runs. The package records a maximum of 128 values at an interval of either 1 or 2 min, whereas the new tool package will record several thousand samples at an interval no larger than 5.12 s. Records from runs at 434.0 and 453.0 mbsf (after Cores 110-674A-46X and -48X, respectively) are reproduced in Figures 51B and 51C and indicate that the T-probe moved while in the sediment on both runs. However, a frictional temperature spike from sediment penetration is present on both records.

From the bottom-water temperature and the sediment temperature measurements with the APC tool at 25.1 mbsf, a thermal gradient of 143°C/km has been calculated (Fig. 52). From the six good T-probe sediment temperature measurements, a linear thermal gradient of 28°C/km has been determined for the depth interval 92–377 mbsf. Variations in thermal conductivity (Fig. 53) were taken into account by calculating the integrated thermal resistance of the sediment column at each temperature-depth (see Seismic Stratigraphy section, Site 672 chapter). Using the thermal resistivity plot (Fig. 54) the calculated heat flow from 0 to 25.1 mbsf is 218 mW/m^2 and from 92 to 377 mbsf is 38 mW/m^2.

Interpretations

The thermal gradient from 0 to 25.1 mbsf of 143°C/km, and the surface heat flow, calculated to be 218 mW/m^2, are some of the highest values ever measured in this region (Speed et al., 1984). A heat-flow transect at 15°30′N (Langseth et al., 1986) found increasing surface heat flow westward on the accretionary complex, with several localized heat-flow highs. This upslope heat flow increase is in contrast to surveys at 14°20′ and 14°35′N which found progressive decreases of heat flow up the slope of the prism, as predicted by models of active margins (Toksoz et al., 1971; Hsui and Toksoz, 1979). The low values measured over the complex on these southern transects are also consistent with calculations of expected heat flow for 90-Ma crust (Anderson and Skilbeck, 1982; Lister, 1977).

The nature of the major change in thermal gradient between 25 and 92 mbsf at Site 674 is unclear. If the two gradients are extrapolated, they intersect at a depth of 48 mbsf. This change in the thermal gradient in the region of 25–92 mbsf has two plausible explanations:

1. Chemical analysis of pore water indicates low Cl$^-$ at 30 m (Geochemistry section, this chapter), which may reflect movement of less saline water through the sediment. Other low-Cl$^-$ anomalies at greater depths may indicate the same, although these are not associated with any change in the thermal gradient. There is considerable brecciation in the section from 20 to 35 mbsf and faulting at 20, 40, and 50 mbsf, sometimes associated with calcite veins. Warm water moving through this zone

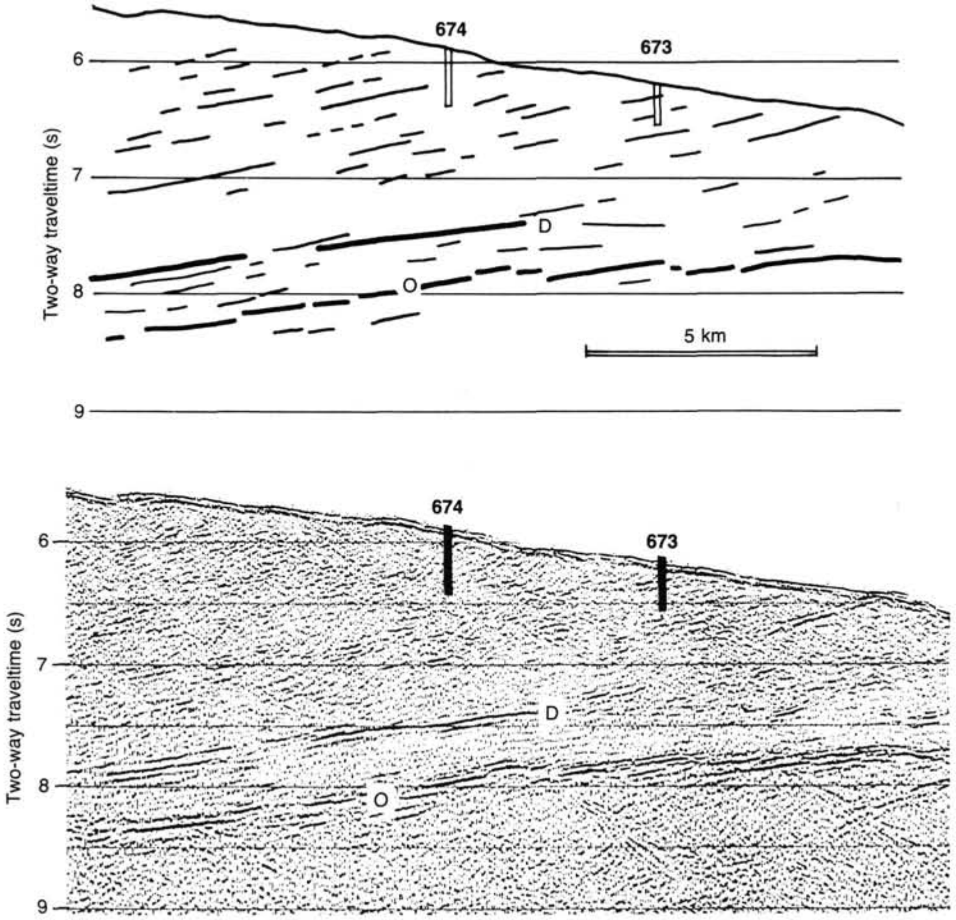

Figure 47. Projection of Sites 673 and 674 on seismic line A3. Site 673 is 0.5 km to the northeast and Site 674 is 5 km to the north. D: Décollement; O: Top of the oceanic crust.

Table 13. Temperature measurement instruments used at Site 674.

Tool	Thermistor housing	Thermistor resolution	Recorder program
APC Tool	Steel annular cylinder ID: 0.0617 m OD: 0.0786 m	0.02°C	15-s, recording interval
T-probe	Steel cylindrical probe 0.0125 m dia	0.05°C	5.12 or 60-s recording interval

Table 14. Temperature measurement summary at Site 674.

Depth (mbsf)	Tool	Equilibrium T (est error) (°C)	Sediment/Water temperature
0.0	APC tool	2.20 (0.05)	Water
25.1	APC tool	5.80 (0.20)	Sediment
92.0	T-probe	10.30 (0.05)	Sediment
168.0	T-probe	12.30 (0.10)	Sediment
206.0	T-probe	13.70 (0.10)	Sediment
244.0	T-probe	14.60 (0.10)	Sediment
301.0	T-probe	16.15 (0.05)	Sediment
377.0	T-probe	18.20 (0.10)	Sediment
434.0	T-probe	>20 Lower bound only	Sediment

would alter the sediment temperatures, increasing the thermal gradient in the upper 25 mbsf and effectively reducing the thermal gradient beneath the conduit. This water would need to maintain a sediment temperature of 5.8°C at 25 mbsf to yield the observed thermal gradients. If this flow stops, the gradient will smooth and become fully linear with time.

2. There has been relative upward movement of structural Units B and C compared to A, bringing these closer to the sediment-water interface, resulting in a thermal gradient from 0 to 377 mbsf which is not in equilibrium (see Structural Geology section, this chapter). At least 200 m of material would need to have been removed from the top of the section, assuming that the present thermal gradient from 92–377 mbsf was also the gradient before this movement. The loss of material could be a result of either tectonic thrusting of Packets B and C upwards, or slumping of sediments above the present sediment-water interface. Site 674 is located in an area of rough bathymetry that appears to be marked by slump scars (Background and Objectives and Seismic Stratigraphy sections, this chapter). Slump features (debris flows) are also present in cores recovered from this site between 9 and 33 mbsf (Structural Geology section) and also at Site 673, downslope of Site 674, which had 20 m of slump material in Hole 673A and 75 m in Hole 673B. Normal diffusive gradients for Mg^{++} and Ca^{++} (Geochemistry section, this chapter) do not support this explanation since they would require that either the displacement involved sedimentary units of similar geochemical composition, or that the time since displace-

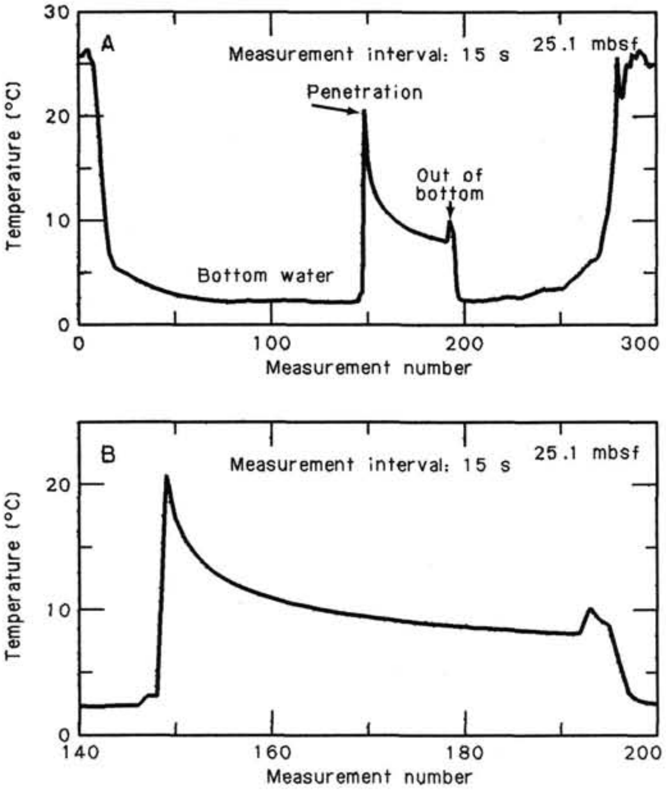

Figure 48. A. Temperature vs. time record for the only deployment of APC tool, Core 110-674A-3H. B. Detail of record of APC tool deployment, Core 110-674A-3H, showing sediment temperature.

ment is great enough to have allowed diffusion of the chemical signal. This geochemical evidence does not suggest upward migration of pore fluids through the sediment column.

Neither of the explanations above is completely consistent with all simple interpretations of the evidence at Site 674, nor does either explain why heat flow is apparently higher on the complex at 15°30′N than it is at 14°20′ and 14°35′N (Langseth, et al., 1986).

CONCLUSIONS

Site 674 is located 17 km arcward of the Barbados Ridge deformation front. It is the shallowest (water depth: 4560 m) and the furthest arcward of a series of penetrations including ODP Sites 671 and 673, and DSDP Sites 541 and 542 downslope, as well as the oceanic reference ODP Site 672. As at Site 673 located only 5 km downslope, the main objectives were to study the continuing structural and hydrologic evolution of accreted deposits and to make comparisons with sequences drilled at the toe of the complex (Site 671) and in the adjacent Atlantic plain (Site 672).

Site 674 penetrated three major tectonic units composed of sediments ranging in age from middle Eocene to early Pleistocene. They are separated by recent low-angle thrust faults which apparently postdate the internal deformation of each unit (Fig. 55). These faults can be correlated with poorly defined arcward dipping reflectors.

Tectonic Unit A (0–101 mbsf) includes five lithologic units (Fig. 56):

Unit 1 (0–9 mbsf) is composed of lower Pleistocene undeformed calcareous mudstones and marls with reworked pebbles of noncalcareous clays and thin ash layers. This unit is probably a slope deposit similar to the upper 40 m drilled at Site 673 and it unconformably overlies Unit 2.

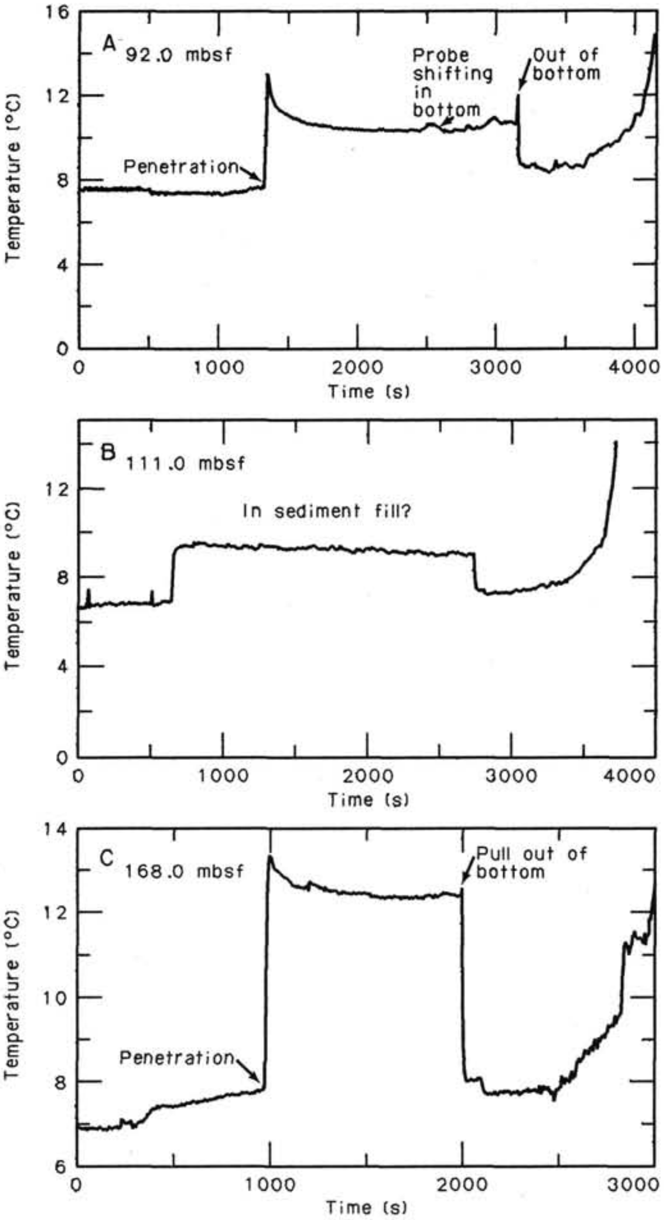

Figure 49. A. Temperature vs. time record for first deployment of T-probe, after Core 110-674A-10X. B. Temperature vs. time record for second deployment of T-probe, after Core 110-674B-12X. C. Temperature vs. time record for third deployment of T-probe, after Core 110-674B-18X.

Unit 2 (9–40 mbsf) is made of claystones with numerous reworked blocks (debris-flows ?) and a few ash layers. The ages of both matrix and blocks are unknown. This unit is similar to the lower half of lithologic Unit 1 in Hole 673B. Both of these units show internal deformation and could represent a large slump of Miocene material in Pleistocene slope deposits. A significantly steeper slope just west of Site 674 may indicate the source for this slump (see Seabeam map in the back pocket). Alternatively, Unit 2 could represent several thin slump deposits in an older, noncalcareous claystone, both subsequently thrust over the Pleistocene slope deposits. This slump unit overlies Unit 3, separated by a sedimentary or tectonic unconformity.

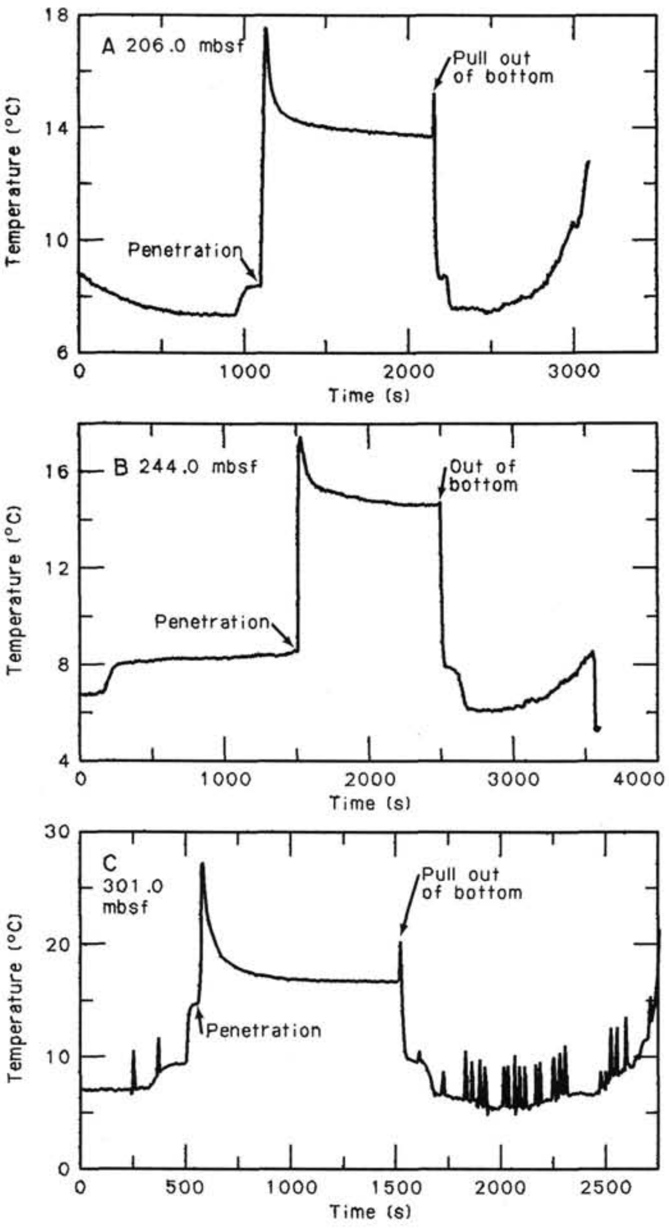

Figure 50. A. Temperature vs. time record for fourth deployment of T-probe, after Core 110-674A-22X. B. Temperature vs. time record for fifth deployment of T-probe, after Core 110-674A-26X. C. Temperature vs. time record for sixth deployment of T-probe, after Core 110-674A-32X.

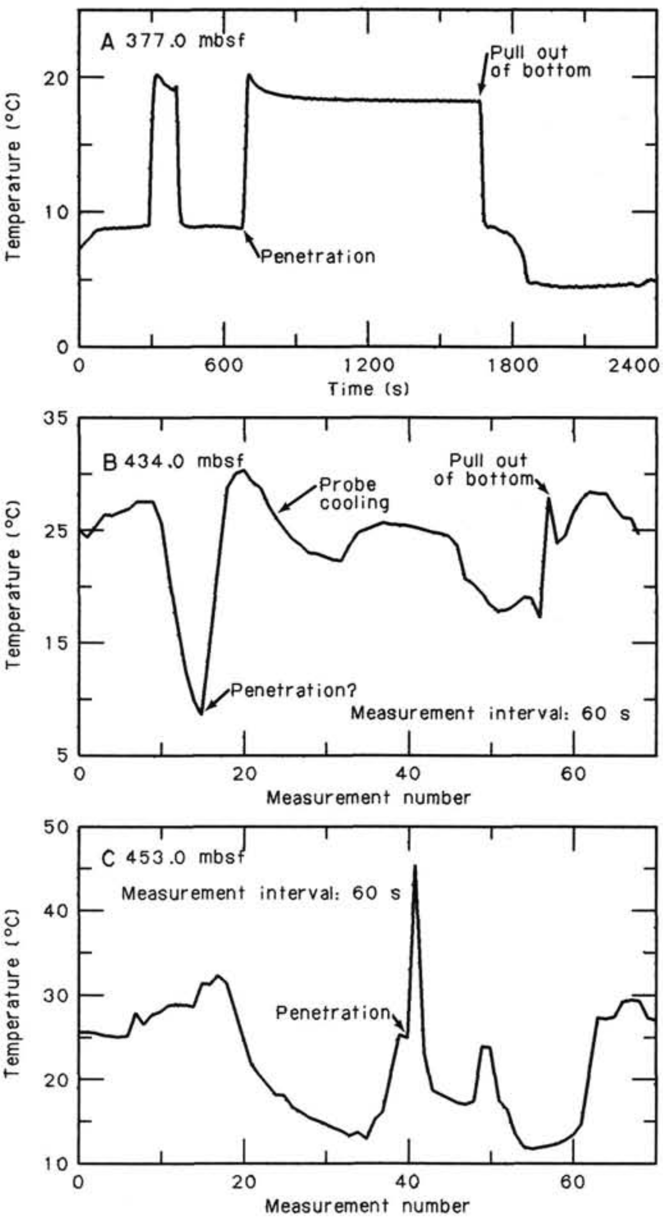

Figure 51. A. Temperature vs. time record for seventh deployment of T-probe, after Core 110-674A-40X. B. Temperature vs. time record for eighth deployment of T-probe, after Core 110-674A-46X. C. Temperature vs. time record for ninth deployment of T-probe, after Core 110-674A-48X.

Unit 3 (40–63 mbsf) is composed of undeformed lower Pleistocene to upper Pliocene calcareous mudstone, claystone and marl with few ash layers. This unit is similar to Unit 1 and is probably part of the slope apron into which Unit 2 has been emplaced. Unit 3 overlies Unit 4 without apparent unconformity.

Unit 4 (63–92 mbsf) is composed of claystones with few ash beds. The bedding dips are horizontal and the water content is still very high (about 70%). The formation is barren of fossils but lithologic correlation with Site 672 suggests a late Miocene age. This unit may represent the base of the slope cover that unconformably overlies lower Oligocene sediments in the top of Unit 5.

Unit 5 (92–101 mbsf) shows a well-developed scaly fabric and an apparent internal age reversal from early to late Oligocene (radiolarian zones R15 to R14) at the top. Lithologic correlation to Site 672 suggests the bottom of this unit could be of early Miocene age. This 10-m-thick unit corresponds to an abrupt change in physical properties and is interpreted as a shear zone in the offscraped sequence. This first occurrence of Oligocene rocks in the accreted complex demonstrates that the décollement has been at a deeper stratigraphic level than it is presently at Site 671. Also a certain amount of Oligocene or Miocene strata was probably eroded before the deposition of the upper Miocene sediments.

The top of tectonic Unit B corresponds to a sharp age reversal (Oligocene–early Miocene over late Pliocene) and is quite obviously related to a large thrust fault of post-late Pliocene age, i.e., younger than 3 Ma (Fig. 56). Tectonic Unit B (101–255 mbsf) includes two lithologic units:

Unit 6 (101–120 mbsf) is formed of steeply dipping lower to upper Pliocene claystone and mudstone with few ash layers. Strongly dissolved lower Pliocene microfaunas suggest that these

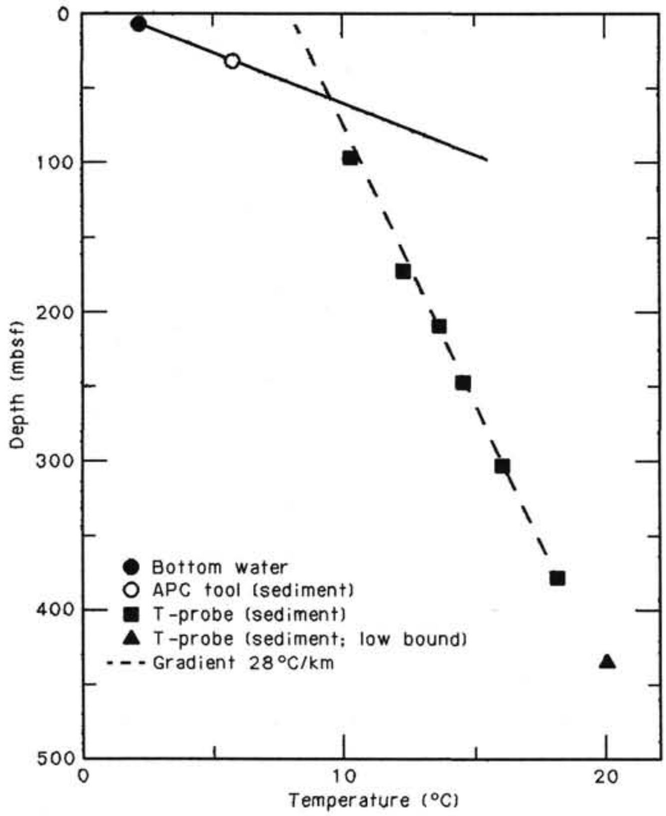

Figure 52. Plot of downhole temperatures in Hole 674A. The thermal gradient for the upper section (depth < 45 m) is 143 °C/km. The thermal gradient for the lower sediment section (depth > 45 m) is 28°C/km.

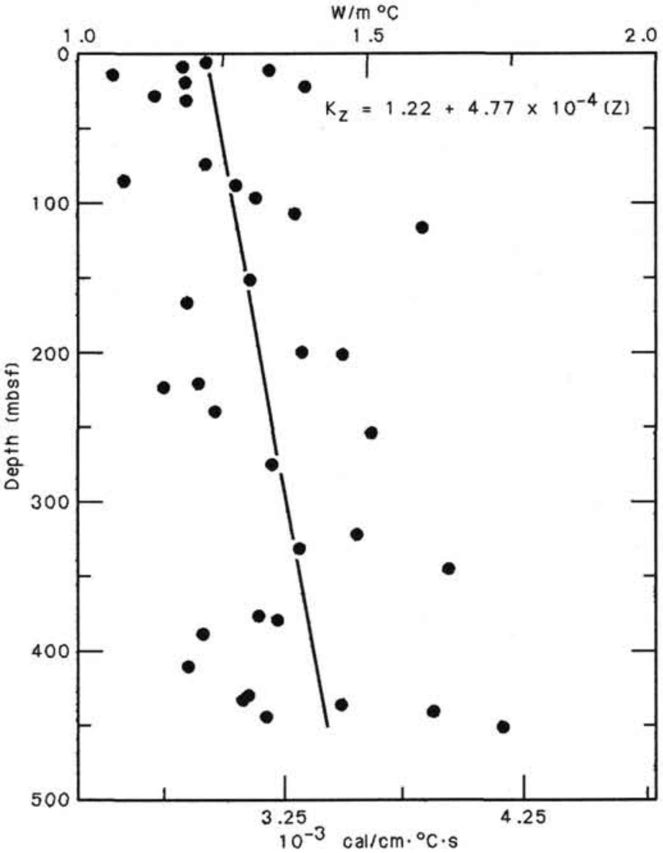

Figure 53. Plot of sediment thermal conductivity determined by the needle-probe method from cores taken from Hole 674A.

sediments were deposited at greater water depth than the equivalent faunas at the oceanic reference Site 672.

Unit 7 (120–255 mbsf) is composed of mudstone and claystone with a few ash layers. This whole sequence is barren of fossils and is tentatively dated as Miocene based on the ash content, lack of carbonate (see Site 672 for comparison), and the apparent continuity with Unit 6 of Pliocene age. However, this interval is much thinner than the Miocene section at Site 672. If the initial thicknesses at both sites were similar, then stratal thinning, related to reverse faulting, is a likely cause for this difference, as suggested by the structural data. The lowermost part of Unit 7 is correlated with the lower Miocene interval drilled at Sites 671 and 672 based on lithologic similarities, but it is lacking the radiolarian faunas found at the latter sites.

Bedding dips are quite steep in Units 6 and 7 (average: 50°) and both units show conspicuous development of moderately dipping scaly fabric. The age relationship between tectonic Units A and B suggests the following sequence of events: a) early-middle Miocene: thrust faulting followed by erosion in Unit 5; b) late Miocene: covering of the eroded surface by a slope cover, and c) underthrusting of Unit B below Unit A. Unit B includes lower and upper Pliocene sediments that can be interpreted either as a slope cover over accreted Miocene strata (but no unconformity has been observed), or as offscraped abyssal plain deposits. This latter scenario would require a large amount of displacement to thrust slope deposits of late Miocene age over late Pliocene sediments.

The lower Miocene mudstones at the bottom of tectonic Unit B are thrust over highly folded sequences of middle Eocene mudstone, limestone, and sandstone (top of tectonic Unit C). The whole Oligocene and the upper Eocene are missing between tectonic Units B and C (Fig. 56). This missing section could be attributed to normal faulting; however, we do not believe that this is the case because of the almost exclusive occurrence of compressive small-scale tectonic features. Tectonic Unit C (255–453 mbsf) is made of six lithologic units:

Unit 8 (255–291 mbsf) is formed of interbedded chalk, limestone, marl, calcareous mudstone, and sandstone. These sediments are dated as middle Eocene according to foraminifer, nannoplankton, and radiolarian assemblages. This sequence is lithologically quite similar to the equivalent age sediments drilled at the oceanic reference Site 672. The presence of scattered early Miocene nannoplankton within this unit is puzzling. There is very little chance that the observed middle Eocene microfossils could be reworked because the unique facies of these rocks correlates exactly to the middle Eocene at Site 672. We propose, instead, that the Miocene nannofossils were incorporated into the Eocene rocks by small-scale tectonic imbrication or intrusion of mud slurry. Unit 8 is probably in thrust contact with Unit 9 below.

Unit 9 (291–301 mbsf) is made of lower Oligocene siliceous claystone and mudstone. This facies differs from equivalent age rocks at Site 672 but it shows some similarities with the Oligocene drilled at Site 543. This Unit 9 probably overthrusts Unit 10.

Unit 10 (301–320 mbsf) is composed of claystone and calcareous mudstone with middle Miocene nannofossils. Unit 10 shows strong scaly fabric and could be interpreted as a single shear zone within disrupted middle Miocene strata.

Units 8, 9, and 10 can be interpreted either as a single sheared overturned sequence or as upright units separated by thrust faults.

Unit 11 (320–339 mbsf) is composed of upper Eocene mudstone and claystone with few siliceous intervals. Scaly fabric is also intensively developed in this unit.

Unit 12 (339–405 mbsf) includes siliceous claystone and mudstone of early Oligocene age with mixed middle Eocene to Oli-

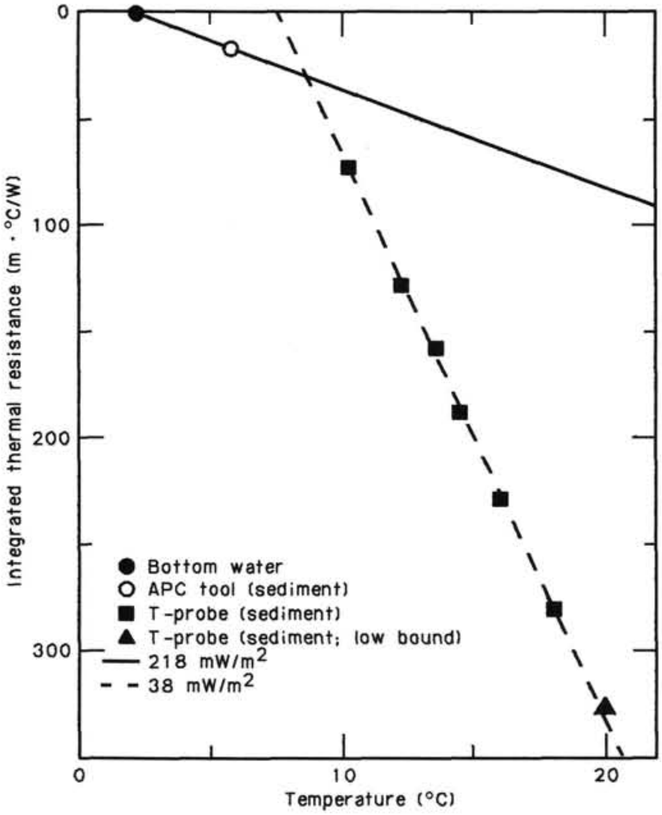

Figure 54. Plot of downhole temperatures vs. integrated thermal resistance at Site 673. Linear-least-squares best-fitted heat flow for the lower section (depth > 45 m) is 38 mW/m^2. Heat flow for the upper section (depth < 45 m) is 218 mW/m^2.

gocene radiolarians in the deepest core. If Unit 12 is stratigraphically continuous with Unit 11 then both units form a single overturned sequence. Alternatively the scaly fabric at the top of Unit 12 and in Unit 11 marks a thrust contact separating two distinct upright units.

Unit 13 (405–453 mbsf), the deepest sequence cored at Site 674, contains claystone and mudstone with a few ash layers. Unit 13 is barren of fossils, and lithologic correlations with sediments from other holes are ambiguous. The unit shows some similarities with Oligocene facies of Units 9 and 12, but it may also correspond to strata of inferred Miocene age (as proposed for Unit 7). The lower 30 m of Unit 13 is composed almost entirely of scaly and stratally disrupted rocks.

The sediment physical properties distinctly show three domains which are, from top to bottom (Fig. 57):

An upper section (0–90 mbsf) has low densities (and correlative high water content and porosity) roughly decreasing with depth. The density data suggest these upper series are slope cover. Two higher density values at depths of 20–30 m could be related to blocks in a debris-flow.

The second physical properties unit shows intermediate values of density with no clear increasing or decreasing trend. This section is correlated with tectonic Unit B and probably the lower 10 m of tectonic Unit A (lithologic Unit 5). Both are part of the accreted complex.

The lower section has the highest densities but the values are particularly scattered and high between 250 and 340 mbsf. This interval is characterized by rapid changes in ages, well-developed scaly fabric and intense shearing. On the other hand, most of the low-density values in this lower section correlate with radiolarian-rich zones, suggesting that the scattering of values is also related to variations in grain density.

An important conclusion from the porosity, density, and water content data is that, although tectonic deformation is intense, dewatering has not been dramatic with respect to the sediments of same ages and facies in the Atlantic abyssal plain (Site 672). For instance, the lower Oligocene sediments at Site 674 still have an average water content of 30% between 340 and 400 mbsf, whereas at Site 672 the same time interval shows an average water content of 35% between 250 and 325 mbsf.

Site 674 was the only site of Leg 110 where temperature measurements were regularly taken from the seafloor to the bottom of the hole. The results show two distinct features: a) a poorly constrained superficial gradient (0–25 mbsf) of 143°C/km and b) a clearly defined gradient at depth (92–453 mbsf) of 28°C/km. The shallow gradient is anomalously high even with respect to the already high gradients at Sites 673 (73°C/km from 0 to 75 mbsf), 671 (103°C/km in the upper 36.4 m), and 672 (79°C/km from 0 to 135 mbsf). This gradient, if linear, will intersect the deeper gradient at 48 mbsf. Two possible explanations have been so far proposed to explain this distribution of temperatures: a) warm waters are being laterally supplied at a depth of about 30 mbsf and create the superficial gradient (this is supported by a low chloride content at this depth), or b) the accretionary complex is heated as a whole along numerous flow paths (as suggested by several low-chloride anomalies between 200 and 453 mbsf) and the upper gradient is owing only to the presence of the 2.2°C isotherm at the water/sediment interface. Both hypotheses imply circulation of water from depth in the accretionary complex and each of them can similarly explain the anomalously high temperature gradients at other sites. However, they do not explain why such high superficial temperature gradients so far have been encountered only at the latitude of the Leg 110 site transect.

Low-chloride contents in formation water provide clear evidence for fluid flow in sediments. The amount of flow could, however, be underestimated if moving waters locally have no geochemical anomalies. The depletion of chloride in formation waters is probably related to membrane filtering under large effective stresses. At Site 674, low-chloride contents occur at 30 mbsf and, with less confidence, at 250, 310, and 440 mbsf. The three deeper minima correlate with major shear zones and scaly fabrics suggesting, as at the previous sites, that advection and higher permeabilities are better developed in fractured zones. The low-chloride value at 30 mbsf occurs in a unit that could either be a debris flow or fault zones, tinging the exclusive correlation of geochemical anomalies and structural features. The simplest explanation for the observed chloride distribution is that faulting has been recently active in the slope cover leading to the advection of low-chloride water. The pore waters are devoid of methane, suggesting that they originate only from moderate depths where temperatures are insufficient for thermogenic gas generation.

Sites 674 and 673 provide unique insights into the tectonic and sedimentary processes occurring in the accretionary complex 17 and 12 km arcward of the deformation front, and 600 m and 400 m, respectively, above the abyssal plain. These sites link present accretionary processes, as observed at Site 671, to rocks of ancient accretionary complexes as exposed on Barbados Island. From the summary of Sites 674 and 673, three major points are especially noteworthy:

1. Slope sediment aprons can develop quite early in the history of the propagating accretionary prism. Sites 673 and 674 document resedimentation of material from upslope as isolated claystone pebbles in the *in-situ* calcareous mud, and as massive debris flows up to few tens of meters thick (here probably of Miocene materials). At Site 674 these deposits may locally be de-

formed by thrust faults propagating from the underlying complex. Continuation of such faulting will lead to the incorporation of the slope sediments in the accretionary complex.

2. Site 674 probably recovered the most highly deformed rocks from an accretionary complex in the history of DSDP-ODP drillings. The structural interpretation of the cores was difficult because: a) observations are only along one (vertical) dimension; b) cores were not oriented horizontally; c) no detailed correlation with seismic data was possible; d) drilling disturbances were superimposed on tectonic features; e) very few unambiguous bedding facing directions were determined; and f) sections barren of fossils encompassed half of the hole. Nevertheless, the detailed structural data provide constraints for any geological model of the deformational history (e.g., Fig. 58). Clearly the out-of-sequence thrusts are relatively young features that have developed after the initial frontal offscrapping. These thrusts separate tectonic units which show relatively homogeneous internal structures but marked differences with adjacent units. The physical properties change rapidly across these tectonic boundaries, but the overall water content of accreted sequences remains high (20–40% of their total weight). Lastly, the intensity of the scaly fabric and of calcite veining increases downsection.

3. Fluid transport in the accreted sequences is clearly documented by the pore-water chemistry. Chloride minima correlate to some biostratigraphically documented fault zones indicating that advection of water is restricted to some discrete pathways with enhanced fracture permeability. The absence of thermogenic methane suggests that most of the fluids originate from dewatering processes in the upper 2 km of the accreted complex. Flow of water is also strongly supported by *in-situ* temperature measurments. Because of the very rapid temporal decay of any temperature anomaly, the high sub-bottom temperatures at Site 674 necessitate a permanent input of warm water.

REFERENCES

Anderson, R. N., and Skilbeck, J. N., 1982. Oceanic heat flow. *In* Emiliani, C. (Ed.), *The Oceanic Lithosphere*, Volume 7, *The Sea*, New York (Wiley and Sons): 489–524.

Berggren, W. A., 1977. Late Neogene planktonic foraminiferal biostratigraphy of the Rio Grande Rise (South Atlantic). *Mar. Micropaleontology*, 2, 3:265–313.

Bolli, H. M., and Premoli Silva, I., 1973. Oligocene to Recent planktonic foraminifera and stratigraphy of the Leg 15 Sites in the Caribbean Sea. *In* Edgar, N. T., Saunders, J. B., et al., *Init. Repts. DSDP*, 15: Washington (U. S. Govt. Printing Office), 475–497.

Boyer, S. E., and Elliott, D., 1982. Thrust systems. *Am. Assoc. Petrol. Geol. Bull.*, 66:1196–1230.

Gartner, S., 1977. Calcareous nannofossil biostratigraphy and revised zonation of the Pleistocene. *Mar. Micropaleontology.*, 2:1–25.

Goll, R. M., 1972. Leg 9 Synthesis, Radiolaria. *In* Hays, J. D., et al., *Init. Repts. DSDP*, 9: Washington (U.S. Govt. Printing Office), 947–1058.

Hamilton, E. L., 1976. Variations of density and porosity with depth in deep-sea sediments, *J. Sediment Petrol.*, 46, 280–300.

Hsui, A. T., and Toksoz, M. N., 1979. The evolution of thermal structures beneath a subduction zone, *Tectonophysics*, 60:43–60.

Langseth, M., Westbrook, G., and Hobart, M., 1986. Geothermal transects of the lower trench slope of the Barbados accretionary prism, [paper presented at the 11th Annual Caribbean Geological Conference, Bridgetown, Barbados].

Lister, C.R.B., 1977. Estimates for heat flow and deep rock properties based on boundary layer theory. *Tectonophysics*, 41:157–171.

Mascle, A., Biju-Duval, B., de Clarens, Ph., and Munsch, H., 1986. Growth of accretionary prism, tectonic processes from Caribbean examples. *In* Wezel, D. (Ed.), *The Origin of Arcs*: New York (Elsevier Scientific).

Okada, H., and Bukry, D., 1980. Supplementary modification and introduction of code numbers to the low-latitude coccolith biostratigraphic zonation (Bukry 1973, 1975). *Mar. Micropaleontology*, 5: 321–325.

Riedel, W. R., and Sanfilippo, A., 1978. Stratigraphy and evolution of tropical Cenozoic radiolarians. *Micropaleontology*, 24:61–96.

Saunders, J. B., Bernoulli, D., Mueller-Merz, E., Oberhaensli, H., Perch-Nielsen, K., Riedel, W. R., Sanfilippo, A., and Torrini, R., Jr., 1984. Stratigraphy of Late Middle Eocene to Early Oligocene in Bath Cliff section Barbados, West Indies. *Micropaleontology*, 30:390–425.

Speed, R. C., Westbrook, G. et al., 1984. Lesser Antilles Arc and adjacent terranes. *In Atlas 10*, Ocean Margin Drilling Program, Regional Atlas Series: Woods Hole (Marine Science International).

Speed, R. C., Westbrook, G. K., Biju-Duval, B., Ladd, J. W., Mascle, A., Moore, J. C., Saunders, J. B., Schoonmaker, J. E., and Stein, S., 1984. *Atlas 10*, Ocean Margin Drilling Program; Lesser Antilles and Adjacent Ocean Floor: Woods Hole (Marine Science Institute Publication).

Toksoz, M. N., Minoar, J. W., and Julian, B. R., 1971. Temperature field and geophysical effects of a downgoing slab, *J. Geophys. Res.*, 76:1113–1138.

Valery, P., Nely, G., Mascle, A., Biju-Duval, B., Le Quellec, P. and Berthon, J., 1985. Structure et croissance d'un prisme d'accretion tectonique proche d'un continent: La ride de la Barbade au Sud de l'arc antillais. *In* Mascle, A. (Ed.), Geodynamique des Caraibes, edition Technip: 173–186.

Westbrook, G. K., Mascle, A., Biju-Duval, B., 1984. Geophysics and the structure of the Lesser Antilles Forearc: *In* Biju-Duval, B., and Moore, J. C., et al., *Init. Repts. DSDP* 78A: Washington (U.S. Govt. Printing Office), 23–38.

Ms 110A-108

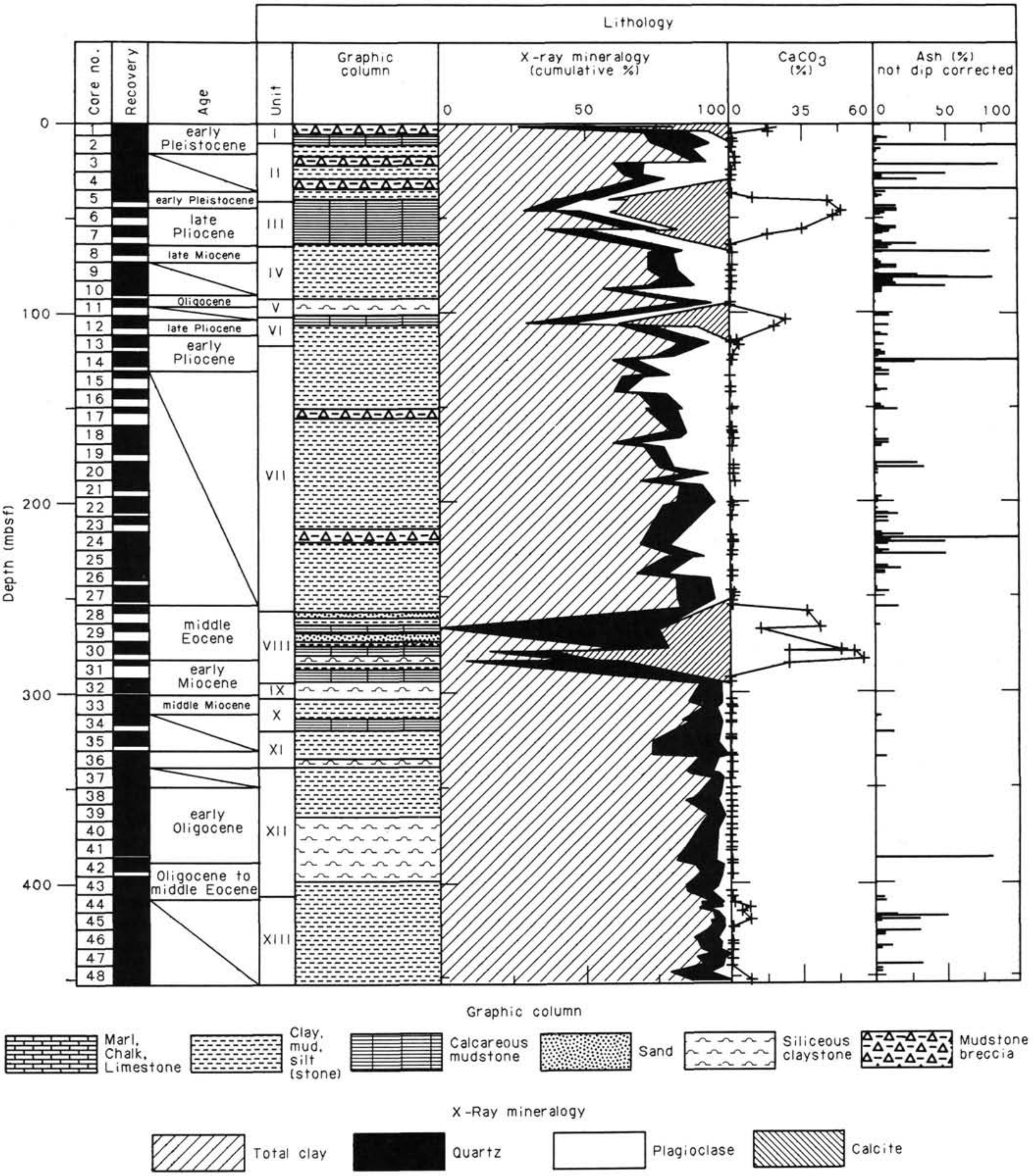

Figure 55. Site summary diagram, Site 674.

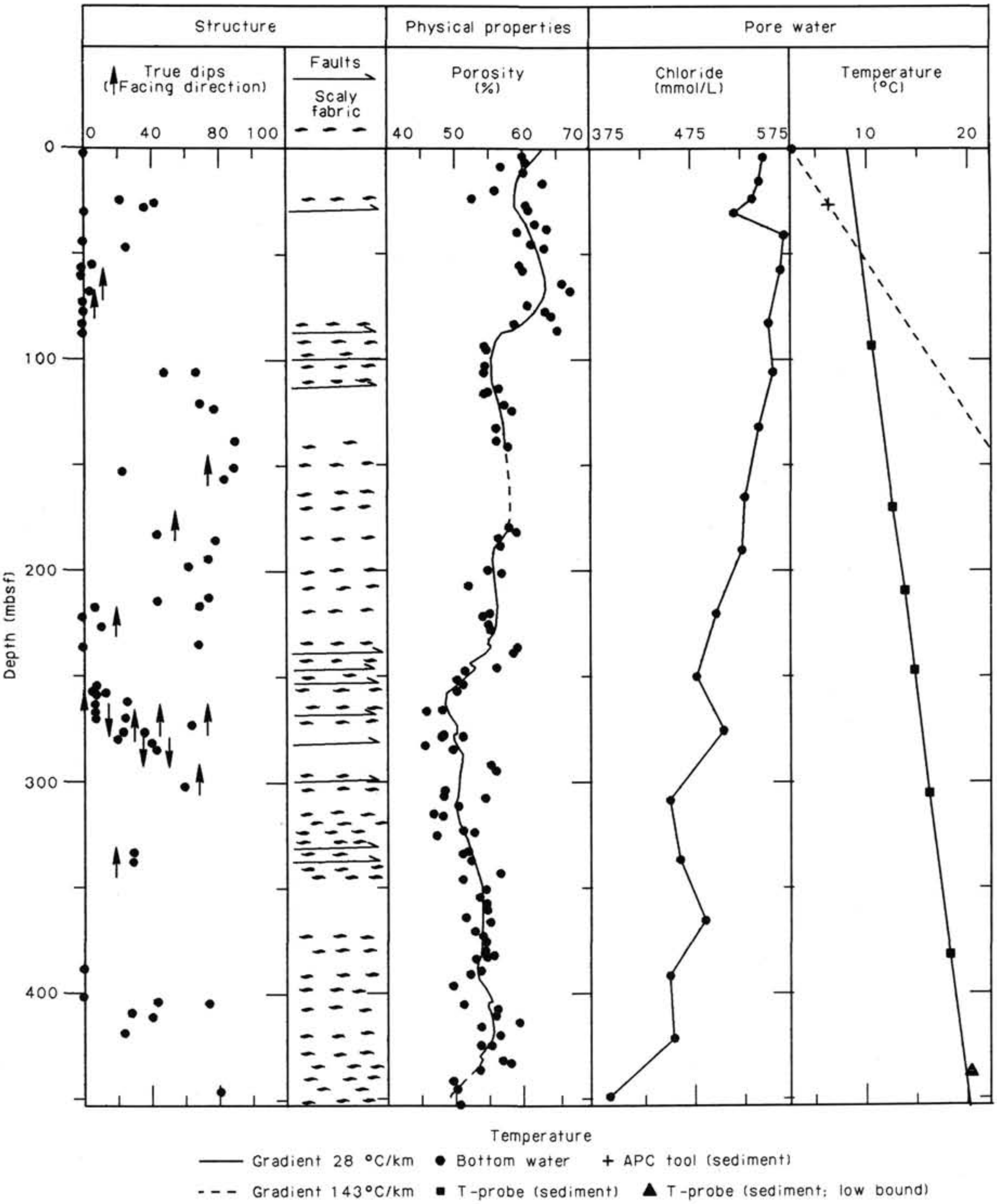

Figure 55 (continued).

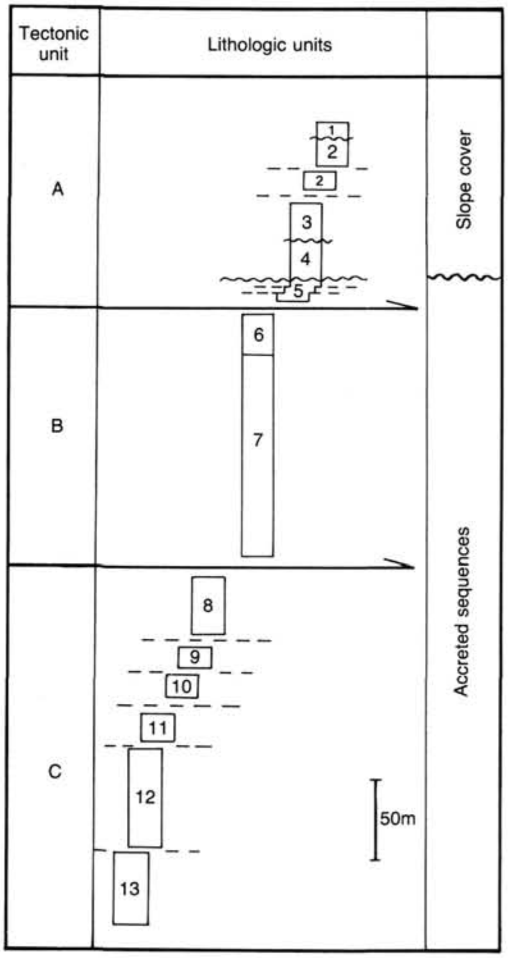

Figure 56. Correlation between tectonic units and lithologic units.

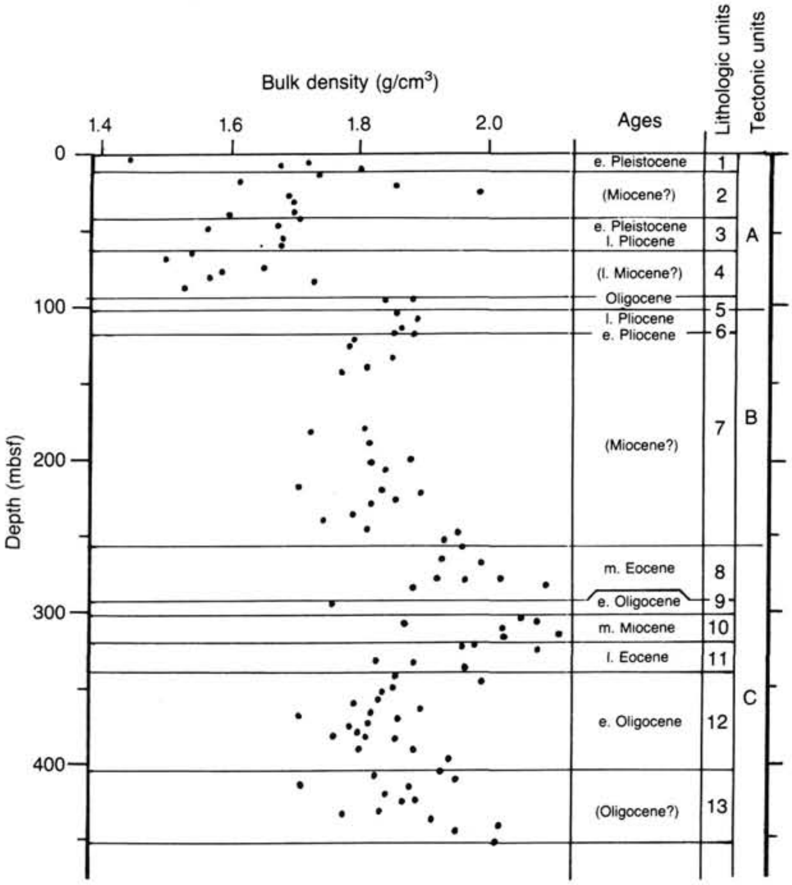

Figure 57. Correlation between densities and lithologic units.

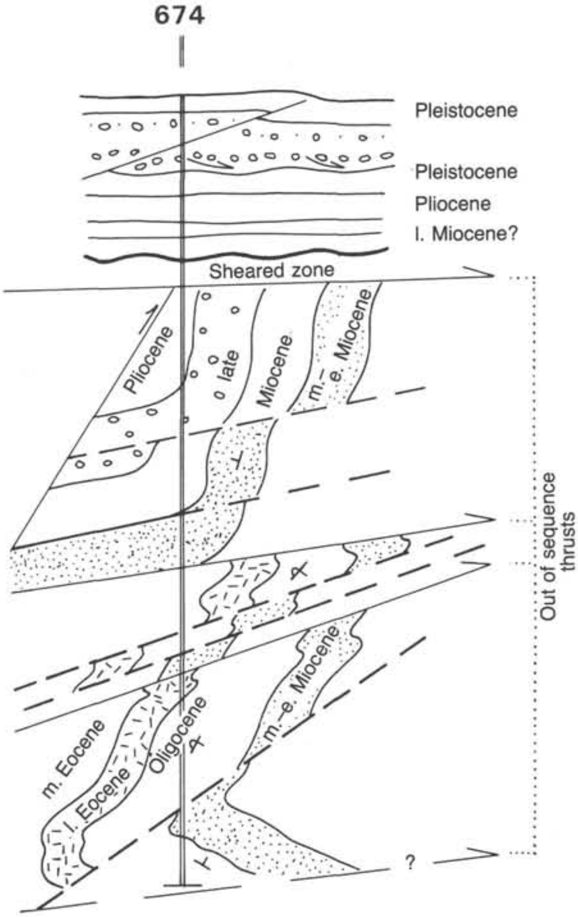

Figure 58. One of the many possible models for Site 674. In this simplified model, the following assumptions are made: a) Beds dip either east or west. This hypothesis is fundamental for any structural interpretation, and is a necessary simplifying assumption because the cores are not orientated. b) Major thrust faults are out-of-sequence types, i.e., there is no direct correlation between beds across these faults. c) The lower half of the cored section (below 256 mbsf) is considered to be overturned down to 410 mbsf. d) Most of the structures are interpreted in terms of a first stage of folding and imbricate thrusting, and a second stage of out-of-sequence thrustings.

SITE 674 HOLE A CORE 1 H CORED INTERVAL 4550.2-4556.3 mbsl; 0.0-6.1 mbsf

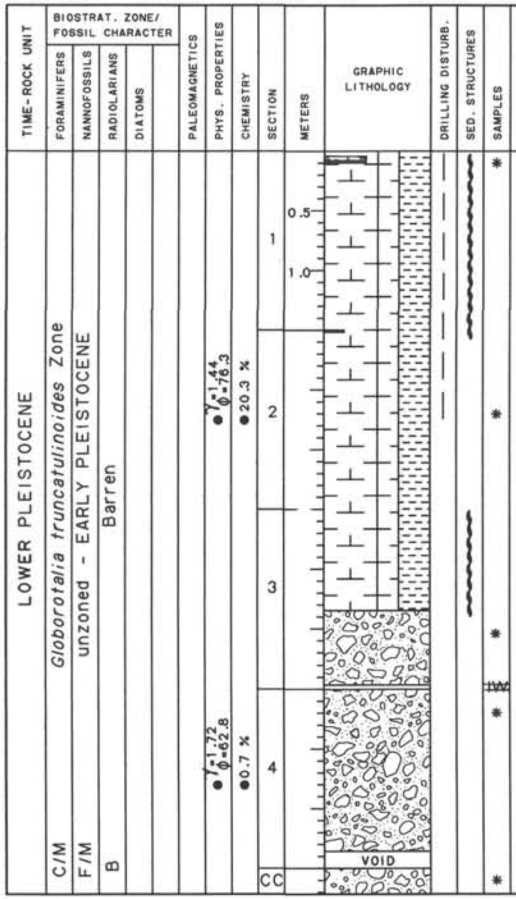

LITHOLOGIC DESCRIPTION

MARL and CALCAREOUS MUD, and CONGLOMERATE with MUDSTONE matrix and CLAYSTONE pebbles

Two dominant lithologies:

Section 1, 0 cm, to Section 3, 84 cm: homogeneous yellowish brown (10YR5/6 to 10YR7/4) MARL and CALCAREOUS MUD (foraminifers and nannofossils), with two thin ash layers at Section 1, 8 cm, and Section 2, 3 cm.

Section 3, 84 cm, to CC, 21 cm: matrix-supported CONGLOMERATE with dark olive-gray (2.5Y5/4) MUDSTONE matrix and dark olive-gray (2.5Y5/4) CLAYSTONE pebbles.

SMEAR SLIDE SUMMARY (%):

	1, 6 M	2, 68 D	3, 105 M	4, 19 M	CC, 1 D
TEXTURE:					
Sand	50	10	—	—	—
Silt	20	20	5	25	15
Clay	30	70	95	75	85
COMPOSITION:					
Quartz	3	—	—	—	2
Feldspar	20	1	Tr	2	3
Clay	55	24	95	73	85
Volcanic glass	—	—	4	—	3
Accessory minerals	2	—	Tr	25	—
Orthopyroxene	4	—	—	—	—
Clinopyroxene	3	Tr	—	—	Tr
Hornblende	5	Tr	—	—	—
Foraminifers	3	20	—	—	2
Nannofossils	4	50	—	—	3
Sponge spicules	1	Tr	—	—	—
Bioclasts	—	5	—	—	2

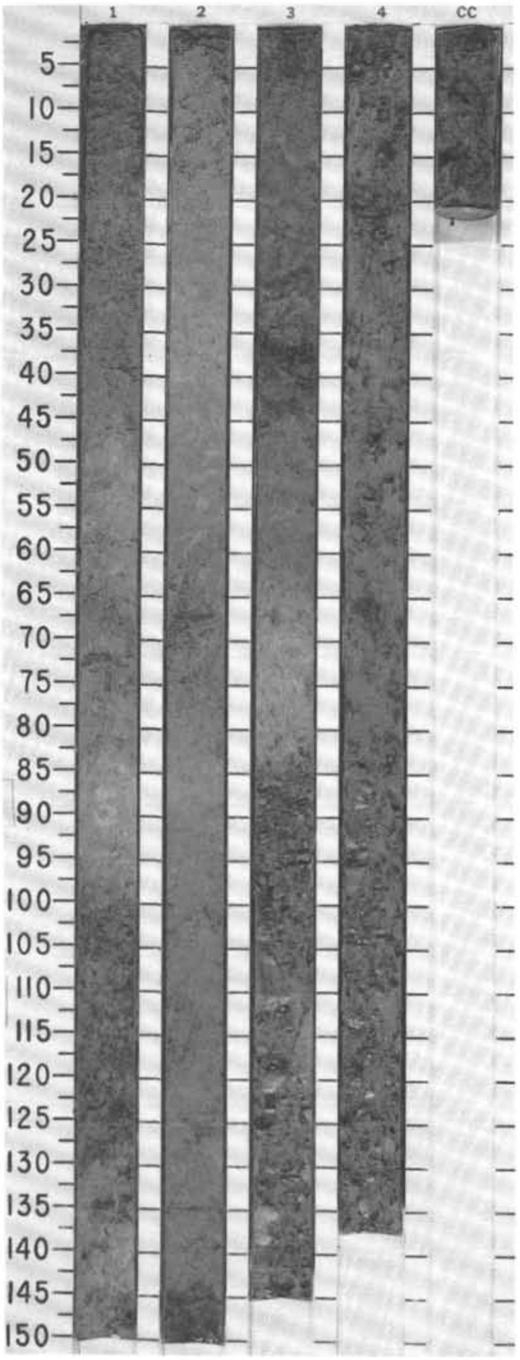

SITE 674 HOLE A CORE 2 H CORED INTERVAL 4556.3-4565.8 mbsl; 6.1-15.6 mbsf

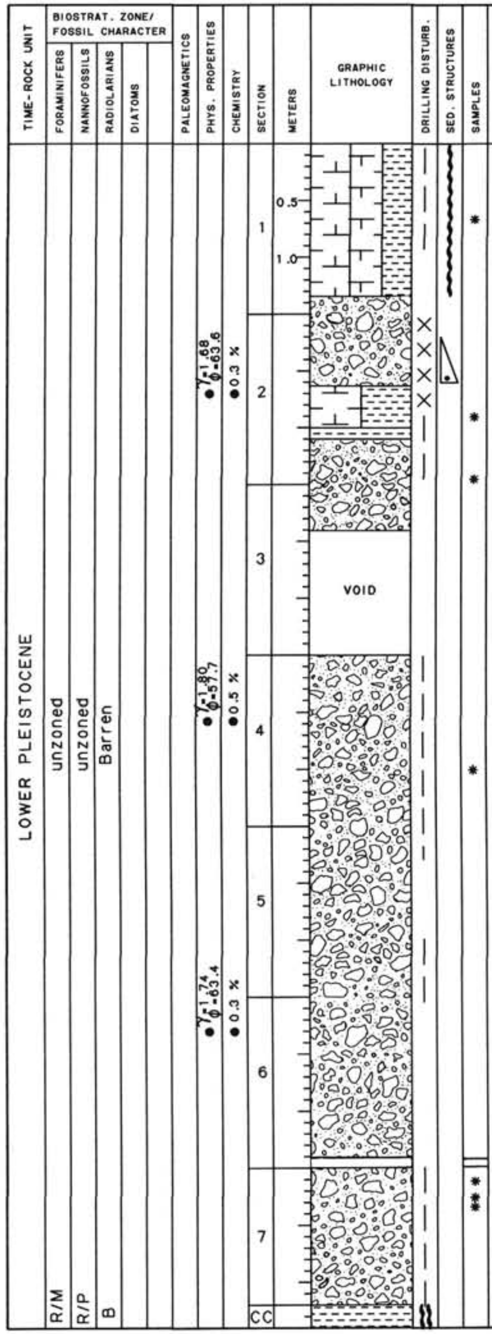

LITHOLOGIC DESCRIPTION

CONGLOMERATE and BRECCIA of CLAYSTONE

Matrix-supported CONGLOMERATE and BRECCIA; matrix is olive-gray (5GY5/1 to 5G4/2) CLAYSTONE; rounded to sub-angular pebbles are dark olive-gray (5G5/2) CLAYSTONE with some dark ashy mottles; minor chalk pebbles.

SMEAR SLIDE SUMMARY (%):

	1, 67 D	2, 84 D	2, 145 M	4, 102 M	7, 18 M	7, 34 D	7, 35 M
TEXTURE:							
Sand	10	—	1	—	—	—	—
Silt	20	5	4	7	—	12	—
Clay	70	95	95	93	100	88	100
COMPOSITION:							
Quartz	Tr	—	—	Tr	—	1	Tr
Feldspar	Tr	1	1	5	—	Tr	Tr
Clay	30	50	95	93	20	88	100
Volcanic glass	—	1	4	—	—	5	—
Calcite/dolomite	—	—	—	—	80	Tr	—
Accessory minerals	—	1	—	—	—	5	—
Hornblende	—	—	—	—	—	Tr	—
Fe/Mn oxide	—	1	—	2	—	—	—
Foraminifers	30	5	—	—	—	—	—
Nannofossils	40	40	—	Tr	—	—	—
Sponge spicules	—	Tr	—	—	—	—	—
Fish remains	—	1	—	—	—	—	Tr

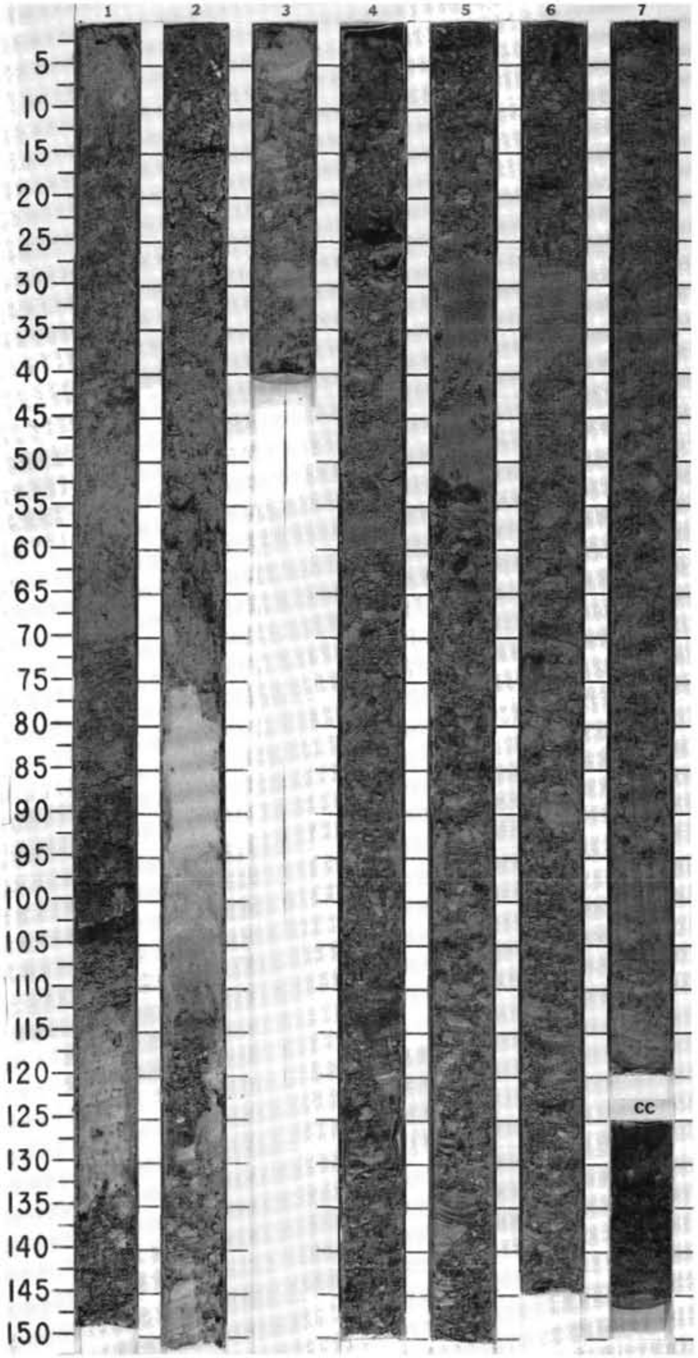

SITE 674 HOLE A CORE 3 H CORED INTERVAL 4565.8-4575.3 mbsl; 15.6-25.1 mbsf

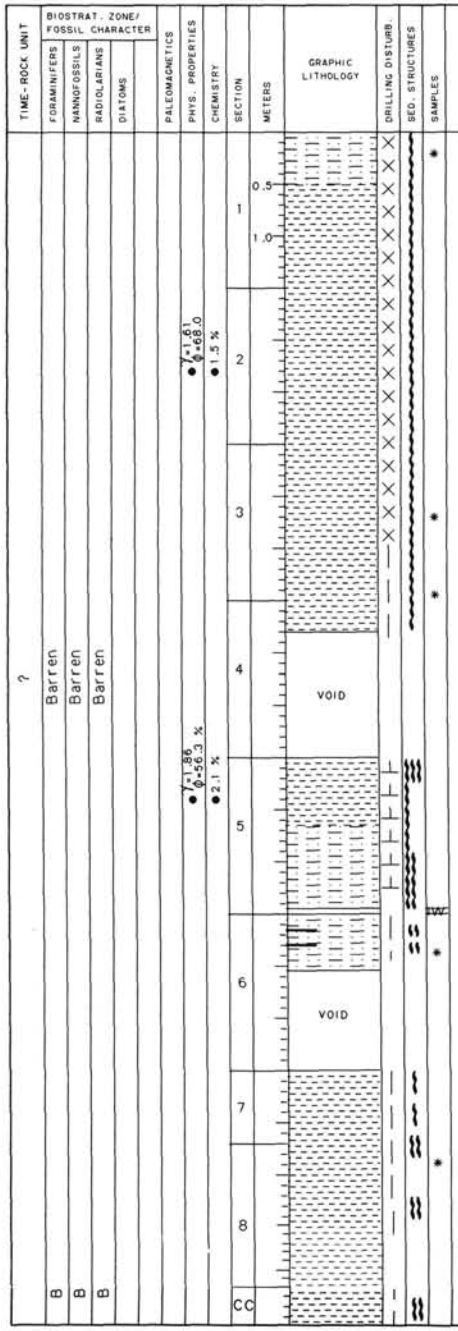

LITHOLOGIC DESCRIPTION

CLAYSTONE and MUDSTONE

Dark olive-gray (5G5/1) to dark brownish (2.5Y4/4), bioturbated CLAYSTONE and MUDSTONE.

Minor lithology: disseminated ash beds.

Structure: abundant syn-tectonic(?) calcite veins; bedding dips 20°; one fault in Section 6, 0–10 cm, dips 45°.

SMEAR SLIDE SUMMARY (%):

	1, 27 D	3, 75 D	3, 143 D	6, 37 M	CC, 8 D
TEXTURE:					
Sand	2	—	—	80	—
Silt	13	3	Tr	20	2
Clay	85	97	100	—	98
COMPOSITION:					
Quartz	Tr	Tr	—	10	—
Feldspar	1	—	Tr	20	—
Clay	87	98	100	—	97
Volcanic glass	2	—	—	67	—
Calcite/dolomite	5	Tr	—	—	—
Accessory minerals	5	2	Tr	2	2
Orthopyroxene	—	—	—	Tr	—
Clinopyroxene	—	—	—	1	—
Fe/Mn hydroxide	—	—	—	—	1

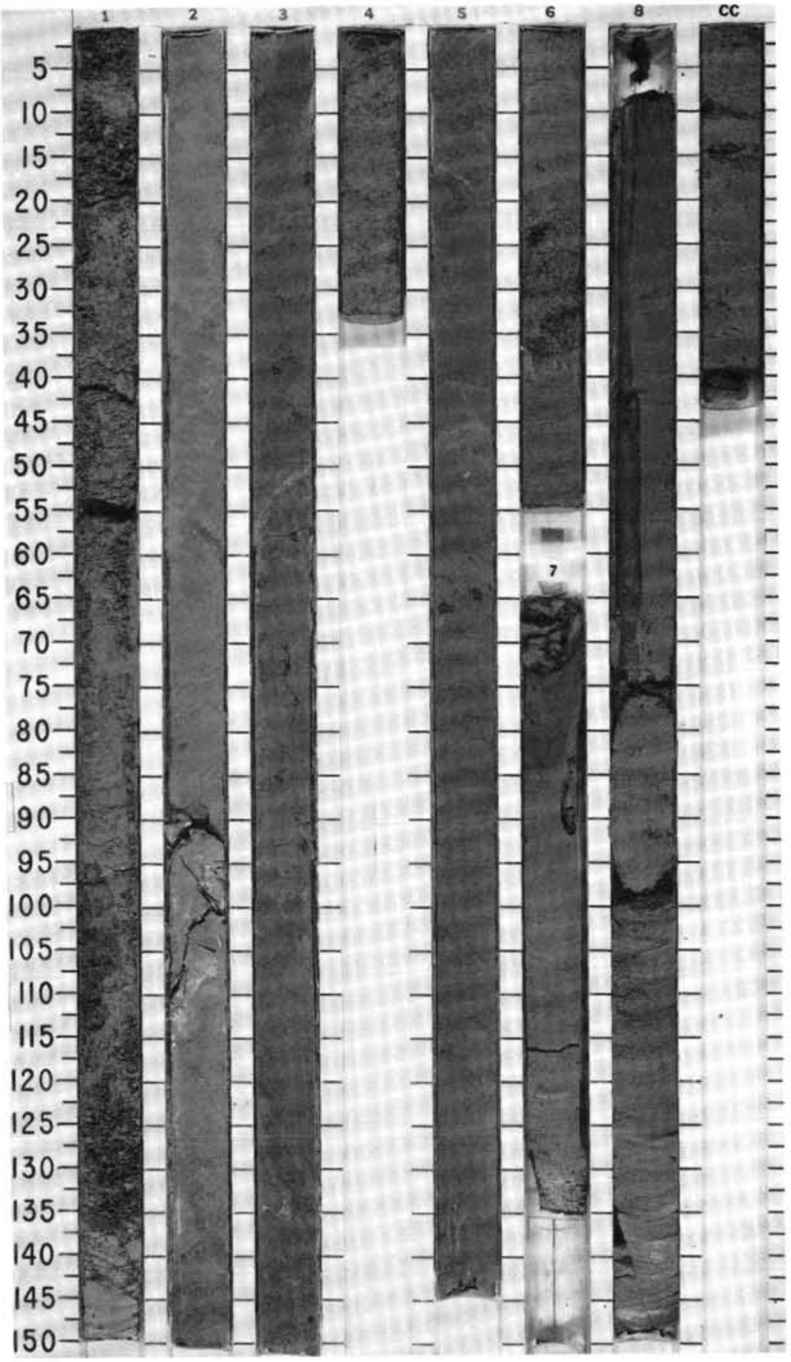

SITE 674 HOLE A CORE 4 H CORED INTERVAL 4575.3-4584.8 mbsl; 25.1-34.6 mbsf

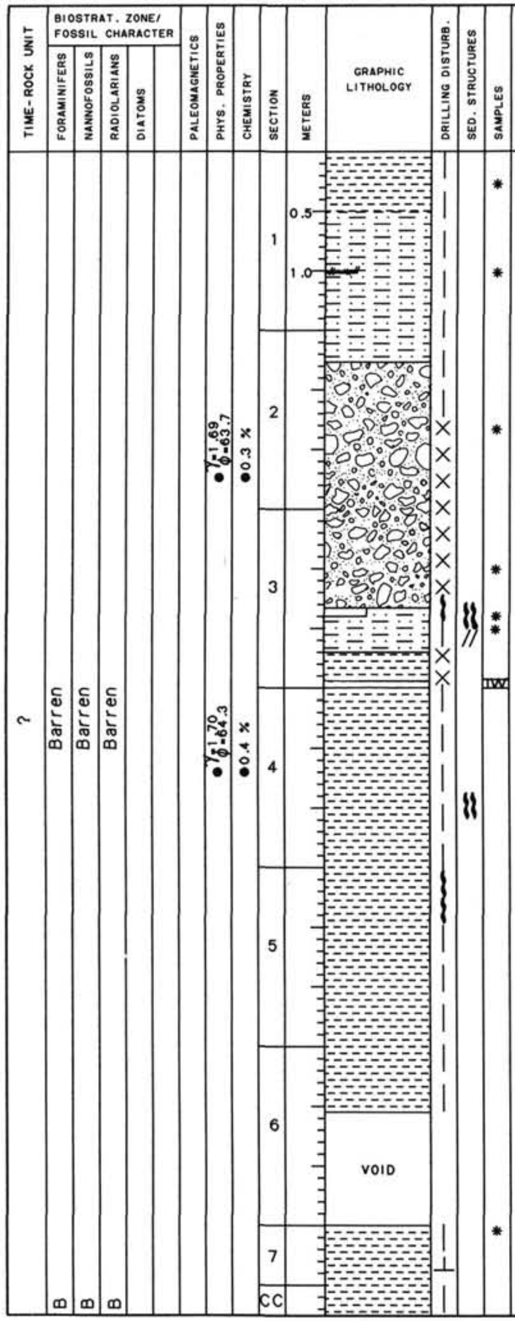

LITHOLOGIC DESCRIPTION

CLAYSTONE, MUDSTONE, and CLAYSTONE BRECCIA

Olive-gray to dark brownish gray (5Y4/2, 5G5/2, 5BG5/1) CLAYSTONE, locally grading into MUDSTONE; local bioturbation; possible interval of CLAYSTONE BRECCIA, Section 2, 25 cm, to Section 3, 85 cm.

Minor lithology: minor ashy beds.

Structure: syn-tectonic(?) calcite veins and vein structure in claystone; bedding dips 25°.

SMEAR SLIDE SUMMARY (%):

	1, 30 M	1, 104 M	2, 85 D	3, 50 D	3, 86 M	3, 90 D	7, 5 D
TEXTURE:							
Sand	—	—	—	—	50	—	—
Silt	68	20	10	1	50	30	—
Clay	32	80	90	99	—	70	100
COMPOSITION:							
Quartz	1	1	1	—	10	2	5
Feldspar	5	5	1	1	20	25	—
Clay	32	79	78	99	—	70	99
Volcanic glass	50	—	—	Tr	10	—	—
Accessory minerals	—	—	—	—	—	4	—
Orthopyroxene	—	—	—	—	1	—	—
Clinopyroxene	—	—	—	—	1	1	—
Mn oxide	12	15	20	—	58	—	1

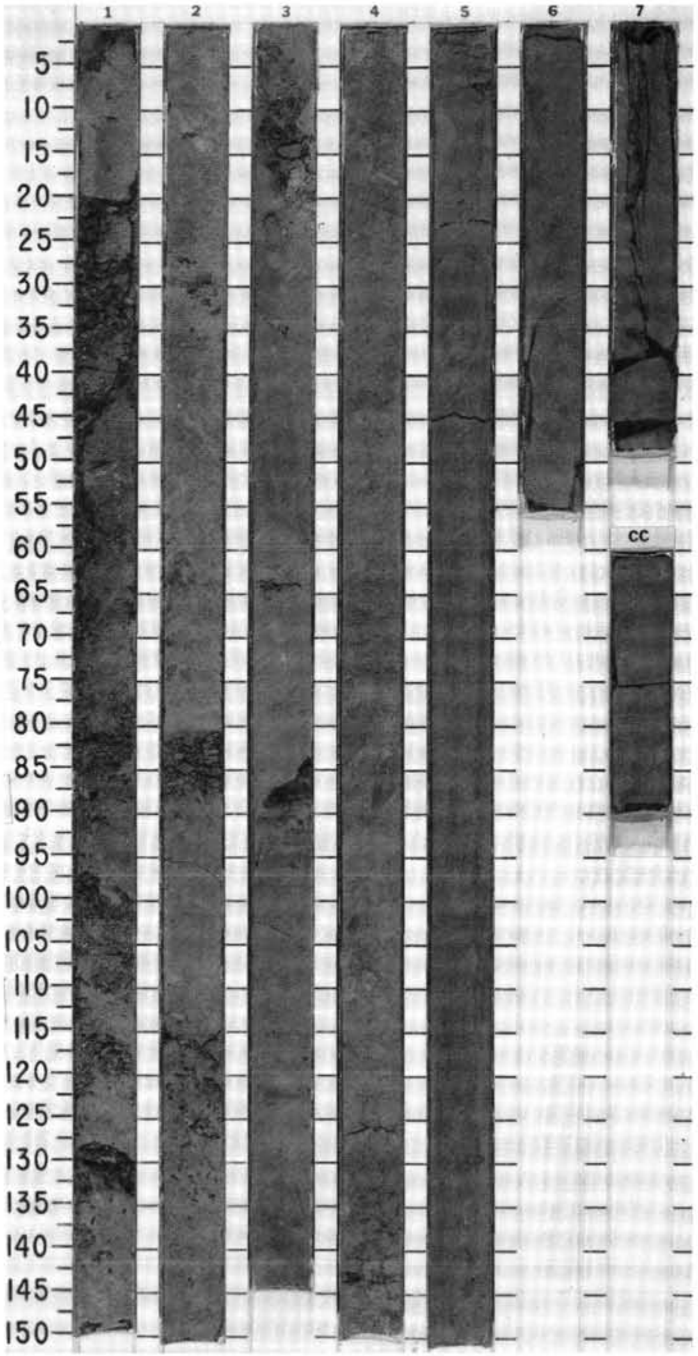

SITE 674 HOLE A CORE 5 X CORED INTERVAL 4584.8-4594.3 mbsl; 34.6-44.1 mbsf

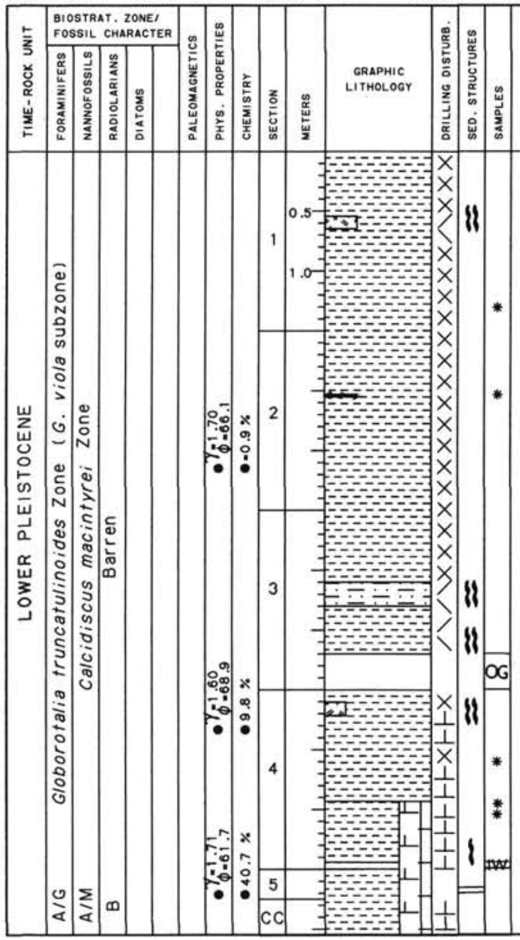

LITHOLOGIC DESCRIPTION

CLAYSTONE grading into MUDSTONE, and MARL

Two dominant lithologies:

Section 1, 0 cm, to Section 4, 93 cm: olive-gray (5G4/1, 10Y5/1) CLAYSTONE, locally grading into MUDSTONE; few bioturbated ashy beds throughout.

Section 4, 93 cm, to CC, 30 cm: light yellowish brown (5Y5/2, 10YR6/3) nannofossil-foraminifer MARL.

Structure: possible horizontal bedding in lower part; the two lithologies are separated by a fault.

SMEAR SLIDE SUMMARY (%):

	1, 122 D	2, 54 M	4, 60 D	4, 93 M	4, 107 D
TEXTURE:					
Sand	—	—	—	—	5
Silt	2	10	1	2	10
Clay	98	90	99	98	85
COMPOSITION:					
Quartz	—	1	Tr	Tr	—
Feldspar	1	2	1	—	2
Rock fragments	—	1	—	—	—
Clay	97	85	98	98	65
Volcanic glass	Tr	8	—	—	Tr
Calcite/dolomite	—	—	1	—	3
Accessory minerals	2	2	—	—	—
Hematite	—	Tr	—	—	—
Mn oxide	—	—	—	2	—
Foraminifers	—	—	—	—	10
Nannofossils	—	Tr	Tr	—	20
Sponge spicules	—	Tr	—	—	—

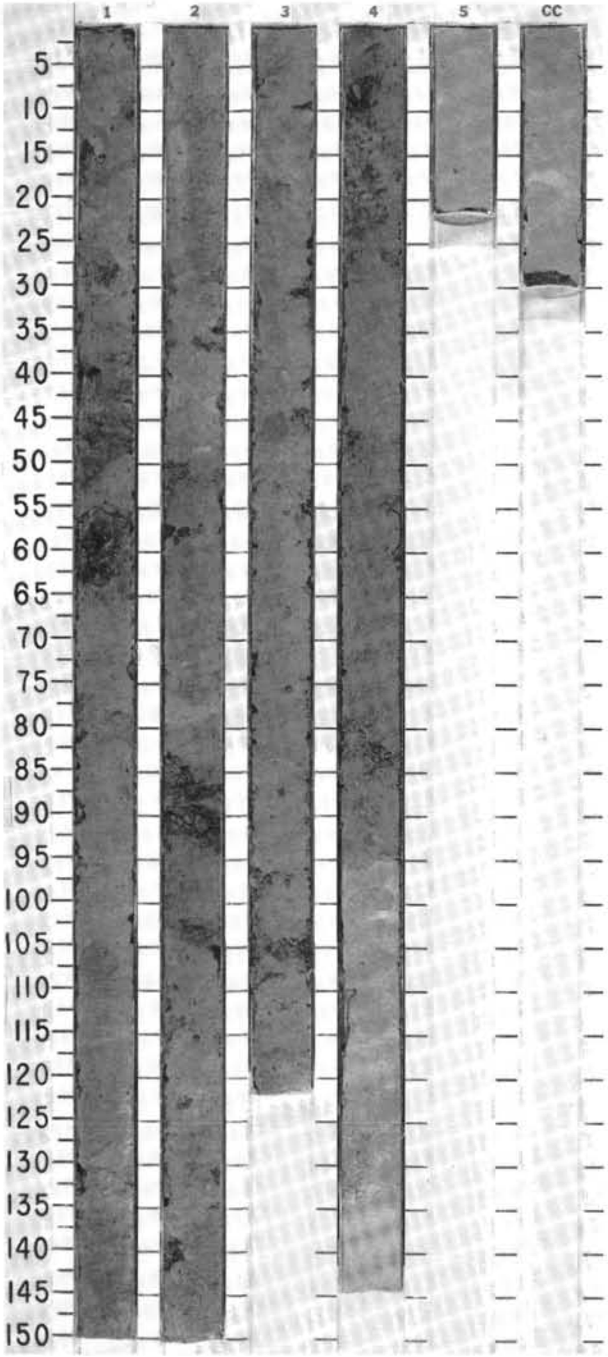

SITE 674 HOLE A CORE 6 X CORED INTERVAL 4594.3-4603.8 mbsl; 44.1-53.6 mbsf

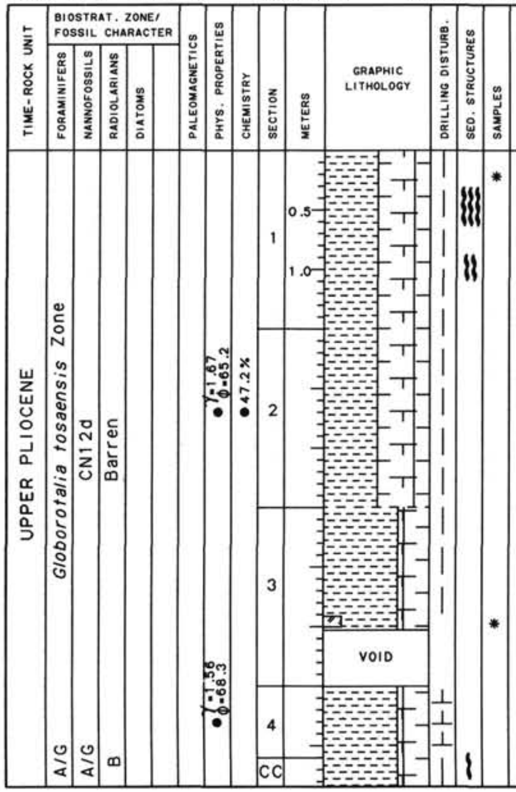

LITHOLOGIC DESCRIPTION

MARL and CALCAREOUS CLAYSTONE

Light yellowish gray (10YR6/4, 2.5Y6/2) MARL and CALCAREOUS CLAYSTONE; local bioturbation; foraminifer content decreases downsection.

Minor lithology: pink (2.5YR6/2) ash bed, Section 3, 95 cm.

SMEAR SLIDE SUMMARY (%):

	1, 27 D	3, 97 D
TEXTURE:		
Sand	20	4
Silt	20	16
Clay	60	80
COMPOSITION:		
Feldspar	—	2
Clay	50	70
Volcanic glass	—	5
Accessory minerals	1	2
Pyroxene	—	Tr
Hornblende	—	Tr
Foraminifers	30	4
Nannofossils	15	15
Bioclasts	5	2

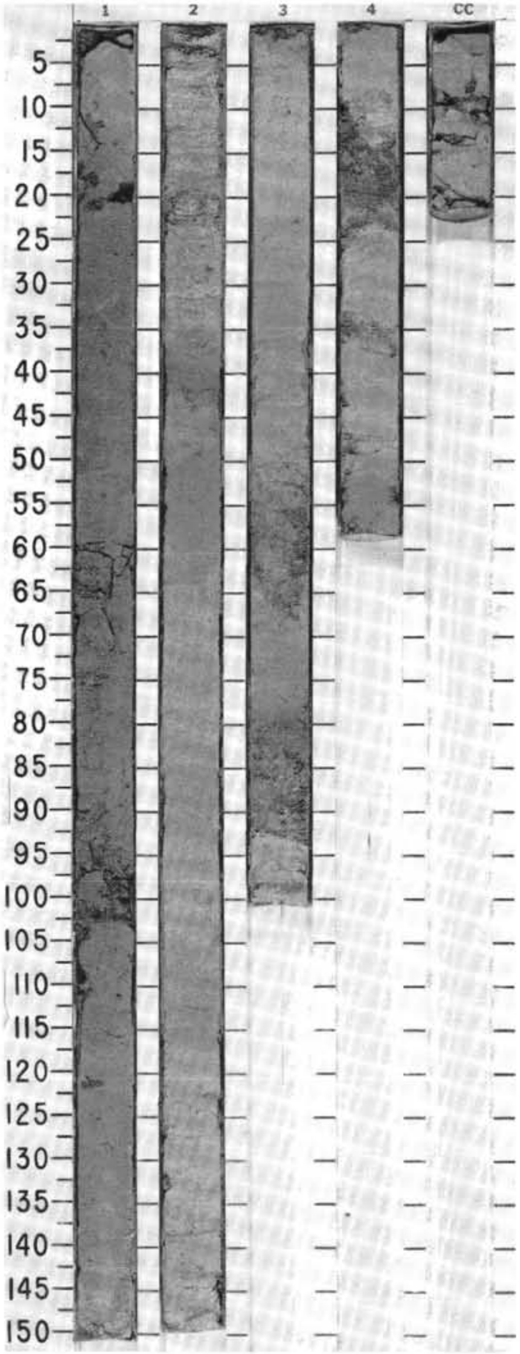

SITE 674 HOLE A CORE 7 X CORED INTERVAL 4603.8-4613.3 mbsl; 53.6-63.1 mbsf

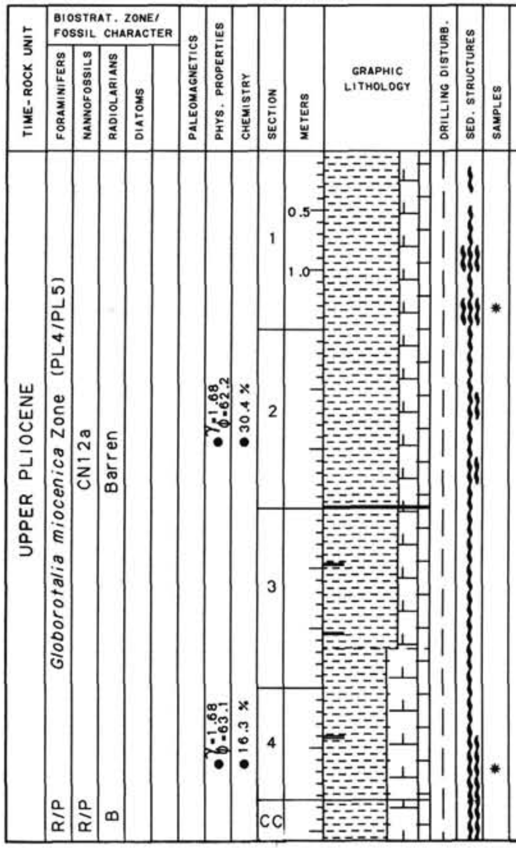

LITHOLOGIC DESCRIPTION

MARL and CALCAREOUS CLAYSTONE

Light olive-gray to light brown (5Y5/2 to 10YR6/2) MARL and CALCAREOUS CLAYSTONE; moderately to highly bioturbated.

Minor lithology: dark gray (N4) ashy layers (Section 3, 46 and 105 cm; and Section 4, 40 cm).

Structure: bedding dips range from subhorizontal to 20°.

SMEAR SLIDE SUMMARY (%):

	1, 85 D	4, 70 D
TEXTURE:		
Sand	12	14
Silt	4	4
Clay	84	82
COMPOSITION:		
Quartz	2	4
Feldspar	1	2
Clay	64	48
Volcanic glass	2	4
Accessory minerals	—	Tr
Pyroxene	—	Tr
Foraminifers	10	10
Nannofossils	20	30
Radiolarians	1	1

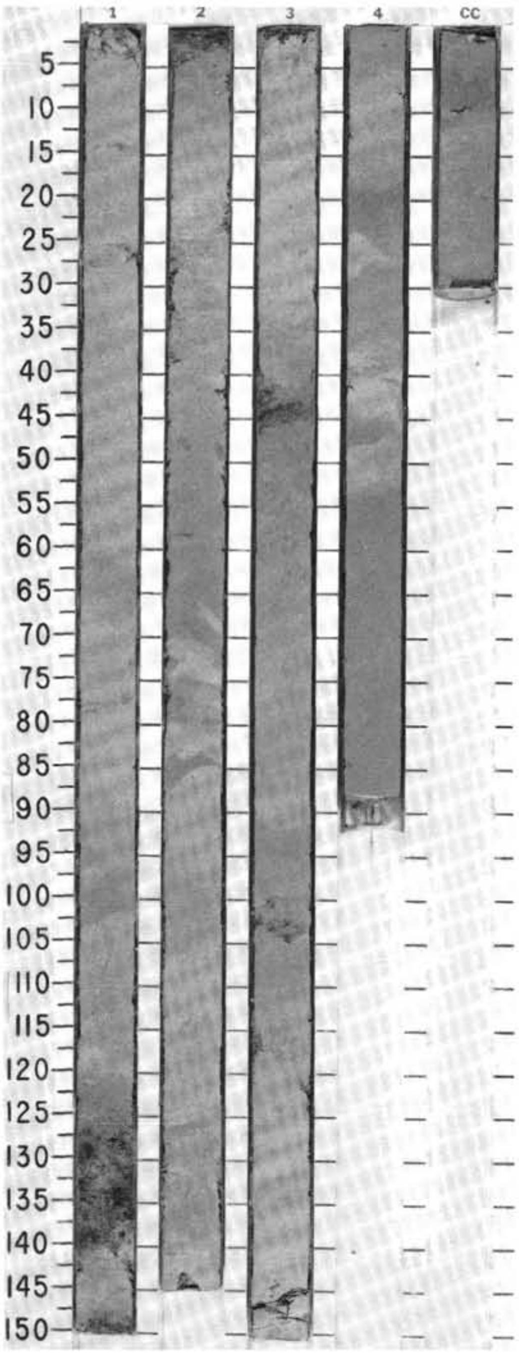

SITE 674 HOLE A CORE 8 X CORED INTERVAL 4613.3-4622.8 mbsl; 63.1-72.6 mbsf

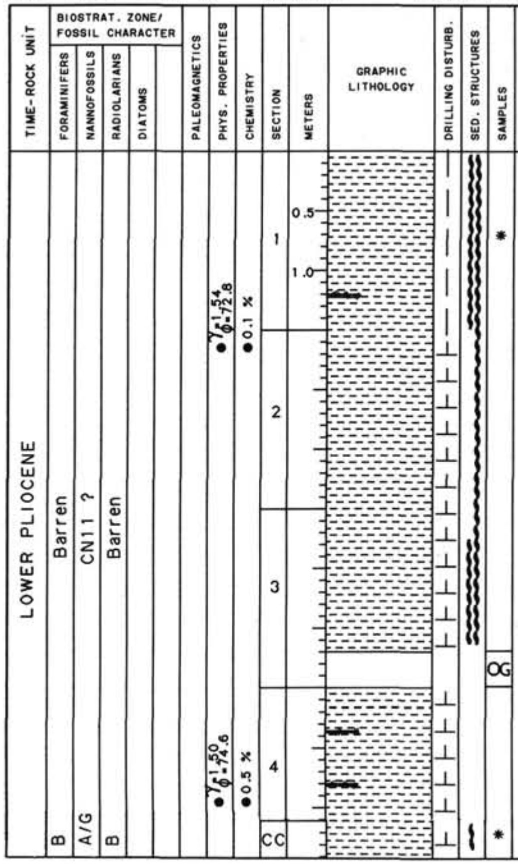

LITHOLOGIC DESCRIPTION

CLAYSTONE

Greenish gray (5GY5/1, 5G5/1, 5G4/1) CLAYSTONE; moderately bioturbated throughout.

Minor lithology: dark gray (N4) ash beds.

Structure: subhorizontal bedding.

SMEAR SLIDE SUMMARY (%):

	1, 62 D	CC, 16 M
TEXTURE:		
Silt	3	6
Clay	97	94
COMPOSITION:		
Quartz	5	2
Feldspar	2	Tr
Clay	88	93
Volcanic glass	5	5
Accessory minerals	—	Tr
Glauconite	—	Tr
Nannofossils	Tr	—
Sponge spicules	—	Tr

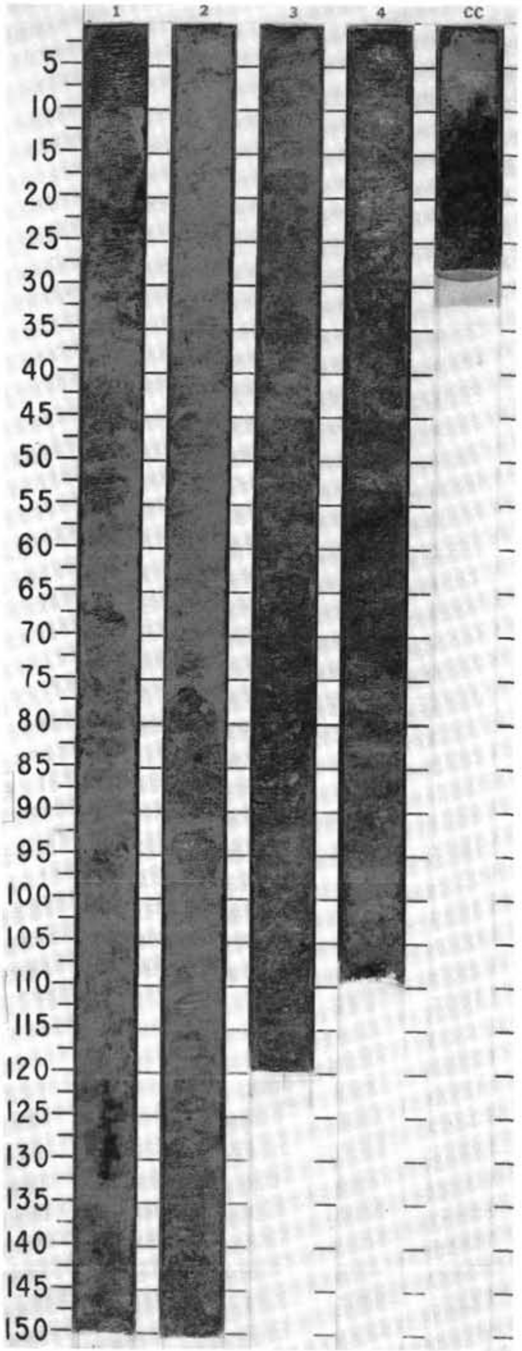

SITE 674 HOLE A CORE 9 X CORED INTERVAL 4622.8-4632.3 mbsl; 72.6-82.1 mbsf

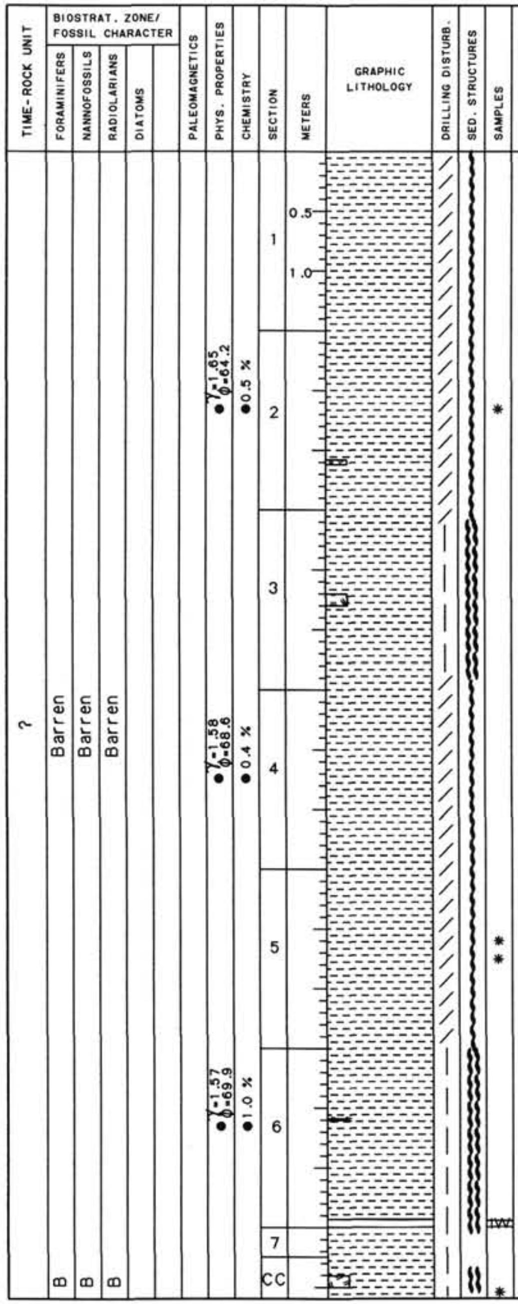

LITHOLOGIC DESCRIPTION

CLAYSTONE

Medium to dark greenish gray (10Y5/1, 5Y5/1) CLAYSTONE, moderately bioturbated, with common darker (5Y6/1) disseminated ashy layers.

Structure: sub-horizontal bedding.

SMEAR SLIDE SUMMARY (%):

	2, 114 M	5, 56 D	5, 79 D	CC, 21 M
TEXTURE:				
Sand	20	—	—	2
Silt	50	3	2	73
Clay	30	97	98	25
COMPOSITION:				
Quartz	5	1	—	5
Feldspar	40	1	1	25
Rock fragments	2	—	—	—
Clay	18	96	97	25
Volcanic glass	30	—	—	35
Calcite/dolomite	—	1	—	—
Accessory minerals	—	—	1	—
Pyroxene	1	—	—	5
Opaques	3	1	1	5
Hornblende	1	—	—	—
Hematite	—	—	—	Tr

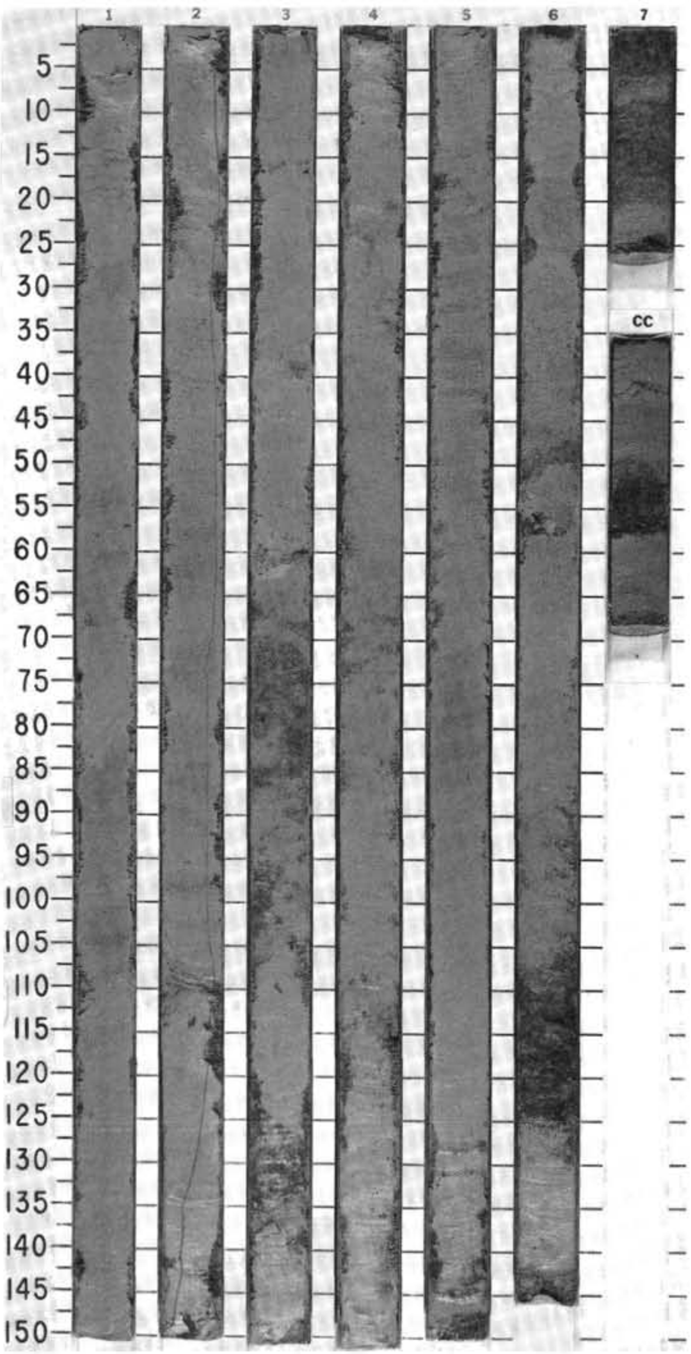

SITE 674 HOLE A CORE 10 X CORED INTERVAL 4632.3-4641.8 mbsl; 82.1-91.6 mbsf

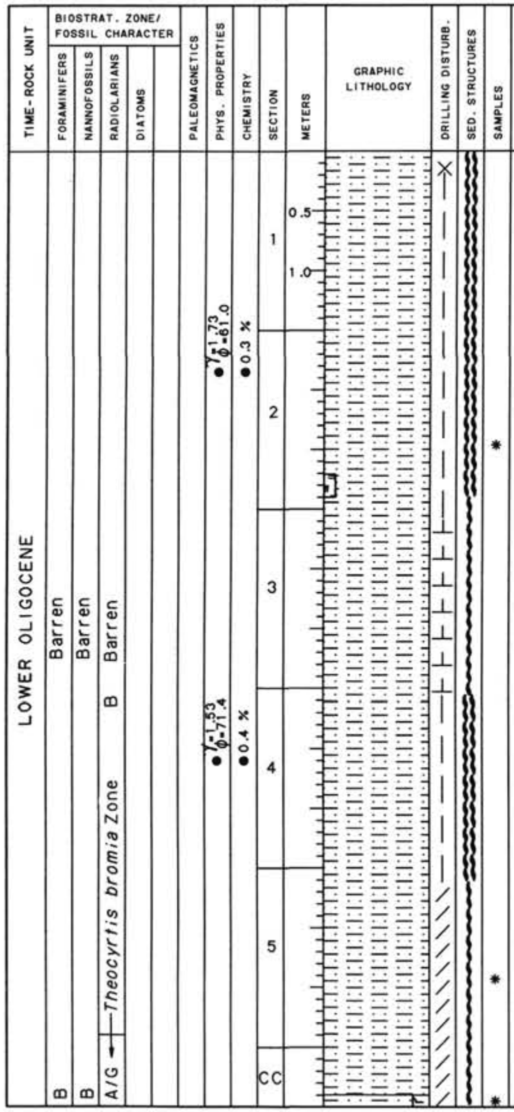

LITHOLOGIC DESCRIPTION

MUDSTONE

Olive-gray to dark greenish gray (5Y5/1, 5G4/1, 5G6/1) MUDSTONE; slightly ash-rich in Section 2, 70–90 cm; moderate bioturbation.

Minor lithology: 1-cm-thick light yellowish gray (5Y6/3) siliceous mudstone in CC, 46–47 cm.

Structure: bedding dips 10°.

SMEAR SLIDE SUMMARY (%):

	2, 94 D	5, 93 D	CC, 47 M
TEXTURE:			
Sand	—	—	2
Silt	15	5	15
Clay	85	95	83
COMPOSITION:			
Quartz	10	7	—
Clay	85	88	84
Volcanic glass	5	5	—
Accessory minerals			
Opaques	—	—	Tr
Diatoms	—	—	2
Radiolarians	—	—	3
Sponge spicules	—	—	10
Silicoflagellates	—	—	1

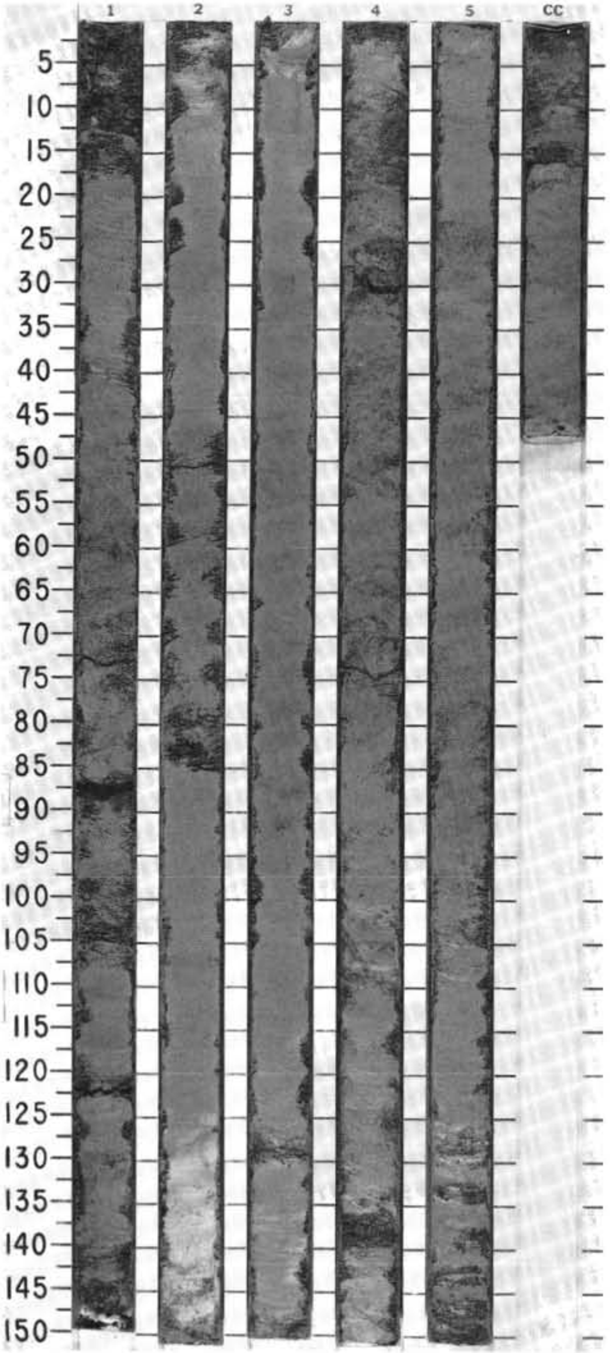

SITE 674 HOLE A CORE 11 X CORED INTERVAL 4641.8-4651.3 mbsl; 91.6-101.1 mbsf

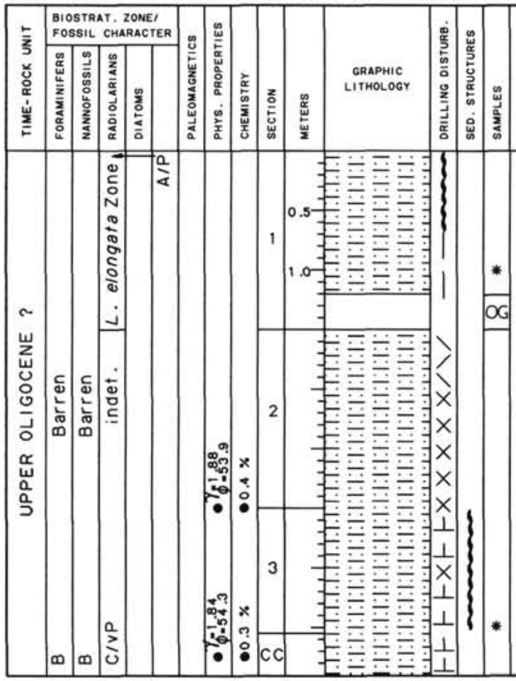

LITHOLOGIC DESCRIPTION

MUDSTONE

Brownish to reddish brown and olive-gray (10YR6/4, 2.5Y6/2, 5Y5/4) MUDSTONE, locally slightly siliceous, darker patches of dispersed ash material throughout core.

SMEAR SLIDE SUMMARY (%):

	1, 100 D	3, 100 D
TEXTURE:		
Silt	11	15
Clay	89	85
COMPOSITION:		
Quartz	11	18
Feldspar	Tr	2
Clay	86	80
Volcanic glass	—	Tr
Radiolarians	Tr	—
Sponge spicules	3	—

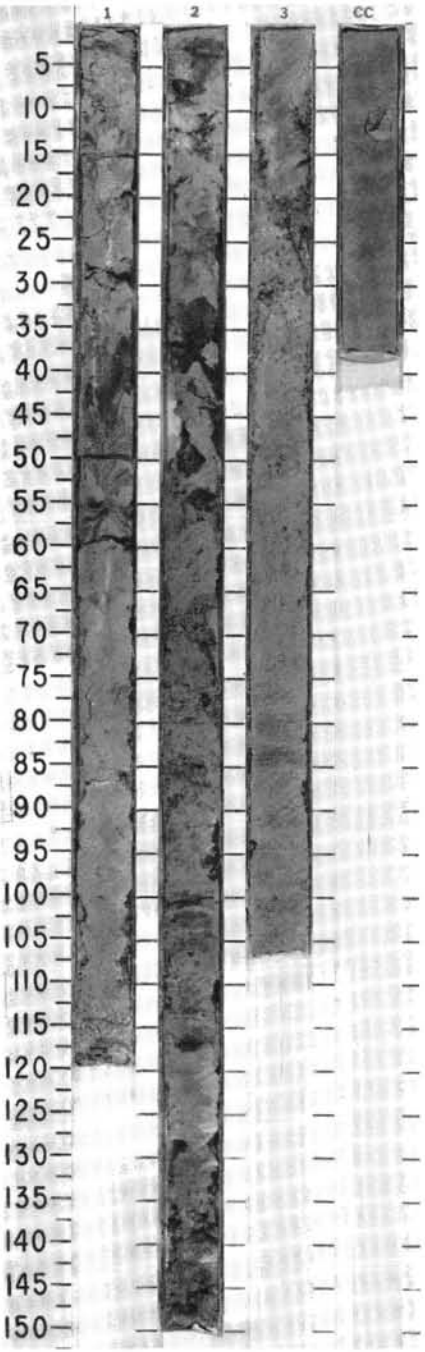

SITE 674 HOLE A CORE 12 X CORED INTERVAL 4651.3-4660.8 mbsl; 101.1-110.6 mbsf

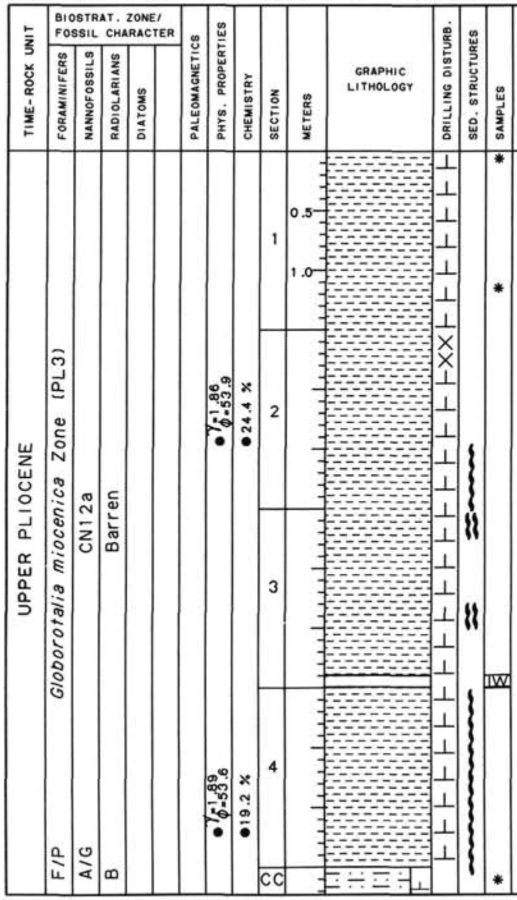

LITHOLOGIC DESCRIPTION

CLAYSTONE

Slightly calcareous gray (5Y5/1) CLAYSTONE, local bioturbation.

Minor lithology: gray (5Y5/1) calcareous mudstone, entire CC.

Structure: moderate bedding dips suggested by 50°-dipping *Zoophycos* burrows.

SMEAR SLIDE SUMMARY (%):

	1, 1 M	1, 115 D	CC, 11 D
TEXTURE:			
Silt	2	11	12
Clay	98	89	88
COMPOSITION:			
Quartz	1	Tr	—
Feldspar	1	10	8
Mica	—	Tr	—
Clay	98	89	68
Calcite/dolomite	—	1	—
Accessory minerals	—	—	1
Glauconite	—	—	1
Pyrite	—	Tr	—
Orthopyroxene	—	—	1
Clinopyroxene	—	—	1
Hornblende	—	—	1
Fe/Mn oxide	Tr	—	—
Foraminifers	—	—	Tr
Nannofossils	—	2	20

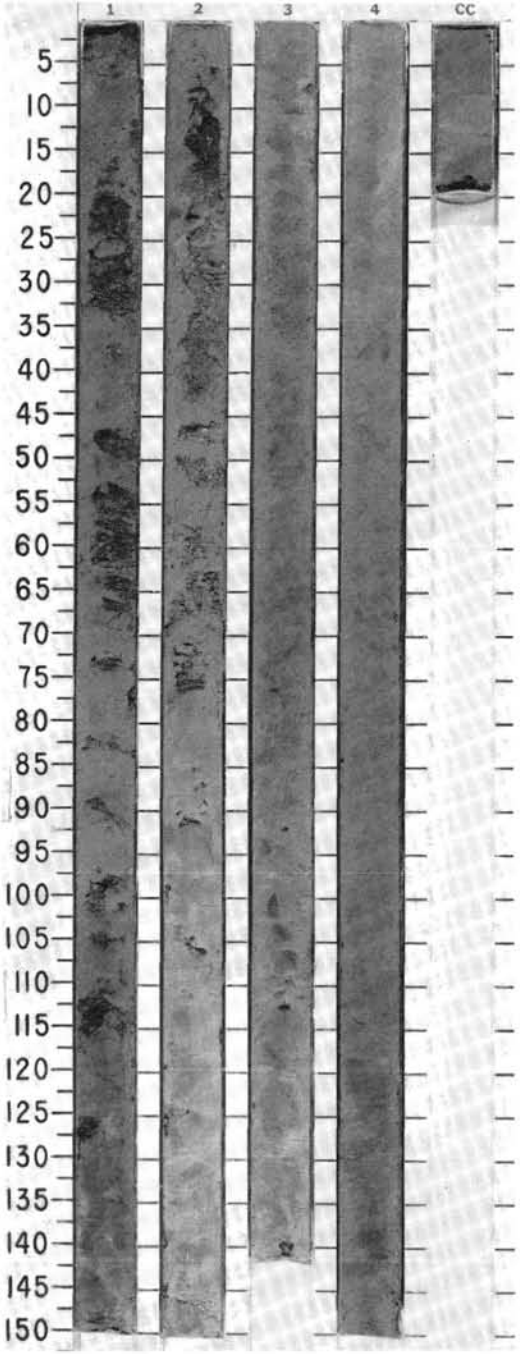

SITE 674 HOLE A CORE 13 X CORED INTERVAL 4660.8-4670.3 mbsl; 110.6-120.1 mbsf

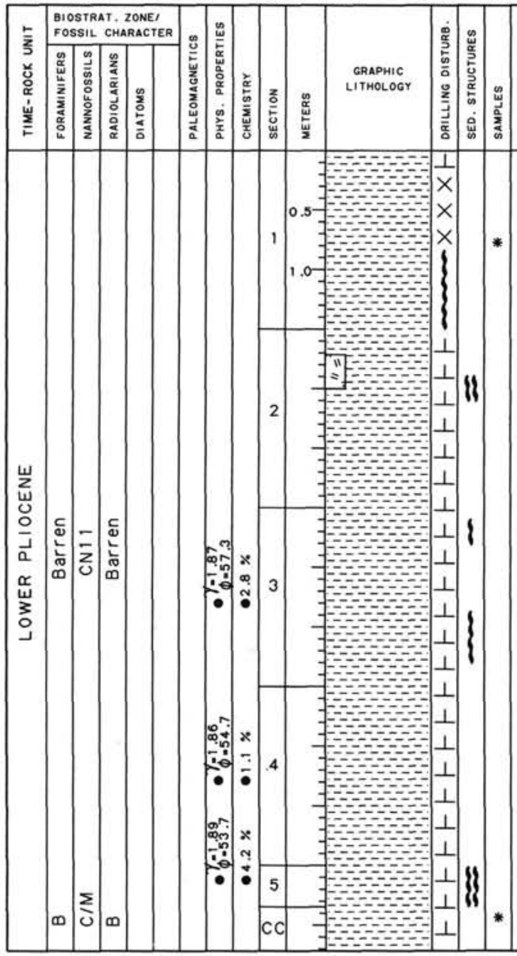

LITHOLOGIC DESCRIPTION

MUDSTONE

Olive-gray to brownish gray (5GY5/1, 5G4/2, 5Y5/2), carbonate-free to slightly calcareous MUDSTONE; disseminated darker ash material throughout; local bioturbation.

SMEAR SLIDE SUMMARY (%):

	1, 73 D	CC, 10 D
TEXTURE:		
Silt	10	10
Clay	90	90
COMPOSITION:		
Feldspar	8	7
Clay	85	90
Volcanic glass	Tr	—
Calcite/dolomite	1	Tr
Accessory minerals	1	1
Pyroxene	Tr	Tr
Hornblende	Tr	1
Fe/Mn oxide	Tr	—
Nannofossils	5	Tr
Sponge spicules	Tr	—

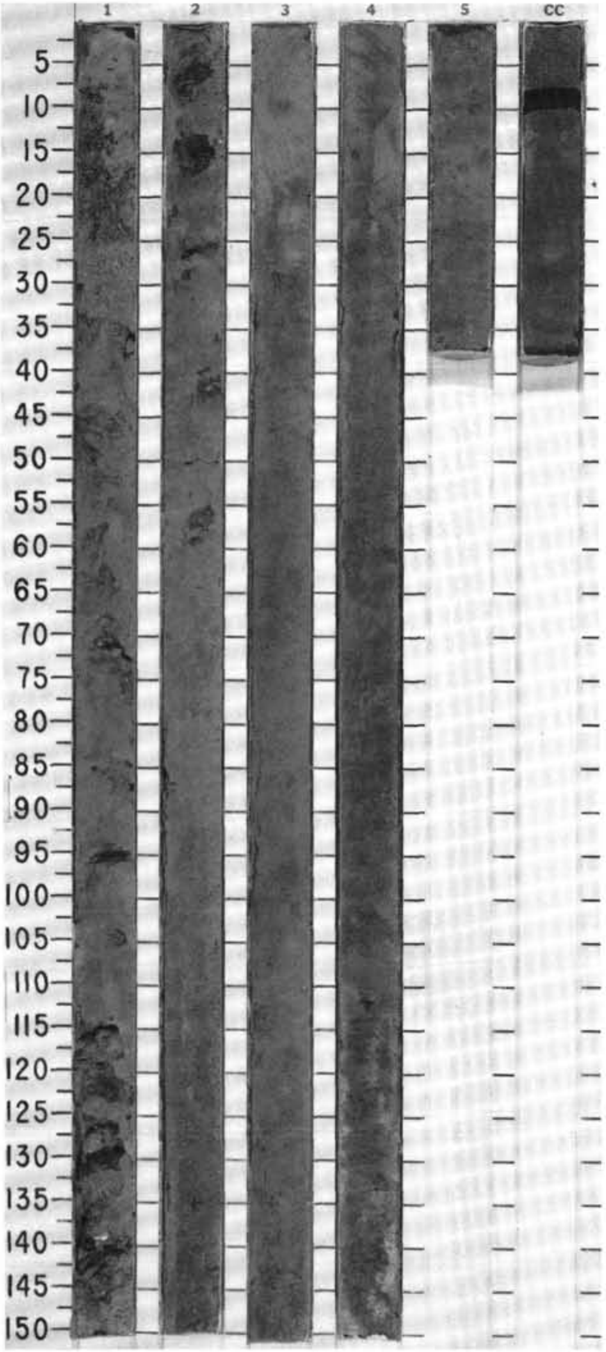

SITE 674 HOLE A CORE 14 X CORED INTERVAL 4670.3-4679.8 mbsl; 120.1-129.6 mbsf

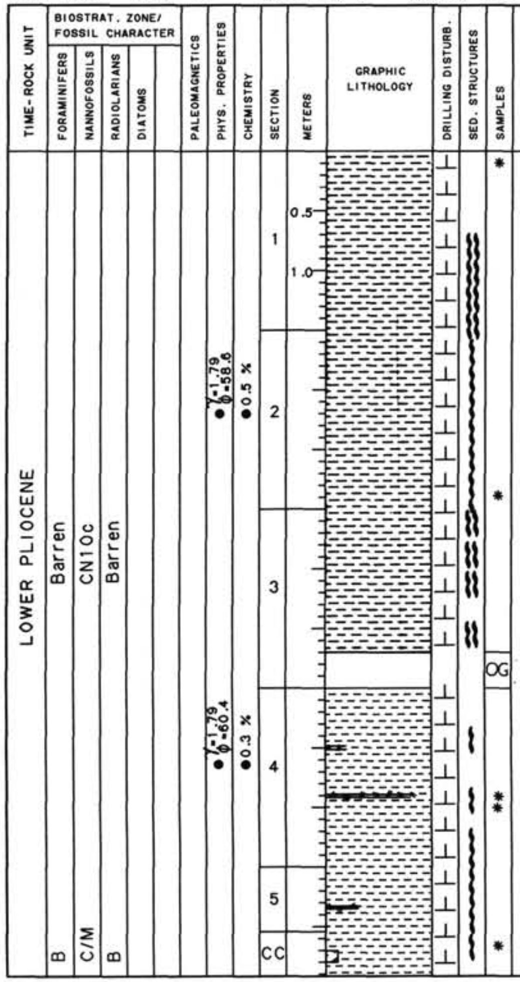

LITHOLOGIC DESCRIPTION

MUDSTONE

Light yellowish to brownish gray (2.5Y5/2, 2.5Y6/4, 10YR5/4), carbonate-free to slightly calcareous MUDSTONE.

Minor lithology: bioturbated ash beds in Sections 4, 5, and CC.

Structure: 55°-dipping fault in Section 1, 40–45 cm.

SMEAR SLIDE SUMMARY (%):

	1, 13 D	2, 145 D	4, 86 D	4, 92 M	CC, 14 D
TEXTURE:					
Sand	Tr	—	—	—	—
Silt	20	10	1	10	1
Clay	80	90	99	90	99
COMPOSITION:					
Quartz	Tr	—	Tr	5	1
Feldspar	Tr	8	Tr	25	Tr
Rock fragments	—	Tr	—	15	—
Clay	90	90	99	—	99
Volcanic glass	—	—	—	49	—
Calcite/dolomite	2	—	—	—	—
Accessory minerals	2	—	Tr	2	—
Pyroxene	—	1	Tr	4	—
Fe/Mn oxide	—	1	—	—	—
Nannofossils	3	Tr	—	—	—
Bioclasts	3	—	—	—	—

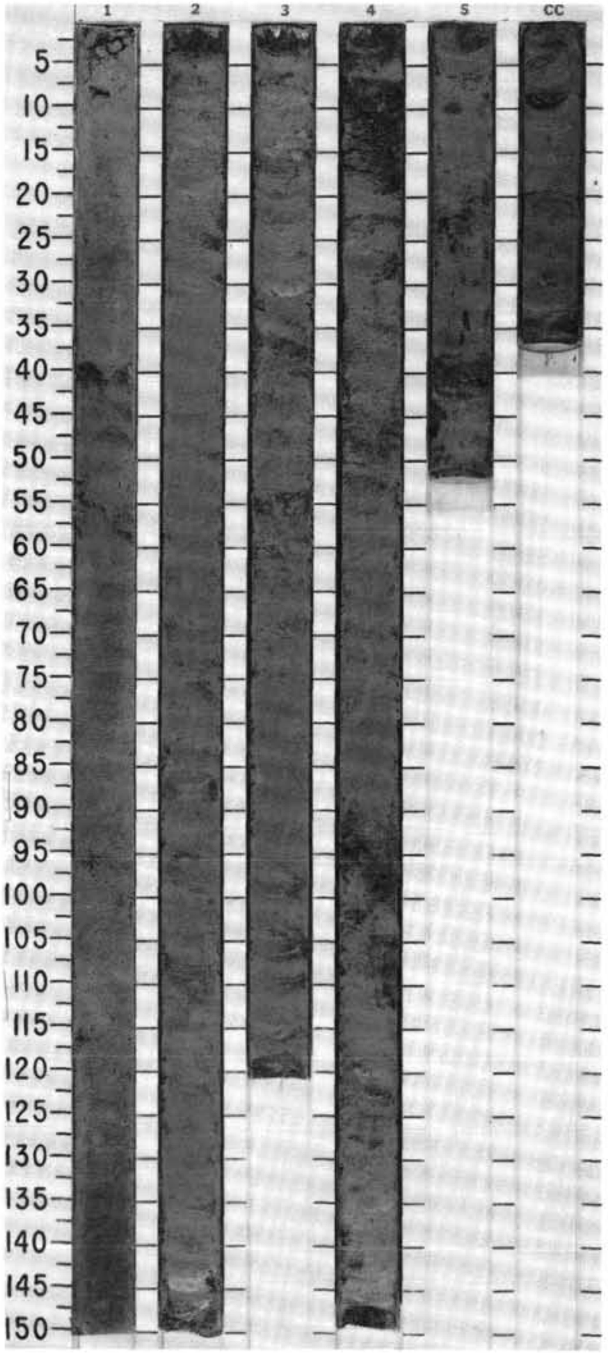

SITE 674 HOLE A CORE 15 X CORED INTERVAL 4679.8-4689.3 mbsl; 129.6-139.1 mbsf

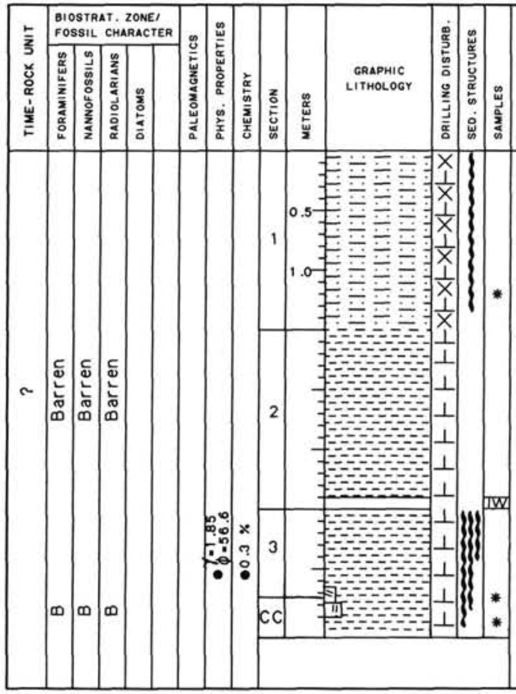

LITHOLOGIC DESCRIPTION

CLAYSTONE

Olive-gray (5Y4.2, 5Y5/2) CLAYSTONE, moderate to strong bioturbation, minor ash disseminated throughout core. CC is ash-rich.

Structure: minor scaly fabric, locally developed.

SMEAR SLIDE SUMMARY (%):

	1, 117 D	CC, 5 M	CC, 22 D
TEXTURE:			
Sand	—	Tr	3
Silt	11	25	20
Clay	89	75	67
COMPOSITION:			
Quartz	1	—	—
Feldspar	8	10	2
Rock fragments	1	—	—
Clay	88	75	67
Volcanic glass	—	5	20
Calcite/dolomite	1	—	—
Accessory minerals			
Glauconite	Tr	Tr	—
Pyroxene	Tr	—	Tr
Hornblende	Tr	Tr	Tr
Opaques (Fe/Mn oxide)	10	10	1

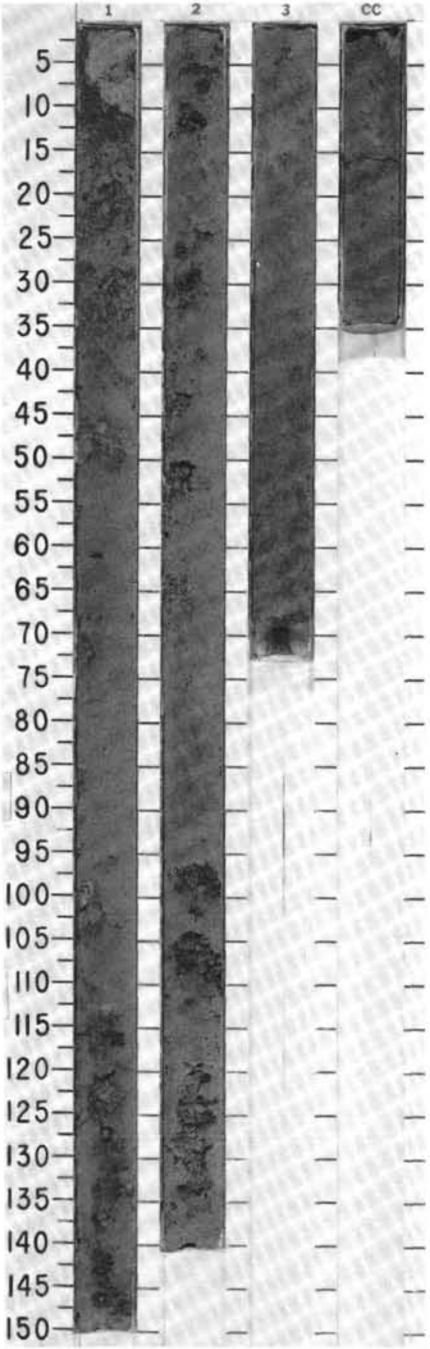

SITE 674 HOLE A CORE 16 X CORED INTERVAL 4689.3-4698.8 mbsl; 139.1-148.6 mbsf

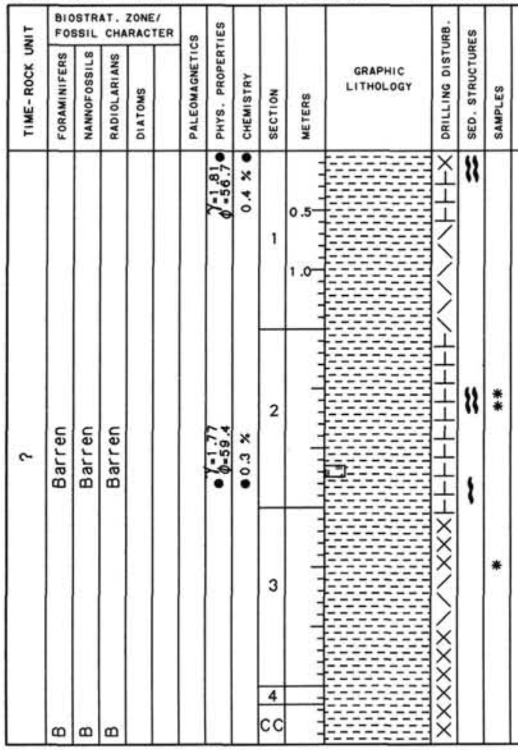

LITHOLOGIC DESCRIPTION

CLAYSTONE

Olive-gray to dark greenish gray (5Y4/2, 5G4/1, 5Y5/1) CLAYSTONE; local discrete bioturbation; entire core contains minor concentrations of ash; Section 2, 117–122 cm, contains a bioturbated ash horizon.

SMEAR SLIDE SUMMARY (%):

	2, 57 D	2, 58 M	3, 43 D
TEXTURE:			
Sand	—	—	1
Silt	10	6	1
Clay	90	94	98
COMPOSITION:			
Quartz	—	—	Tr
Feldspar	8	5	1
Rock fragments	Tr	—	—
Clay	90	94	89
Accessory minerals	1	Tr	—
Orthopyroxene	Tr	Tr	—
Clinopyroxene	Tr	—	—
Hornblende	1	Tr	—
Mn oxide	Tr	Tr	10

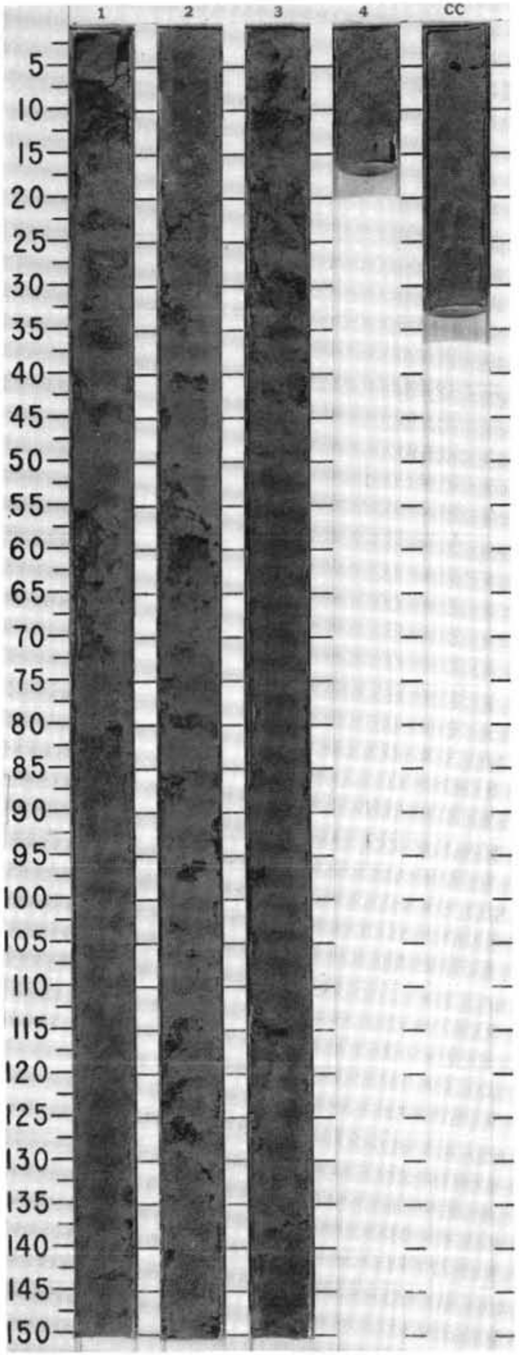

SITE 674 HOLE A CORE 17 X CORED INTERVAL 4698.8-4708.3 mbsl; 148.6-158.1 mbsf

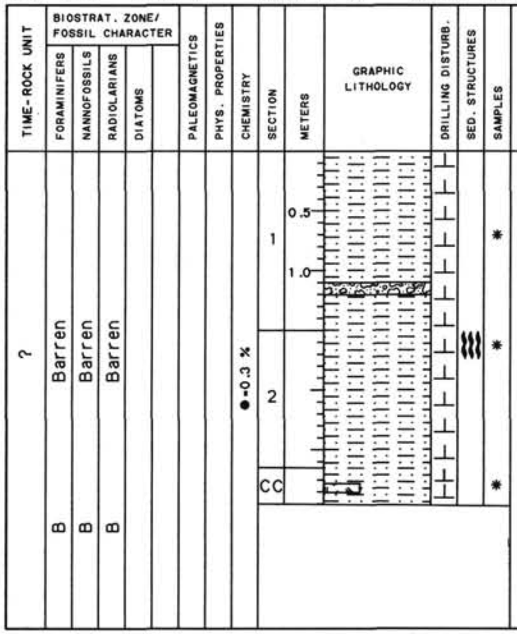

LITHOLOGIC DESCRIPTION

MUDSTONE

Olive-gray to pale greenish gray (5Y4/1, 5Y3/1) MUDSTONE; silt-size fraction consists mostly of ash material; thin conglomerate bed in Section 1, 110–120 cm.

Structure: conglomerate bed dips 80°, scaly fabric, dips variable but generally 0–15°, intensely developed throughout core.

SMEAR SLIDE SUMMARY (%):

	1, 69 D	2, 17 M	CC, 10 M
TEXTURE:			
Sand	—	2	6
Silt	18	10	24
Clay	82	88	70
COMPOSITION:			
Quartz	20	10	5
Feldspar	2	1	11
Clay	75	86	77
Volcanic glass	3	3	6
Accessory minerals			
Pyrite	—	Tr	1

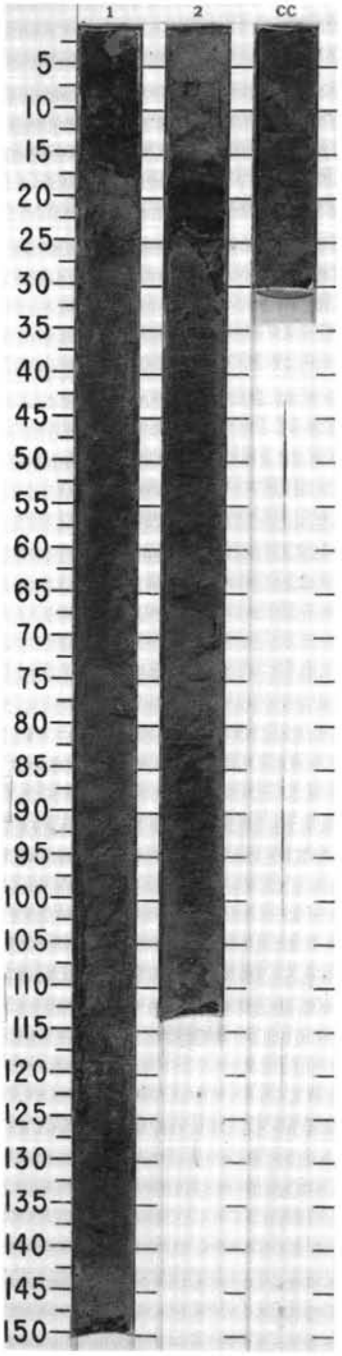

SITE 674 HOLE A CORE 18 X CORED INTERVAL 4708.3-4717.8 mbsl; 158.1-167.6 mbsf

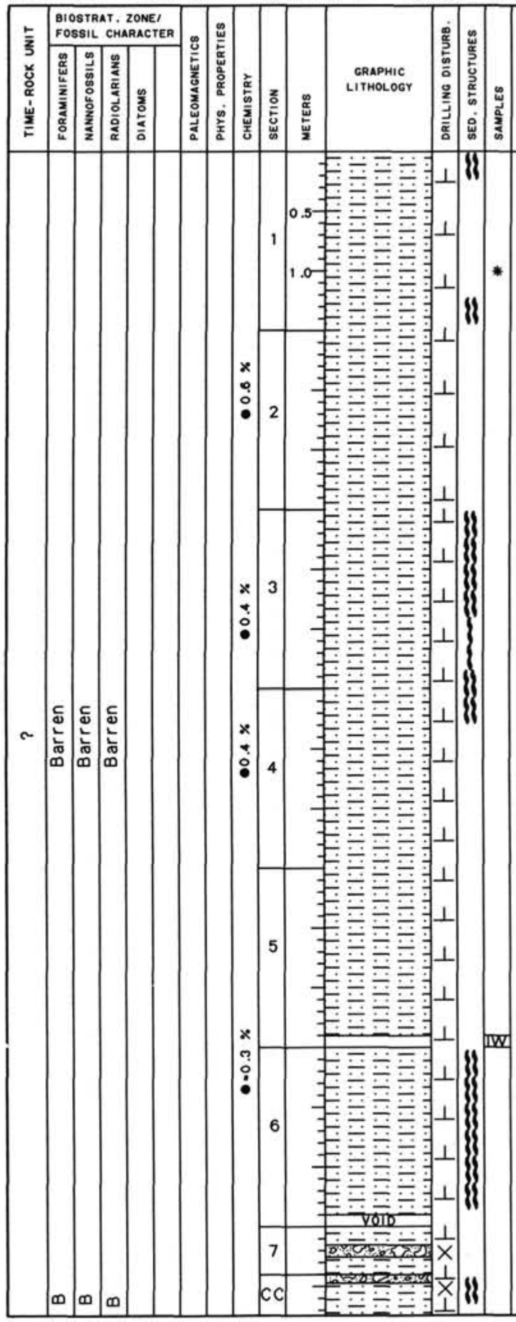

LITHOLOGIC DESCRIPTION

MUDSTONE

Olive (5Y5/1) and olive-gray (5Y5/2) MUDSTONE; local moderate bioturbation.

Structure: moderate to intense scaly fabric (30–45° dips) developed throughout core.

SMEAR SLIDE SUMMARY (%):

	1, 98 D
TEXTURE:	
Silt	10
Clay	90
COMPOSITION:	
Quartz	10
Feldspar	5
Clay	85

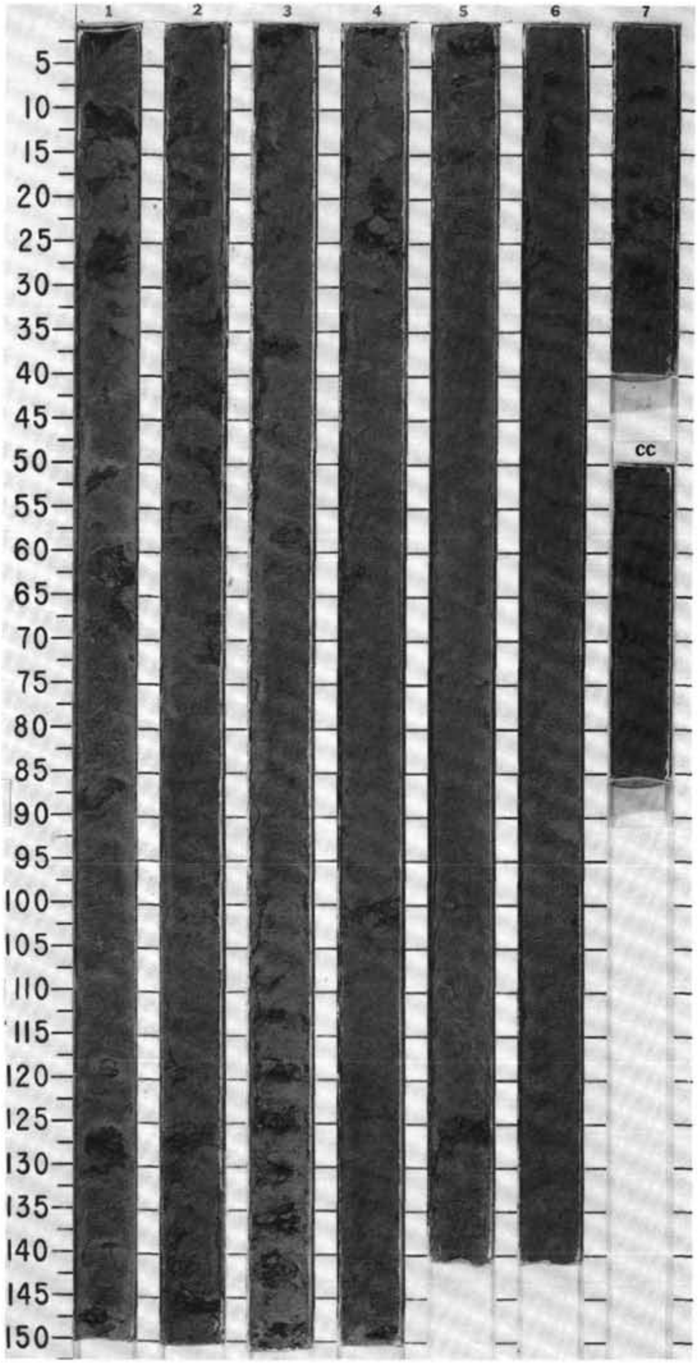

SITE 674 HOLE A CORE 19 X CORED INTERVAL 4717.8-4727.3 mbsl; 167.6-177.1 mbsf

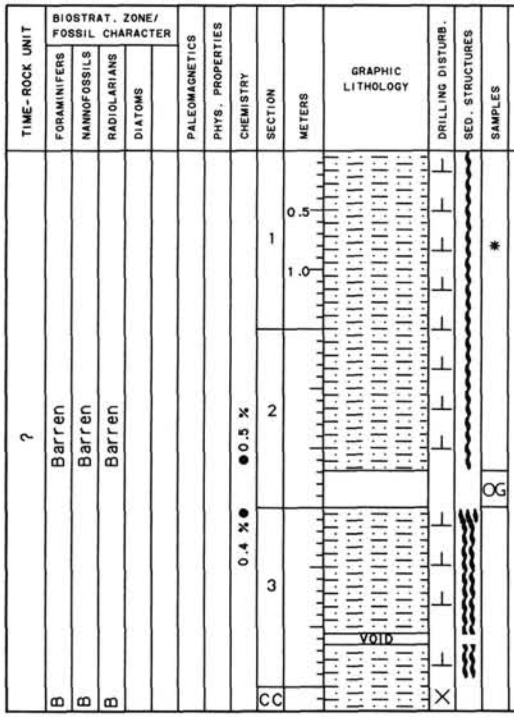

LITHOLOGIC DESCRIPTION

MUDSTONE

Olive-green (5GY4/1, 5Y4/1) MUDSTONE, moderate bioturbation throughout core but more strongly developed in Section 3.

Structure: local, moderately intense, scaly fabric, 0–40° dips.

SMEAR SLIDE SUMMARY (%):

	1, 75 D
TEXTURE:	
Silt	25
Clay	75
COMPOSITION:	
Quartz	20
Feldspar	6
Clay	66
Volcanic glass	8
Accessory minerals	
Hornblende(?)	Tr
Tektites(?)	Tr

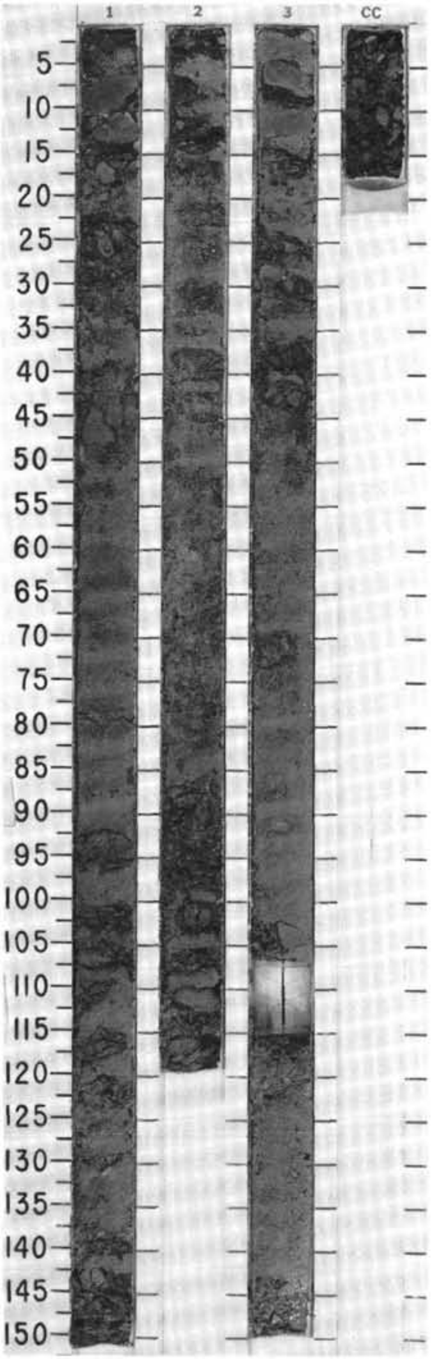

SITE 674 HOLE A CORE 20 X CORED INTERVAL 4727.3-4736.8 mbsl; 177.1-186.6 mbsf

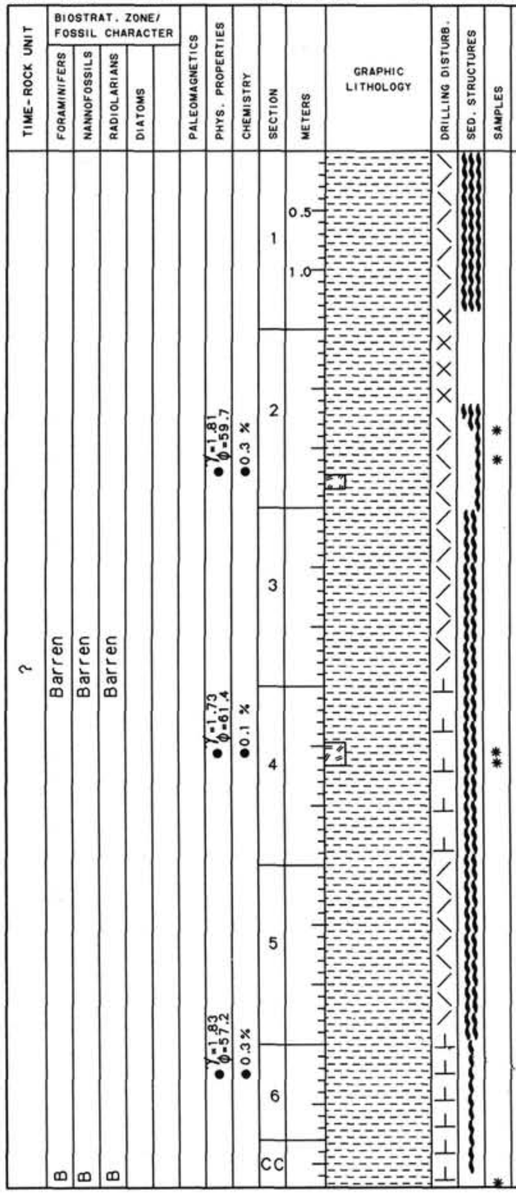

LITHOLOGIC DESCRIPTION

MUDSTONE

Olive-green (10Y4/2) and grayish green (5GY4/1) CLAYSTONE, moderate to intense bioturbation.

Structure: moderately well-developed scaly fabric; calcite-filled veins in Sections 4, 5, and 6.

SMEAR SLIDE SUMMARY (%):

	2, 96 D	2, 110 D	4, 56 M	4, 58 M	CC, 27 D
TEXTURE:					
Sand	—	—	10	40	—
Silt	2	5	35	10	Tr
Clay	98	95	55	50	100
COMPOSITION:					
Quartz	—	10	10	2	—
Feldspar	1	Tr	15	20	2
Clay	98	90	54	50	98
Volcanic glass	Tr	—	20	20	Tr
Accessory minerals					
Pyroxene	—	—	1	4	—
Opaques	Tr	—	Tr	3	—
Hornblende	—	—	—	1	—

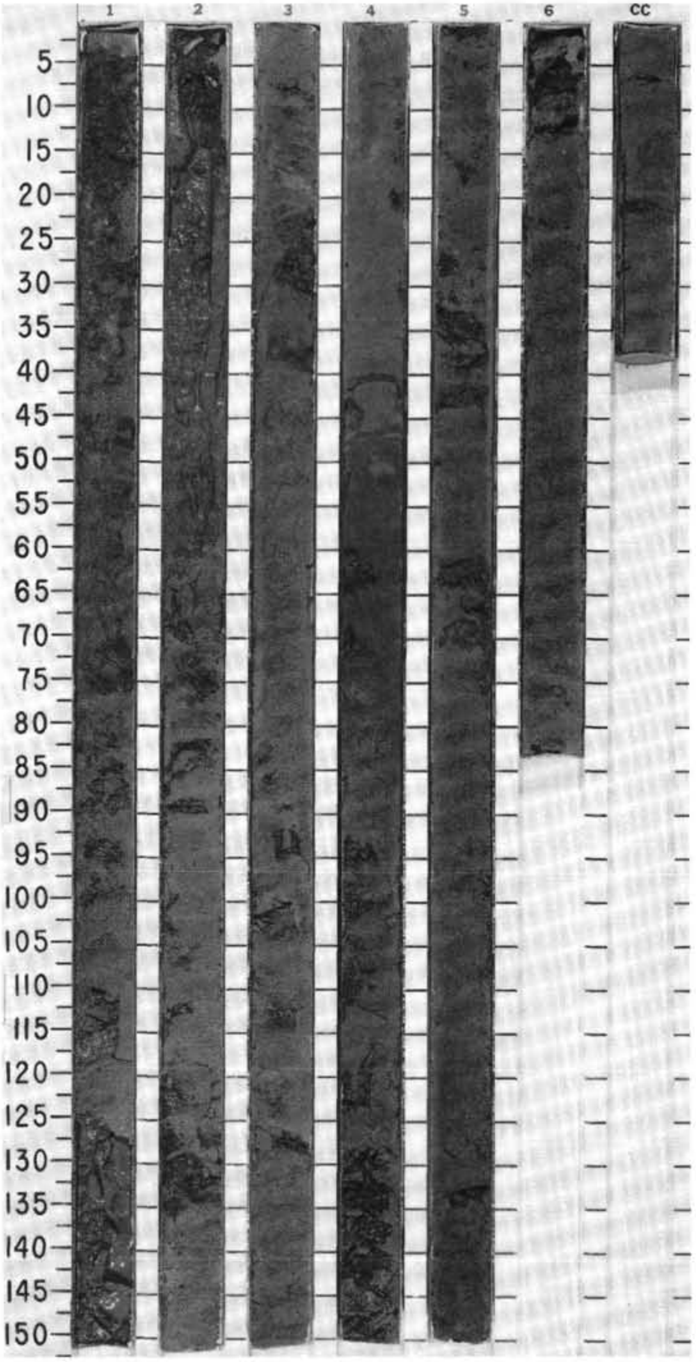

SITE 674 HOLE A CORE 21 X CORED INTERVAL 4736.8-4746.3 mbsl; 186.6-196.1 mbsf

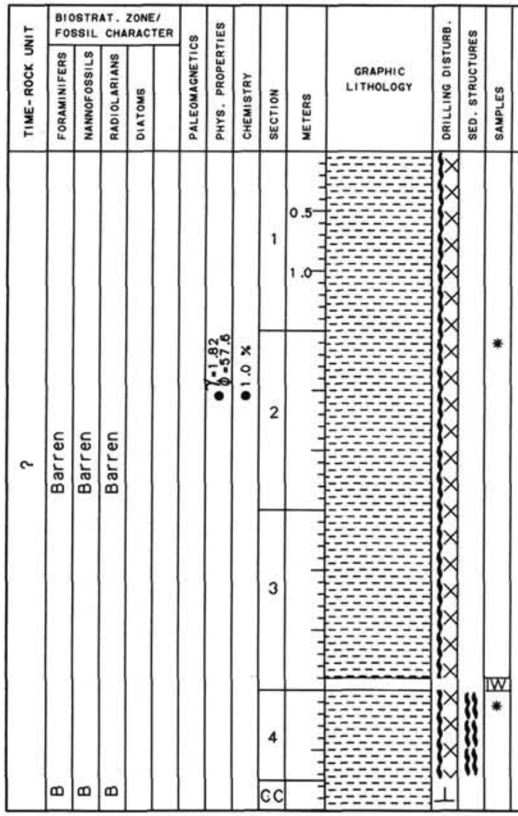

LITHOLOGIC DESCRIPTION

CLAYSTONE

Homogeneous, greenish gray (5GY5/1, 5G4/2) CLAYSTONE; entire core is drilling breccia and slurry.

SMEAR SLIDE SUMMARY (%):

	2, 98	4, 11
TEXTURE:		
Silt	2	2
Clay	98	98
COMPOSITION:		
Feldspar	1	2
Mica	Tr	—
Clay	98	98
Accessory minerals		
Hornblende	—	Tr
Mn oxide	1	—

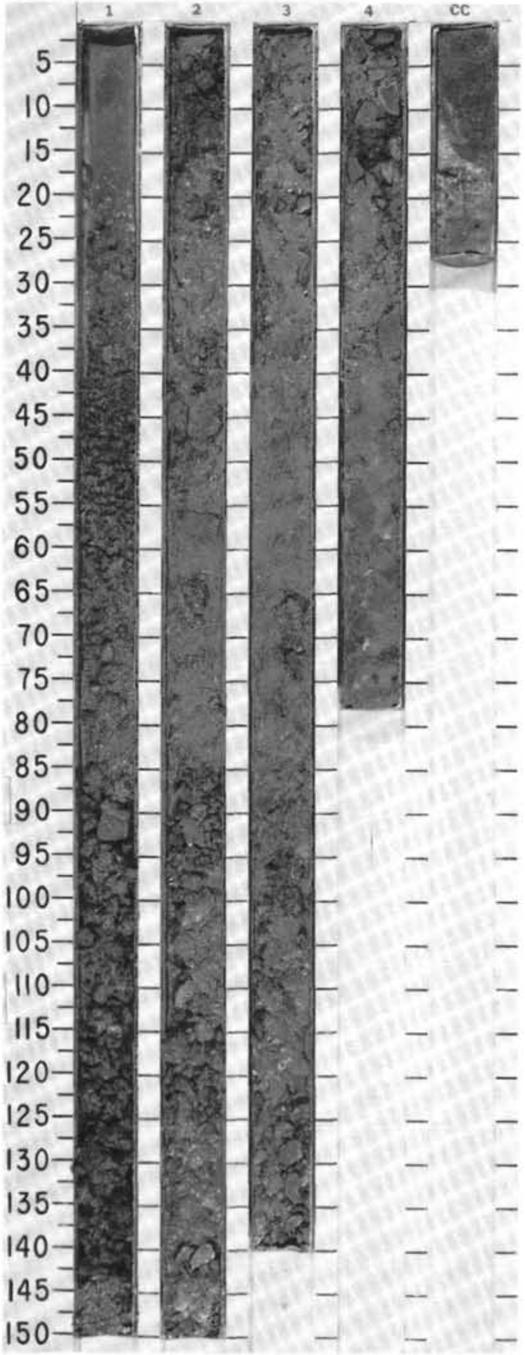

SITE 674 HOLE A CORE 22 X CORED INTERVAL 4746.3-4755.8 mbsl; 196.1-205.6 mbsf

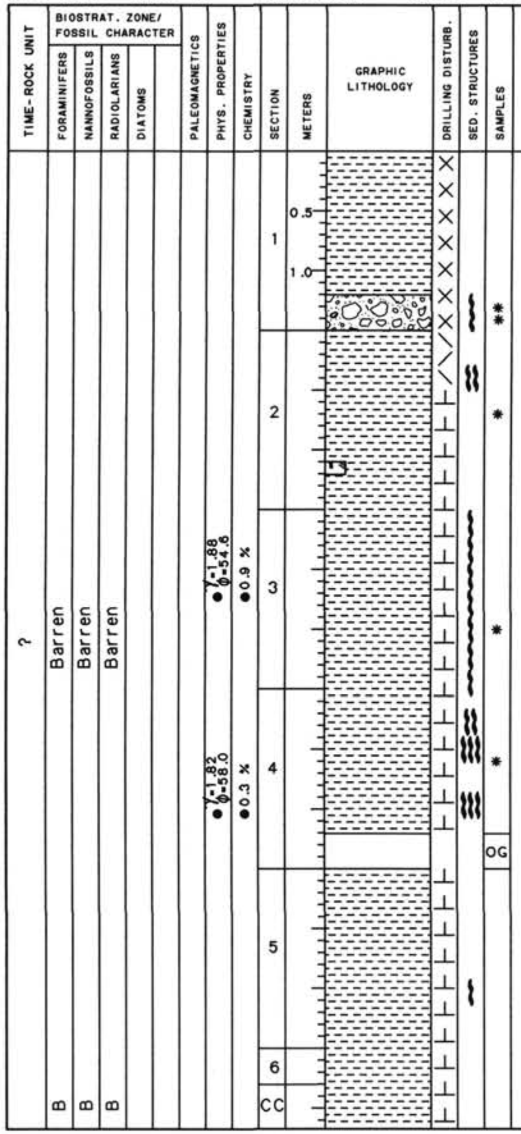

LITHOLOGIC DESCRIPTION

CLAYSTONE

Homogeneous olive-gray to brownish gray (5GY4/1, 5G5/2), carbonate-free CLAYSTONE; minor disseminated ash throughout; strong local bioturbation. Breccia beds in Section 1, 120–150 cm, contain clasts apparently more indurated than sediment.

Structure: bedding dips steeply, 65° and 85°.

SMEAR SLIDE SUMMARY (%):

	1, 133 M	1, 135 M	2, 66 D	3, 102 M	4, 58 D
TEXTURE:					
Sand	Tr	2	—	—	—
Silt	72	18	1	11	3
Clay	28	80	99	89	97
COMPOSITION:					
Quartz	Tr	—	Tr	—	—
Feldspar	—	3	Tr	3	2
Rock fragments	—	—	—	4	—
Clay	28	35	99	90	97
Volcanic glass	—	2	—	—	—
Accessory minerals	—	—	—	2	—
Glauconite	Tr	—	—	—	—
Pyroxene	—	—	Tr	—	—
Hornblende	1	—	—	Tr	—
Mn oxide	70	60	—	Tr	1

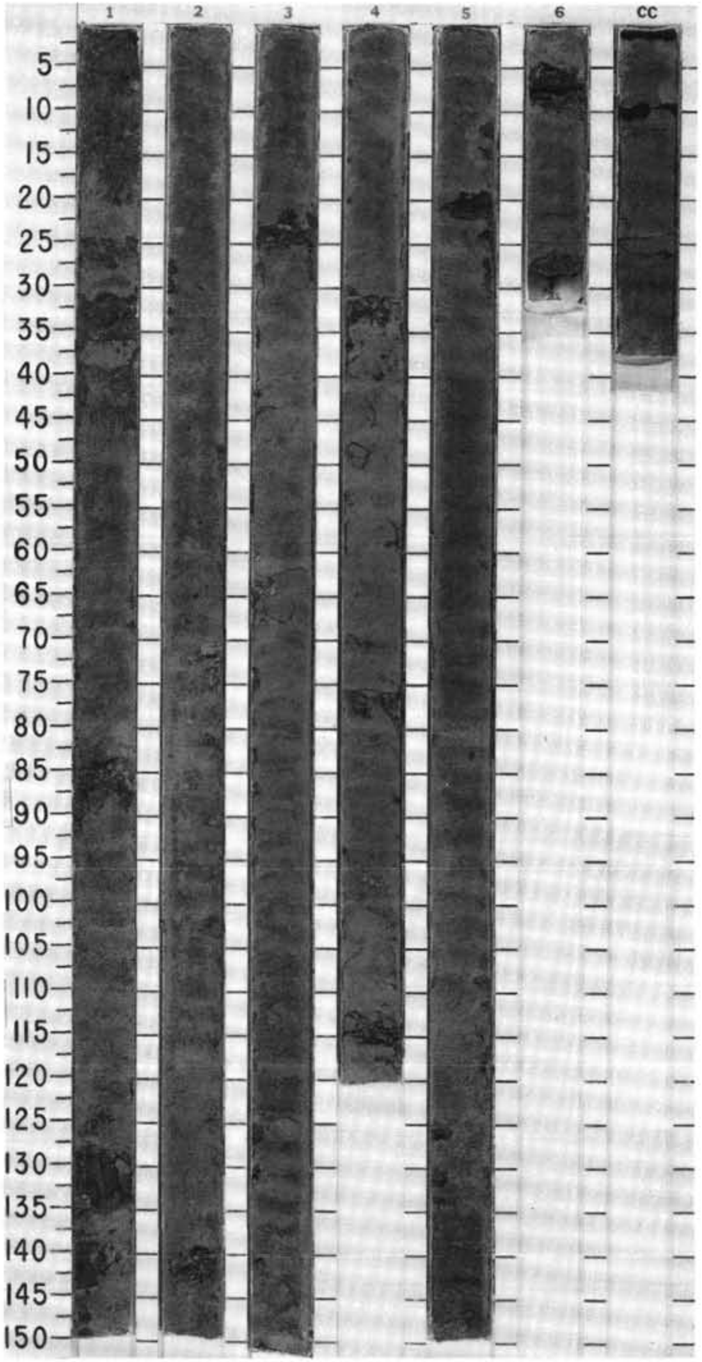

SITE 674 HOLE A CORE 23 X CORED INTERVAL 4755.8-4765.3 mbsl; 205.6-215.1 mbsf

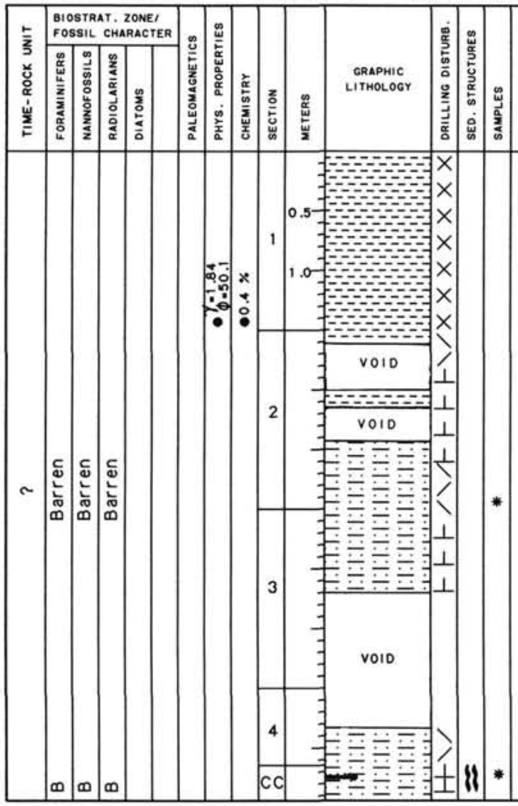

LITHOLOGIC DESCRIPTION

CLAYSTONE and MUDSTONE

Gray to olive-gray (5GY5/1, 5GY4/1) CLAYSTONE and MUDSTONE with minor disseminated ash.

Structure: steeply dipping scaly fabric, probably tectonic, developed throughout.

SMEAR SLIDE SUMMARY (%):

	2, 147 D	CC, 19 M
TEXTURE:		
Sand	5	—
Silt	15	90
Clay	85	10
COMPOSITION:		
Quartz	1	—
Feldspar	8	40
Rock fragments	Tr	10
Clay	80	10
Accessory minerals	2	Tr
Glauconite	—	Tr
Pyroxene	Tr	Tr
Mn oxide	9	40

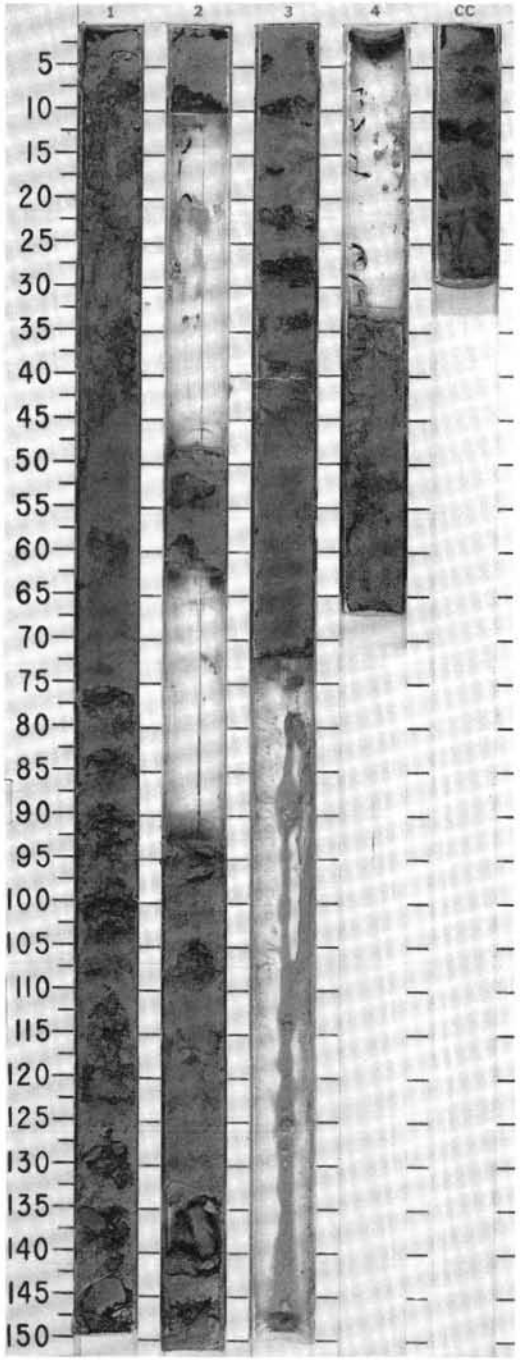

SITE 674 HOLE A CORE 24 X CORED INTERVAL 4765.3-4774.8 mbsl; 215.1-224.6 mbsf

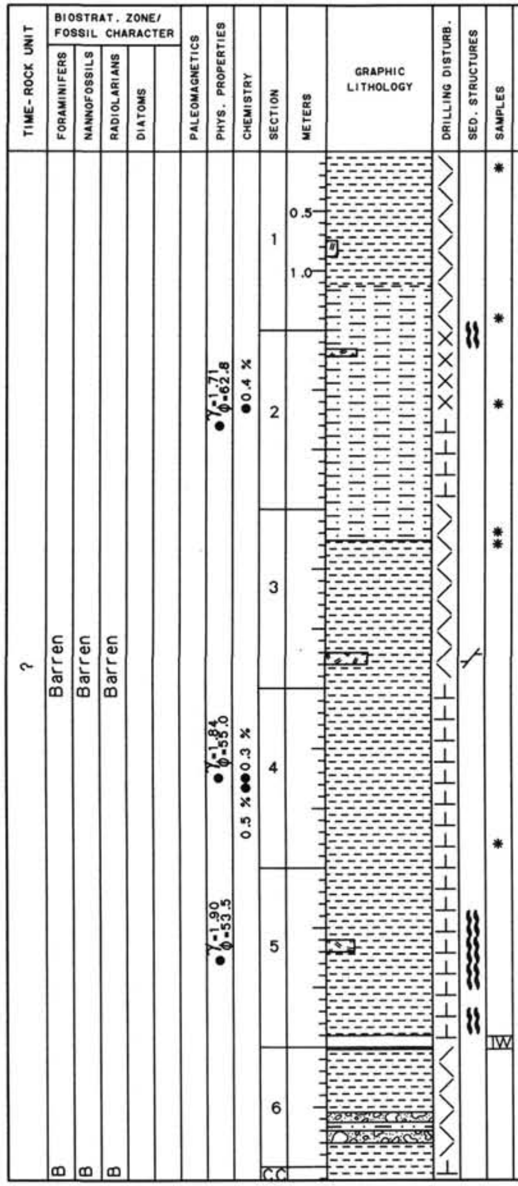

LITHOLOGIC DESCRIPTION

CLAYSTONE and MUDSTONE

Dark greenish gray (5GY4/1, 5G4/2) CLAYSTONE and MUDSTONE; frequent disseminated ash beds; conspicuous intervals of mud-matrix-supported conglomerate with reworked claystone and ash pebbles.

Structure: bedding dips vary 10–80°; normal fault in Section 3, 130–135 cm, dips 60°; scaly fabric dips steeply.

SMEAR SLIDE SUMMARY (%):

	1, 16 D	1, 143 M	2, 63 M	3, 17 M	3, 21 D	4, 123 M
TEXTURE:						
Sand	—	15	20	60	—	50
Silt	5	15	77	30	15	28
Clay	95	70	3	10	85	22
COMPOSITION:						
Quartz	Tr	—	5	20	—	10
Feldspar	1	15	30	50	—	40
Rock fragments	—	—	—	10	—	20
Clay	69	70	3	—	85	22
Volcanic glass	—	Tr	—	—	—	—
Accessory minerals	—	—	—	2	10	3
Orthopyroxene	—	—	—	2	—	1
Clinopyroxene	—	—	—	2	—	1
Hornblende	—	—	—	—	—	Tr
Mn oxide	30	25	60	5	5	5

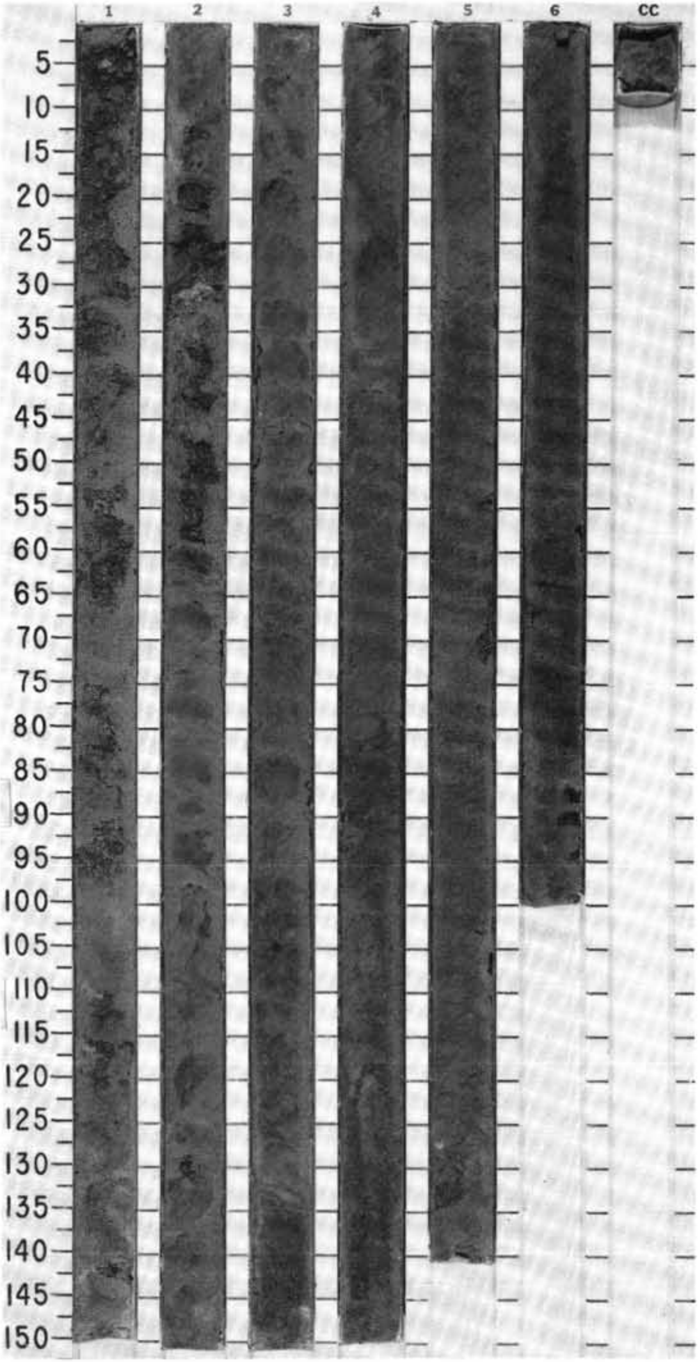

SITE 674 HOLE A CORE 25 X CORED INTERVAL 4774.8-4784.3 mbsl; 224.6-234.1 mbsf

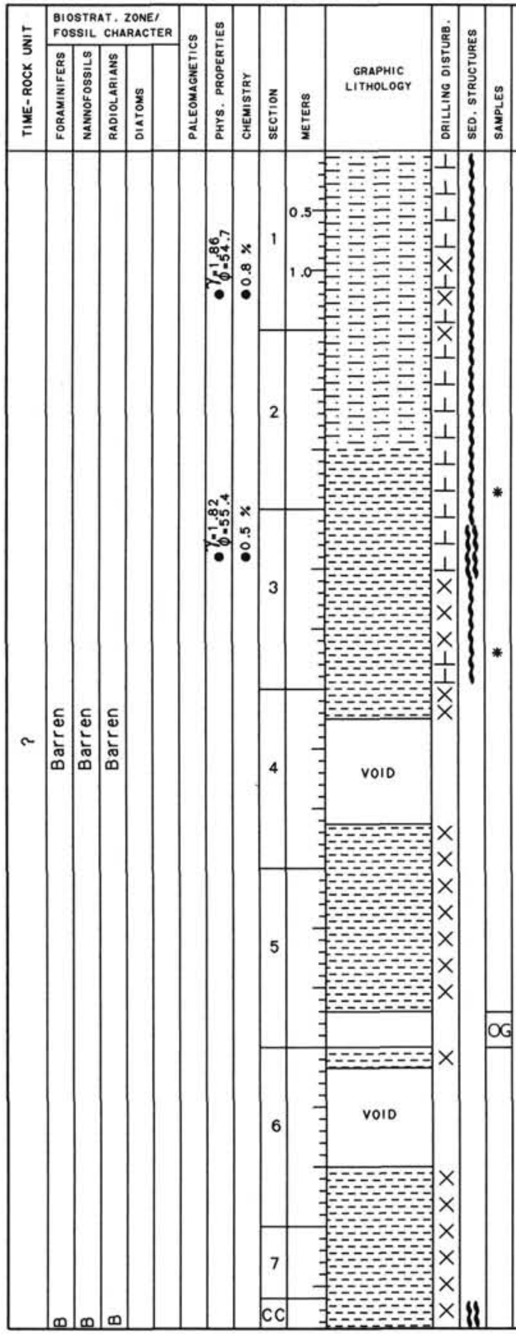

LITHOLOGIC DESCRIPTION

CLAYSTONE and MUDSTONE

Dark greenish gray to dark olive-gray (5GY4/1, 5Y4/2, 5Y4/1) CLAYSTONE and MUDSTONE, minor disseminated ash, moderate bioturbation. A few 1-mm-thin calcite veins in Section 3, 95–120 cm.

SMEAR SLIDE SUMMARY (%):

	2, 140 D	3, 122 D
TEXTURE:		
Silt	12	5
Clay	88	95
COMPOSITION:		
Feldspar	6	Tr
Rock fragments	1	Tr
Clay	88	95
Calcite/dolomite	2	5
Accessory minerals	3	—
Glauconite	—	Tr
Pyroxene	Tr	Tr
Mn oxide	—	Tr

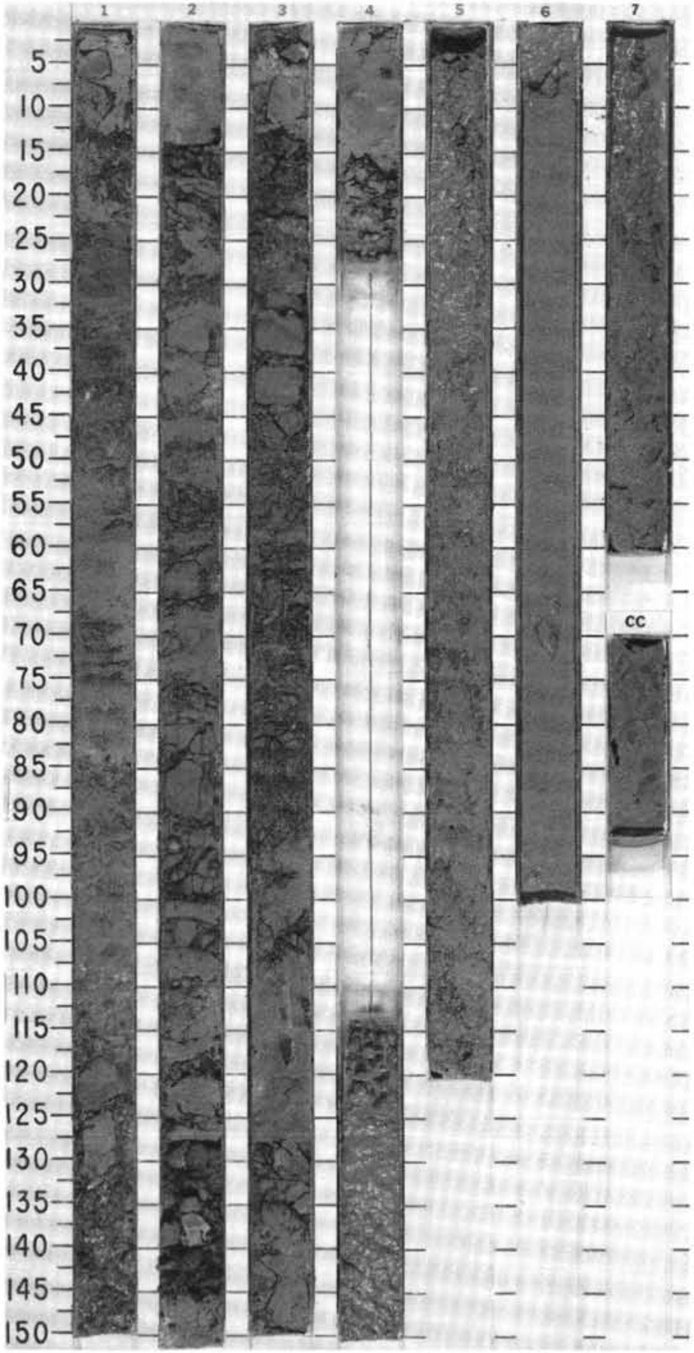

SITE 674 HOLE A CORE 26 X CORED INTERVAL 4784.3-4793.8 mbsl; 234.1-243.6 mbsf

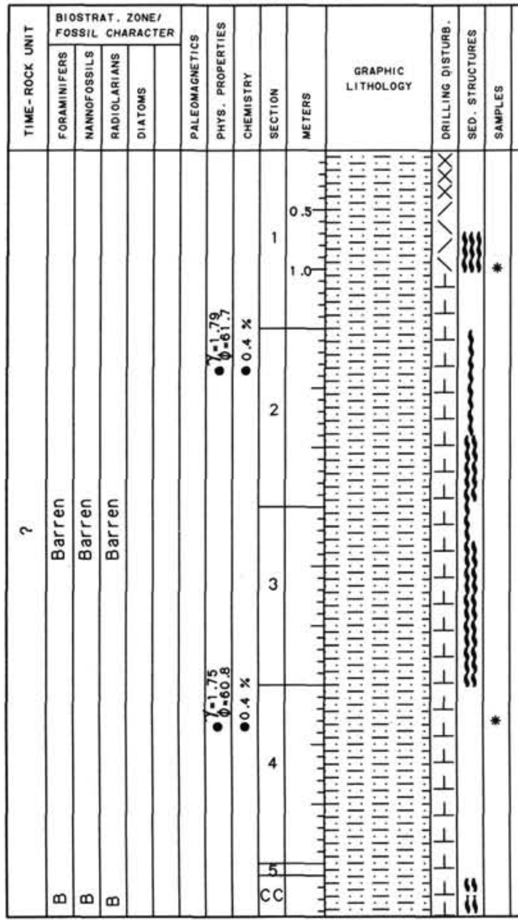

LITHOLOGIC DESCRIPTION

MUDSTONE

Homogeneous, moderately bioturbated, carbonate-free, greenish gray to brownish gray (5GY4/1, 5Y4/2) MUDSTONE with minor disseminated ash.

Structure: discrete, brownish, scaly fault zone in Section 4, 50–115 cm.

SMEAR SLIDE SUMMARY (%):

	1, 99 D	4, 33 D
TEXTURE:		
Sand	1	—
Silt	15	15
Clay	84	85
COMPOSITION:		
Quartz	5	—
Feldspar	2	5
Rock fragments	—	3
Clay	84	79
Volcanic glass	9	3
Accessory minerals	—	10
Sponge spicules	Tr	—

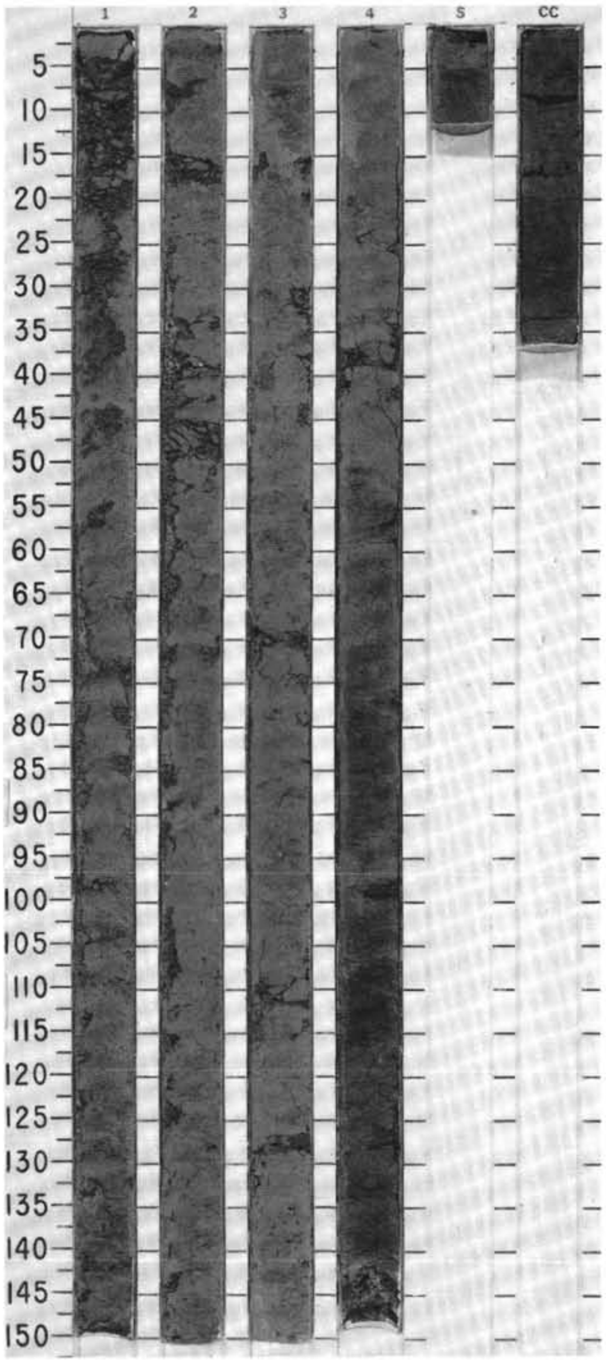

SITE 674 HOLE A CORE 27 X CORED INTERVAL 4793.8-4803.3 mbsl; 243.6-253.1 mbsf

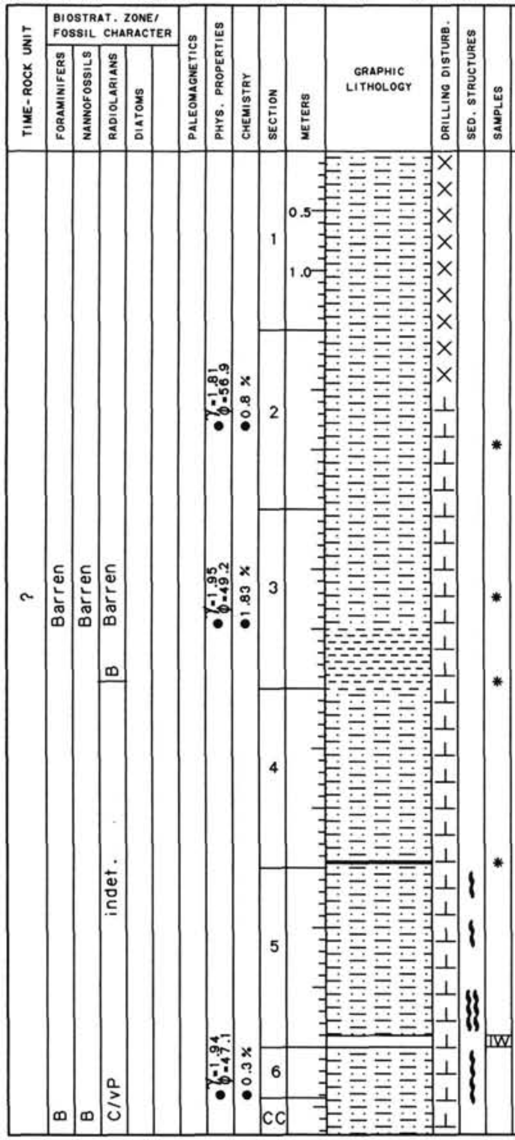

LITHOLOGIC DESCRIPTION

MUDSTONE and CLAYSTONE

Dark to light brownish gray (10YR6/3, 10YR5/4, 5GY5/1) MUDSTONE and CLAYSTONE, local mild bioturbation.

Structure: subhorizontal, scaly shear zone in Section 3; moderate to intense scaly fabric with subhorizontal to shallow dips from Section 3 through CC.

SMEAR SLIDE SUMMARY (%):

	2, 96 D	3, 76 D	3, 139 D	4, 148 M
TEXTURE:				
Sand	—	Tr	—	10
Silt	15	20	2	40
Clay	85	80	98	50
COMPOSITION:				
Quartz	10	5	—	25
Feldspar	Tr	10	1	10
Rock fragments	—	—	—	10
Clay	85	75	98	50
Volcanic glass	5	10	Tr	—
Accessory minerals	—	—	1	5
Hematite	—	—	Tr	—
Radiolarians	—	Tr	—	—

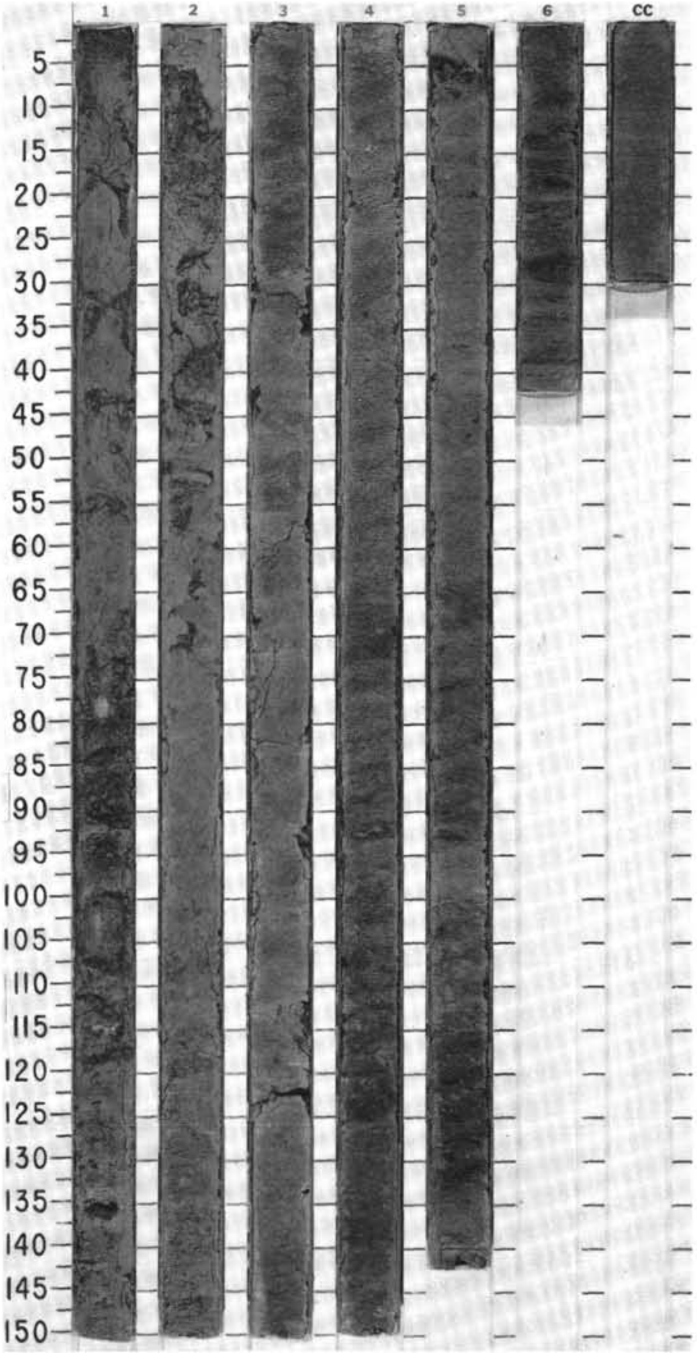

SITE 674 HOLE A CORE 28 X CORED INTERVAL 4803.3-4812.8 mbsl; 253.1-262.6 mbsf

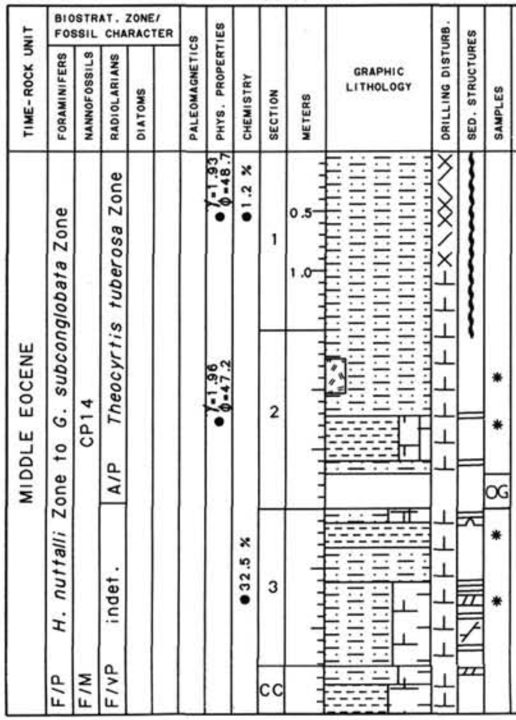

LITHOLOGIC DESCRIPTION

CLAYSTONE, MUDSTONE, and MARLSTONE

Interbedded, dark greenish gray or orange-brown (5G5/2, 10YR5/5) CLAYSTONE; orange-brown (10YR5/5) MUDSTONE; and laminated pale green (5GY6/1) silty MARLSTONE.

Structure: pervasive scaly fabric dipping 50–70° in claystone; reverse fault in Section 3, 110–115 cm, dips 40°; bedding dips from 5–25°.

SMEAR SLIDE SUMMARY (%):

	2, 42 D	2, 80 D	3, 24 D	3, 77 D
TEXTURE:				
Sand	—	20	Tr	10
Silt	20	5	5	40
Clay	80	75	95	50
COMPOSITION:				
Quartz	5	2	10	5
Feldspar	2	—	—	2
Clay	78	63	75	38
Volcanic glass	15	5	10	15
Accessory minerals				
Pyroxene	Tr	—	—	Tr
Foraminifers	—	20	Tr	5
Nannofossils	Tr	10	5	35

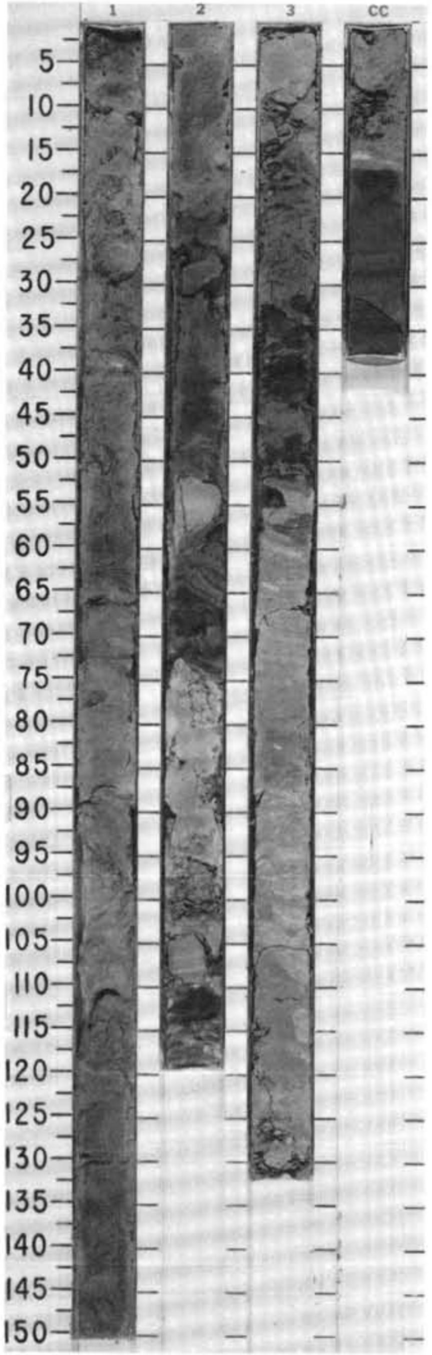

SITE 674 HOLE A CORE 29 X CORED INTERVAL 4812.8-4822.3 mbsl; 262.6-272.1 mbsf

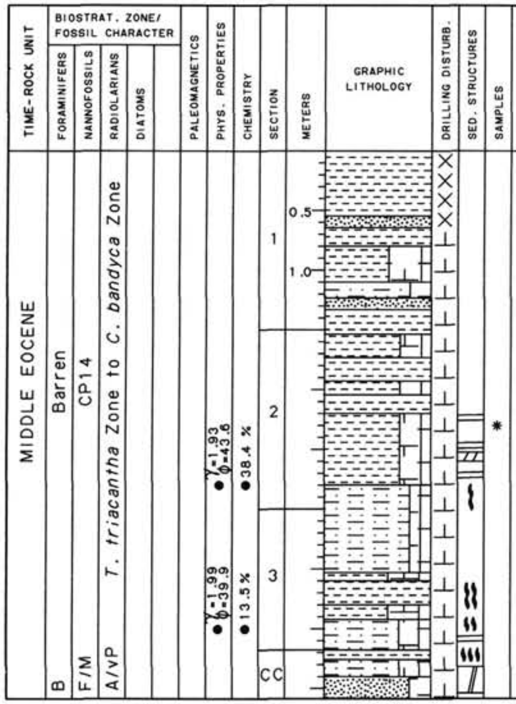

LITHOLOGIC DESCRIPTION

CLAYSTONE, SILTSTONE, and CALCAREOUS SANDSTONE

Interbedded green to dark green (5G5/1) CLAYSTONE, laminated greenish gray (5Y6/1) SILTSTONE, dark greenish gray to olive (5GY5/1, 5Y6/1, 5Y3/1) cross-laminated CALCAREOUS SANDSTONE, and pale greenish gray (5Y6/2, 5GY7/1) MARL.

Structure: possibly overturned bedding (10° dip); intensely scaly interval in Section 1.

SMEAR SLIDE SUMMARY (%):

	2, 80 D
TEXTURE:	
Sand	20
Silt	5
Clay	75
COMPOSITION:	
Quartz	2
Clay	67
Volcanic glass	5
Foraminifers	20
Nannofossils	10

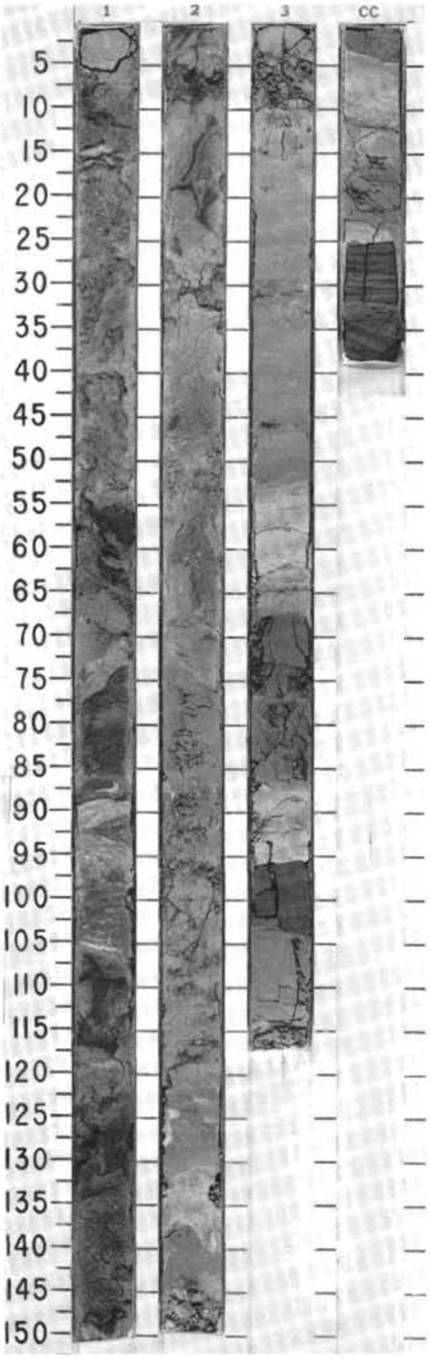

SITE 674 HOLE A CORE 30 X CORED INTERVAL 4822.3-4831.8 mbsl; 272.1-281.6 mbsf

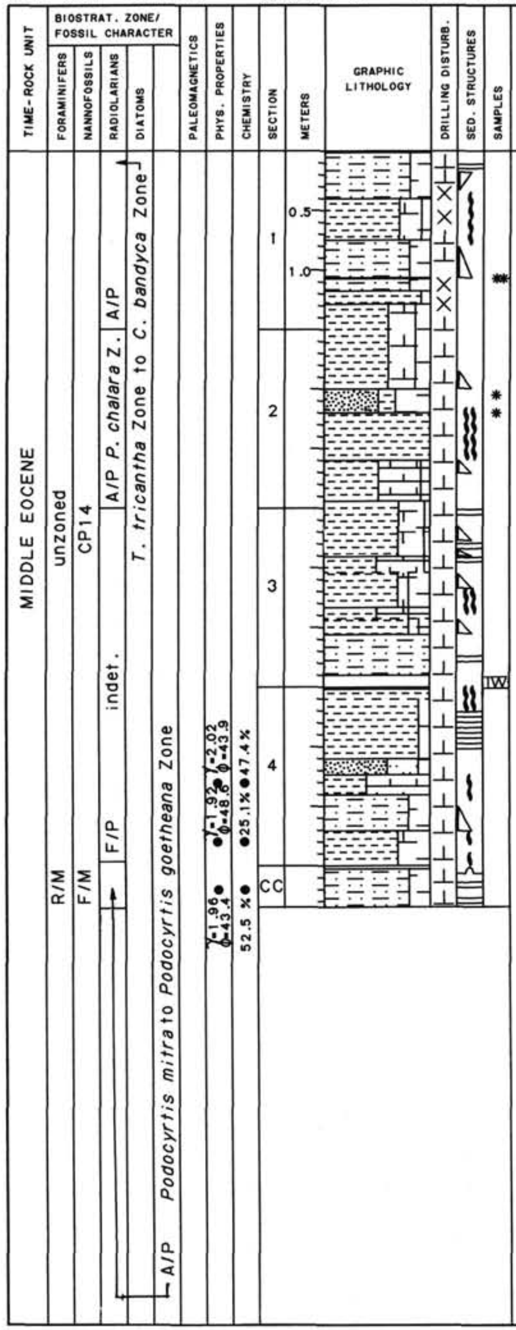

CALCAREOUS MUDSTONE, CHALK, MUDSTONE, CLAYSTONE, and SANDSTONE

Interbedded greenish gray (5GY6/1, 5G6/1) CALCAREOUS MUDSTONE; light gray (5G7/1) CHALK; light brown (5Y4/1), laminated calcareous sandy MUDSTONE; dark green (5G5/2) CLAYSTONE; and dark brown (5Y3/2), calcareous silty SANDSTONE.

Structure: bedding dips range from subhorizontal to 50°; probably upright bedding, although grading in Section 1, 15–35 cm, suggests overturned beds.

SMEAR SLIDE SUMMARY (%):

	1, 102 M	1, 103 D	2, 53 D	2, 66 D
TEXTURE:				
Sand	—	—	65	—
Silt	5	50	19	12
Clay	95	50	16	88
COMPOSITION:				
Quartz	5	20	45	6
Feldspar	—	—	3	—
Clay	95	45	15	88
Calcite/dolomite	—	5	3	—
Accessory minerals	—	5	—	—
Glauconite	—	—	1	Tr
Pyroxene	—	—	Tr	—
Opaques	—	—	3	—
Zircon	—	—	Tr	—
Foraminifers	—	15	25	—
Nannofossils	Tr	10	3	Tr
Radiolarians	—	—	—	5
Sponge spicules	Tr	—	—	—
Fish remains	—	—	—	Tr
Plant debris	Tr	—	Tr	—
Bioclasts	—	—	2	—

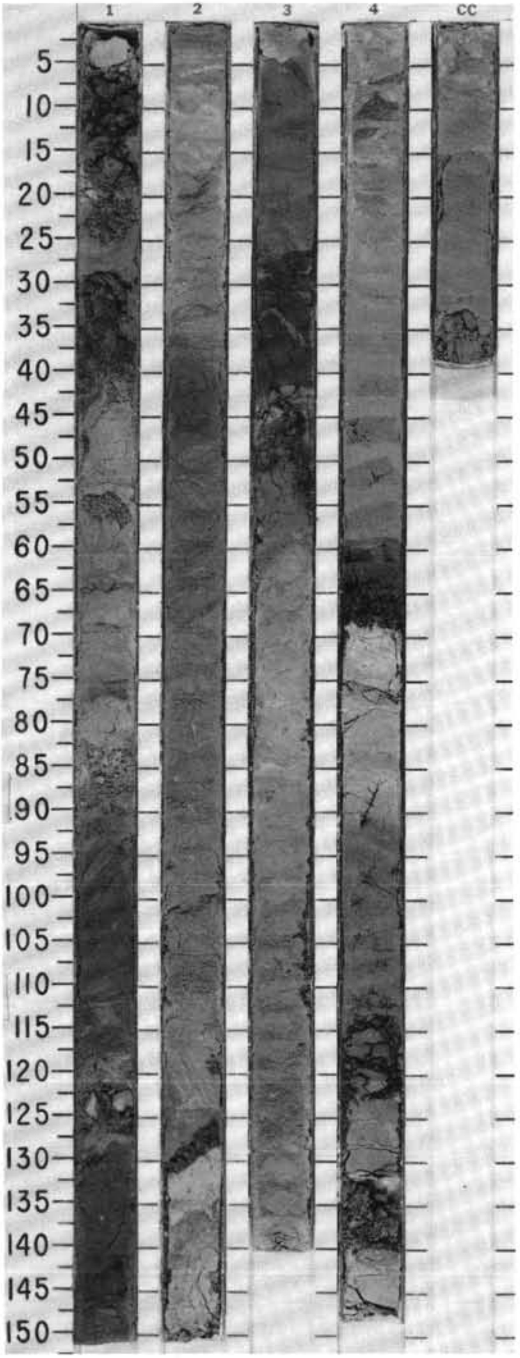

SITE 674 HOLE A CORE 31 X CORED INTERVAL 4831.8-4841.3 mbsl; 281.6-291.1 mbsf

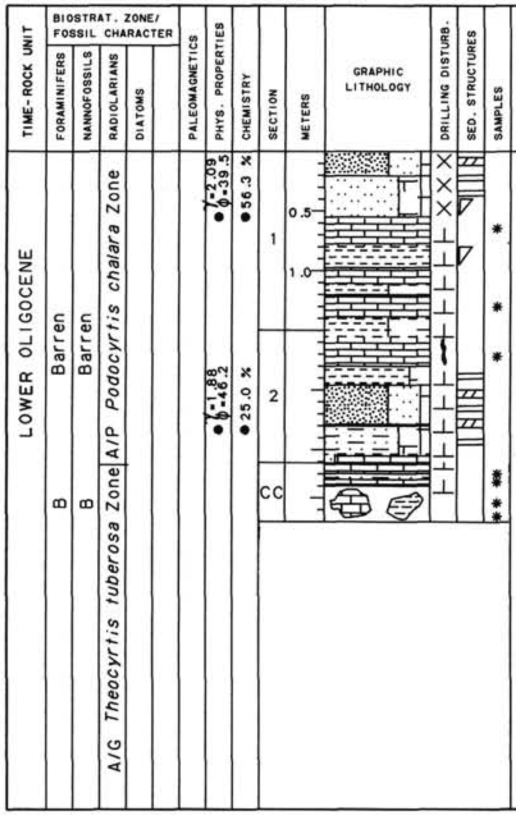

LITHOLOGIC DESCRIPTION

CHALK, CALCAREOUS MUDSTONE, CLAYSTONE, and SANDSTONE

Interbedded white to light greenish gray (5GY7/1) CHALK and silty CHALK, local bioturbation; light brown (5Y4/1) laminated CALCAREOUS MUDSTONE; dark green (5G5/2) CLAYSTONE, and dark brown (5Y2.5/1) laminated and cross-laminated SANDSTONE.

Structure: Sections 1 and 2 are overturned, beds dip 45°.

SMEAR SLIDE SUMMARY (%):

	1, 66 D	1, 128 M	2, 26 D	CC, 4 D	CC, 12 M	CC, 32 M	CC, 45 D
TEXTURE:							
Sand	—	—	—	17	—	—	3
Silt	55	1	40	78	95	20	20
Clay	45	99	60	5	5	80	77
COMPOSITION:							
Quartz	—	1	1	15	75	—	—
Feldspar	—	—	—	2	2	—	—
Rock fragments	—	—	—	—	10	—	—
Clay	15	—	20	—	5	—	77
Calcite/dolomite	45	49	44	78	—	80	1
Accessory minerals	—	—	—	—	4	—	—
Glauconite	—	—	—	—	1	—	—
Micronodules	—	—	—	—	1	—	—
Fe/Mn oxide	—	—	—	—	2	—	10
Foraminifers	Tr	—	Tr	—	—	20	—
Nannofossils	40	50	35	5	—	—	—
Diatoms	—	—	—	—	—	—	3
Radiolarians	—	—	—	—	—	—	4
Sponge spicules	—	—	—	—	—	—	5

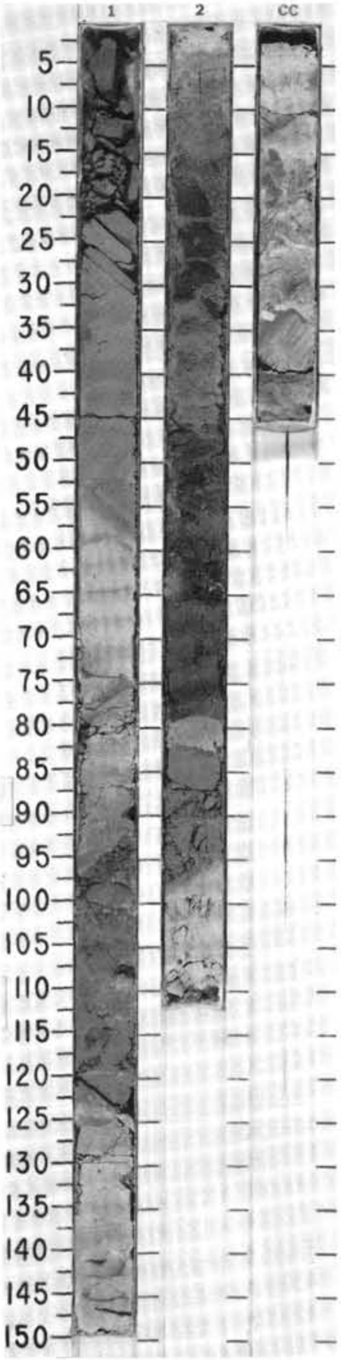

SITE 674 HOLE A CORE 32 X CORED INTERVAL 4841.3-4850.8 mbsl; 291.1-300.6 mbsf

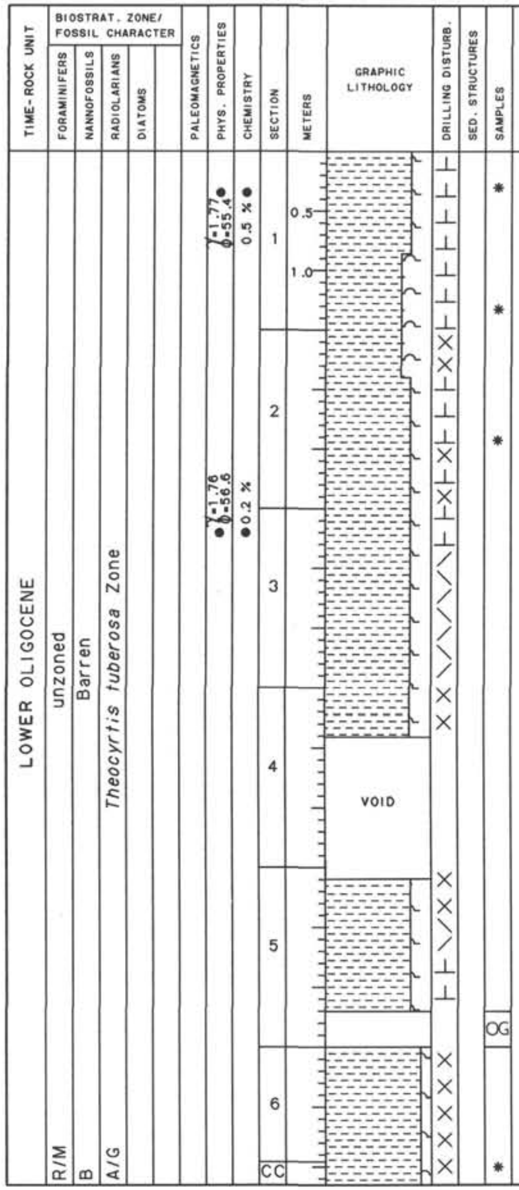

LITHOLOGIC DESCRIPTION

CLAYSTONE and MUDSTONE

Homogeneous light yellowish brown (2.5Y6/4) to light olive-brown (2.5Y5/4, 2.5Y5/6) and brownish gray (2.5Y6/2) radiolarian-bearing CLAYSTONE in Sections 1, 6, and CC; MUDSTONE in Sections 1 through 5; sporadic greenish gray (5G6/1) alteration.

SMEAR SLIDE SUMMARY (%):

	1, 31 M	1, 139 D	2, 89 D	CC, 4 D
TEXTURE:				
Sand	Tr	10	3	—
Silt	25	30	27	18
Clay	75	60	70	82
COMPOSITION:				
Quartz	Tr	—	—	3
Feldspar	Tr	—	—	—
Clay	75	60	70	82
Diatoms	—	—	—	1
Radiolarians	20	30	20	10
Sponge spicules	5	7	8	4
Silicoflagellates	—	3	2	—

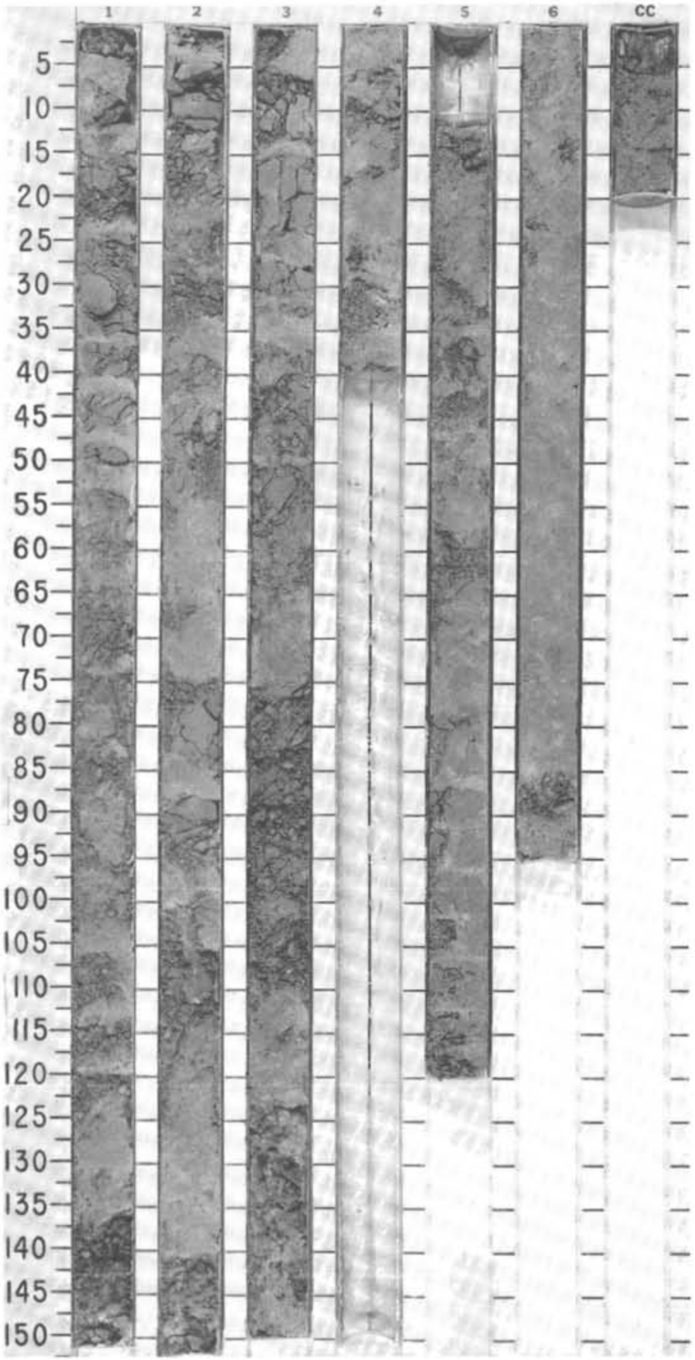

SITE 674 HOLE A CORE 33 X CORED INTERVAL 4850.8-4860.3 mbsl; 300.6-310.1 mbsf

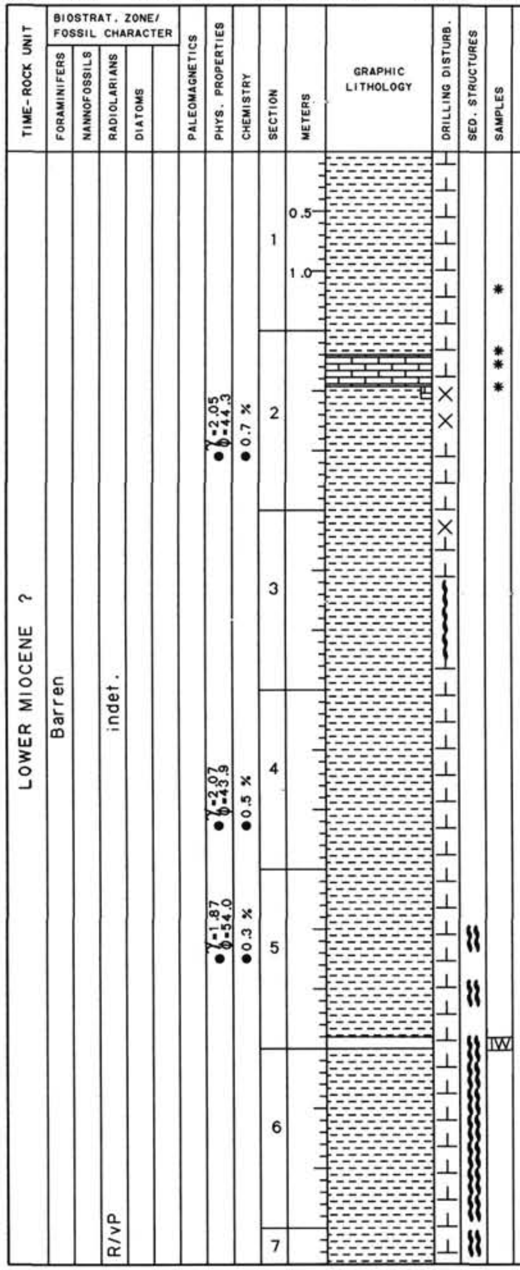

LITHOLOGIC DESCRIPTION

CLAYSTONE

Dark greenish gray (5BG4/1, 5GY4/1), dark gray (5Y4/1), and olive-gray (5Y4/2), to dark olive-gray (5Y3/2) homogeneous CLAYSTONE; locally weakly calcareous; Sections 5 and 6 show bioturbation.

Minor lithology: gray (5Y6/1), laminated, micritic indurated chalk in Section 2, 22–47 cm, underlain by 10 cm of calcareous mudstone.

Structure: scaly fabrics developed throughout core; bedding dips 60° in Section 2, 50 cm; calcite veins in Section 2, 23–27 cm, and Section 6, 110–140 cm.

SMEAR SLIDE SUMMARY (%):

	1, 111 D	2, 22 M	2, 29 M	2, 48 D
TEXTURE:				
Silt	Tr	50	60	10
Clay	100	50	40	90
COMPOSITION:				
Quartz	Tr	—	1	1
Feldspar	—	—	—	1
Clay	100	10	—	90
Calcite/dolomite	—	90	98	5
Accessory minerals				
Glauconite	—	—	—	Tr
Opaques	—	—	Tr	Tr
Foraminifers	—	—	—	1
Nannofossils	—	—	—	1
Fish remains	—	—	—	Tr

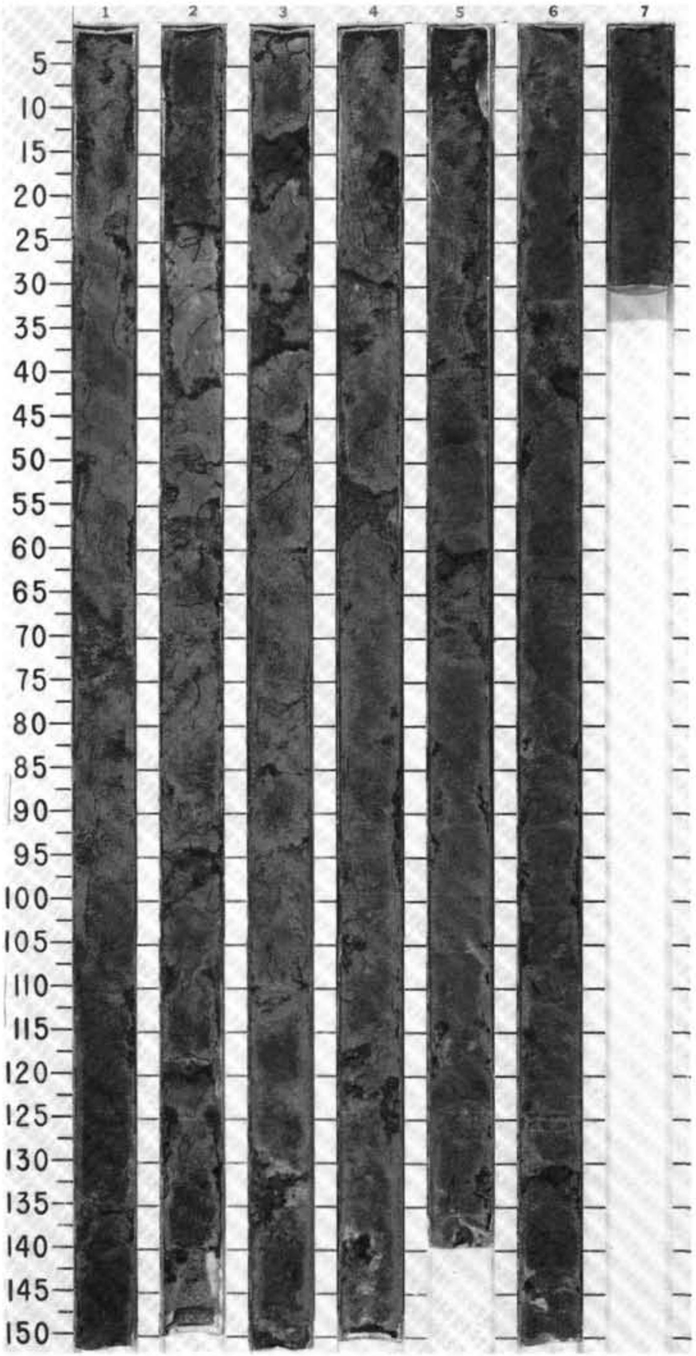

SITE 674 HOLE A CORE 34 X CORED INTERVAL 4860.3-4869.8 mbsl; 310.1-319.6 mbsf

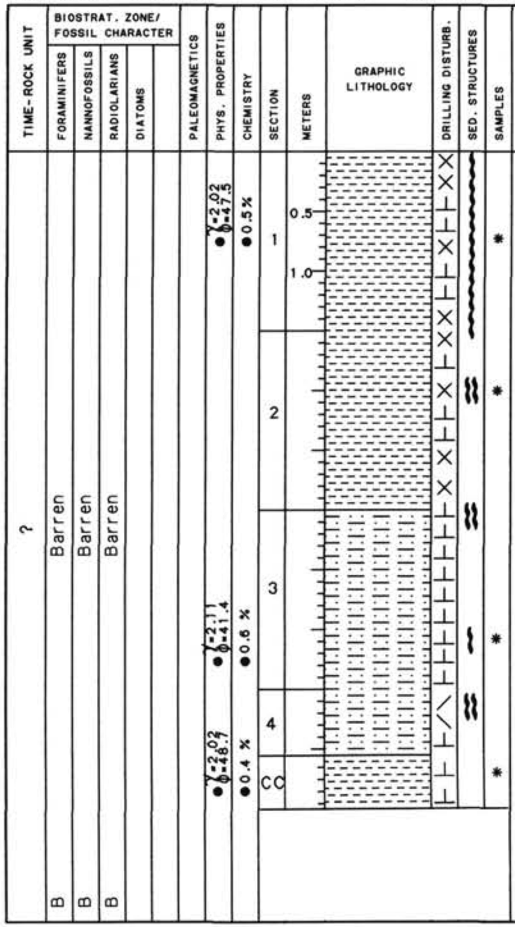

LITHOLOGIC DESCRIPTION

CLAYSTONE and MUDSTONE

Dark greenish gray (5GY4/1), dark gray (5Y4/1), dark olive-gray (5Y3/2), and dark brown (10YR3/3) CLAYSTONE and MUDSTONE; locally slightly to moderately bioturbated.

Structure: scaly fabrics developed in Section 4, 33–55 cm, and CC.

SMEAR SLIDE SUMMARY (%):

	1, 79 D	2, 54 M	3, 107 D	5, 19 D
TEXTURE:				
Sand	—	2	—	—
Silt	1	38	12	2
Clay	99	60	88	98
COMPOSITION:				
Quartz	1	1	2	Tr
Feldspar	—	5	—	Tr
Mica	—	—	—	Tr
Clay	99	33	88	98
Volcanic glass	—	1	—	—
Accessory minerals				
Opaques	Tr	—	—	1
Semi-opaque oxide	—	60	10	—
Possible Anglesite or Maguesite	—	—	—	Tr

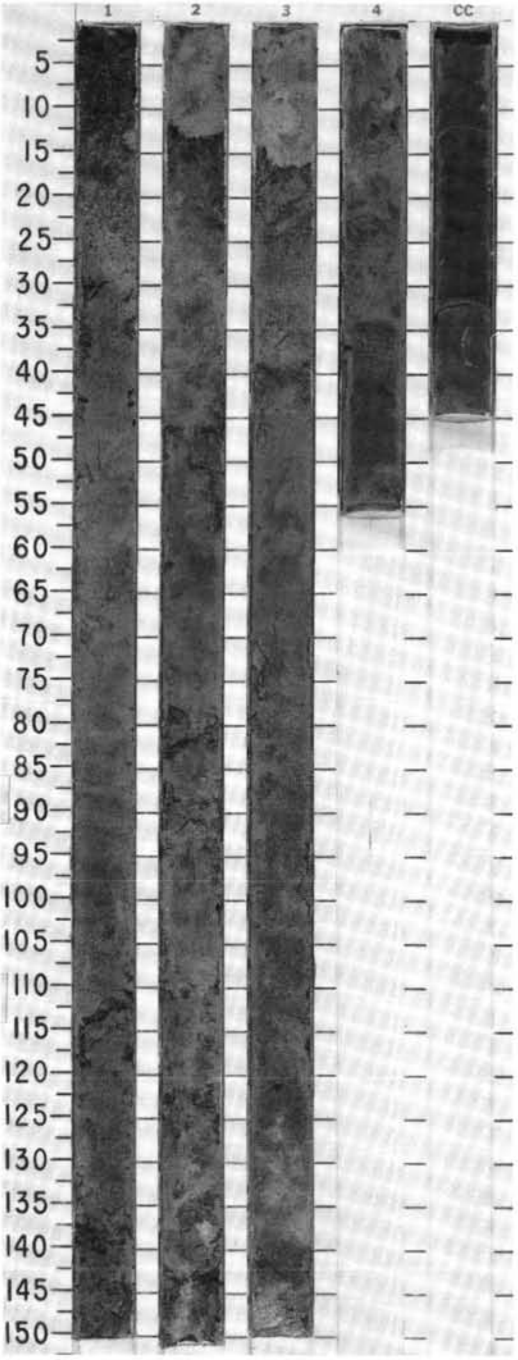

SITE 674 HOLE A CORE 35 X CORED INTERVAL 4869.8-4879.3 mbsl; 319.6-329.1 mbsf

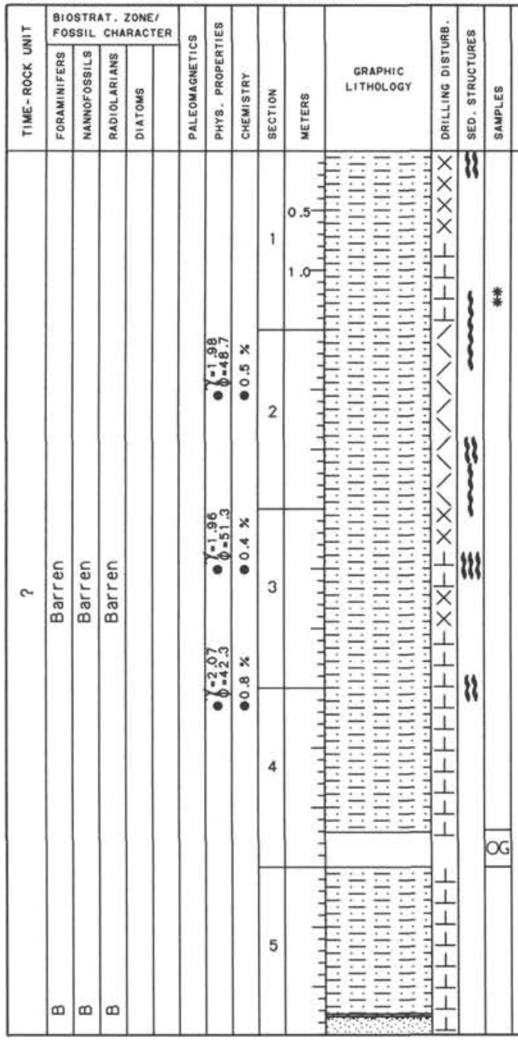

LITHOLOGIC DESCRIPTION

MUDSTONE

Varicolored gray (5GY3/1, 5G4/1, 5Y4/1, 10Y4/1, 5GY4/1) MUDSTONE with dark reddish brown (5YR3/3) and dark olive-gray (5Y3/2) intervals in Section 5, 56–122 cm; local mild to strong bioturbation.

Minor lithology: light gray (5BG4/1 and 2.5Y7/0) sandstone; minor calcite veins around margins and cross-cutting the sandstone in Section 5, 122–128 cm.

Structure: sandstone is stratally disrupted; scaly fabrics throughout mudstone.

SMEAR SLIDE SUMMARY (%):

	1, 119 M	1, 128 D
TEXTURE:		
Silt	20	25
Clay	80	75
COMPOSITION:		
Quartz	3	23
Feldspar	3	2
Clay	75	75
Volcanic glass	15	Tr
Accessory minerals		
Pyrite	3	—
Fe hydroxide	1	Tr

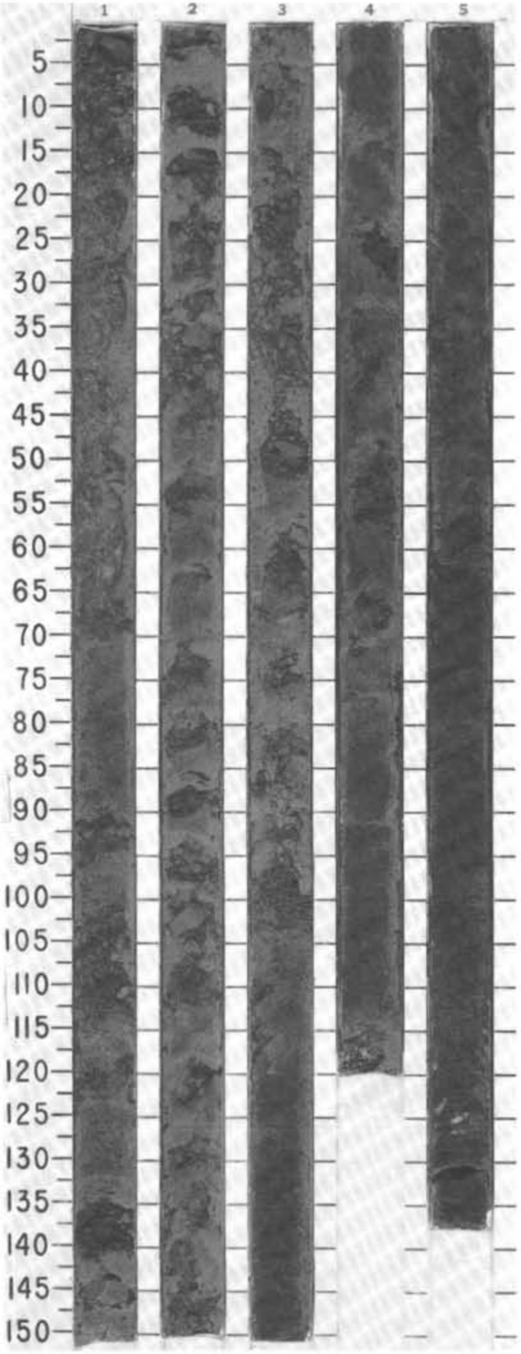

SITE 674 HOLE A CORE 36 X CORED INTERVAL 4879.3-4888.8 mbsl; 329.1-338.6 mbsf

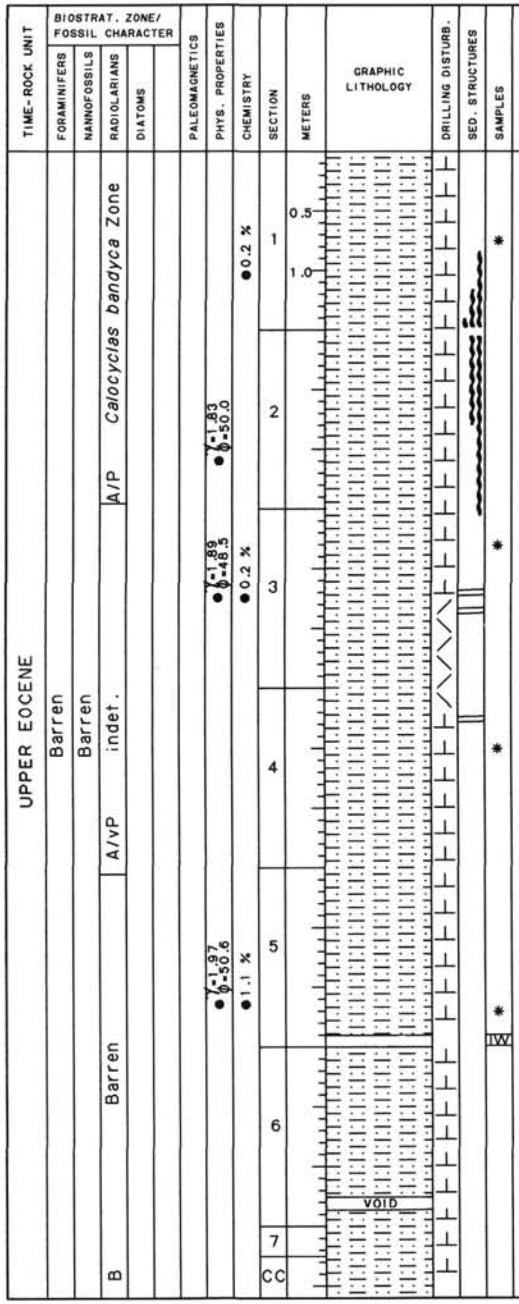

LITHOLOGIC DESCRIPTION

MUDSTONE

Varicolored gray (5GY5/1, 5G5/1, 5Y4/1), grayish green (5G5/2, 10G4/2), olive (10Y4/2), light olive-brown (2.5Y5/4), dark yellowish brown (10YR4/4), dark grayish brown (10YR4/2), brown (10YR5/3), and dark grayish brown (10YR5/3) MUDSTONE; slightly to strongly bioturbated in Sections 1 and 2; silty laminations in Sections 3 and 4.

Structure: scaly fabrics in Sections 1–2, 4–7, and CC; web structure in Sections 3 and 4. Bedding dips 30° in Section 3, 75 cm, and 30° in Section 6, 103 cm. Calcite veins in Section 6, 90 cm, crosscut scaly fabric.

SMEAR SLIDE SUMMARY (%):

	1, 75 D	3, 32 M	4, 55 M	5, 124 D
TEXTURE:				
Sand	2	—	6	—
Silt	13	20	34	20
Clay	85	80	60	80
COMPOSITION:				
Quartz	16	20	34	20
Feldspar	—	—	5	2
Clay	80	80	58	78
Volcanic glass	Tr	Tr	3	—
Accessory minerals				
Pyrite	—	Tr	—	—
Clinopyroxene	—	Tr	—	—
Hornblende(?)	—	—	—	Tr
Radiolarians	2	—	—	—
Sponge spicules	2	—	—	—

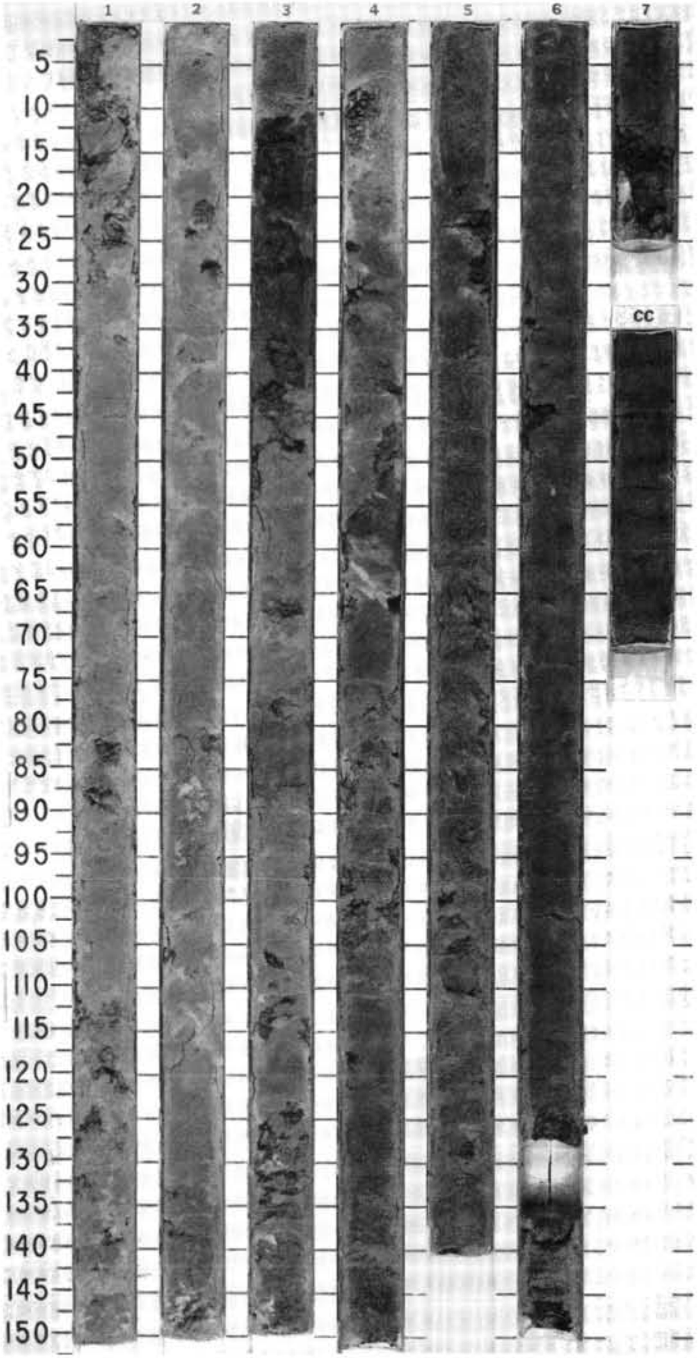

SITE 674 HOLE A CORE 37 X CORED INTERVAL 4888.8-4898.3 mbsl; 338.6-348.1 mbsf

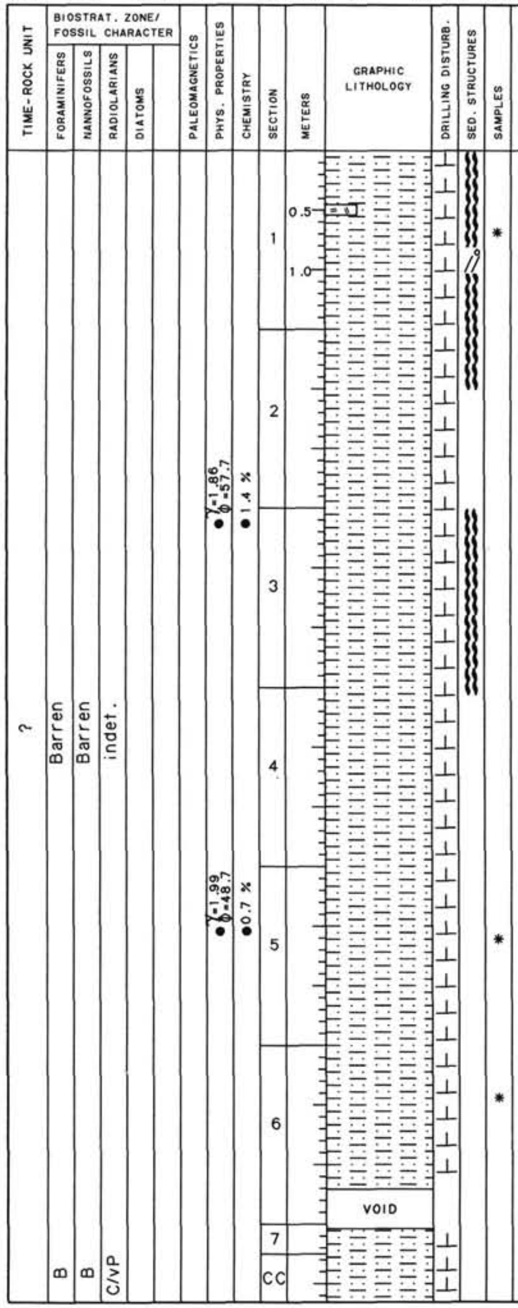

LITHOLOGIC DESCRIPTION

MUDSTONE

Homogeneous, greenish gray (5BG4/1, 5G4/1), bioturbated MUDSTONE; grades down to orangish brown (10YR5/8) MUDSTONE; minor disseminated ash throughout.

Structure: scaly fabric, well developed, Section 4 through CC (mostly steeply dipping); local calcite veins in Section 1, 0–35 and 105–110 cm, and CC, 16–22 cm; stratal disruption in Section 5, 98–107 cm; and web structure(?) in Section 3, 82–88 cm.

SMEAR SLIDE SUMMARY (%):

	1, 69 D	5, 68 D	6, 46 M
TEXTURE:			
Sand	5	—	—
Silt	25	25	5
Clay	70	75	95
COMPOSITION:			
Quartz	—	5	—
Feldspar	5	8	5
Clay	65	68	40
Volcanic glass	30	19	52
Accessory minerals			
Pyroxene	Tr	—	—
Fe/Mn oxide	—	—	3

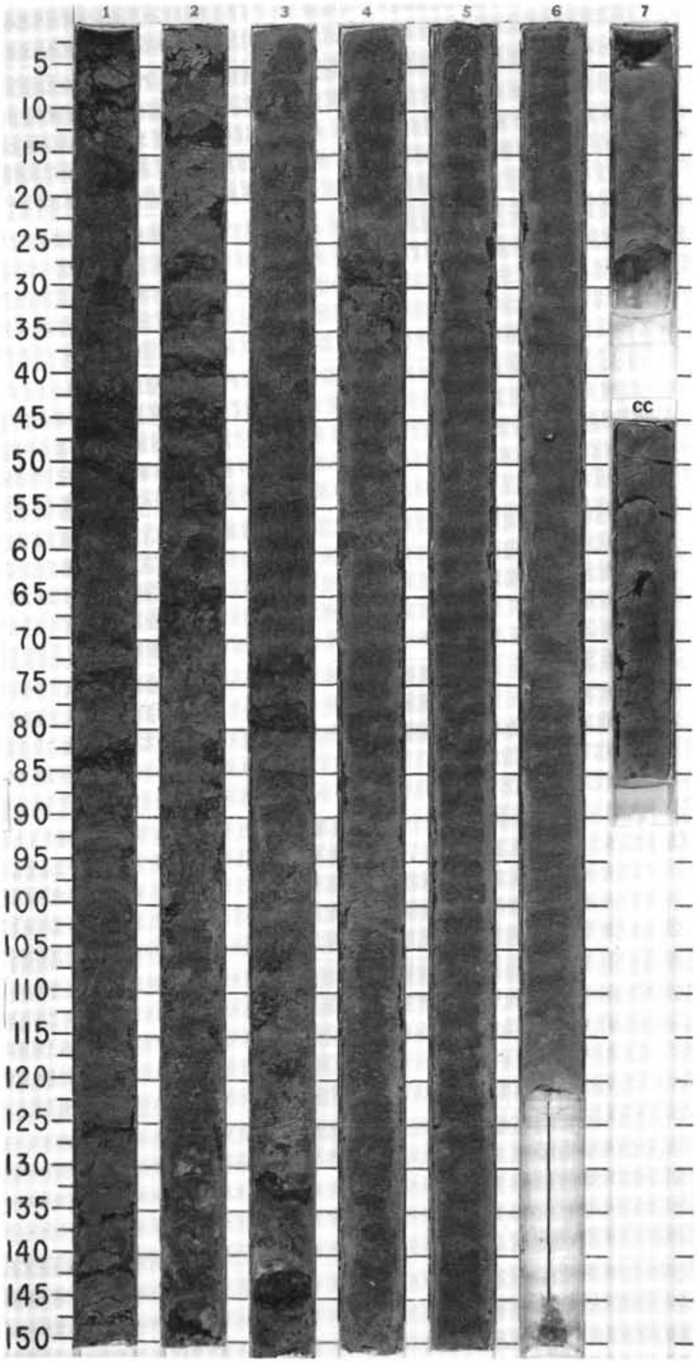

SITE 674 HOLE A CORE 38 X CORED INTERVAL 4898.3-4907.8 mbsl; 348.1-357.6 mbsf

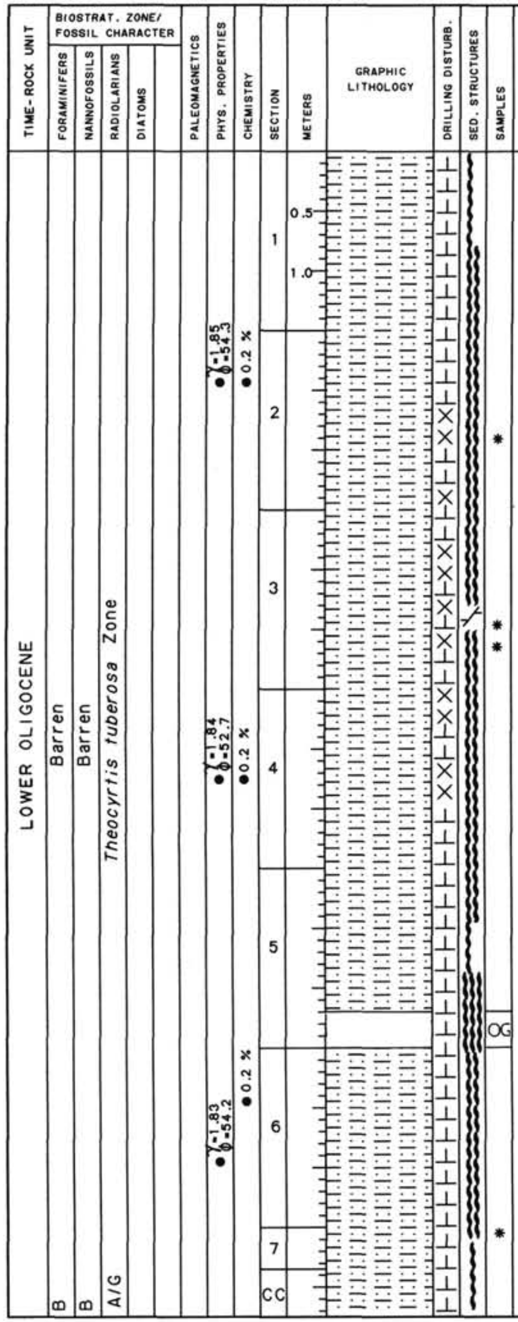

LITHOLOGIC DESCRIPTION

MUDSTONE

Olive to pale olive (5G4/2) MUDSTONE; locally greenish gray (5GY5/2) and brownish (5Y5/3); minor disseminated ash material; moderate to intense bioturbation.

Structure: scaly fabric, well developed in Sections 1 through 5 (generally steeply dipping); strike-slip fault dips 65° in Section 3, 88–89 cm.

SMEAR SLIDE SUMMARY (%):

	2, 100 D	3, 100 M	3, 113 D	7, 8 M
TEXTURE:				
Silt	25	15	20	20
Clay	75	85	80	80
COMPOSITION:				
Quartz	10	—	5	—
Feldspar	Tr	Tr	Tr	—
Clay	63	83	79	90
Volcanic glass	25	10	15	10
Diatoms	—	Tr	—	—
Radiolarians	—	5	—	Tr
Sponge spicules	2	2	1	—

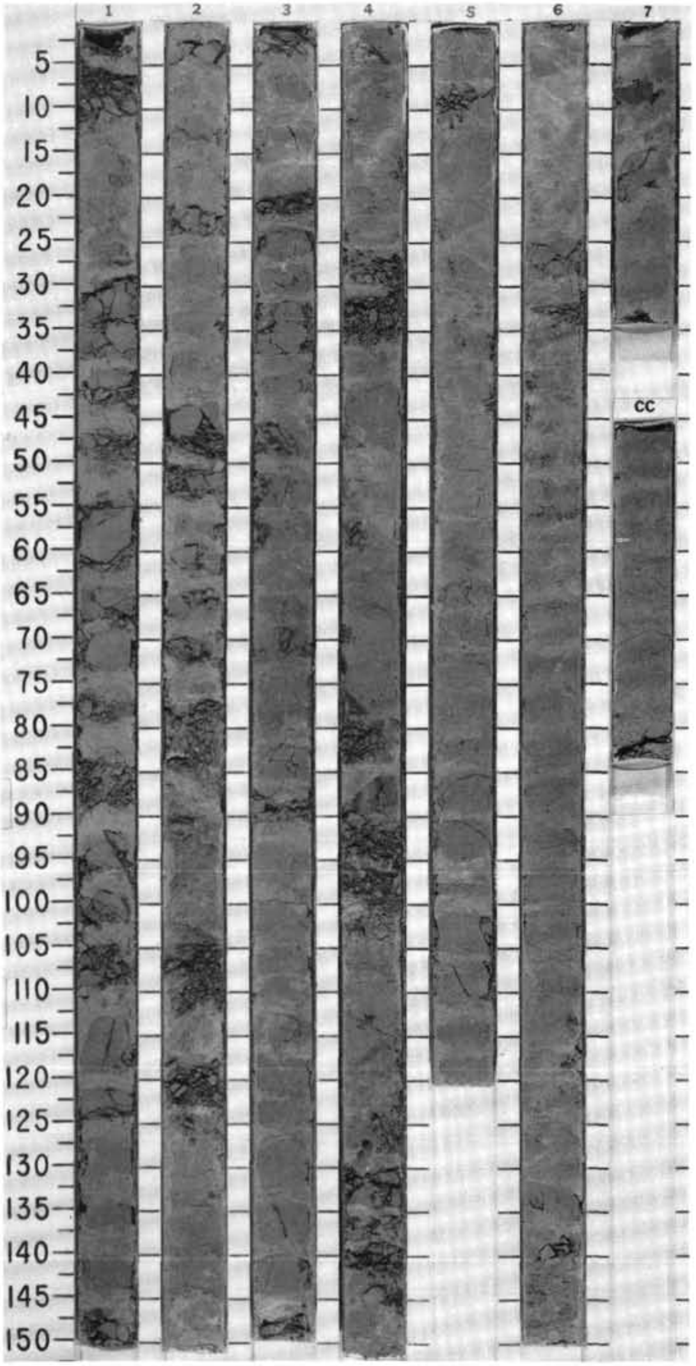

SITE 674 HOLE A CORE 39 X CORED INTERVAL 4907.8-4917.3 mbsl; 357.6-367.1 mbsf

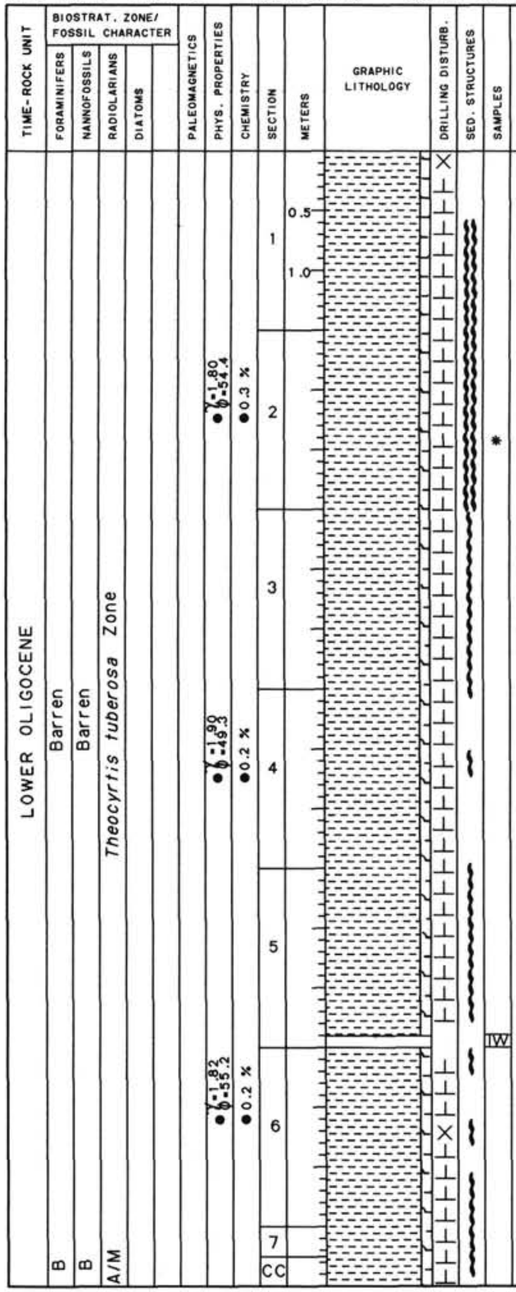

LITHOLOGIC DESCRIPTION

CLAYSTONE and MUDSTONE

Olive-gray (5Y5/2) to brownish (5Y5/3, 5Y6/2), slightly siliceous CLAYSTONE and MUDSTONE; moderately bioturbated; greenish gray staining along fractures throughout (5G6/1).

SMEAR SLIDE SUMMARY (%):

	2, 94 D
TEXTURE:	
Silt	10
Clay	90
COMPOSITION:	
Quartz	2
Clay	90
Radiolarians	5
Sponge spicules	3

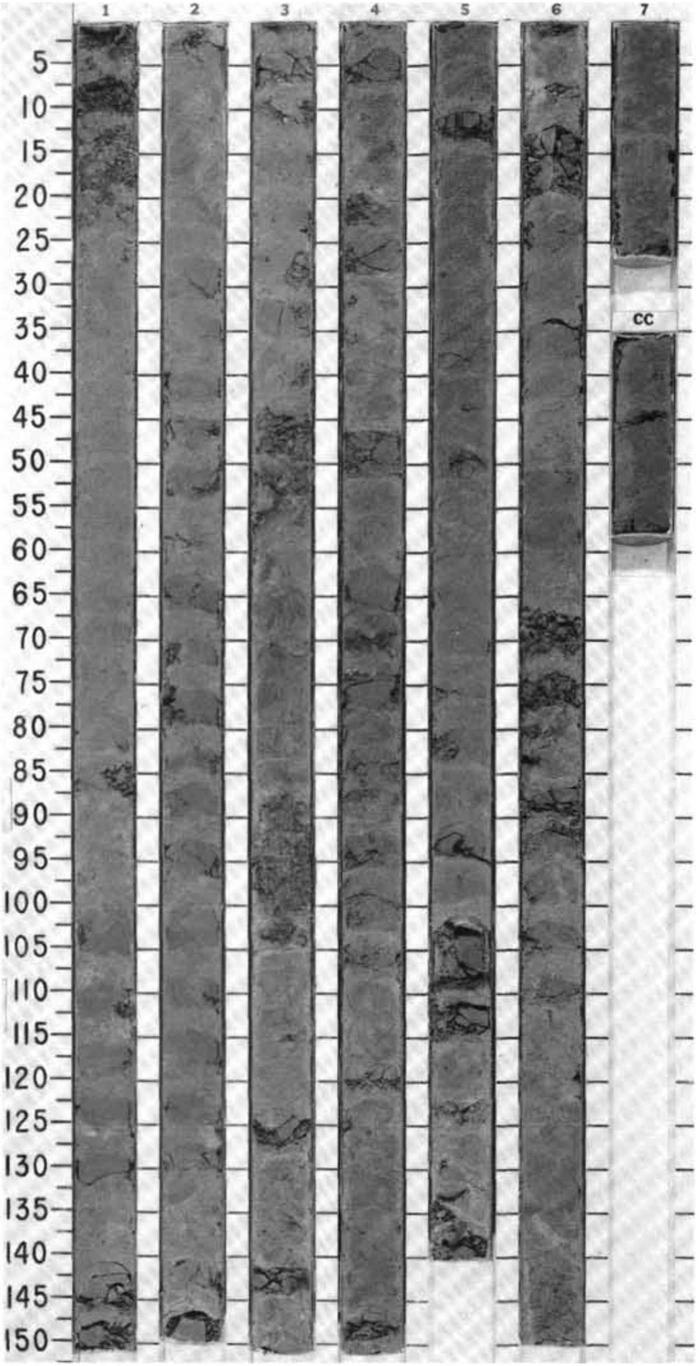

SITE 674 HOLE A CORE 40 X CORED INTERVAL 4917.3-4926.8 mbsl; 367.1-376.6 mbsf

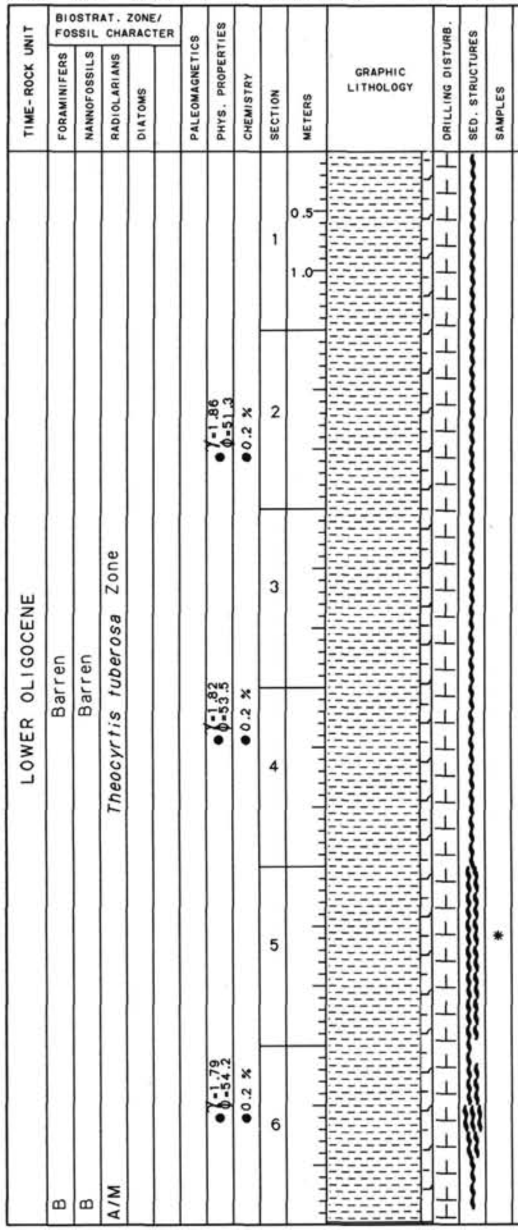

LITHOLOGIC DESCRIPTION

SILICEOUS MUDSTONE and SILICEOUS CLAYSTONE

Olive-gray (5Y5/2, 5G5/1) to brownish gray (5Y5/2) SILICEOUS MUDSTONE and SILICEOUS CLAYSTONE; moderately bioturbated; local greenish gray alteration (5G5/1); minor fracturing.

SMEAR SLIDE SUMMARY (%):

	5, 60 D
TEXTURE:	
Sand	2
Silt	20
Clay	78
COMPOSITION:	
Quartz	Tr
Feldspar	Tr
Clay	78
Accessory minerals	
Mn oxide	2
Radiolarians	15
Sponge spicules	5

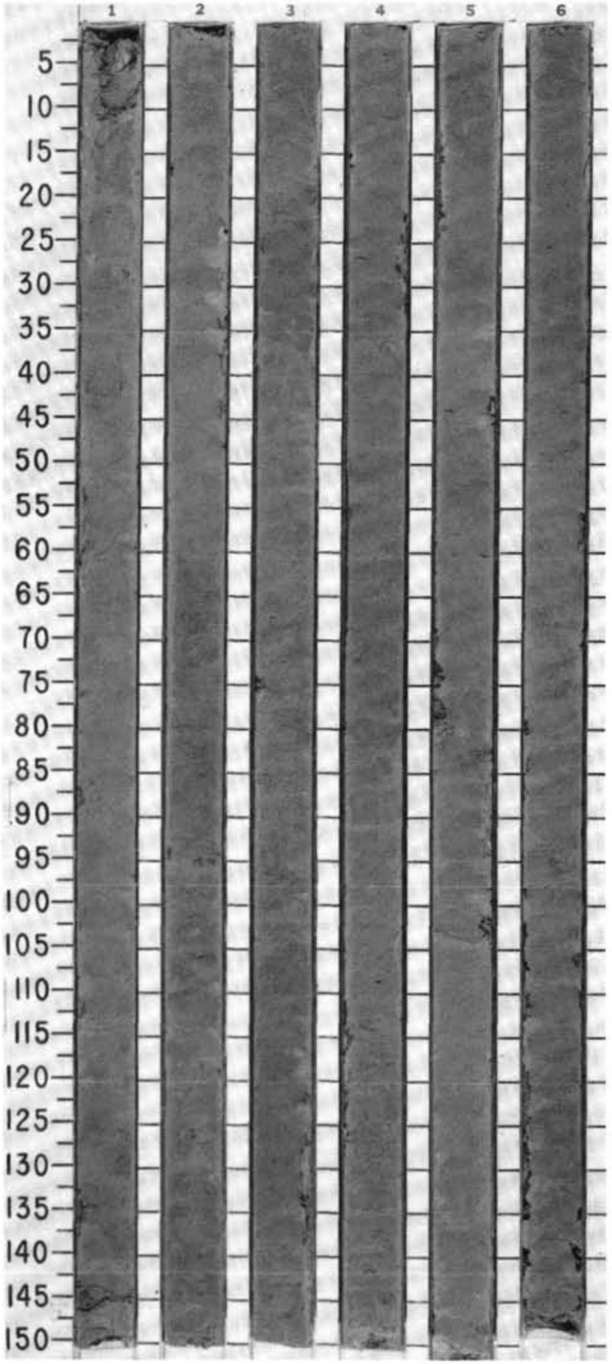

SITE 674 HOLE A CORE 41 X CORED INTERVAL 4926.8-4936.3 mbsl; 376.6-386.1 mbsf

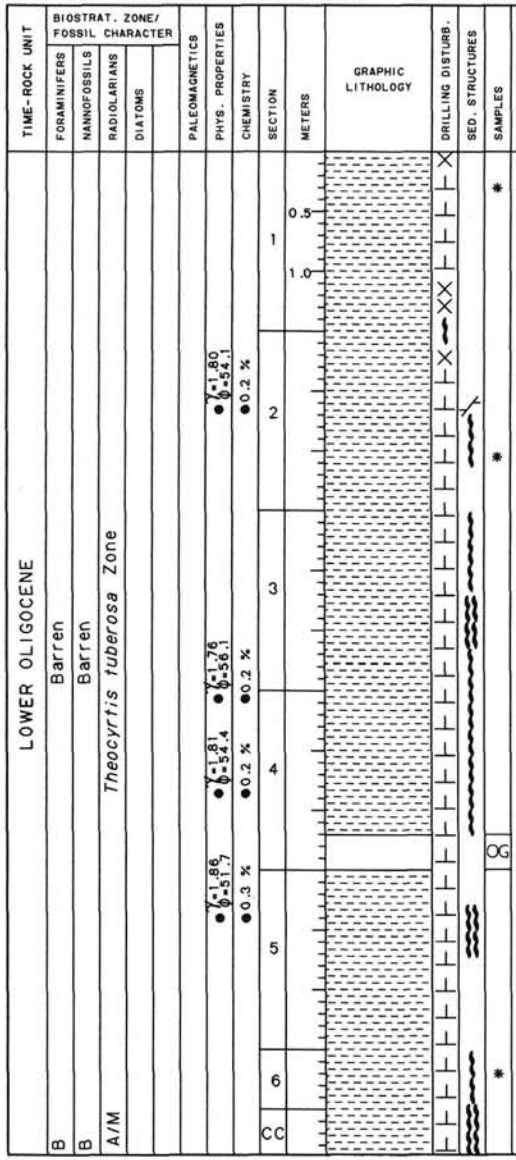

LITHOLOGIC DESCRIPTION

SILICEOUS MUDSTONE

Light brown (10YR6/3, 10YR6/4), light yellow-brown (10YR6/4), and light gray (2.5Y7/2 and 2.5Y6/2) SILICEOUS MUDSTONE; slightly zeolitic in Section 6; local slight to moderate bioturbation (in Section 5 by *Teichnius*).

Structure: subvertical fault with associated scaly fabrics in Section 2, 70 cm; sporadic scaly fabric with steep dips in Sections 5 and 6.

SMEAR SLIDE SUMMARY (%):

	1, 30 D	2, 110 M	6, 24 D
TEXTURE:			
Sand	Tr	3	—
Silt	30	20	13
Clay	70	77	87
COMPOSITION:			
Quartz	Tr	—	Tr
Feldspar	Tr	—	Tr
Clay	70	77	87
Accessory minerals			
Opaques	Tr	—	—
Diatoms	—	3	Tr
Radiolarians	25	15	10
Sponge spicules	5	5	3
Silicoflagellates	—	Tr	Tr
Fish remains	Tr	—	—

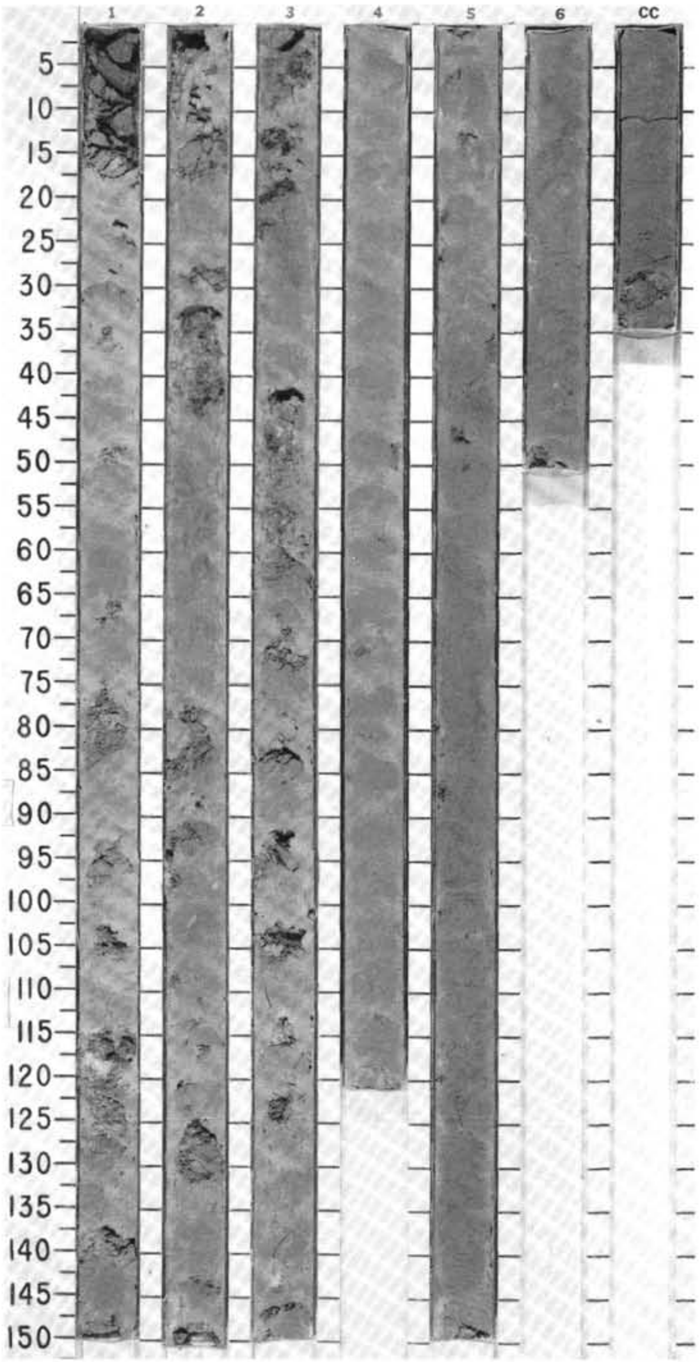

SITE 674 HOLE A CORE 42 X CORED INTERVAL 4936.3-4945.8 mbsl; 386.1-395.6 mbsf

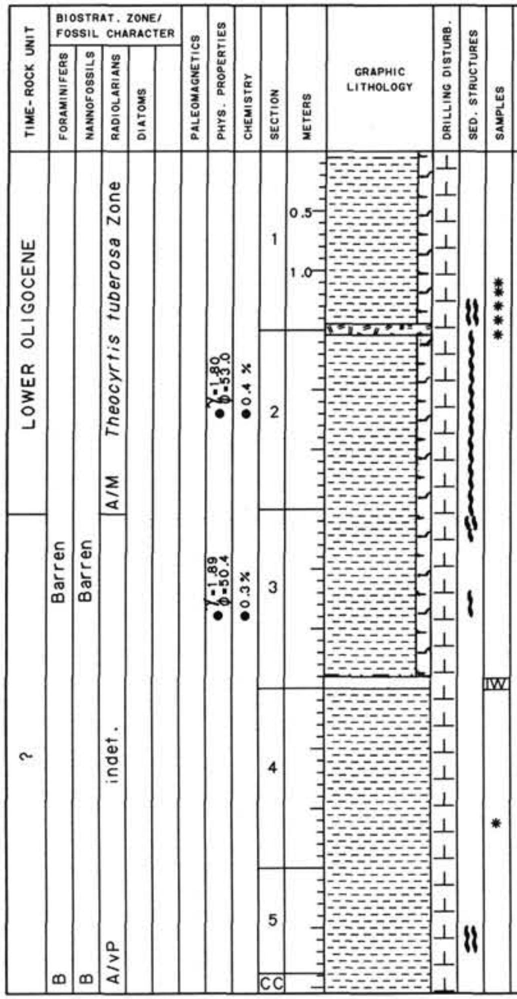

LITHOLOGIC DESCRIPTION

MUDSTONE and CLAYSTONE

Light olive-brown (5Y5/2, 5Y6/2, 2.5Y5/4), light green (5G5/2, 5G6/2), and gray-brown (2.5Y5/2) MUDSTONE and CLAYSTONE; locally slightly bioturbated.

Minor lithology: gray (N4), clay-rich vitric ash in Section 1, 145 cm, to Section 2, 2 cm.

SMEAR SLIDE SUMMARY (%):

	1, 107 D	1, 117 D	1, 123 M	1, 147 M	2, 2 M	4, 122 D
TEXTURE:						
Sand	—	—	5	10	—	—
Silt	19	10	5	33	90	2
Clay	81	90	90	57	10	98
COMPOSITION:						
Quartz	1	Tr	Tr	—	2	2
Feldspar	Tr	Tr	Tr	2	10	—
Clay	81	90	90	57	10	98
Volcanic glass	—	Tr	Tr	40	76	—
Accessory minerals	—	—	—	1	2	—
Zeolites	—	—	—	—	—	Tr
Orthopyroxene	—	—	—	—	Tr	—
Mn oxides	3	—	—	—	—	—
Fe/Mn hydroxides	—	—	—	—	—	Tr
Nannofossils	—	—	—	—	—	Tr
Diatoms	2	—	2	—	—	—
Radiolarians	10	8	5	—	—	Tr
Sponge spicules	3	2	3	—	—	Tr

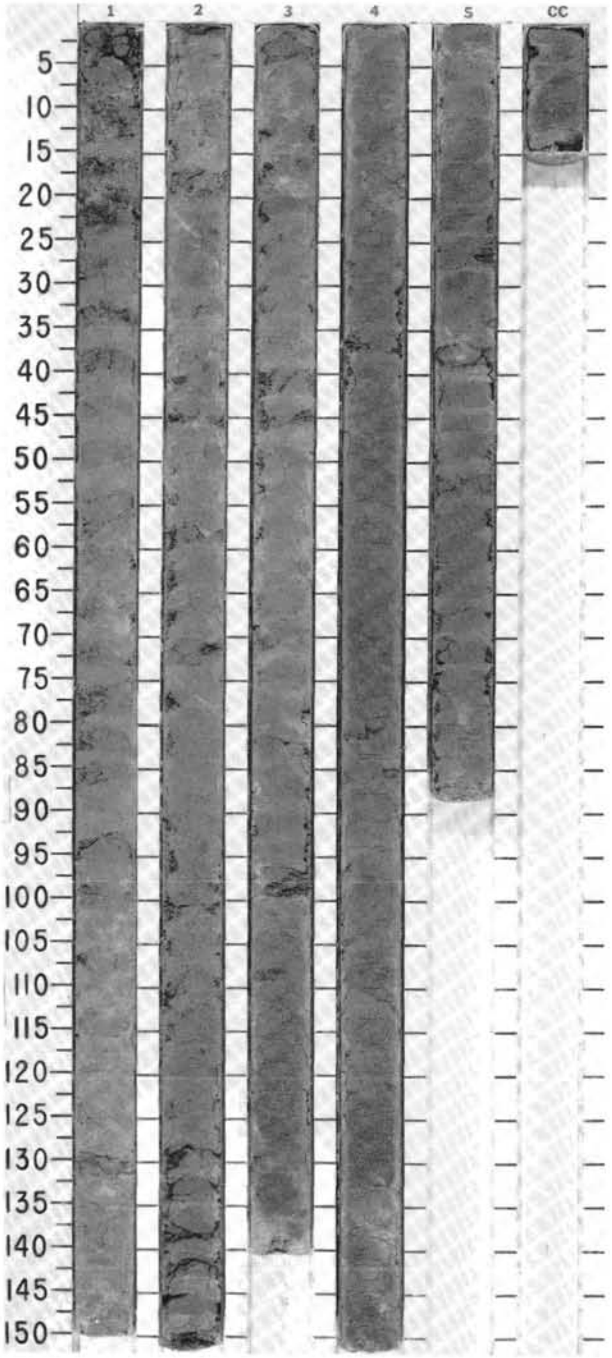

SITE 674 HOLE A CORE 43 X CORED INTERVAL 4945.8-4955.3 mbsl; 395.6-405.1 mbsf

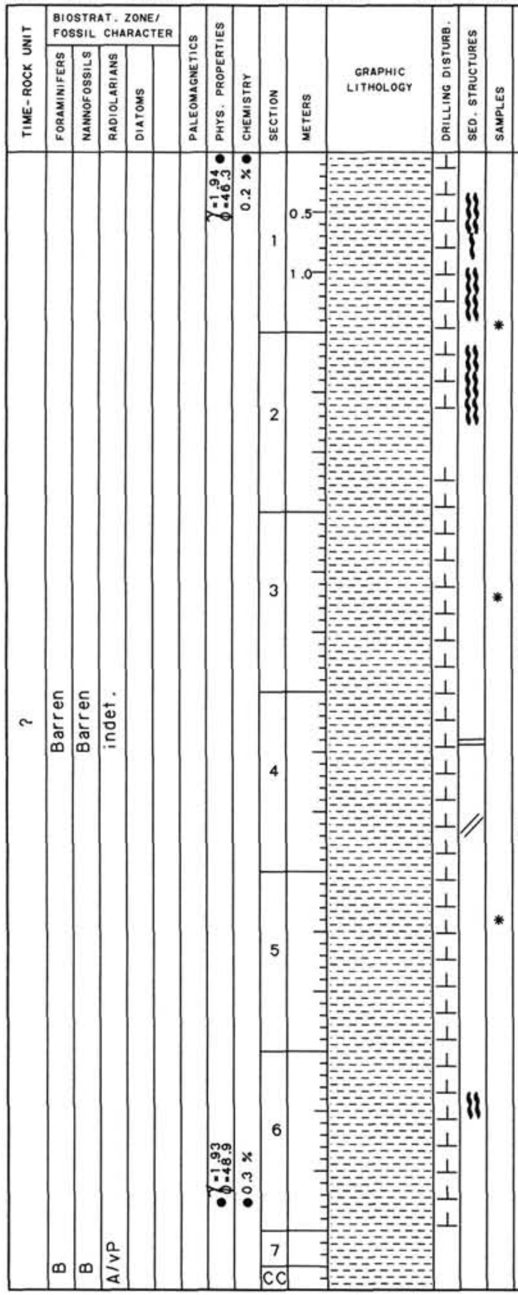

LITHOLOGIC DESCRIPTION

CLAYSTONE

Light olive-gray (5Y5/2, 5Y5/3, 2.5Y5/3, 5G6/2, 5G7/1) and light olive-brown (2.5Y5/4, 5Y6/3) CLAYSTONE in Sections 1 through 5, grading to reddish brown (7.5YR5/4) CLAYSTONE in Sections 6 through CC; Sections 1 and 2 are moderately bioturbated.

Minor lithology: light gray (5GY6/1) siltstone in Section 4, 45 and 113–118 cm, and in Section 5, 35 cm.

Structure: fault (80° dip) with associated scaly fabric in Section 2, 90 cm; fault breccias in Section 3, 30–60 cm, and Section 4, 75–110 cm; pervasive scaly fabric with variable dips. Bedding dips 0° at Section 3, 45 cm, and 45° at Section 3, 120 cm.

SMEAR SLIDE SUMMARY (%):

	1, 145 D	3, 75 D	5, 60 M	CC, 27 D
TEXTURE:				
Silt	5	5	100	9
Clay	95	95	—	91
COMPOSITION:				
Quartz	—	—	85	—
Feldspar	—	—	5	—
Rock fragments	—	—	5	—
Clay	95	95	—	91
Calcite/dolomite	—	—	2	—
Clinopyroxene	—	—	1	—
Accessory minerals				
Glauconite	—	—	Tr	Tr
Opaques	—	—	2	—
Orthopyroxene	—	—	Tr	—
Zeolite(?)	Tr	Tr	—	—
Fe/Mn hydroxide	Tr	Tr	—	2
Blue-green hornblende	—	—	Tr	—
Gray hornblende	—	—	Tr	—
Zircon	—	—	Tr	—
Radiolarians	5	5	—	5
Sponge spicules	—	—	—	2
Fish remains	—	Tr	—	—

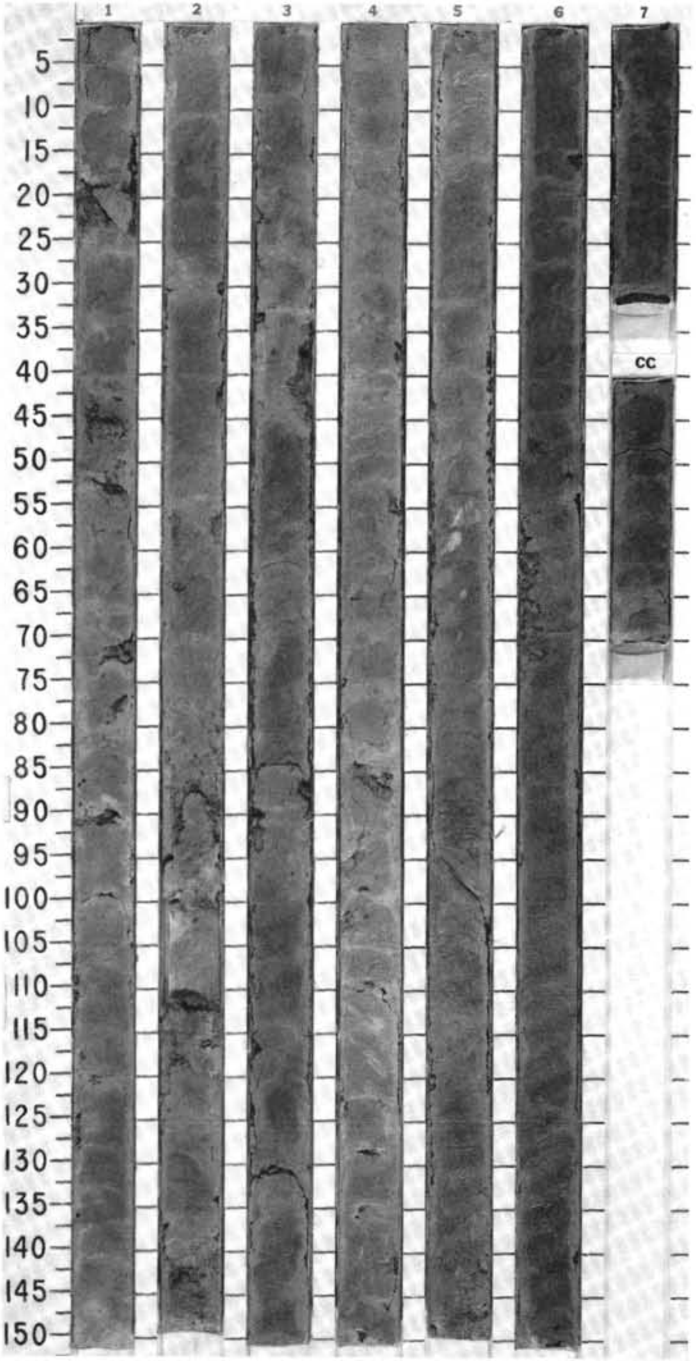

SITE 674 HOLE A CORE 44 X CORED INTERVAL 4955.3-4964.8 mbsl; 405.1-414.6 mbsf

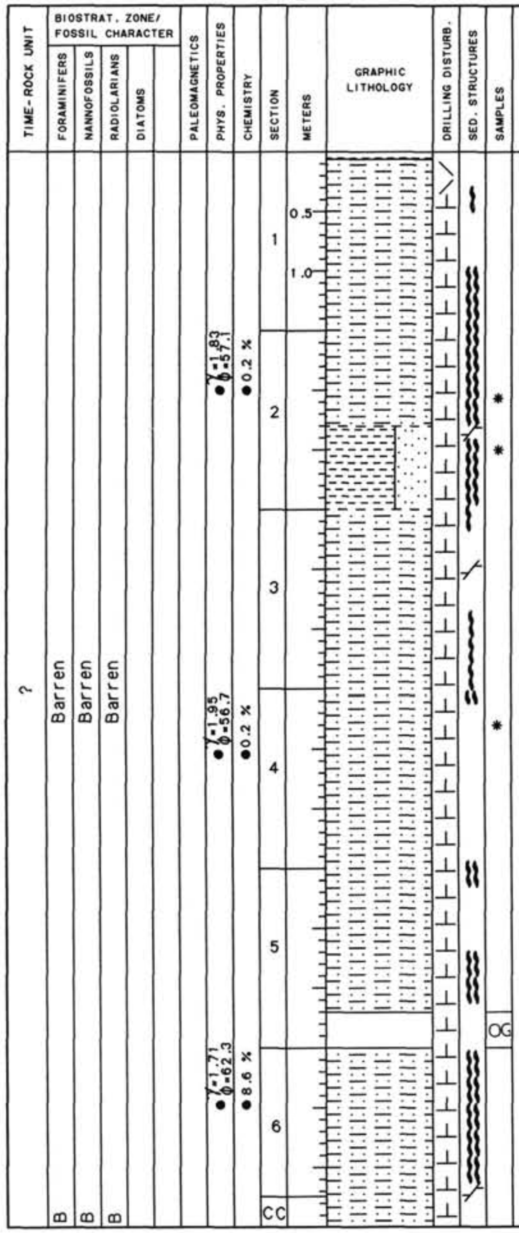

LITHOLOGIC DESCRIPTION

MUDSTONE, CLAYSTONE, and SILTY MUDSTONE

Pale olive (5Y6/3), dark olive-gray (5G4/1, 5G5/1), and brownish olive (2.5Y4/2) MUDSTONE, CLAYSTONE, and SILTY MUDSTONE; moderately bioturbated.

Structure: common anastomosing calcite veins; local intense scaly fabric (45–90° dips); faults at Section 2, 80 cm (30° dip), Section 3, 39–51 cm (vertical), and CC, 0–3 cm (40° dip, thrust). Bedding dip of 35° at Section 2, 75 cm.

SMEAR SLIDE SUMMARY (%):

	2, 58 D	2, 103 M	4, 23 M
TEXTURE:			
Sand	—	—	2
Silt	10	35	18
Clay	90	65	80
COMPOSITION:			
Quartz	10	—	17
Feldspar	—	5	—
Clay	90	65	76
Volcanic glass	—	30	—
Accessory minerals			
Pyrite	—	—	5
Clinopyroxene	—	—	2

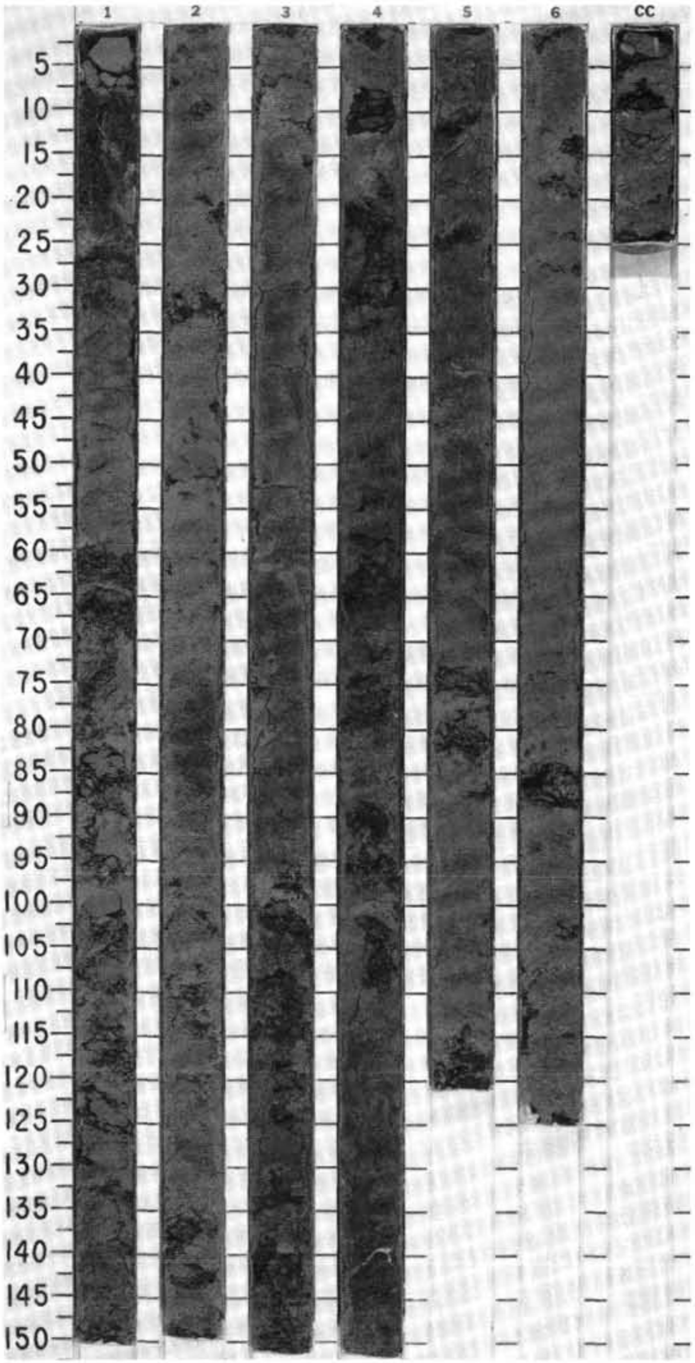

SITE 674 HOLE A CORE 45 X CORED INTERVAL 4964.8-4974.3 mbsl; 414.6-424.1 mbsf

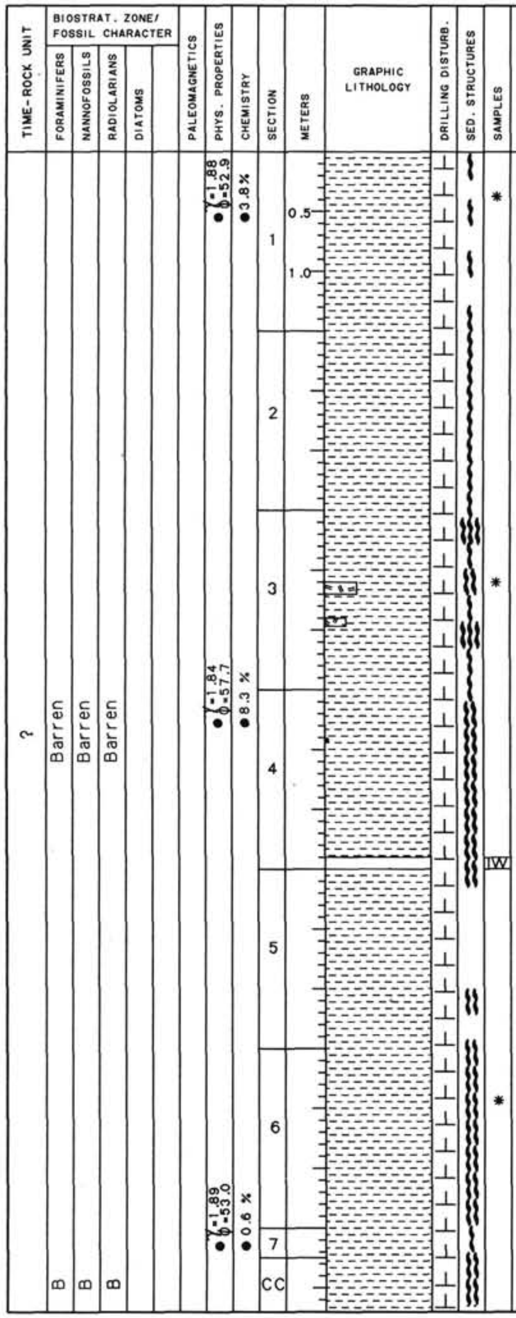

LITHOLOGIC DESCRIPTION

CLAYSTONE

Greenish gray (5GY4/1, 10Y4/1) to brown (10YR3/3) CLAYSTONE; moderately bioturbated.

Minor lithology: gray (N3) vitric ash beds in Section 3, 0–5, 59–66, and 92–96 cm, and in Section 4, 110–132 cm.

Structure: frequent anastomosing calcite veins (25–80° dips); local scaly fabric with variable, but steep, dips; fault in Section 5, 142–150 cm (40° dip).

SMEAR SLIDE SUMMARY (%):

	1, 39 D	3, 63 M	6, 44 D
TEXTURE:			
Silt	5	35	3
Clay	95	65	97
COMPOSITION:			
Quartz	5	8	2
Feldspar	2	2	2
Clay	90	50	94
Volcanic glass	—	20	—
Calcite/dolomite	3	10	—
Accessory minerals	—	10	2
Fish remains	Tr	—	—

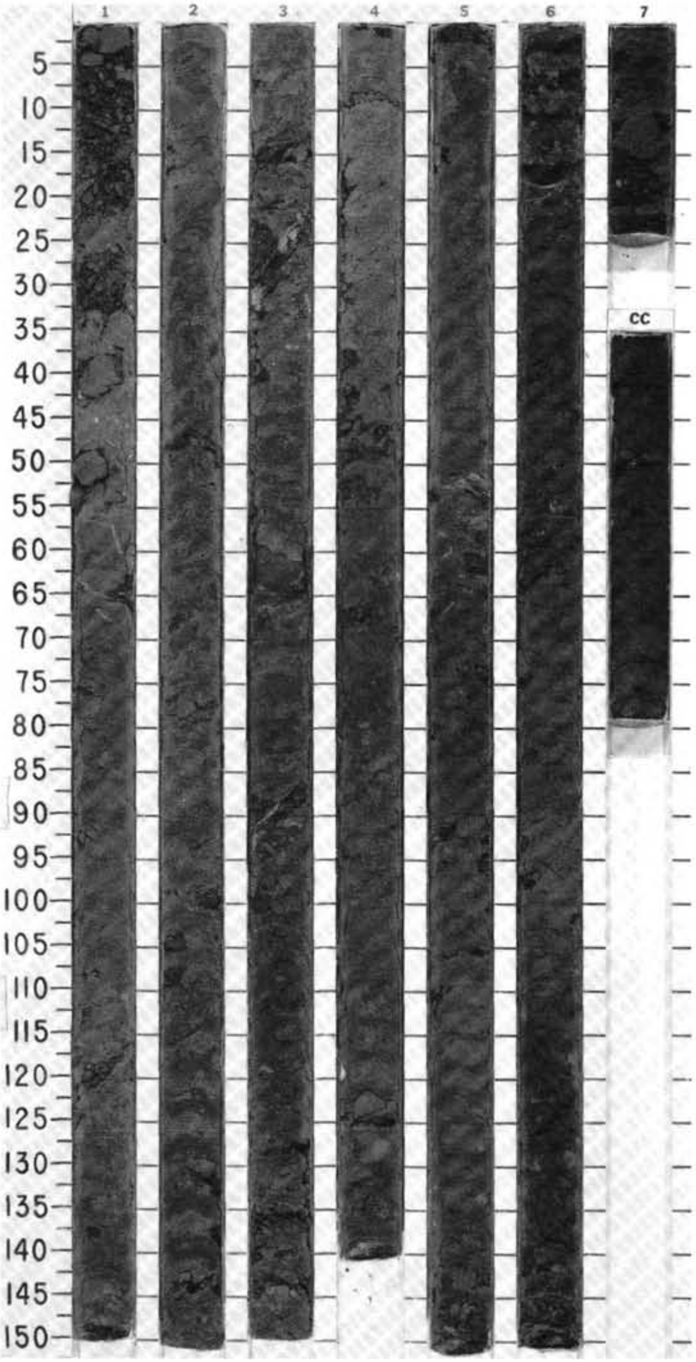

SITE 674 HOLE A CORE 46 X CORED INTERVAL 4974.3-4983.8 mbsl; 424.1-433.6 mbsf

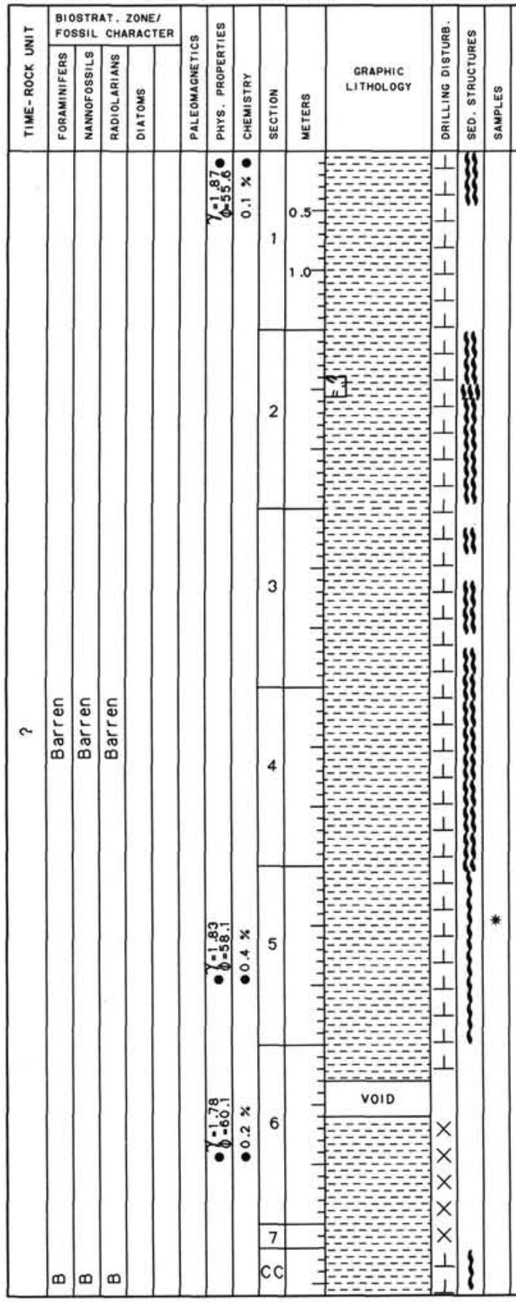

LITHOLOGIC DESCRIPTION

CLAYSTONE

Olive (10Y4/1), dark green (5GY4/1), and olive-brown (5Y4/2) CLAYSTONE; moderately bioturbated.

Minor lithology: gray-brown (5Y2.5/2) ash-rich layer in Section 2, 45–56 cm.

Structure: numerous calcite veins associated with steeply dipping scaly fabric.

SMEAR SLIDE SUMMARY (%):

	5, 48 D
TEXTURE:	
Silt	5
Clay	95
COMPOSITION:	
Quartz	6
Clay	93
Accessory minerals	1

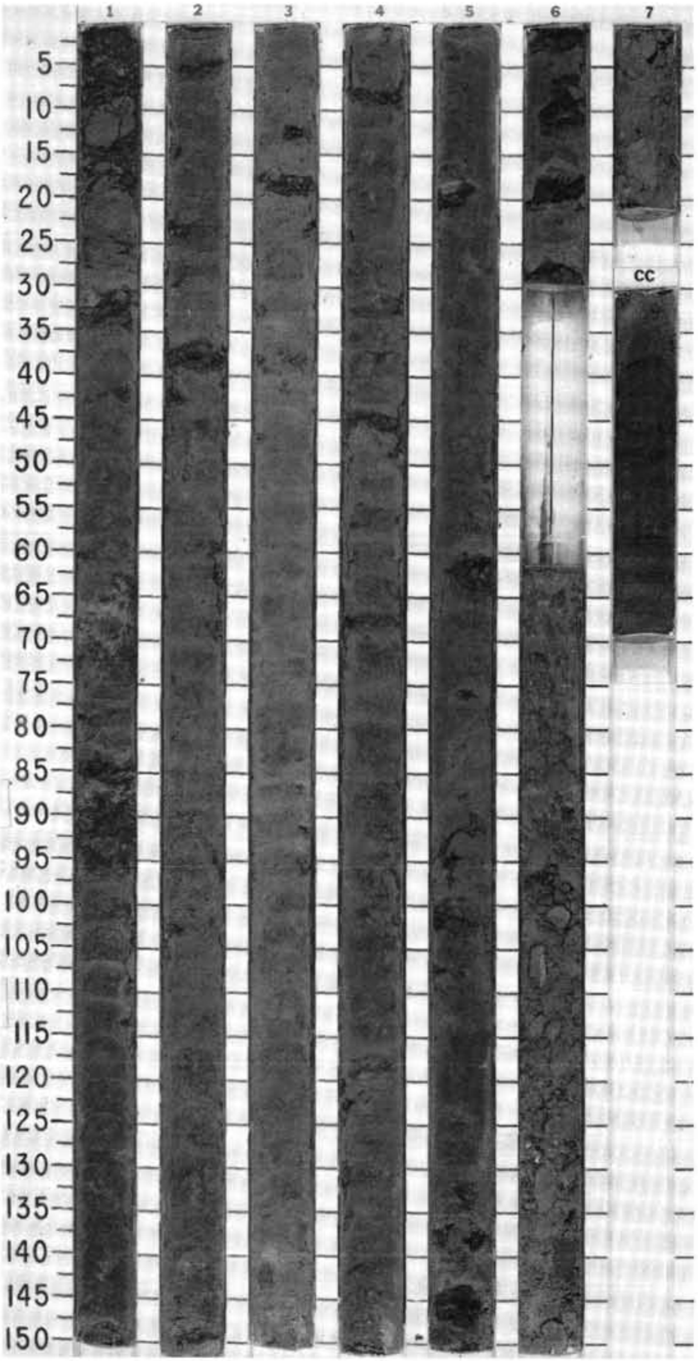

SITE 674 HOLE A CORE 47 X CORED INTERVAL 4983.8-4993.3 mbsl; 433.6-443.1 mbsf

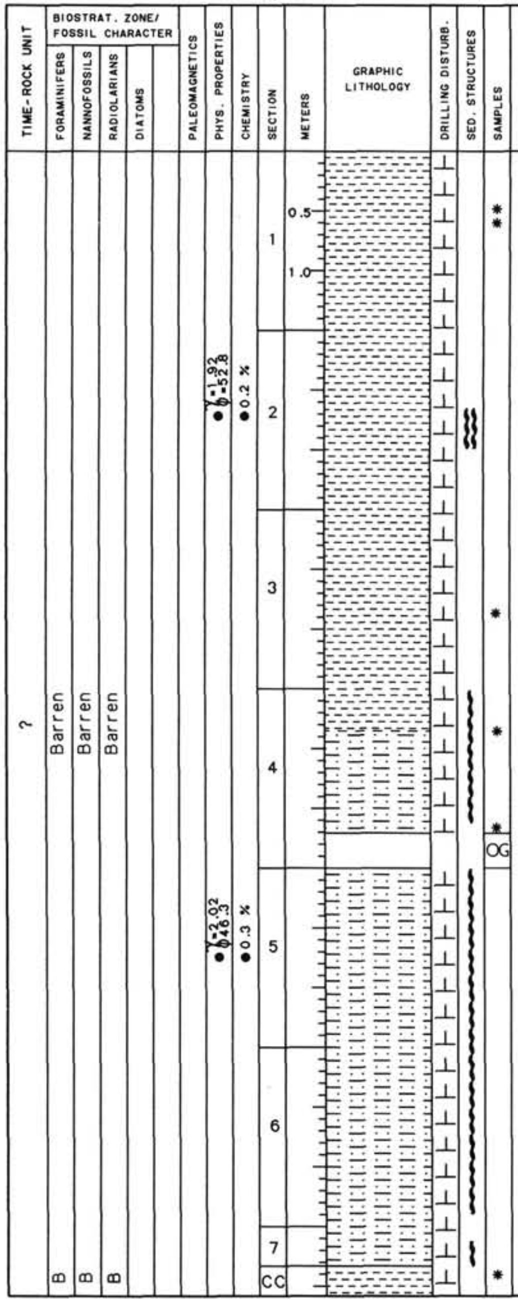

LITHOLOGIC DESCRIPTION

CLAYSTONE and MUDSTONE

Varicolored orange-brown (7.5YR4/2), brown (10YR4/3), blue-green (5G5/1), and red-brown (7.5YR4/6) CLAYSTONE and MUDSTONE.

Structure: pervasive, steeply dipping, scaly fabric throughout the core.

SMEAR SLIDE SUMMARY (%):

	1, 50 D	1, 63 M	3, 85 D	4, 30 D	4, 118 D	CC, 2
TEXTURE:						
Silt	—	14	8	—	12	5
Clay	100	86	92	100	88	95
COMPOSITION:						
Quartz	—	1	10	—	13	3
Feldspar	—	2	—	—	1	1
Clay	100	86	88	98	86	90
Volcanic glass	—	—	2	—	Tr	1
Calcite	—	—	—	—	—	1
Accessory minerals	Tr	1	Tr	—	—	3
Fibrous zeolite	Tr	—	—	Tr	—	—
Orthopyroxene	—	Tr	—	—	—	—
Mn oxide	Tr	10	—	2	—	—
Sponge spicules	—	—	—	—	—	1

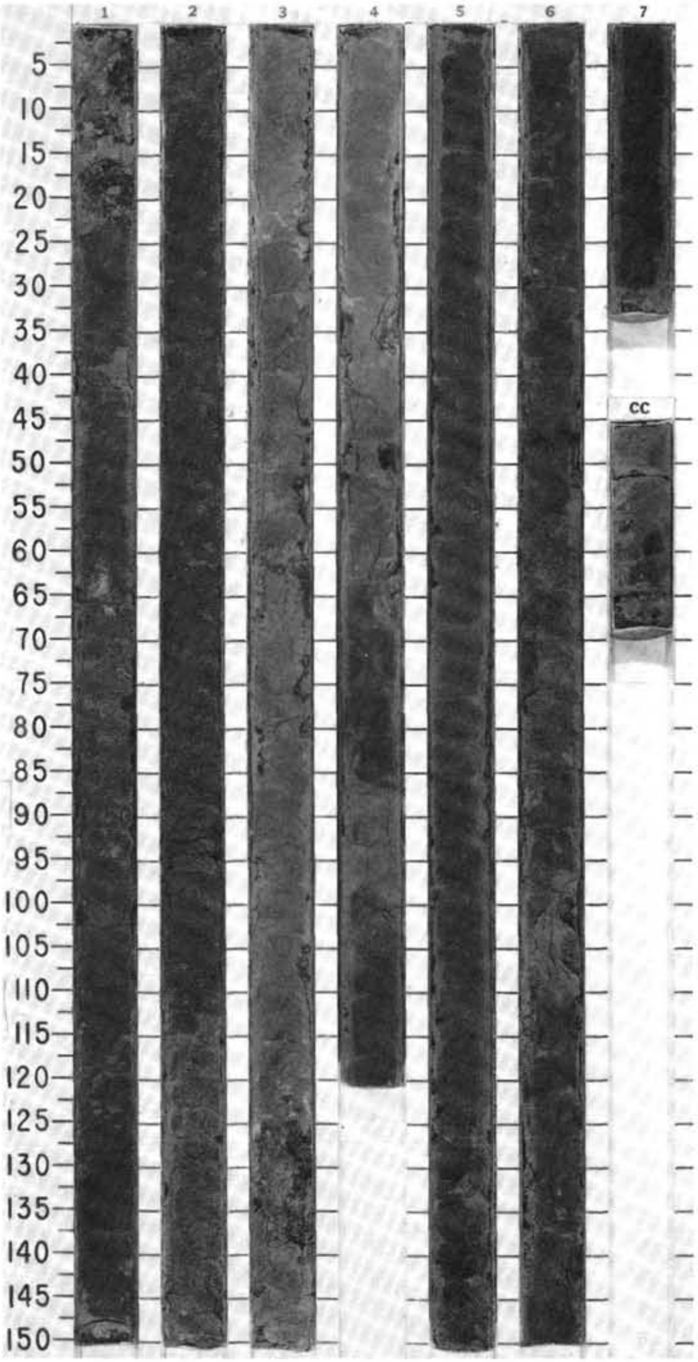

SITE 674 HOLE A CORE 48 X CORED INTERVAL 4993.3-5002.8 mbsl; 443.1-452.6 mbsf

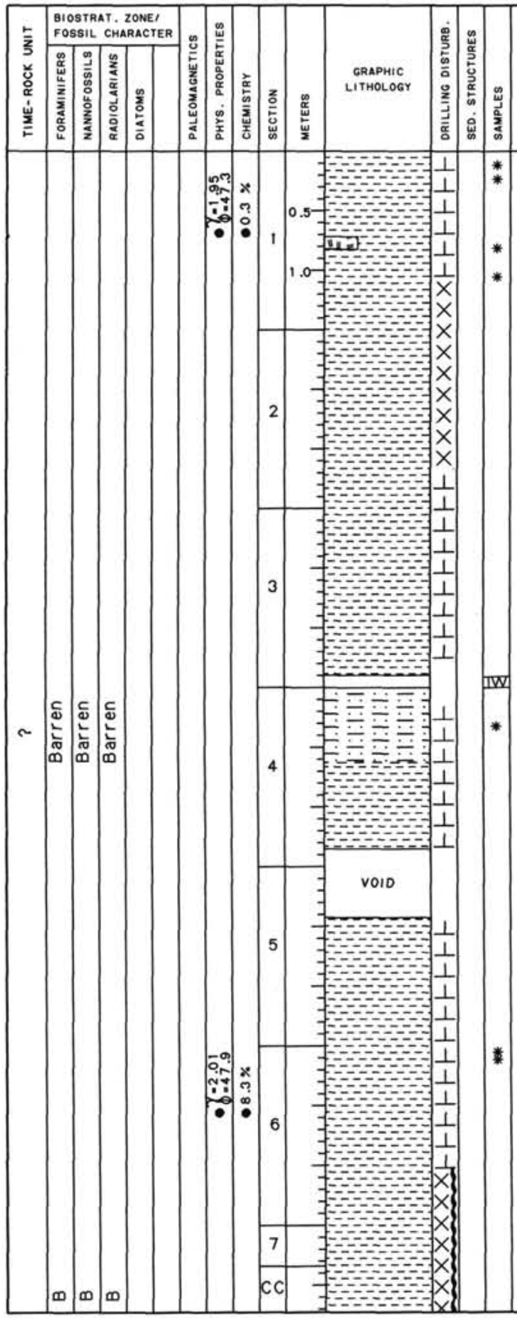

LITHOLOGIC DESCRIPTION

CLAYSTONE and MUDSTONE

Varicolored, orange-brown (7.5YR4/2, 7.5YR4/3), green-gray (5GY6/1), brown-gray (5Y6/1), and dark olive-gray (5GY6/1) CLAYSTONE; locally grading into MUDSTONE.

Structure: entire core is highly sheared; pervasive, intense, steeply to vertically dipping scaly fabric; frequent faults in Sections 1, 3, and 5, all with subvertical dips.

SMEAR SLIDE SUMMARY (%):

	1, 12 D	1, 22 M	1, 77 M	1, 103 D	4, 26 M	6, 6 M	6, 9 D
TEXTURE:							
Sand	—	1	—	—	—	Tr	—
Silt	5	10	25	Tr	22	5	2
Clay	95	89	75	100	78	95	98
COMPOSITION:							
Quartz	1	5	—	Tr	2	Tr	Tr
Feldspar	1	Tr	—	—	2	Tr	—
Rock fragments	3	—	—	2	—	—	—
Clay	96	89	75	100	78	15	98
Volcanic glass	—	—	10	—	—	—	—
Calcite/dolomite	—	—	5	—	—	85	1
Accessory minerals	—	—	—	—	10	—	—
Mn oxide	2	2	10	—	14	—	1